

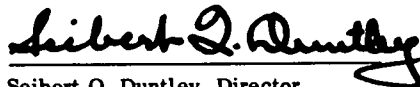
**AIRBORNE AND GROUND-BASED MEASUREMENTS OF OPTICAL
ATMOSPHERIC PROPERTIES IN SOUTHERN ILLINOIS**

by

Seibert Q. Duntley, Richard W. Johnson, Jacqueline I. Gordon


Visibility Laboratory
University of California, San Diego
Scripps Institution of Oceanography
San Diego, California 92152

Approved:



Seibert Q. Duntley, Director
Visibility Laboratory

Approved:



William A. Nierenberg, Director
Scripps Institution of Oceanography

CONTRACT NO. F19628-73-C-0013

Project No. 7621

Task No. 762104

Work Unit No. 76210401

Scientific Report No. 4

June 1974

Contract Monitor: Dr. Robert W. Fenn, Optical Physics Laboratory

Approved for public release; distribution unlimited.

Prepared for

**AIR FORCE CAMBRIDGE RESEARCH LABORATORIES
AIR FORCE SYSTEMS COMMAND
UNITED STATES AIR FORCE
HANSCOM AFB, MASSACHUSETTS 01730**

ABSTRACT

This report presents daytime atmospheric optical data collected chiefly with airborne instruments during a field expedition to southern Illinois in the summer of 1971. Results from four flights and selected ground-based data are presented. The data include the natural irradiance upon horizontal plane surfaces, scalar irradiances, total volume scattering coefficients, atmospheric beam transmittances, path radiances, directional path reflectances, and directional terrain reflectances. Data for sunlight conditions were derived for downward-looking paths of sight inclined at six zenith angles (95, 100, 105, 120, 150, and 180 degrees) from maximum altitudes of 3000 to 5100 meters above ground level and lower in three spectral regions, as follows: two narrow band optical filters with mean wavelengths of 478 and 664 nanometers; and one broad band sensitivity representing the photopic response with a mean wavelength of 557 nanometers.

SUMMARY

This report, which describes the second increment of the Visibility Laboratory's Project METRO effort, was prepared under AFCRL Contract F19628-73-C-0013. The first increment was reported in AFCRL-TR-73-0422, Duntley *et al.* (1973). The principal project task was to take daytime atmospheric optical measurements in southern Illinois and, from these measurements, to determine optical properties for various downward-inclined paths of sight. These properties include the natural irradiance upon horizontal plane surfaces, scalar irradiances, total volume scattering coefficients, atmospheric beam transmittances, directional path reflectances, directional terrain reflectances, and path radiances. The data previously reported in AFCRL-TR-73-0422 described flight profiles representing mostly cloud-free upper hemispheres. The data in this report describe those flight profiles having more severe cloud conditions.

The field trip was made to Illinois during August 1971. Data were recorded on several flight tracks located in the area surrounding St. Louis, Missouri. The typical terrains were either rolling wooded hills or flat cultivated farmland.

The radiometric instrumentation developed at the Visibility Laboratory and mounted in Air Force C-130A, aircraft No. 50022, consisted of a total scattering meter (or integrating nephelometer) for determining the total scattering coefficient, two sky scanning radiometers for recording upper and lower sky radiances, a dual irradiator for recording alternately the downwelling and upwelling irradiances, an equilibrium radiance telephotometer, and a variable direction path function meter. The meteorological instrumentation included a Royco particle counter, pressure transducers, a dewpoint hygrometer, and an AN/AMQ-17 aerograph for measuring ambient temperature and pressure. Unfortunately, the dewpoint hygrometer failed to perform adequately, as did the AN/AMQ-17 pressure channel, and the data were not recoverable.

Each optical instrument was fitted with five optical filters causing it to measure at three narrow band wavelengths of the spectrum and two broad pass bands. The measurements were made using two narrow band filters at mean wavelengths of 478 and 664 nanometers and a filter representing the photopic response with a mean wavelength of 557 nanometers.

All but the Royco data were recorded on magnetic tape in the aircraft by means of a 42-channel magnetic tape data logger. The data tapes were returned to the Visibility Laboratory to be processed using the computer facilities at the University of California, San Diego.

A Visibility Laboratory ground-based data station was located at Scott Air Force Base. It contained effectively duplicate instrumentation for obtaining optical data.

TABLE OF CONTENTS

ABSTRACT	iii
SUMMARY	v
LIST OF ILLUSTRATIONS	ix
RELATED CONTRACTS AND PUBLICATIONS	xi
GLOSSARY AND NOTATION	xiii
1. INTRODUCTION	1-1
2. THEORY	2-1
2.1 Contrast Transmittance in the Troposphere	2-1
2.2 Ground-Based Measurements of Vertical Earth-To-Space Contrast Transmittance.	2-12
3. INSTRUMENTATION	3-1
3.1 Radiometric Systems	3-4
3.2 Meteorological Systems	3-6
3.3 Control and Communication Systems	3-7
3.4 Photographic Systems	3-7
3.5 Radiometric Calibration Procedures	3-8
3.6 Standard Response Characteristics for Broad Band Sensors	3-14
4. DATA COLLECTION METHODS	4-1
4.1 Airborne System	4-1
4.2 Ground-Based System	4-3
5. DATA PROCESSING	5-1
5.1 Airborne Data	5-1
5.2 Ground-Based Data	5-1
5.3 Calibration Data	5-3
5.4 Data Tapes	5-4
6. WEATHER SUMMARY	6-1
6.1 Summary	6-1
6.2 Synoptic Conditions	6-6
6.3 Tabular Summary and Glossary	6-6
6.4 Analysis of Radiometric and Meteorological Relationships	6-12

7.	DATA PRESENTATION	7-1
7.1	Airborne Data and Flight Summary	7-1
7.2	Description of Airborne Data Tables and Graphs.	7-6
7.3	Presentation of Airborne Data.	7-10
7.4	Ground-Based Data Summary.	7-81
7.5	Description and Presentation of Ground-Based Data Tables	7-85
8.	DATA INTERPRETATION AND EVALUATION	8-1
8.1	Meteorological Data	8-1
8.2	Airborne Radiometric Data	8-4
8.3	Ground-Based Radiometric Data.	8-13
8.4	Summary	8-19
9.	ACKNOWLEDGEMENTS	9-1
10.	REFERENCES	10-1

LIST OF ILLUSTRATIONS

Figure	Title	Page
1-1	Computations From Basic Airborne Data	1-2
1-2	Computations From Backup Airborne Data	1-3
1-3	Computations From Specialized Ground Data	1-4
1-4	Typical METRO Flight Tracks	1-5
1-5	Standard Spectral Responses – Project METRO	1-6
2-1	Path Length Geometry for Steeply Inclined Paths of Sight	2-4
2-2	Path Length Geometry for Grazing Paths of Sight in Refractive Spherical Atmospheres	2-5
2-3	Scattering Angle Relationships for Typical CRM Operations	2-15
3-1	C-130 Airborne Instrument System	3-3
3-2	Ground-Based Instrument System	3-4
3-3	Typical Computer-Generated Linearity Calibration Curve	3-9
3-4	Typical Absolute Calibration Form	3-10
3-5	Computer-Generated Plot of Standard Spectral Responses for Project METRO	3-15
4-1	Typical Visibility Laboratory Flight Profile	4-2
5-1	Atmospheric Visibility Program Data Processing Schedule	5-2
6-1	Synoptic Charts of St. Louis Area During Project METRO	6-2
6-2	Temperature Versus Altitude for Six Project METRO flight profiles	6-4
7-1	Typical Sky and Terrain Photographs for Flight C-183	7-4
7-2	Typical Sky and Terrain Photographs for Flight C-185	7-5
8-1	AN/AMQ-17 Temperature Calibration Curves	8-2
8-2	Temperature for METRO Flights With Some Scattered Clouds Compared to 30°N July and 45°N July Temperatures from the U. S. Standard Atmosphere Supplements	8-3
8-3	Total Volume Scattering Coefficient for Filter 4 (Pseudo-Photopic) for Six METRO Flights	8-5
8-4	Project METRO Low Altitude Downwelling Irradiance for Filter 4 (Pseudo-Photopic) Compared to Brown (1952) and a Rayleigh Atmosphere	8-6
8-5	Comparison of Equilibrium Nadir Radiance With Several Computed Apparent Nadir Terrain Radiances and the Measured Scanner Nadir Radiance from Flight C-180 Filter 4 (Pseudo-Photopic)	8-9
8-6	Contrast Transmittance for Several Different Backgrounds and Beam Transmittance for Flight C-180 Filter 4 (Pseudo-Photopic) Nadir Path of Sight	8-13
8-7	Ground-Based Downwelling Irradiance for Filter 4 (Pseudo-Photopic) Compared to Brown (1952)	8-18
8-8	Directional Reflectance of Mowed Grass, Dry and Browning for Filter 4 (Pseudo-Photopic)	8-19

RELATED CONTRACTS AND PUBLICATIONS

Related Contracts: None

Publications:

S. Q. Duntley, R. W. Johnson, and J. I. Gordon, "Airborne Measurements of Optical Atmospheric Properties in Southern Germany," AFCRL-72-0255, SIO Ref. 72-64 (July 1972)

S. Q. Duntley, R. W. Johnson, and J. I. Gordon, "Airborne and Ground-Based Measurements of Optical Atmospheric Properties in Central New Mexico," AFCRL-72-0461, SIO Ref. 72-71 (September 1972)

S. Q. Duntley, R. W. Johnson, and J. I. Gordon, "Airborne Measurements of Optical Atmospheric Properties, Summary and Review," AFCRL-72-0593, SIO Ref. 72-82 (November 1972)

J. I. Gordon, J. L. Harris, Sr., and S. Q. Duntley, "Measuring Earth-to-Space Contrast Transmittance from Ground Stations," Appl. Opt. **12**, 1317 - 1324 (1973)

S. Q. Duntley, R. W. Johnson, and J. I. Gordon, "Airborne Measurements of Optical Atmospheric Properties in Southern Illinois," AFCRL-TR-73-0422, SIO Ref. 73-24 (July 1973)

J. I. Gordon, C. F. Edgerton, and S. Q. Duntley, "Signal-Light Nomogram," submitted to the Journal of the Optical Society of America in March 1974

GLOSSARY AND NOTATION

The notation used in reports and journal articles produced by the Visibility Laboratory staff follow, in general, the rules set forth in pages 499 and 500, Duntley *et al* (1957). These rules are:

Each optical property is indicated by a basic (parent) symbol.

A presubscript may be used with the parent symbol as an identifier, e.g., b indicates background while t denotes an object.

A postsubscript may be used to indicate the length of a path of sight, e.g., r denotes an *apparent* property as measured at the end of a path of sight of length r , while o denotes an *inherent* property based on the hypothetical concept of a photometer located at zero distance from an object.

A postsuperscript*, or a postsubscript*, is employed as a mnemonic symbol signifying that the radiometric quantity has been generated by the scattering of ambient light reaching the path from all directions.

The parenthetical attachments to the parent symbol denote altitude and direction. The letter z indicates altitude in general; z_t is used to specify the altitude of an object. The direction of a path of sight is specified by the zenith angle θ and the azimuth ϕ . In the case of irradiances, the downwelling irradiance is designated by d , the upwelling by u .

The glossary for meteorological symbols is presented in Section 6.

$A(z)$	Albedo at altitude z , defined by the equation $A(z) \equiv H(z,u)/H(z,d)$.
${}_sA(z)$	Scalar albedo at altitude z , defined by the equation ${}_sA(z) \equiv h(z,u)/h(z,d)$.
AGL	Above ground level.
$C_o(z_t, \theta, \phi)$	Inherent universal contrast determined for a path of sight of zero length at altitude of the object z_t in the direction of zenith angle θ and azimuth ϕ . This property is defined by the equation

$$C_o(z_t, \theta, \phi) \equiv \frac{{}_tN_o(z_t, \theta, \phi) - {}_bN_o(z_t, \theta, \phi)}{{}_bN_o(z_t, \theta, \phi)}$$

$C_r(z, \theta, \phi)$ Apparent universal contrast as determined at altitude z from the end of path of sight of length r in the direction of the zenith angle θ and azimuth ϕ . This property is defined by the equation

$$C_r(z, \theta, \phi) \equiv \frac{{}_tN_r(z, \theta, \phi) - {}_bN_r(z, \theta, \phi)}{{}_bN_r(z, \theta, \phi)}$$

g Acceleration of gravity.

$H(z)$ Scale height at altitude z , the height of a homogeneous atmosphere having the density of the layer at altitude z .

$H(z, d)$ Irradiance produced by downwelling flux as determined on a horizontal flat plate at altitude z . In this report d is used in place of the minus sign in the notation $H(z, -)$ which appears in Duntley (1969). This property may be defined by the equation

$$H(z, d) \equiv \int_{2\pi} N(z, \theta', \phi') \cos\theta' d\Omega .$$

$H(z, u)$ Irradiance produced by upwelling flux as determined on a horizontal flat plate at altitude z . Here u is substituted for the plus sign formerly used in the notation $H(z, +)$.

$h(z)$ Scalar irradiance. This may be defined as the radiant flux arriving at a point, from all directions about that point, at altitude z (Tyler and Preisendorfer, 1962):

$$h(z) \equiv h(z, d) + h(z, u) .$$

$h(z, d)$ Scalar irradiance produced by downwelling flux. This may be defined as the radiant flux from the upper hemisphere arriving at a point at altitude z .

${}_k h(z, d)$ Scalar irradiance defined as the radiant flux from the upper hemisphere sky (flux from the sun is not included) arriving at a point at altitude z .

${}_s h(z)$ Scalar irradiance defined as the radiant flux from the sun arriving at a point at altitude z .

$h(z, u)$ Scalar irradiance produced by upwelling flux. This may be defined as the radiant flux from the lower hemisphere arriving at a point at altitude z .

$L(z)$ Attenuation length at altitude z . This property is the reciprocal of the attenuation coefficient, that is,

$$L(z) \equiv a(z)^{-1} .$$

$\bar{L}(z)$ Equivalent attenuation length is defined as

$$\bar{L}(z) = \frac{-z}{\ln T_z(0,0)} .$$

$m_\infty(z,\theta)/m_\infty(z,0)$ Relative optical airmass.

$N(z,\theta,\phi)$ Radiance as determined from altitude z in the direction specified by zenith angle θ and azimuth ϕ .

${}_b N_o(z_t,\theta,\phi)$ Inherent background radiance as determined at altitude of the photometer z_t at zenith angle θ and azimuth ϕ .

${}_b N_r(z,\theta,\phi)$ Apparent background radiance as determined at altitude z from the end of a path of sight of length r at zenith angle θ and azimuth ϕ . This property may be defined by the equation

$${}_b N_r(z,\theta,\phi) \equiv {}_b N_o(z_t,\theta,\phi) T_r(z,\theta) + N_r^*(z,\theta,\phi) .$$

${}_s N_\infty(0,\theta_s,0^\circ)$ Apparent radiance of the center of the solar disk as determined at ground-level altitude from the end of path of sight of length ∞ from out of the atmosphere to ground at zenith angle of the sun θ_s .

${}_t N_o(z_t,\theta,\phi)$ Inherent radiance of an object as determined at altitude of the photometer z_t at zenith angle θ and azimuth ϕ .

${}_t N_r(z,\theta,\phi)$ Apparent radiance of an object as determined at altitude z from the end of a path of sight of length r at zenith angle θ and azimuth ϕ . This property may be defined by the equation

$${}_t N_r(z,\theta,\phi) \equiv {}_t N_o(z_t,\theta,\phi) T_r(z,\theta) + N_r^*(z,\theta,\phi) .$$

$N_q(z, \theta, \phi)$ Equilibrium radiance at altitude z with the direction of the path of sight specified by zenith angle θ and azimuth ϕ . This property is a point function of position and direction.

$\bar{N}_q(z, \theta, \phi)$ Effective equilibrium radiance for a path of sight from out of the atmosphere to altitude z in the direction specified by zenith angle θ and azimuth ϕ . This property may be defined by the equation

$$\bar{N}_q(z, \theta, \phi) \equiv N_{\infty}^*(z, \theta, \phi) / [1 - T_{\infty}(z, \theta)] .$$

This property may also be denoted as a function of angle from light source (sun or moon) β , i.e., $\bar{N}_q(z, \beta)$.

$N_*(z, \theta, \phi)$ Path function at altitude z with the direction of the path of sight specified by zenith angle θ and azimuth ϕ . This property is defined by the equation

$$N_*(z, \theta, \phi) \equiv \int_{4\pi} \sigma(z, \beta') N(z, \theta', \phi') d\Omega .$$

This property also is a point function of position and direction.

$N_r^*(z, \theta, \phi)$ Path radiance as determined at altitude z at the end of a path of sight of length r in the direction specified by zenith angle θ and azimuth ϕ .

$N_{\infty}^*(0, \gamma_s, 180^\circ)$ Sky radiance at a scattering angle of 90° from the sun. Also the path radiance for the path of sight of length ∞ from out of the atmosphere to ground-level altitude at a zenith angle equal to the solar elevation angle γ_s .

$n(z)$ Index of refraction at altitude z .

$P(z)$ Pressure at altitude z .

psia Pressure, absolute, pounds per square inch.

psid Pressure, differential, pounds per square inch.

${}_bR_o(z_t, \theta, \phi)$ Inherent background reflectance as determined at the altitude of an object z_t and viewed at zenith angle θ and azimuth ϕ .

$R_q(z, \theta, \phi)$ Equilibrium reflectance is defined as $R_q(z, \theta, \phi) \equiv N_q(z, \theta, \phi) \pi / H(z, d)$.

$R_r^*(z, \theta, \phi)$ Directional path reflectance as determined at altitude z at the end of a path of sight of length r in the direction specified by zenith angle θ and azimuth ϕ .

$R/M(0)$ Universal gas constant.

$\overline{S_\lambda T_\lambda}$ Standardized relative spectral response of filter/cathode combination where S_λ is spectral sensitivity of the multiplier phototube cathode and T_λ is spectral transmittance of optical filter.

$s(z)$ Total volume scattering coefficient as determined at altitude z . This property may be defined by the equation

$$s(z) \equiv \int_{4\pi} \sigma(z, \beta) d\Omega .$$

In the absence of atmospheric absorption, the total volume scattering coefficient is numerically equal to the attenuation coefficient.

${}_M s(z)$ Total volume scattering coefficient for Mie scattering at altitude z .

${}_R s(z)$ Total volume scattering coefficient for Rayleigh scattering at altitude z .

$T(z)$ Temperature in degrees Kelvin at altitude z .

$T_r(z, \theta)$ Beam transmittance as determined at altitude z for a path of sight of length r at zenith angle θ . This property is independent of azimuth in atmospheres having horizontal uniformity. It is always the same for the designated path of sight or its reciprocal.

W_λ Spectral emittance (power/unit of area) of electromagnetic flux from a plane surface.

${}_c W_\lambda$ Spectral emittance of calibration source.

W'_λ Spectral emittance of anticipated field scene.

\bar{y} Symbol for visual efficiency function.

ZSV Zero scale value. The zero point on the linear scale when the radiometric or photometric quantity x is equal to a reference radiometric or photometric quantity x_0 as shown in the equation

$$\log[x_0/x] = 0 .$$

z Altitude, usually used as above ground level.

z_t	Altitude of an object.
$\alpha(z)$	Volume attenuation coefficient as determined at altitude z . In the absence of atmospheric absorption, the attenuation coefficient is numerically equal to the volume scattering coefficient.
β	Symbol for scattering angle of flux from a light source. It is equal to the angle between the line from the source to the observer and the path of sight.
β'	Symbol for scattering angle of flux from a discrete part of the sky. It is equal to the angle between the direction specified by θ' and ϕ' and the path of sight.
γ_s	Elevation angle of the sun. The solar elevation angle is the complement of the sun zenith angle, $\gamma_s = 90^\circ - \theta_s$.
Δ	Symbol to indicate incremental quantity and used with r and z to indicate small, discrete increments in path length r and altitude z .
δ_λ	Response area is defined as $\delta_\lambda = \overline{S_\lambda T_\lambda} \Delta \lambda$.
ϵ_λ	Spectral emissivity of tungsten filament.
ζ	Symbol for radius of the earth in Eq. 2.13 and 2.15 and Figure 2-2.
θ	Symbol for zenith angle. This symbol is usually used as one of two coordinates to specify the direction of a path of sight.
θ'	Symbol for zenith angle usually used as one of two coordinates to specify the direction of a discrete portion of the sky.
λ	Symbol for wavelength.
$\bar{\lambda}$	Mean wavelength is defined as $\bar{\lambda} \equiv \overline{\lambda(S_\lambda T_\lambda)} \Delta \lambda / \delta \lambda$.
$\rho(z)$	Density at altitude z .
σ	Symbol for volume scattering function. Parenthetical symbols may be added for example, β may be used to designate the scattering angle from a source. In Gordon (1969) the parenthetical symbols are z and β for altitude and scattering angle.
$\sigma(z, \beta) / s(z)$	Proportional directional volume scattering function. This may be defined by the equation

$$\int_{4\pi} [\sigma(z, \beta) / s(z)] \equiv 1 .$$

$\tau_r(z, \theta, \phi)$ Contrast transmittance as determined at altitude z at the end of a path of sight of length r and specified by zenith angle θ and azimuth ϕ . This property is *not* independent of azimuth and is *not* the same for the designated path of sight and its reciprocal.

ϕ Symbol for azimuth. The azimuth is the angle in the horizontal plane of the observer between a fixed point and the path of sight. The fixed point may be, for example, true north, the bearing of the sun, or the bearing of the moon. This symbol is usually used as one of two coordinates to specify the direction of a path of sight.

ϕ' This symbol for azimuth is usually used as one of two coordinates to specify the direction of a discrete portion of the sky.

Ψ Angular solar radius at true earth-to-sun distance.

$\bar{\Psi}$ Angular solar radius at mean solar distance.

Ω Symbol for solid angle. For a hemisphere

$$\Omega = 2\pi \text{ steradians;}$$

for a sphere $\Omega = 4\pi \text{ steradians.}$

1. INTRODUCTION

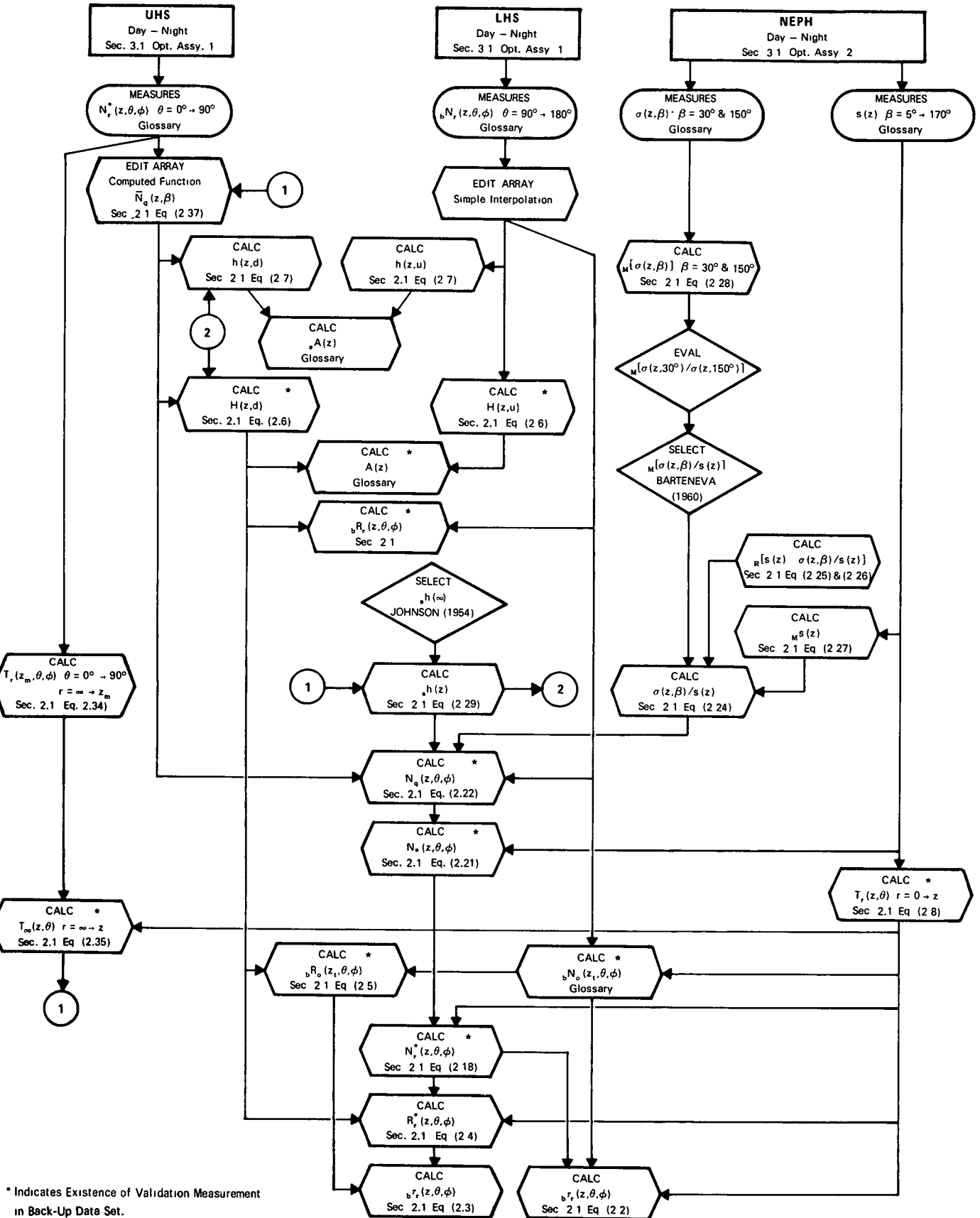
The field measurement program described in this report was organized under the project title METRO*. It was conducted during August 1971 in the area surrounding St. Louis, Missouri. The overall operation of this project was coordinated as a part of Air Force Cambridge Research Laboratory's Project 7621.

The METRO deployment was planned for the St. Louis area in August for several reasons. The turbid character of the heavy summer atmosphere in the vicinity of a densely urbanized population center was not available in our existing data bank. Since this class of atmosphere is typical of many modern environments, we felt it should be documented as promptly as possible. The Metropolitan Meteorological Experiment (METROMEX), Changnon *et al.* (1971), was being coordinated for the St. Louis area during the same summer interval, and the availability of a broad spectrum of coordinated measurements was an attractive inducement to participate. Not incidentally, Scott Air Force Base offered excellent support facilities for the project aircraft and ground-based data station.

The measurements obtained and the computations related to their use are examples of the Visibility Laboratory's continuing development of improved techniques for predicting, by calculation from physical data, the probabilities with which any object can be visually detected and recognized. The instrumental and computational organization for pursuing the development of these improved techniques is illustrated in Figures 1-1, 1-2, and 1-3. These three figures illustrate the experimental inter-relationships between the various pieces of project hardware, discussed in Section 3, the radiometric measurements made by them, and the subsequent computational chains accomplished in accordance with the theoretical considerations of Section 2. Through an examination of these generalized flow charts one can readily evaluate the experimental program's flexibility and self-checking redundancies. The capability to generate equivalent optical properties from separate and independent data sources, indicated in these figures, is the key feature in ensuring advancements in technical expertise and data quality.

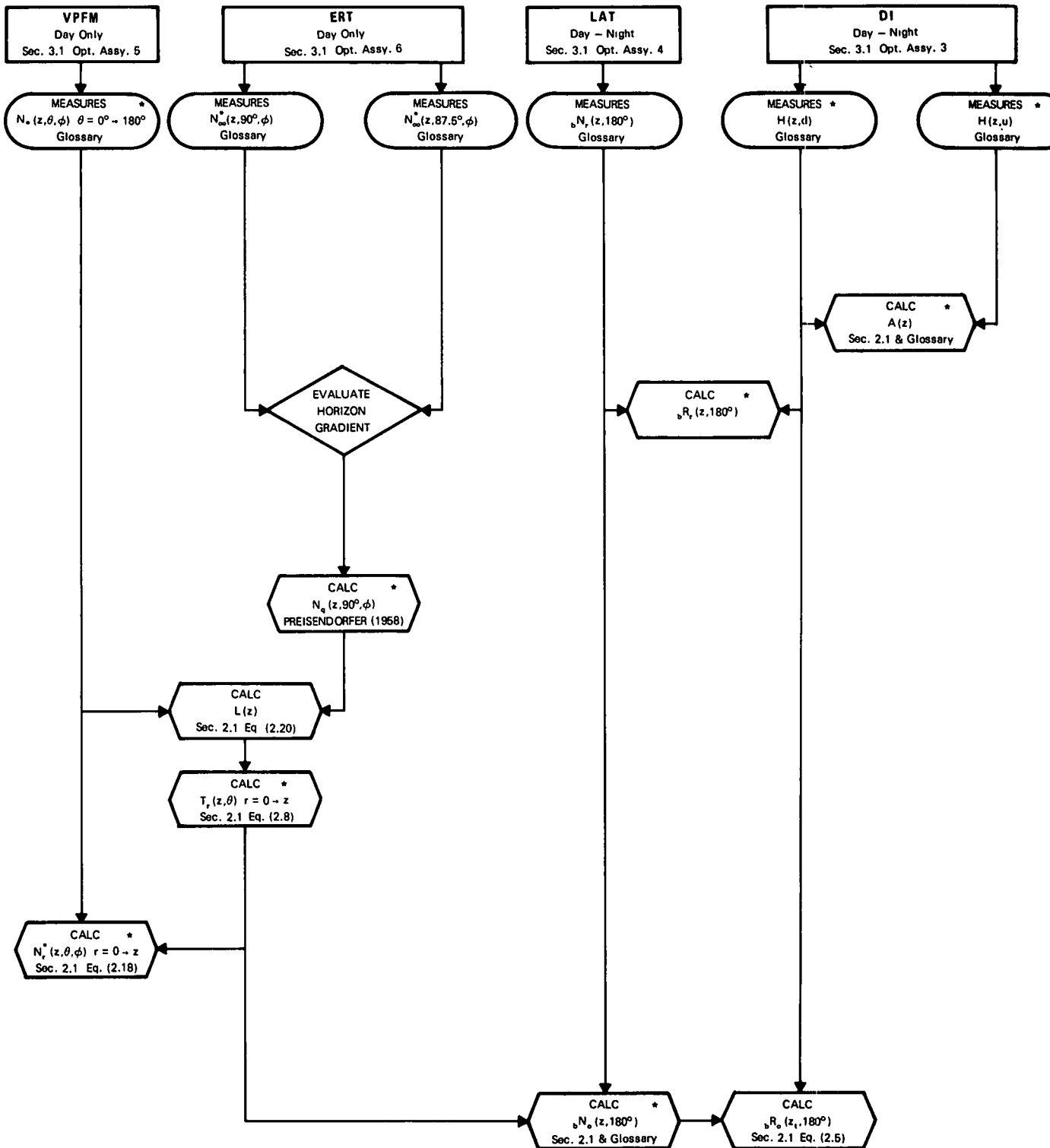
* The project title METRO has been assigned to this activity for procedural identification only and is not necessarily utilized or recognized by agencies or organizations outside the Visibility Laboratory. The relationship between this activity and other similar activities conducted by the Visibility Laboratory is well-illustrated in AFCRL-72-0593, "Airborne Measurements of Optical Atmospheric Properties, Summary and Review," Duntley *et al.* (1972c).

COMPUTATIONS FROM BASIC AIRBORNE DATA



* Indicates Existence of Validation Measurement in Back-Up Data Set.

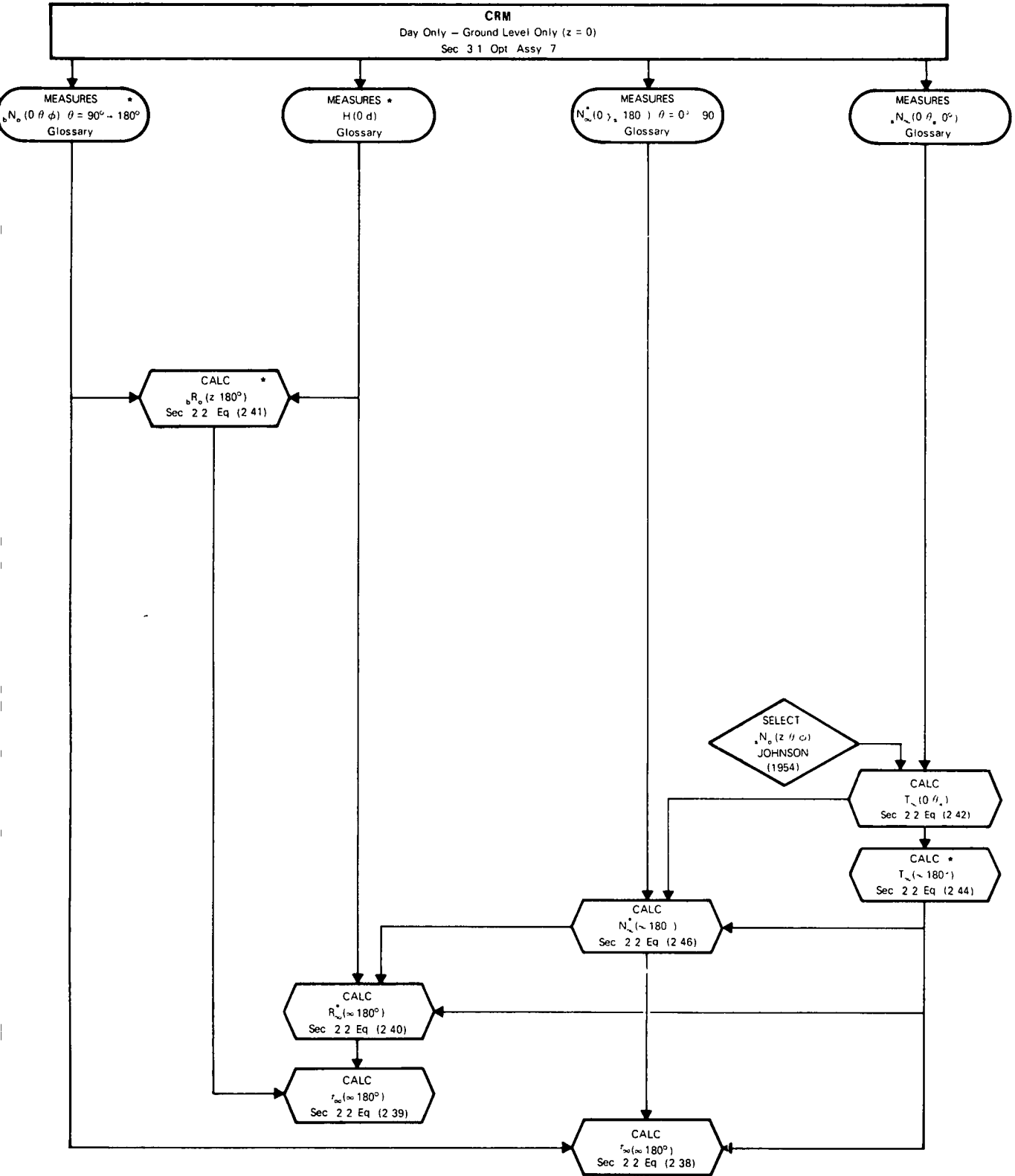
COMPUTATIONS FROM BACK-UP AIRBORNE DATA



* Indicates Utilization as Direct Validation of Computed Values.

Fig. 1-2. Computations From Backup Airborne Data.

COMPUTATIONS FROM SPECIALIZED GROUND DATA



* Indicates Utilization as Direct Validation of Computed Values

This report has been prepared under Contract No. F19628-73-C-0013. It is the second report issued which relates to the project METRO data. The first, Scientific Report No. 3, AFCRL-TR-73-0422, Duntley *et al.* (1973), was issued under the title "Airborne Measurements of Optical Atmospheric Properties in Southern Illinois."

This report, Scientific Report No. 4, also contains the optical properties of various downward-inclined paths of sight based upon daytime atmospheric optical measurements. These properties include natural irradiance upon horizontal plane surfaces, scalar irradiance, total volume scattering coefficient, atmospheric beam transmittance, path radiance, directional path reflectance, and directional terrain reflectance. The measurements were made along the flight tracks illustrated in Figure 1-4.

In addition, this report includes selected data from 11 sets of ground-based measurements. These ground-based measurements were made at Scott Air Force Base during the same general time interval that the aircraft was in operation along its flight track. They are restricted to ground-level scattering coefficient, downwelling irradiance, and terrain reflectance.

The methods used in the derivation of these optical properties are discussed in Section 2 and are similar to those presented in AFCRL-72-0255 and -0461, Duntley *et al.* (1972a and b). The most significant variation from earlier methods is in the computation of beam transmittance. For the data contained in this report, beam transmittance values for the path interval from space to the highest flight altitude are determined from sky radiance ratios in a manner suggested by Kushpil' and Petrova (1971).

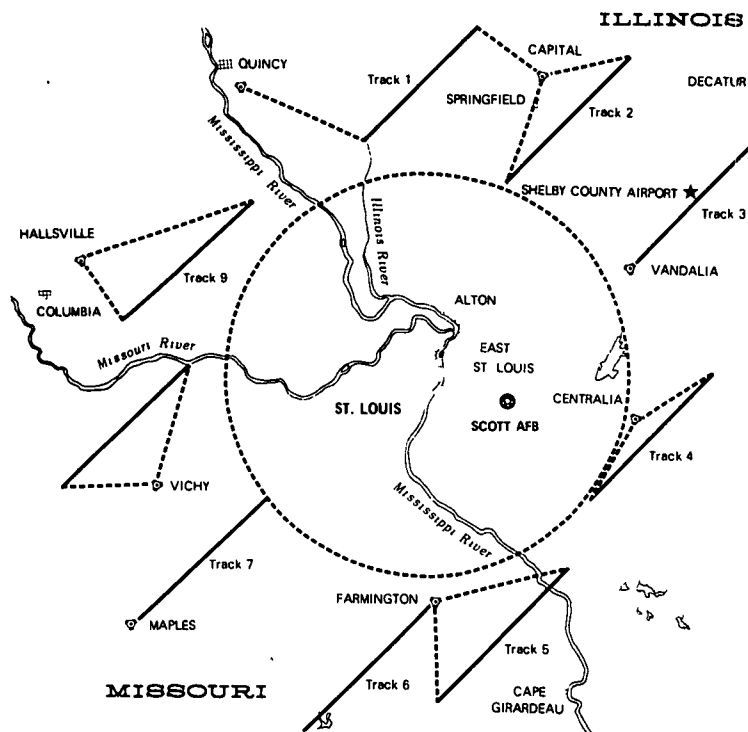


Fig. 1-4. Typical METRO Flight Tracks.

The optical instrumentation, developed at the Visibility Laboratory and installed in Air Force C-130A aircraft No. 50022, is reported in detail in Duntley *et al.* (1970). The instrumentation that generated the raw data upon which the reported properties are based consisted of an integrating nephelometer for determining the total scattering coefficient and two sky scanning radiometers for recording upper and lower sky radiances. A ground-based integrating nephelometer similar to the airborne instrument provided a ground-level value of the total volume scattering coefficient. Additionally, a ground-based scanning radiometer was used for the determination of downwelling irradiance and terrain reflectance. The radiometer spectral responses were standardized for the METRO deployment in the manner illustrated in Figure 1-5. A brief review of the instrumentation utilized during the METRO deployment is presented in Section 3.

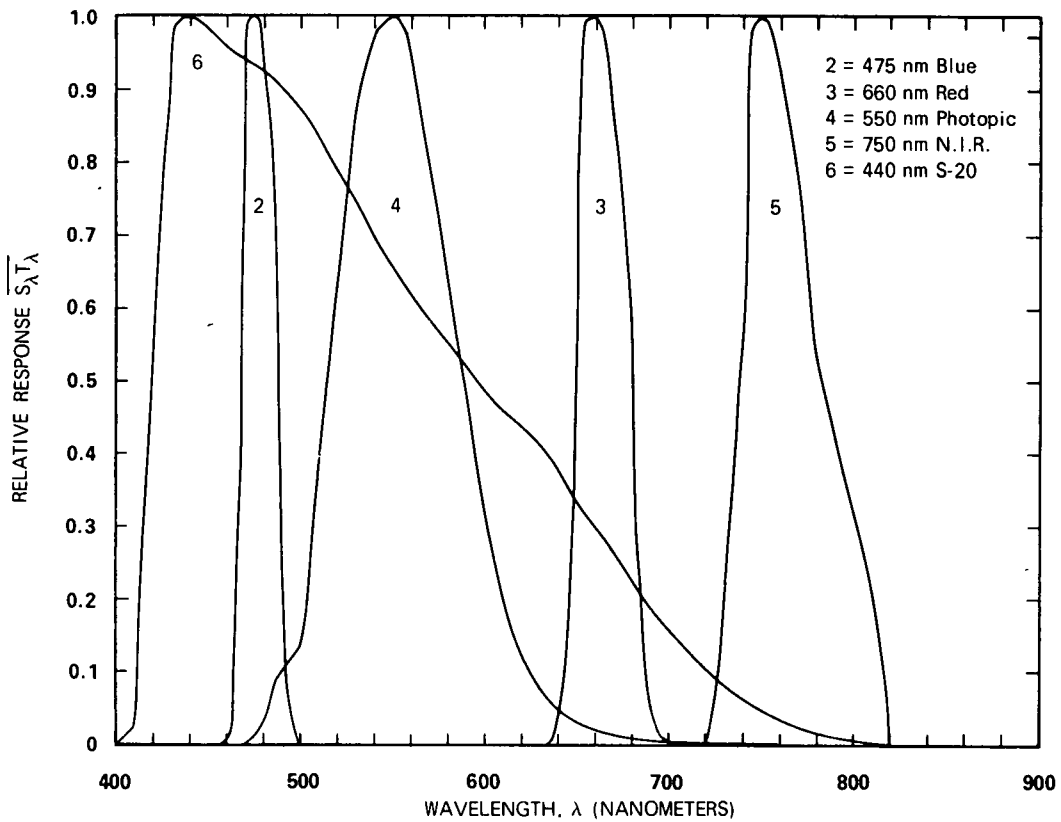


Fig. 1-5. Standard Spectral Responses – Project METRO.

Data collection methods are similar to those reported in AFCRL-72-0461, Duntley *et al.* (1972b). Although the first flight, C-180, was flown in accordance with the typical flight profile illustrated in Figure 4-1, all subsequent flights were modified to contain only three straight and level altitudes, with the highest at 10 000 feet (3050 meters) above ground level. All project METRO data flights were daytime flights. The basic features of these stylized flight profiles are summarized in Section 4.

The computer techniques used for processing the data included in this report are summarized in Section 5. They are, in general, the same as the techniques reported in AFCRL-72-0593, Duntley *et al.* (1972c).

A general discussion of the weather patterns that predominated in the St. Louis area during the data collection interval is presented in Section 6. This section, in conjunction with the flight track photographs shown in Section 7, is intended as an aid to the data user's generalized interpretation and evaluation. The inclusion of the graphical presentations is intended to further facilitate the user's rapid orientation with the overall weather situation.

The radiometric data representing four separate flights and containing six separate profiles are presented in Section 7, as is the ground-based data. The presentation format resembles that used in AFCRL-72-0461, Duntley *et al.* (1972b).

Discussion related to the interpretation and evaluation of the data herein is found in Section 8.

2. THEORY

2.1 CONTRAST TRANSMITTANCE IN THE TROPOSPHERE

Contrast transmittance ${}_b\tau_r(z, \theta, \phi)$ is defined as the ratio of the apparent contrast $C_r(z, \theta, \phi)$ to the inherent contrast $C_o(z_t, \theta, \phi)$:

$${}_b\tau_r(z, \theta, \phi) = C_r(z, \theta, \phi) / C_o(z_t, \theta, \phi). \quad (2.1)$$

The parenthetical modifiers indicate the altitude z of the sensor and the zenith angle θ and azimuth ϕ of the path of sight. In this report, ϕ will always be in terms of azimuth from light source (sun or moon). The path length r in the direction of the path of sight is between the altitude of the target z_t and the sensor altitude z . For the inherent contrast the path length is zero. The presubscript b on the contrast transmittance ${}_b\tau_r(z, \theta, \phi)$ indicates background. The contrast transmittance is a function of the inherent background radiance ${}_bN_o(z_t, \theta, \phi)$, the atmospheric beam transmittance $T_r(z, \theta)$, and the path radiance $N_r^*(z, \theta, \phi)$ of the path of sight as shown in Eq. 2.2 (Duntley (1964) Eq. 2.4):

$${}_b\tau_r(z, \theta, \phi) = [1 + N_r^*(z, \theta, \phi) / {}_bN_o(z_t, \theta, \phi) T_r(z, \theta)]^{-1}. \quad (2.2)$$

As noted in the glossary, beam transmittance is considered as being independent of azimuth, and thus its notation is typically simplified from the general form by omitting the azimuth designator ϕ .

DIRECTIONAL PATH REFLECTANCE

The concept of directional path reflectance (Duntley (1969) p. 3) is utilized in an alternate form of Eq. 2.2,

$${}_b\tau_r(z, \theta, \phi) = [1 + R_r^*(z, \theta, \phi) / {}_bR_o(z_t, \theta, \phi)]^{-1}, \quad (2.3)$$

where ${}_bR_o(z_t, \theta, \phi)$ is the directional background reflectance. By definition, the directional path reflectance is

$$R_r^*(z, \theta, \phi) = \pi N_r^*(z, \theta, \phi) / [H(z_t, d) T_r(z, \theta)] , \quad (2.4)$$

where $H(z_t, d)$ is the downwelling irradiance. We have chosen to present the atmospheric data in the form of directional path reflectance since, in this form, it can be easily utilized with the directional reflectance of a variety of backgrounds smaller in extent but different from the heterogeneous background which contributed to the path radiance and downwelling irradiance. The directional path reflectance is also the most convenient form of presenting the atmospheric data for easy use to obtain contrast transmittance.

BACKGROUND REFLECTANCE

The inherent background reflectance is defined as

$${}_bR_o(z_t, \theta, \phi) = \pi {}_bN_o(z_t, \theta, \phi) / H(z_t, d) , \quad (2.5)$$

where $H(z_t, d)$ is the downwelling irradiance at the target altitude (Gordon (1964) p. 558 or Boileau and Gordon (1966) p. 805). The inherent background reflectance may be obtained from either (1) a measurement by a ground-based telephotometer[†] or (2) measurements by an airborne telephotometer. In this report airborne telephotometer data from the lowest altitude of flight not extrapolated to ground level were used to obtain the terrain reflectances reported here for each flight.

DOWNWELLING AND UPWELLING IRRADIANCE

The downwelling irradiance used to compute the directional path reflectance $R_r^*(z, \theta, \phi)$ and the apparent terrain reflectance is computed from data at the lowest altitude of flight by the equation

$$H(z, d) = {}_s h(z) \cos \theta_s + \int_{2\pi} N(z, \theta', \phi') \cos \theta' d\Omega , \quad (2.6)$$

where ${}_s h(z)$ is the sun scalar irradiance at altitude z , θ_s is the sun zenith angle, and $N(z, \theta', \phi')$ is the sky radiance at direction θ', ϕ' .

[†] Although the measurements are radiometric as opposed to photometric, the instrument used to perform these measurements is referred to herein as a "telephotometer" in lieu of the more precise term "teleradiometer". This is in keeping with the practice established in previous publications.

The upwelling irradiance $H(z,u)$ is computed by deleting the first term in Eq. 2.6 and replacing the sky radiances with apparent terrain radiances from the lower hemisphere scanner. The θ' would then be the nadir angle so that $\cos\theta'$ is positive. The albedo $A(z)$ is the ratio of the upwelling to downwelling irradiance $H(z,u)/H(z,d)$.

A second type of irradiance is the scalar or nondirectional irradiance:

$$h(z,d) = {}_s h(z) + \int_{2\pi} N(z,\theta',\phi') d\Omega \quad (2.7)$$

The scalar irradiance is not weighted by the cosine. The upwelling irradiance from zenith angles between 90 and 180 degrees is designated by $h(z,u)$ and computed by using Eq. 2.7 without the first term. The total scalar irradiance is the sum of the upwelling and downwelling scalar irradiances, $h(z) = h(z,u) + h(z,d)$. The scalar albedo is defined as the ratio of upwelling to downwelling scalar irradiance, $h(z,u)/h(z,d)$. For a full discussion of scalar irradiances and scalar albedo uses refer to Gordon (1969).

BEAM TRANSMITTANCE

The beam transmittance $T_r(z,\theta)$ is obtained directly from the total scattering coefficient $s(z)$ by means of Eq. 2.8. (Refer also to Boileau (1964) p. 570.) When there is no significant atmospheric absorption in the passbands of the measurements, e.g., from smoke, dust, or smog, the attenuation coefficient $\alpha(z)$ is equivalent to the scattering coefficient $s(z)$. Therefore,

$$T_r(z,\theta) = \exp \left[- \sum_{i=1}^n \alpha(z_i) \Delta r \right] = \exp \left[- \sum_{i=1}^n s(z_i) \Delta r \right] \quad (2.8)$$

The incremental path length Δr used is 30 meters (98.4 feet). The measured total scattering coefficient data are extrapolated to ground level when no ground-based measurements are available. The extrapolation assumes that the scattering particles are the same at all altitudes, but decrease or increase according to the density at each altitude $\rho(z)$:

$$s(o) = \frac{s(z)\rho(o)}{\rho(z)} \quad (2.9)$$

Similarly, upward extrapolations are made to the highest reported altitude above ground level (6 kilometers maximum) when the highest flight altitude is less. Extrapolation in this case is based on the scattering coefficient measured at highest flight altitude. The densities used for the extrapolations are from the U. S. Standard Atmosphere (1962). The density at each altitude is obtained by truncated Chebyshev expansion using the coefficients for the atmosphere between 0 and 80 kilometers (U. S. Standard Atmosphere Supplements (1966) p. 69).

All altitudes reported are between ground level and 6 kilometers. For all paths of sight at zenith angles greater than 95 degrees, Δr equals $\Delta z \sec\theta$ for these altitudes. The Δr is always nonnegative since Δz is defined as $z_1 - z_2$ (the subscripts increase with the flux direction). See Fig. 2-1. For zenith angles greater than 95 degrees, the beam transmittance can also be expressed as a function of the vertical beam transmittance $T_r(z,180)$ as follows:

$$T_r(z,\theta) = T_r(z,180)^{|\sec\theta|} . \quad (2.10)$$

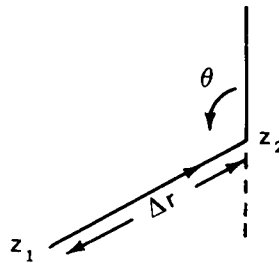


Fig. 2-1. Path Length Geometry for Steeply Inclined Paths of Sight.

ATTENUATION LENGTH

The attenuation length $L(z)$ is defined as the reciprocal of the atmospheric attenuation coefficient $\alpha(z)$. Therefore, when there is no significant absorption, it is also equivalent to the reciprocal of the atmospheric scattering coefficient:

$$L = \frac{1}{\alpha(z)} = \frac{1}{s(z)} . \quad (2.11)$$

The equivalent attenuation length $\bar{L}(z)$ is a pseudo-attenuation length which, when combined with its altitude z , can be used directly in the equation (Boileau (1964) Eq. 6.1)

$$T_r(z,\theta) = \exp[-z/\bar{L}(z)] \sec\theta, \quad (2.12)$$

where $\theta > 95^\circ$.

EARTH CURVATURE AND REFRACTION

For the paths of sight at 90 to 95 degree zenith angles, the Δr for $\Delta z = 30$ meters (98.4 feet) is significantly longer at ground level than at 6 kilometers due to the curvature of the earth. Therefore, for these paths of sight, the incremental path length Δr_i is computed from

$$\Delta r_i = \left\{ 1 - \left[\frac{n(z)}{n(z_1)} \frac{(\zeta + z)}{(\zeta + z_1)} \sin\theta \right]^2 \right\}^{-1/2} \Delta z . \quad (2.13)$$

This is the classical equation for computing incremental path length at paths of sight affected by earth curvature and refraction. The $n(z)$ is the refractive index, z is the sensor or observer altitude, ζ is the radius of the earth. Equation 2-13 was derived as follows. The Δr_i due to earth curvature is a function of the angle θ'' which is the angle of the flux path at altitude z_1 (see Fig. 2-2 for the relationship of θ and θ'' for the downward path of sight):

$$\Delta r_i = \sec\theta'' \Delta z = (1 - \sin^2\theta'')^{-1/2} \Delta z . \quad (2.14)$$

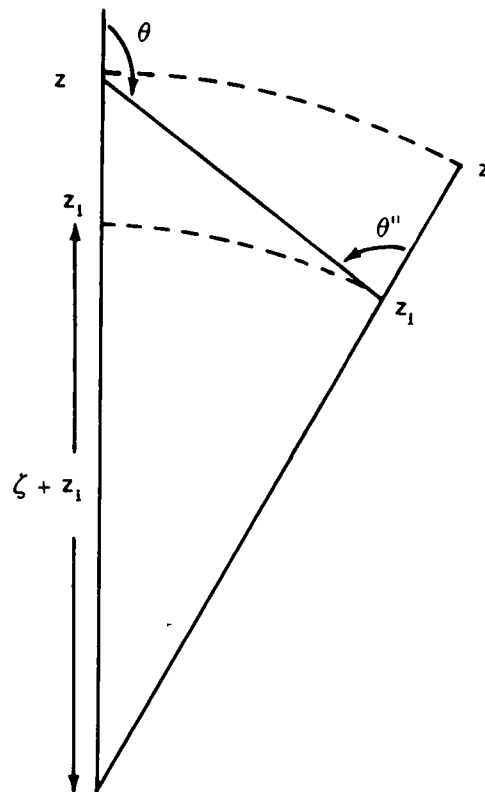


Fig. 2-2. Path Length Geometry for Grazing Paths of Sight in Refractive Spherical Atmospheres.

Since $\sin x = \sin(180^\circ - x)$, the law of sines can be used to express Δr as a function of the path of sight θ :

$$\sin\theta'' = \frac{\zeta + z}{\zeta + z_i} \sin\theta . \quad (2.15)$$

The refraction effect is added by recourse to Snell's law, thus resulting in Eq. 2.13.

The square of the refractive index ratio is given in an alternate form by Kasten (1965) as

$$\left[\frac{n(z)}{n(z_i)} \right]^2 = 1 + 2[n(z) - 1] [1 - \rho(z_i) / \rho(z)] . \quad (2.16)$$

This can be rewritten in terms of the refractive index at ground level $z = 0$ as follows:

$$\left[\frac{n(z)}{n(z_i)} \right]^2 = 1 + 2[n(0) - 1] \left[\frac{\rho(z)}{\rho(0)} - \frac{\rho(z_i)}{\rho(0)} \right] . \quad (2.17)$$

The density values for computing the refraction effect are, as before, based on the U. S. Standard Atmosphere (1962). The refractive index used for ground level was 1.000276, appropriate to a wavelength of 700 nanometers at 15 degrees centigrade. The maximum error in using the Δr based on 700 nanometers for wavelengths of 478 to 770 nanometers is 0.2 percent.

PATH RADIANCE

Path radiance $N_r^*(z, \theta, \phi)$ for the downward-looking path of sight is the integration or summation of the path function $N_*(z, \theta, \phi)$ weighted by the beam transmittance $T_{ri}(z, \theta)$. Path length r_i is from the incremental path Δr to the sensor at z :

$$N_r^*(z, \theta, \phi) = \sum_{i=1}^m N_*(z_i, \theta, \phi) T_{ri}(z, \theta) \Delta r . \quad (2.18)$$

Refer to Duntley *et al.* (1957) Eq. 17 on p. 502.

PATH FUNCTION

Image-forming light is lost by scattering and absorption in each elementary segment of the path of sight, and contrast-reducing path radiance is generated by the scattering of the ambient light which reaches the segment from all directions. The quantitative description of this scattered component of path-segment radiance involves a quantity called the "path function", $N_*(z, \theta, \phi)$. The "path function" depends upon the directional distribution of the lighting on the segment due to its surroundings. It can be operationally defined in terms of the (limiting) ratio of the path radiance associated with a short path to the path length by the relation (Duntley *et al.* (1957) p. 501)

$$N_*(z, \theta, \phi) = \lim (\Delta r \rightarrow 0) N_{\Delta r}^*(z, \theta, \phi) / \Delta r . \quad (2.19)$$

In experimental practice, the path length Δr should be sufficiently short so that no change in the ratio can be detected if Δr is made shorter.

In lieu of a direct measurement of path function, it may be derived from related quantities. Path function, attenuation length and equilibrium radiance are related by (Duntley *et al.* (1957) Eq. 11)

$$N_q(z, \theta, \phi) = N_*(z, \theta, \phi) L(z) . \quad (2.20)$$

By substituting Eq. 2.11 into Eq. 2.20 and rearranging, path function is expressed as a function of the total scattering coefficient and the equilibrium radiance :

$$N_*(z_i, \theta, \phi) = N_q(z_i, \theta, \phi) s(z_i) . \quad (2.21)$$

EQUILIBRIUM RADIANCE

The equilibrium radiance (Duntley *et al.* (1957) p. 502, and Gordon (1969) p. 15) is first computed from the measurements made at each of the altitudes of level flight and then interpolated and extrapolated to obtain values at each 30-meter (98.4-foot) interval z_i . Equilibrium radiance is interpolated rather than path function since the equilibrium radiance is relatively invariant with altitude, whereas path function is sensitive to changes in aerosol scattering as well as the lighting distribution. To compute the equilibrium radiance the following equation is used (refer to Gordon (1969), Eq. 16* on p. 16) :

* Equation 16 applies equally well to real and model atmospheres.

$$N_q(z, \theta, \phi) = {}_s h(z) \frac{\sigma(z, \beta)}{s(z)} + \int_{4\pi} N(z, \theta', \phi') \frac{\sigma(z, \beta')}{s(z)} d\Omega, \quad (2.22)$$

where ${}_s h(z)$ is the scalar irradiance of the sun (or full moon), β is the angle between the sun and the path of sight, and $N(z, \theta', \phi')$ is the apparent radiance of the sky or ground for direction θ' and ϕ' . The ratio $\sigma(z, \beta')/s(z)$ is the proportional directional scattering coefficient at angle β' and altitude z . The β' is the angle between the path of sight at θ, ϕ and the radiance θ', ϕ' . It is found by

$$\cos\beta' = \sin\theta \sin\phi \sin\theta' \sin\phi' + \sin\theta \cos\phi \sin\theta' \cos\phi' + \cos\theta \cos\theta' \quad (2.23)$$

It is the scalar irradiance which designates the flux that enters into the computations of equilibrium radiance and path function when the directional radiances are not known or used. It is the directionality of that flux combined with the directionality of the volume scattering function which produces the unique equilibrium radiance associated with each path of sight.

PROPORTIONAL DIRECTIONAL SCATTERING FUNCTION

The proportional directional scattering function is found by combining the Rayleigh scattering component and the Mie scattering component:

$$\sigma(z, \beta')/s(z) = \left\{ {}_R s(z) \left[\frac{\sigma(z, \beta')}{s(z)} \right] + {}_M s(z) \left[\frac{\sigma(z, \beta')}{s(z)} \right] \right\} / s(z). \quad (2.24)$$

The Rayleigh scattering coefficient ${}_R s(z)$ for each passband is based upon monochromatic values of Rayleigh volume scattering coefficient computed using the Penndorf (1957) Eq. 14 for 15 degrees centigrade sea level pressure. The Rayleigh scattering coefficient is corrected to ambient temperature and pressure by the ideal gas law equation. Since the Rayleigh scattering is a direct function of density,

$${}_R s(z) = {}_R s(0) P(z) / [T(z) 3.516E3], \quad (2.25)$$

where $P(z)$ is pressure in dynes cm^{-2} , $T(z)$ is temperature in degrees Kelvin, and $3.516E3^*$ has units of dynes $\text{cm}^{-2} \text{°K}^{-1}$ and is the density at standard sea level pressure and 15 degrees centigrade temperature times the universal gas constant. The proportional directional scattering function for Rayleigh scattering ${}_R[\sigma(\beta)/s]$ is not a function of altitude so the parenthetical modifier is not used. It is found by

* The form of 3.516E3 is an alternate format for 3.516×10^3 . This computer form is used throughout this report.

$${}_R[\sigma(\beta)/s] = (1 + \cos^2\beta)3/(16\pi) . \quad (2.26)$$

The Mie scattering coefficient at measurement altitude z is the measured scattering coefficient minus the Rayleigh coefficient computed from Eq. 2.25 above :

$${}_M s(z) = s(z) - {}_R s(z) . \quad (2.27)$$

The Mie volume scattering function ${}_M[\sigma(z,\beta)/s(z)]$ is taken from a catalog of values derived from data on photopic volume scattering functions published by Barteneva (1960) for a range of total scattering coefficients from near Rayleigh atmosphere to heavy fog. The Barteneva volume scattering functions show a good correlation with the ratio of directional scattering coefficients at scattering angles $\beta = 30^\circ$ and 150° : $({}_M[\sigma(z,30)/\sigma(z,150)])$. The Mie volume scattering functions at 30 and 150 degrees are obtained from the measured volume scattering function at 30 and 150 degrees by subtracting the Rayleigh component, as follows :

$${}_M\sigma(\beta) = \sigma(\beta) - {}_R s(z) {}_R[\sigma(\beta)/s] . \quad (2.28)$$

SUN IRRADIANCE

Although the scanner radiance measurements include a measure of the apparent sun radiance, that value is beyond the calibrated span of the instrument. Therefore, the sun irradiance used in the computations of the irradiance and the equilibrium radiance is based upon the sun irradiance out of the atmosphere ${}_s h(\infty)$ for the appropriate broadband filter and the beam transmittance from out of the atmosphere to altitude z , $T_\infty(z,\theta_s)$:

$${}_s h(z) = {}_s h(\infty) T_\infty(z,\theta_s) . \quad (2.29)$$

The sun irradiance values for mean solar distance ${}_s h(\bar{\infty})$ are computed from spectral sun irradiance from Johnson (1954). The sun irradiance at true solar distance ${}_s h(\infty)$ is equal to the irradiance at mean distance times the square of the ratio of the angular solar radius at true solar distance Ψ to the radius at mean distance $\bar{\Psi}$:

$${}_s h(\infty) = {}_s h(\bar{\infty}) \left(\frac{\Psi}{\bar{\Psi}} \right)^2 . \quad (2.30)$$

The angular solar radius at mean solar distance is 16.016 minutes of arc. The radii at true distance are obtained from the ephemeris for the appropriate date.

The transmittance from out of the atmosphere to the highest flight altitude is computed from the ratio of sky radiances at equivalent scattering angles from the sun. This method stems from the suggested nomographic method of Kushpil' and Petrova (1971) for obtaining beam transmittance from sky radiance ratios at equivalent scattering angles from the sun. Kushpil' and Petrova do not give equations for the sky radiance ratio as a function of beam transmittance, but such an equation is derived in the following paragraph.

A sky radiance is a path radiance from out of the atmosphere to the altitude of measurement $N_{\infty}^*(z, \theta, \phi)$. On clear days with no absorption, we have found the sky radiance to be a function of an effective equilibrium radiance \bar{N}_q and the beam transmittance (Gordon *et al.* (1963), Gordon (1969), and Gordon *et al.* (1973)):

$$N_{\infty}^*(z, \theta, \phi) = \bar{N}_q(z, \theta, \phi) [1 - T_{\infty}(z, \theta)] . \quad (2.31)$$

Thus the ratio of two sky radiances, at angles θ and θ' , would be

$$\frac{N_{\infty}^*(z, \theta, \phi)}{N_{\infty}^*(z, \theta', \phi')} = \frac{\bar{N}_q(z, \theta, \phi) [1 - T_{\infty}(z, \theta)]}{\bar{N}_q(z, \theta', \phi') [1 - T_{\infty}(z, \theta')]} . \quad (2.32)$$

When the scattering angle from the sun is equivalent for the two paths of sight, the equilibrium radiances are equivalent. Thus Eq. 2.32 simplifies to

$$\frac{N_{\infty}^*(z, \theta, \phi)}{N_{\infty}^*(z, \theta', \phi')} = \frac{[1 - T_{\infty}(z, \theta)]}{[1 - T_{\infty}(z, \theta')]} . \quad (2.33)$$

Equation 2.33 can be expressed as a function of the vertical transmittance $T(z, 0^\circ)$ and the relative optical airmass $m_{\infty}(z, \theta) / m_{\infty}(z, 0^\circ)$:

$$\frac{N_{\infty}^*(z, \theta, \phi)}{N_{\infty}^*(z, \theta', \phi')} = \frac{[1 - T_{\infty}(z, 0^\circ)^{m_{\infty}(z, \theta) / m_{\infty}(z, 0^\circ)}]}{[1 - T_{\infty}(z, 0^\circ)^{m_{\infty}(z, \theta') / m_{\infty}(z, 0^\circ)}]} \quad (2.34)$$

Equation 2.34 cannot be directly solved for the vertical transmittance, but by using iterative means, which is a simple task with a computer, a vertical transmittance is obtained which provides a solution to Eq. 2.34 within a tolerance of 0.1 percent.

An error analysis of the transmittance obtained by Eq. 2.34 indicates that the precision error difference of the two radiances is generally multiplied by a factor of between 1 and 2 for many zenith angle combinations. Thus, a series of measurements is used and the transmittances are averaged to enhance the reliability of the resultant transmittance. A validation of the sky radiance ratio method of obtaining beam transmittance was presented in Duntley *et al.* (1972c) Section 2.1.

The transmittance for the lower flight altitudes is the product of the transmittance from out of the atmosphere to the highest altitude $T_{\infty}(z_m, 0^\circ)$ and the transmittance between the two flight altitudes $T_r(z, 0^\circ)$:

$$T_{\infty}(z, 0^\circ) = T_{\infty}(z_m, 0^\circ) T_r(z, 0^\circ) . \quad (2.35)$$

The conversion from vertical transmittance to transmittance at the zenith angle of the sun is made using the relative airmass $m_{\infty}(z, \theta_s)/m_{\infty}(z, 0^\circ)$:

$$T_{\infty}(z, \theta_s) = T_{\infty}(z, 0^\circ)^{m_{\infty}(z, \theta_s)/m_{\infty}(z, 0^\circ)} . \quad (2.36)$$

The relative airmass equals $\sec\theta$ for $\theta_s \leq 70^\circ$ to an accuracy of 1 percent. Also, the relative airmass at altitudes up to 6 kilometers equals the relative airmass at sea level, $m_{\infty}(6, \theta_s)/m_{\infty}(6, 0^\circ) = m_{\infty}(0, \theta_s)/m_{\infty}(0, 0^\circ)$, to an accuracy of 1 percent for $\theta_s \leq 86^\circ$. Sea level relative airmass values from Kasten (1965) are used for $\theta_s 70 \rightarrow 86^\circ$.

The sun zenith angle θ_s changes during the flight interval. In order to reduce this source of variability in the resultant data, an average sun zenith angle for the flight is used in Eq. 2.36 as well as in computing the irradiance in Eq. 2.6 and the scattering angle β in Eq. 2.22.

SKY AND TERRAIN RADIANCE

The measurements of sky and terrain radiance include values which are questionable due to: slow phototube decay after sensing high radiances; portions of the airplane such as tail or propellers extending into path of sight; values above or below the calibrated range of the sensor; and premature ending of the spiral angular pattern. In order to obtain a basic data array of optimum quality, these well-defined but improper values must be removed. To do this, the upper and lower hemisphere data arrays are handled separately, and in the following manner.

Since the terrain radiances have a relatively narrow range, questionable values are simply replaced by interpolations between adjacent valid data points.

In order to evaluate and replace the questionable sky radiance measurements, the effective equilibrium radiance as a function of angle from sun β is established on the basis of the sky radiance measurements $N_{\infty}^*(z, \theta, \phi)$ of known validity. The effective equilibrium radiance \bar{N}_q is computed by rearranging Eq. 2.31 as follows:

$$\bar{N}_q(z, \beta) = N_{\infty}^*(z, \theta, \phi) / [1 - T_{\infty}(z, \theta)] . \quad (2.37)$$

An average effective equilibrium radiance for each 5 degrees of β is then calculated and the proportional standard deviation from that average function established. The value of the average effective equilibrium radiance at $\beta = 0^\circ$ is determined using Barteneva's method of assuming $\log \bar{N}_q(\beta)$ linear with $\cos\beta$ for small values of β . All sky radiance measurements including the questionable measurements are tested to see if the $\bar{N}_q(\beta)$ resulting from use of Eq. 2.37 is within three standard deviations of the average equilibrium radiance function. All sky radiance values not meeting that test are replaced using the average equilibrium radiance function and Eq. 2.31.

2.2 GROUND-BASED MEASUREMENTS OF VERTICAL EARTH-TO-SPACE CONTRAST TRANSMITTANCE

The earth-to-space contrast transmittance for the vertical path of sight is found by rewriting Eq. 2.2 in terms of the earth-to-space path length ∞ and the vertical downward path of sight at zenith angle 180° :

$${}_b\tau_{\infty}(0, 180^\circ) = [1 + N_{\infty}^*(0, 180^\circ) / {}_bN_o(0, 180^\circ) T_{\infty}(0, 180^\circ)]^{-1} . \quad (2.38)$$

The azimuth ϕ has been deleted from the parenthetical modifiers of the path radiance $N_{\infty}^*(0, 180^\circ)$ and the inherent background radiance ${}_bN_o(0, 180^\circ)$ since ϕ is undefined when the path of sight is vertically downward.

DIRECTIONAL PATH REFLECTANCE

An alternate form for obtaining contrast transmittance is by use of the vertical path reflectance $R_{\infty}^*(0, 180^\circ)$. Thus, Eq. 2.3 is similarly rewritten,

$${}_b\tau_{\infty}(0, 180^\circ) = [1 + R_{\infty}^*(0, 180^\circ) / {}_bR_o(0, 180^\circ)]^{-1} . \quad (2.39)$$

Ground-based data are often presented in the form of vertical path reflectance for convenient use in obtaining contrast transmittance. The path reflectance may be used with the directional reflectance of various backgrounds which are smaller in extent but different from the heterogeneous background which contributes to the path radiance and downwelling irradiance $H(0, d)$. The vertical path reflectance is defined by

$$R_{\infty}^*(\infty, 180^\circ) = \pi N_{\infty}^*(\infty, 180^\circ) / H(0, d) T_{\infty}(\infty, 180^\circ) . \quad (2.40)$$

BACKGROUND REFLECTANCE

The inherent vertical background reflectance is defined as

$${}_bR_o(0,180^\circ) = \pi {}_bN_o(0,180^\circ) / H(0,d) . \quad (2.41)$$

Terrain radiances ${}_bN_o(z,\theta,\phi)$ are measured directly by orienting a contrast reduction meter (CRM) telescope toward the ground.

DOWNWELLING IRRADIANCE

Total downwelling irradiance $H(z,d)$ is measured directly by orienting a CRM assembly and its attached cosine collector cap in a horizontal position. In this position, the measurement represents total downwelling irradiance from the full 2π upper hemisphere on a flat plate, cosine-weighted collector.

BEAM TRANSMITTANCE

The beam transmittance for the path of sight from space to earth in the direction of the sun $T_\infty(0,\theta_s)$ is obtained directly from solar transmissometer measurements of the apparent radiance ${}_sN_\infty(0,\theta_s,0^\circ)$ at the center of the solar disk and from the inherent solar radiance[†] ${}_sN_o(\infty,\theta_s,0^\circ)$ by the following equation :

$$T_\infty(0,\theta_s) = \frac{{}_sN_\infty(0,\theta_s,0^\circ)}{{}_sN_o(\infty,\theta_s,0^\circ)} . \quad (2.42)$$

The vertical earth-to-space beam transmittance is equal to the vertical space-to-earth beam transmittance, and therefore Eq. 2.36 can be rewritten to obtain the vertical downward transmittance from the transmittance at the angle of the sun :

$$T_\infty(0,180^\circ) = T_\infty(0,0^\circ) = T_\infty(0,\theta_s)^{m_\infty(0,0^\circ) / m_\infty(0,\theta_s)} \quad (2.43)$$

For $\theta_s \leq 70^\circ$, the inverse of the relative airmass $m_\infty(0,0^\circ) / m_\infty(0,\theta_s) = \cos\theta_s$ to an accuracy of 1 percent. Since the solar elevation angle γ_s , which equals $90^\circ - \theta_s$, is read directly off of the ground-based equipment, Eq. 2-43 is rewritten as

$$T_\infty(\infty,180^\circ) = T_\infty(0,\theta_s)^{\sin \gamma_s} . \quad (2.44)$$

This eliminates the need for ephemeris or tabular data in the field in reducing data for $\theta_s \leq 70^\circ$.

[†] The values for inherent solar radiance at the center of the disk are based upon the solar irradiances out of the atmosphere from Johnson (1954).

For $\theta_s > 70^\circ$, the sea level relative airmass values $m_\infty(0, \theta_s) / m_\infty(0, 0^\circ)$ from Kasten (1965) are used. As noted before, for ground-level altitudes up to 6 kilometers, $m_\infty(6, \theta_s) / m_\infty(6, 0^\circ) = m_\infty(0, \theta_s) / m_\infty(0, 0^\circ)$ within 1 percent for $\theta_s \leq 86^\circ$.

PATH RADIANCE

The path radiance for the vertically downward path of sight is derived from an appropriate ground-based measurement of sky radiance and beam transmittance (Gordon *et al.* (1973) Eq. 8):

$$N_\infty^*(\infty, 180^\circ) = N_\infty^*(0, \theta', \phi') \left[\frac{1 - T_\infty(\infty, 180^\circ)}{1 - T_\infty(0, \theta')} \right] \quad (2.45)$$

where $N_\infty^*(0, \theta', \phi')$ is the path radiance of an upward-inclined path of sight at zenith angle θ' and azimuth ϕ' , which has the same angle β from the sun as does the vertically downward path of sight. This quantity is in fact the apparent sky radiance as measured from the surface of the earth in the direction θ', ϕ' . The $T_\infty(0, \theta')$ is the beam transmittance of the upward-inclined path of sight in the direction θ', ϕ' .

The scattering at 90 degrees from the sun is assumed to be reasonably equivalent to the scattering toward the vertically downward path of sight. This assumption simplifies the definition of the equivalent look-angle θ' to $90^\circ - \theta_s$, or simply γ_s , and ϕ' becomes 180° . See Fig. 2-3. The CRM illustrated in Fig. 3-2 is built to mechanically insure that the sky radiance is measured at a 90-degree angle from the sun. Equation 2.45 can now be rewritten as

$$N_\infty^*(\infty, 180^\circ) = N_\infty^*(0, \gamma_s, 180^\circ) \left[\frac{1 - T_\infty(\infty, 180^\circ)}{1 - T_\infty(0, \gamma_s)} \right] \quad (2.46)$$

When $\gamma_s \leq 70^\circ$, the transmittance for the upward inclined path at θ' is

$$T_\infty(0, \gamma_s) = T_\infty(0, 0^\circ)^{\sec \gamma_s} \quad (2.47)$$

For $\gamma_s > 70^\circ$, the relative optical airmass from Kasten (1965) is used instead of $\sec \gamma_s$ in Eq. 2.47.

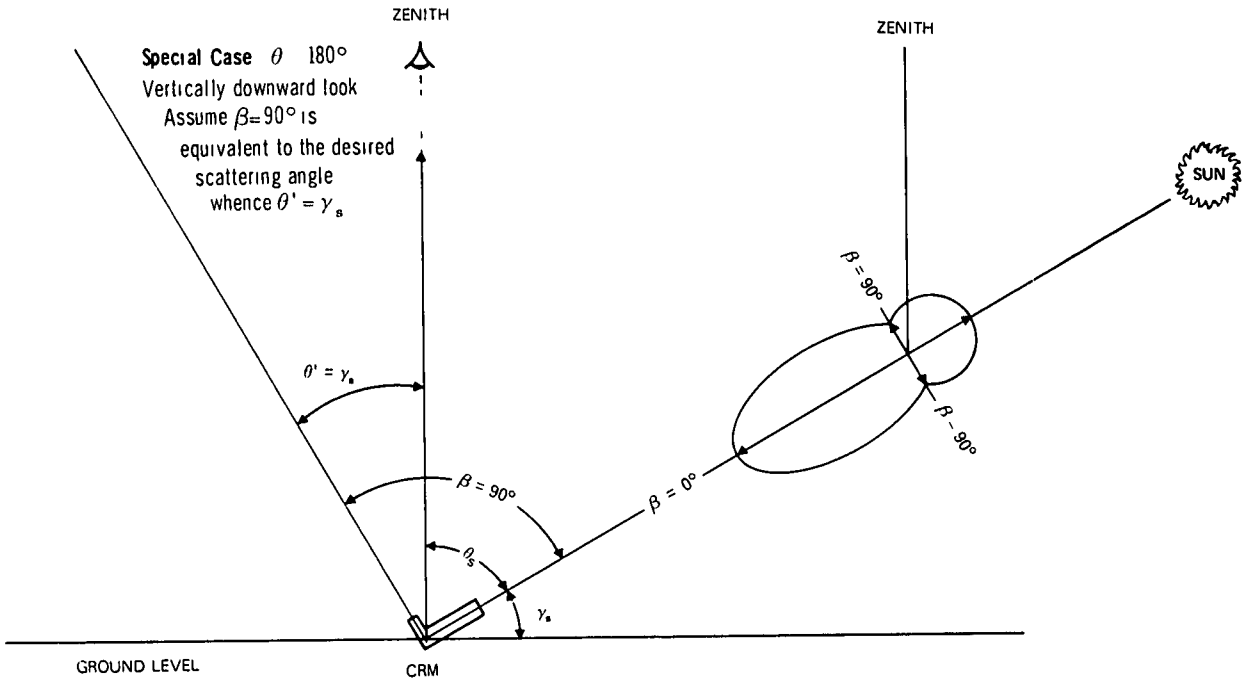


Fig. 2-3. Scattering Angle Relationships for Typical CRM Operations.

3. INSTRUMENTATION

The scientific instrumentation utilized for the Project METRO task was basically the same as that reported in AFCRL-72-0593, Duntley *et al.* (1972c).

For convenience of the reader, all significant instrument systems assigned during the Project METRO exercise are tabulated in Table 3-1 and depicted in Fig. 3-1 and 3-2.

Table 3-1. Project METRO Instrumentation

- I. Radiometric
 - A. Multiplier Phototube Assembly
 - B. Temperature Control Housing Assembly
 - C. Optical Filter Assembly
 - D. Radiometer Measuring Circuit Assembly
 - E. Optical Collector Assembly
 1. Automatic 2π Scanner Assembly
 2. Integrating Nephelometer Mode Selector Head Subassembly
 3. Dual Irradiometer Assembly

4. Large Aperture Telescope Assembly
5. Variable Path Function Meter Assembly
6. Equilibrium Radiance Telephotometer
7. Contrast Reduction Meter

II. Meteorological

- A. Royco Model 220 Particle Counter
- B. Cambridge Model 137-C3 Aircraft Hygrometer System
- C. AN/AMQ-17 Aerograph Set
- D. Bourns Model 430/530 Absolute Pressure Transducer
- E. Bourns Model 509 Differential Pressure Transducer
- F. Bendix Model 566 Aspirated Hygrometer
- G. Science Associates Windspeed and Direction Set
- H. Taylor Model SMT-5-51 Aneroid Barometer

III. Control and Communication

- A. 2π Scanner Control Console
- B. Photometer Temperature Control Panel
- C. Optical Filter Control Panel
- D. Ten Slide Photometer Module
- E. Camera Control Panel
- F. Flight Dynamics Display Panel
- G. 42 Channel Data Logger
- H. 20 Channel Data Logger

IV. Photographic

- A. Airborne Automax G-1 Camera System
- B. Ground-Based Soligor System

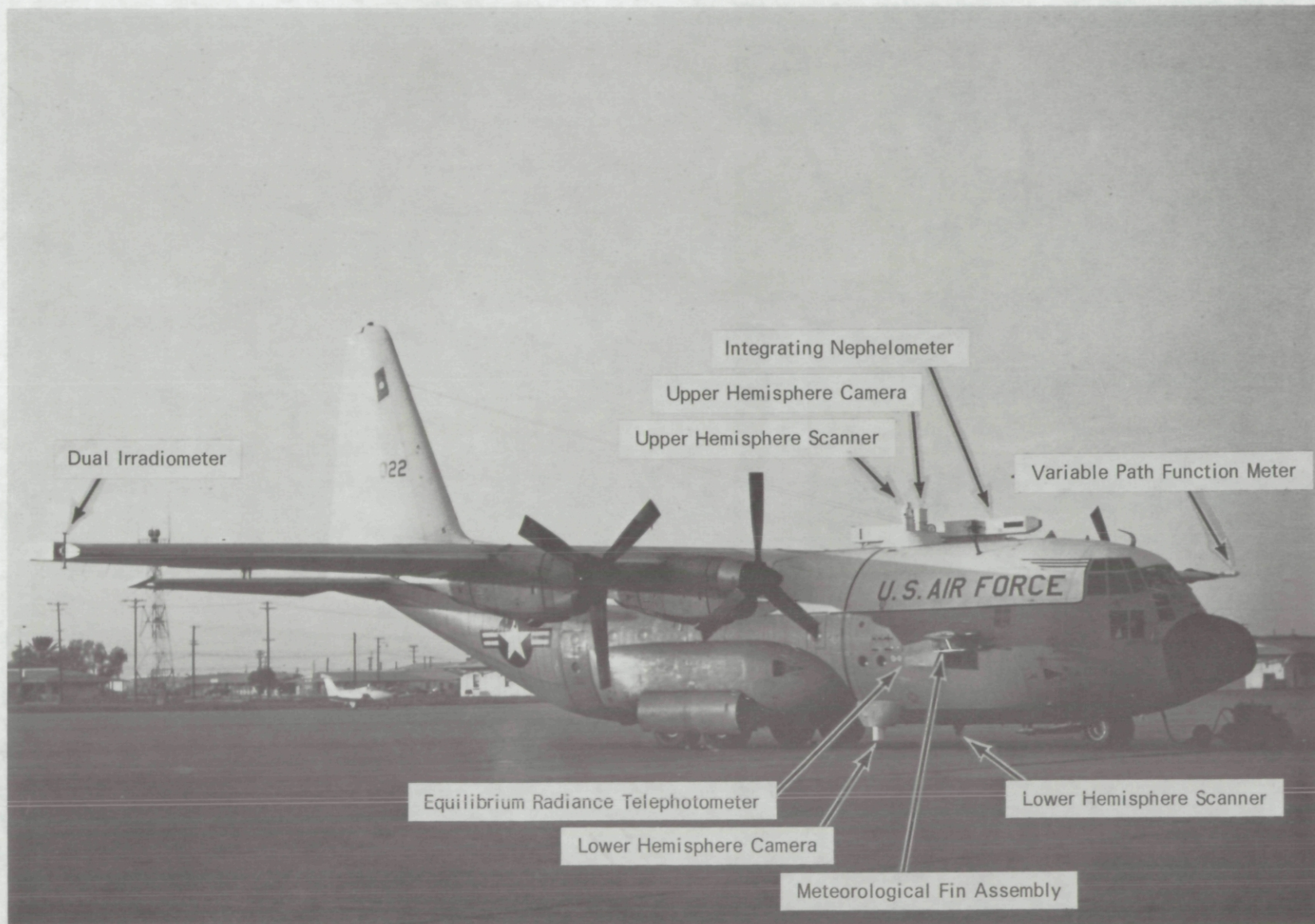


Fig. 3-1. C-130 Airborne Instrument System.

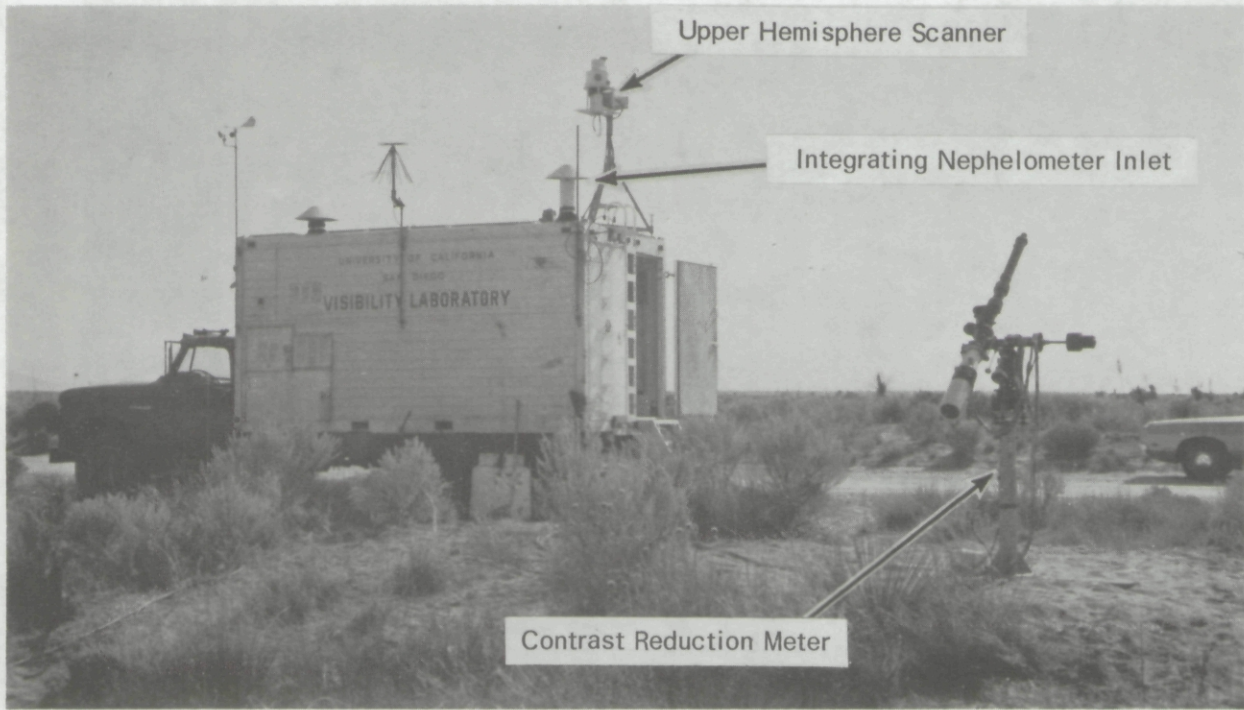


Fig. 3-2. Ground-Based Instrument System.

3.1 RADIOMETRIC SYSTEMS

A standardized radiometer, typical of those used during this data collection interval, consists of five major assemblies as listed below.

1. Multiplier Phototube Assembly
2. Temperature Control Housing Assembly
3. Optical Filter Assembly
4. Radiometer Measuring Circuit Assembly
5. Optical Collector Assembly

These assemblies are generally interchangeable between different radiometer systems, allowing easy field cannibalization in the event of a catastrophic failure of any assembly within a key system. For use in Project METRO, these five assemblies are unchanged from the configuration reported in AFCRL-72-0461, Duntley *et al.* (1972b).

OPTICAL COLLECTOR ASSEMBLIES

Seven basic collector assemblies were used in combination with the basic detector configurations described in AFCRL-72-0461, Duntley *et al.* (1972b). The only major differences between the various radiometer systems described in this report are the differences in these seven collector assemblies. The basic assembly differences are summarized in the following paragraphs.

The first five items discussed below were described in Duntley *et al.*, AFCRL-70-0137 (1970) and AFCRL-72-0255 (1972a). The last two items were discussed in AFCRL-72-0461, Duntley *et al.* (1972b). For more comprehensive information regarding the characteristics of these devices the reader is referred to these readily available sources.

Automatic 2 π Scanner Assembly (UHS and LHS). This collector assembly is essentially a small telescope that can be directed to optically scan any point within a 2π steradian field of view. The telescope itself has a 5-degree field of view. For the METRO mission, the airborne scanners were directed in a spiral pattern which covered the full hemisphere in 160 seconds. The output is converted to an array of radiance values at selected azimuth and elevation angles, such that Δ azimuth = 6° and Δ elevation = 5° between adjacent array elements.

Integrating Nephelometer Assembly (NEPH). In order to measure and evaluate the total scattering coefficient of typical real aerosols, the Visibility Laboratory has devised and built an instrument referred to as an integrating nephelometer. This device measures the radiant flux scattered from the well-defined flux beam of a high-intensity projector. The scattered flux is collected through three different optical channels: two telescopes oriented to collect the flux scattered in the $\beta = 30^\circ$ and $\beta = 150^\circ$ directions, and one irradiator assembly oriented to collect the flux scattered between the scattering angles of $\beta = 5^\circ$ and $\beta = 170^\circ$. From these measurements, the directional scattering functions $\sigma(30)$ and $\sigma(150)$ and the total volume scattering coefficient s may be derived.

Dual Irradiometer Assembly (DI). The dual irradiator assembly is a two channel irradiator. It has two optical input channels but only one optical output. A rotating prism subassembly allows the system operator to select either input channel for optical coupling with the output channel, while simultaneously occulting the other. The resultant time-sharing of a single detector assembly yields a device optimized for ratio type measurements.

The flat plate diffuse collector surfaces used in this assembly are mechanically corrected to yield a cosine collection characteristic within ± 2 percent for all angles of incidence between 0 and 80 degrees.

The dual irradiator assembly is mounted in the aircraft wingtip so that the flat plate collectors are horizontal. In this configuration the upper channel receives radiant flux from the entire hemisphere above the aircraft, and the lower channel receives radiant flux from the entire hemisphere below the aircraft. These measurements of downwelling and upwelling irradiance can be used both in the calculation of directional terrain reflectances and in intersystem data validation checks.

Large Aperture Telescope Assembly (LAT). This telescope assembly is used in the radiometer system which functions as a backup system for measuring very low flux levels. The airborne telescope assembly has a 5-degree circular field of view and an objective lens 6.2 centimeters in diameter. With

this larger collection aperture, flux levels significantly lower than the detection threshold of the 2π scanner assembly can be reached and adequately measured. This system was not deployed during Project METRO.

Variable Path Function Meter (VPFM). The variable path function meter is a radiometer and shroud assembly designed to measure the radiant flux scattered by a small, well-defined volume of aerosol into a given direction when illuminated from all directions. The scattering volume is 1.27 centimeters in diameter and 22.9 centimeters long. It is defined by the cylindrically-limited field of view of the component telephotometer and by two long cylindrical sunshades. Measurements of path function can be made at zenith angles between 0 and 180 degrees at azimuths corresponding to the aircraft heading.

Equilibrium Radiance Telephotometer (ERT). The concept of equilibrium radiance is defined and discussed in Duntley *et al.* (1957). In the special case of a horizontal path of sight which is optically uniform in terms of both the composition of the aerosol and its lighting, the equilibrium radiance is equal to the horizon radiance. It is this horizon radiance which is measured by the ERT.

The optical collector assembly is basically a servo-controlled telescope. Its field of view is 1.0 degrees wide and 0.2 degrees high. The ERT is oriented with a horizontal path of sight and with the wide dimension of the field of view parallel to the horizon. This orientation is maintained by use of a vertical reference gyro. At the discretion of the operator, a 2.5-degree step function can be superimposed on the normal reference signal. In this condition the path of sight is alternately directed horizontally and 2.5 degrees above horizontal. The radiance measurements made at these two zenith angles determine the near horizon radiance gradient.

Contrast Reduction Meter (CRM). The contrast reduction meter consists of a standard detector and filter changing assembly, fitted with a multiple purpose optical collector.

The function of the CRM is to measure apparent solar radiance, sky and terrain radiance, and downwelling irradiance, all with the same detector and measuring circuit. These measurements allow direct computation of earth-to-space universal contrast transmittance.

The optical collectors include a cosine collector for measuring the downwelling irradiance; a telescope with a 5-degree field of view for measuring sky and terrain radiances; and a Pinhole Gershun tube with a 2-minute field of view for measuring solar disk radiances.

3.2 METEOROLOGICAL SYSTEMS

All of the meteorological systems utilized in this project were purchased items. The operating characteristics of each are available in the appropriate manufacturer's brochures. For use in Project METRO, the meteorological systems are unchanged from the configurations reported in AFCRL-72-0461, Duntley *et al.* (1972b).

The airborne meteorological package consists of one Royco model 220 particle counter, one Cambridge model 137-C3 aircraft hygrometer system, one AN/AMQ-17 aerograph set, and two Bourns aneroid pressure transducers. The Cambridge system did not perform adequately during Project METRO and thus no

dewpoint data are available. Also, the AN/AMQ-17 pressure channel failed, resulting in the backup Bourns channel being used for altitude determinations.

The ground-based meteorological package was less extensive, consisting only of one Royco model 220 particle counter, one Bendix model 566 aspirated hygrometer, one Science Associates windspeed and direction set, and one Taylor model SMT-5-51 aneroid barometer.

Since all of the meteorological systems were described in AFCRL-72-0255, Duntley *et al.* (1972a), no further discussion is included in this report.

3.3 CONTROL AND COMMUNICATION SYSTEMS

The control panels, consoles, and other support facilities listed in Table 3-1 are described fully in AFCRL-70-0137, Duntley *et al.* (1970), and are not discussed further in this report.

No significant modifications from the updated configurations, reported in AFCRL-72-0593, Duntley *et al.* (1972c), have been accomplished on any of the control and communication systems.

3.4 PHOTOGRAPHIC SYSTEMS

Photographic documentation of the experimental environment performed simultaneously with the radiometric and meteorological measurements has always been a highly desirable adjunct to any field activity. For Project METRO, this photographic capability was accomplished through the use of two camera systems.

AIRBORNE AUTOMAX G-1 CAMERA SYSTEM

Two 35 millimeter Automax G-1 cameras, modified to accept Traid 735 Periphoto (180-degree) lenses, are mounted on the project aircraft (Fig. 3-1). One camera is oriented to photograph the 2π upper hemisphere and the other covers the 2π lower hemisphere. Either or both cameras may be run in either cine or single frame modes at the discretion of the operator.

The photographs from these cameras are used only as general background for the interpretation of the radiometric measurements. Thus, no special controls are placed upon the film or its processing. For this general purpose application, the cameras are normally loaded with Kodak Ektacolor Professional S, No. 5026 film. Typical photographs from this system are used as illustrations in Section 7 of this report and were shot with a fixed f6.3 aperture in the single frame mode.

GROUND-BASED SOLIGOR SYSTEM

The ground-site documentation photographs have historically been limited to 35 millimeter color snapshots, taken on a casual basis during lulls in the experimental sequences. For Project METRO this

procedure was supplemented with a scheduled routine of site photographs using a Soligor Conversion Fish-eye lens. This lens possesses almost universal adaptability to a wide variety of cameras and prime lenses. During Project METRO it was used on a Yashica, Lynx 1000.

3.5 RADIOMETRIC CALIBRATION PROCEDURES

All the radiometers used in this project are calibrated in essentially the same manner. In each case, the system is calibrated first by determining its relative flux versus high voltage characteristics over the anticipated operating span and second by establishing known absolute flux levels on this voltage curve. The entire calibration procedure is conducted using standard photometric practices, a 3-meter optical bench, and incandescent standards of luminous intensity traceable to the National Bureau of Standards.

A detailed discussion of these calibration procedures is contained in Duntley *et al.* (1970 and 1972a,b,c) and is, therefore, only summarized in this report.

LINEARITY CALIBRATION PROCEDURE

The process of establishing the relative flux versus high voltage characteristic curve for each system is simple and direct. The radiometer system is positioned on the optical bench and irradiated with flux from a stabilized incandescent lamp. The mechanical and optical arrangement is such that the amount of flux presented to the detector can be readily varied in increments of 0.10 log unit. The mechanical constraints on positioning the movable lamp housing ensure compliance with the desired inverse square relationship between lamp position and flux at the detector. Therefore, through an iterative process of relocating the lamp housing at a predetermined set of locations on the optical bench and recording the resulting radiometer output signal, one can generate a set of data illustrating the system electrical response to known changes of input radiance. This set of data is commonly referred to as the system linearity calibration.

The linearity calibrations for all radiometers employed in the Project METRO task extended over a radiance span of 5 log cycles. The electrical circuitry was adjusted to yield an output signal which swung from +250 to -1000 millivolts for this five-decade swing in radiant input. The pseudo-logarithmic characteristic of the radiometer measuring circuit results in a linearity calibration curve typified in Fig. 3-3.

ABSOLUTE CALIBRATION PROCEDURE

Once the linearity calibration for the radiometer system has been established, a similar procedure is followed to convert the calibration into absolute units. For this portion of the calibration sequence, an incandescent standard of luminous intensity is used as the flux source. Then absolute levels of irradiance can be presented to the radiometer either directly or via a calibrated reflectance standard.

Nine determinations of the calibration constant are made during each calibration run. The average value of the nine determinations is assumed to be the most probable value for the calibration constant. Due to precision limitations, stray light, and related procedural errors, typical standard deviations for the calibration constant are on the order of ± 2 percent. Table 3-2 illustrates the quality of typical calibration

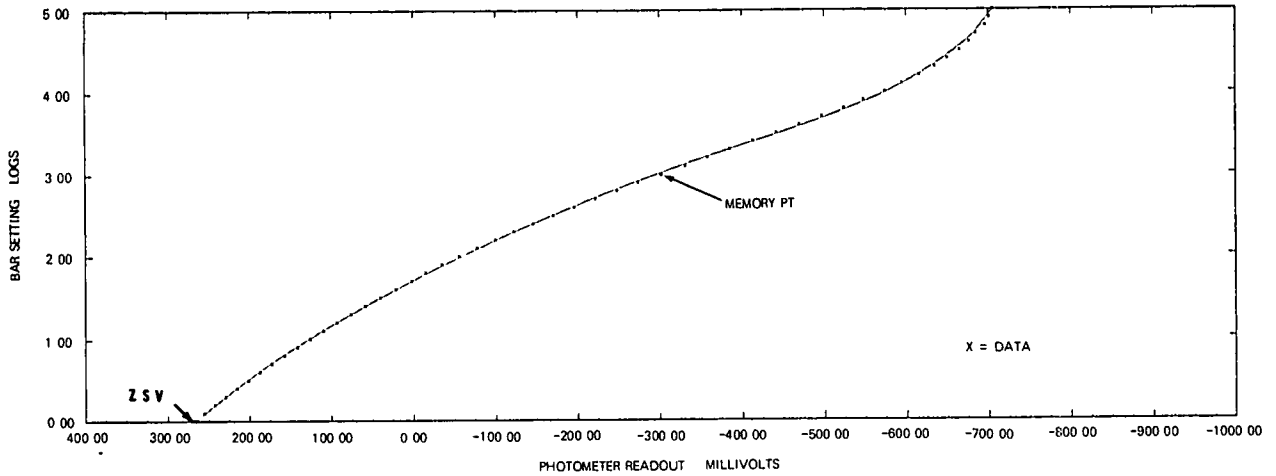


Fig. 3-3. Typical Computer-Generated Linearity Calibration Curve.

Table 3-2

Project METRO
Radiometer Calibration Constants (ZSV) and Related Fractional Standard Deviations ($\delta\%$) for Daylight Flights

Radiometer Ident		Calib Mode	Calib Units	Filter 2		Filter 3		Filter 4		Filter 5		Filter 6		Average % for System
System	MPT SN			ZSV	$\delta\%$	ZSV	$\delta\%$	ZSV	$\delta\%$	ZSV	$\delta\%$	ZSV	$\delta\%$	
SCAN3	9846	Night*	w/ $\Omega m^2 \mu m$	9.43E+04	± 1	1.27E+05	± 1	4.40E+04	± 1	2.48E+05	± 2	4.81E+03	± 1	± 1
SCAN4	9858	Night*	w/ $\Omega m^2 \mu m$	9.09E+03	± 1	1.35E+04	± 1	4.63E+03	± 1	2.56E+04	± 2	4.97E+02	± 1	± 1

NEPH1- Σ	9828	Night	w/m ² μm	1.47E-01	± 3	2.66E-01	± 3	6.88E-02	± 3	1.01E+00	± 2	8.97E-03	± 1	± 2
NEPH1- β	9828	Night	w/ $\Omega m^2 \mu m$	1.58E-01	± 1	3.67E-01	± 1	8.09E-02	± 1	2.70E+00	± 4	1.08E-02	± 1	± 2

D.I. 1	11783	Night*	w/m ² μm	6.72E+04	± 3	6.34E+04	± 3	2.46E+04	± 2	4.94E+04	± 2	2.82E+03	± 2	± 2
LAT 1	9869	N/A	-	-	-	-	-	-	-	-	-	-	-	

VPFM	14531	Night	w/ $\Omega m^2 \mu m$	2.31E+01	± 1	7.14E+01	± 1	6.95E+00	± 1	1.40E+03	± 4	9.61E-01	± 1	± 1
ERT	10697	Night*	w/ $\Omega m^2 \mu m$	8.47E+02	± 1	1.69E+03	± 1	4.62E+02	± 1	1.39E+03	± 3	9.31E+01	± 1	± 1

NEPH3- Σ	14509	Night	w/m ² μm	6.90E-02	± 3	8.69E-02	± 4	3.45E-02	± 5	1.07E-01	± 2	3.60E-03	± 2	± 3
NEPH3- β	14509	Night	w/ $\Omega m^2 \mu m$	6.68E-02	± 1	9.23E-02	± 1	3.15E-02	± 2	1.52E-01	± 1	3.82E-03	± 1	± 1

CRM/SS	9861	Night*	w/ $\Omega m^2 \mu m$	1.78E+04	± 1	3.13E+04	± 1	3.89E+03	± 1	2.09E+03	± 1	3.69E+02	± 1	± 1
CRM/E	9861	Night*	w/m ² μm	1.97E+05	± 2	2.85E+05	± 2	3.86E+04	± 1	1.74E+04	± 2	3.56E+03	± 1	± 2
CRM/STD	9861	***	w/ $\Omega m^2 \mu m$	1.88E+09	± 1	3.65E+09	± 1	4.68E+08	± 1	4.04E+08	± 1	4.09E+07	± 1	± 1

SCAN1	10650	Night*	w/ $\Omega m^2 \mu m$	2.96E+05	± 1	3.84E+05	± 1	1.26E+05	± 1	1.93E+05	± 2	1.21E+04	± 1	± 1
SCAN1/E	10650	***	w/m ² μm	4.18E+06	± 2	4.40E+06	± 1	1.56E+06	± 1	2.06E+06	± 1	1.47E+05	± 1	± 1

* Indicates that the basic night mode absolute calibration was adjusted for daylight using calibrated day/night neutral density filter.

*** Indirect field calibration using CRM/SS channel as reference.

constants associated with data tabulated in Section 7. It should be noted that the term "standard deviation" is not rigorously correct in this application since the calibration data set includes some obvious systematic errors due to detector dynamic response, as well as some procedural stray light errors. These systematic errors are not removed from the calibration data and, as a result, the standard deviation of the calibration constant determination represents a worst-case type of index.

It should also be noted that, in some cases, the basic calibration of the radiometer system is accomplished in the night mode. The conversion of the calibration constant to day mode, which allows calibrated measurements at daylight flux levels, is made by applying the day/night neutral density factor. Obviously, an error in the determination of this factor will also contribute to the overall probable error.

A typical data sheet for the absolute calibration of a Project METRO radiometer is shown in Fig. 3-4. Five different levels of input radiance are used in the determination of the calibration constant for the system. The calibration constant is referred to as the zero scale value and is labeled ZSV on the calibration forms.

```

ABSOLUTE CALIBRATION FOR  CRM/SS VITE 117A (9861  NS) DATE = 11OCT71 FOR SET POST MET FILTER NO. 2 DAY SKY 7000 DEG
INSTRUMENT TYPE          RADIOMETER

REFLECTANCE OF PATH ATTENUATOR =  5.0 PERCENT          REFLECTANCE OF CALIBRATION TARGET 96.0 PERCENT

D1 = LAMP POSITION = D1 + D2          D2 = 164.0 CM.
TOTAL DISTANCE = D1+D2

SPAN  ID      D1      TOTAL      TOTAL      CALC.TGT.  DETEC.  LOG      RAW      AV.      F1      F2      CORRECTED
ID      CM      DIST.     DIST.SQ.   CM.SQ.     B OR F   RAW     OF      ZSV      RAW      LUM. TO RAD.  COLOR  ZSV
          CM          CM          CM          CM          CM          OF      (K0/K)  ZSV      ZSV      WATTS/LUM.    MATCH
          CM          CM          CM          CM          CM          CM          CM          CM          CM          CM          CM          CM

1      40      204.000   4.162E 04   8.701E-06  -403    3.311   1.780E-02  1.771E-02  1.304E-04  9.765E-01  2.256E-06
2      70      234.000   5.476E 04   6.613E-06  -443    3.427   1.768E-02
3      120     284.000   8.066E 04   4.490E-06  -501    3.592   1.754E-02
4      200     364.000   1.325E 05   2.733E-06  -578    3.809   1.762E-02
5      300     464.000   2.153E 05   1.692E-06  -652    4.025   1.780E-02
3      40      204.000   4.162E 04   8.701E-06  -403    3.311   1.780E-02
4      200     364.000   1.325E 05   2.733E-06  -578    3.810   1.763E-02
3      120     284.000   8.066E 04   4.490E-06  -503    3.597   1.777E-02
2      70      234.000   5.476E 04   6.613E-06  -443    3.429   1.774E-02
1      40      204.000   4.162E 04   8.701E-06  -403    3.311   1.782E-02

          RADIOMETER UNITS
CALCULATED TARGET LUMINANCE EXPRESSED AS LUMENS/STERADIAN SQ. CM.
CORRECTED ZERO SCALE VALUE IS 2.2557E-06 WATTS/STERADIAN SQ. CM.
TO CHNGE POSTLOC3 FLT 2 FROM(W/SR SQ.CM)TO(W/SR SQ.M PICK) MULTIPLY BY 5.03100E 05
WITH ABOVE UNIT CONVERSION APPLIED, NEW ZSV IS 1.13484E 00 WATTS/STER. SQ M MICRO M.

STANDARD DEVIATION = 9.9628E-05
FRACTIONAL STANDARD DEVIATION = .96 PERCENT

COMPONENTS OF FILTER FACTORS F1 AND F2 ARE
680YBARSUM= 2.6874E 07  WESTSTD= 3.5090E 03  WSTSTD= 4.100E- 06  WESTINST= 3.6930E 03  WSTINST= 4.4240E 06

CALIBRATION LAMP IDENTIFICATION
SERIAL NUMBER = VL40201
LUMINOUS INTENSITY = 23.70
DISTRIBUTION TEMPERATURE = 2854

IF MILLIVOLT DATA IS LESS THAN THE END OF RULF CUTOFF = -765.0 IGNORE DATA

```

Fig. 3-4. Typical Absolute Calibration Form.

All procedural and precision uncertainties are, of course, independent of the absolute accuracy of the standard lamp calibration, which is assumed to be ± 3 percent.

At regular intervals during the calibration procedure, the radiometer is automatically exposed to its internal reference source, i.e., Isolite standard of luminous intensity. Since this integral, exceptionally stable source is always available for reinspection by the radiometer during subsequent measurement activities, the long term stability of the detector can be monitored and, when necessary, automatic adjustments to the calibration constant can be readily effected.

CALIBRATION CORRECTION FACTORS

Several calibration correction factors are used with the calibration data illustrated in Fig. 3-4 to generate the calibration constants listed in Table 3-2. In general, the factors are used at will to convert radiometric units into photometric units and reconvert them, and to adjust the value of measurements taken with an instrument having a nearly standard spectral response to the value that would have been obtained using the exact standard spectral response specified in Section 3.6.

These correction factors are discussed at length in AFCRL-70-0137 and AFCRL-72-0461, Duntley *et al.* (1970 and 1972b). Thus, they are only summarized here as Table 3-3.

Table 3-3

Calibration Correction Factor Summary

Factor Designator	Operational Identification	Defining Equations
F1	luminance-to-radiance conversion (lumens to watts)	$F1 = \frac{\sum_c W_{\lambda} \epsilon_{\lambda} (\overline{S_{\lambda} T_{\lambda}}) \Delta \lambda}{680 \sum_c W_{\lambda} \epsilon_{\lambda} \bar{y} \Delta \lambda}$
F2	color-matching adjustment (dimensionless)	$F2 = \frac{\sum W'_{\lambda} (\overline{S_{\lambda} T_{\lambda}}) \Delta \lambda}{\sum W'_{\lambda} (S_{\lambda} T_{\lambda}) \Delta \lambda} \times \frac{\sum_c W_{\lambda} \epsilon_{\lambda} (S_{\lambda} T_{\lambda}) \Delta \lambda}{\sum_c W_{\lambda} \epsilon_{\lambda} (\overline{S_{\lambda} T_{\lambda}}) \Delta \lambda}$
F3	unit conversion (watts/cm ² to watts/m ² μm)	$F3 = \frac{10^4}{\delta \lambda} = \frac{10^4}{\sum (\overline{S_{\lambda} T_{\lambda}}) \Delta \lambda}$
F4	photometric reconversion (watts/m ² μm to lu/m ²)	$F4 = \frac{680 \sum W_{\lambda} \bar{y} \Delta \lambda \delta \lambda 10^{-3}}{\sum W'_{\lambda} (\overline{S_{\lambda} T_{\lambda}}) \Delta \lambda}$
<p>Where W_{λ} = the known spectral emittance of the standard lamp used as a calibration source.</p> <p>W'_{λ} = the approximate spectral emittance of the field scene anticipated for later measurement.</p>		

The four correction factors shown in Table 3-3 are calculated in Program SUPERCK6. Several key factors generated by Program SUPERCK6 for use with the METRO data are listed in Tables 3-4 and 3-5.

Table 3-4

Luminance-to-Radiance Conversion Factor, $c_{W\lambda} = 2854^\circ\text{K}$

Spectral Filter Identification					
Factor Designator	Filter 2 478 nm	Filter 3 664 nm	Filter 4 557 nm	Filter 5 765 nm	Filter 6 532 nm
F1 (w/lu)	1.306 E-04	6.958 E-04	1.052 E-03	1.492 E-03	2.111 E-03

Table 3-5

Radiance-to-Luminance Reconversion Factors, F4,
for Selected Typical Distribution Temperatures

Factor Designator	Distribution Temperature of Typical Data Scenes					
	4000°K	5500°K	7000°K	10 000°K	20 000°K	Night Sky
F4 (lu $\mu\text{m}/\text{w}$)	7.299E+01	7.222E+01	7.200E+01	7.195E+01	7.211E+01	6.834E+01

CALIBRATION SUMMARY

The pre-METRO calibration data are dated June–August 1971. The post-METRO calibration data are dated September–October 1971. A review of the data related to each calibration set has led to the selection of preferred calibration constants for application to all Project METRO field data. These preferred calibration constants are those presented in Table 3-2.

IN-FLIGHT CROSS-CALIBRATION CHECK

The Project METRO deployment was the first major series of data flights which incorporated the cross-calibration (X-CAL) data sequence. During this routine the automatic 2π scanners (UHS and LHS) and the equilibrium radiance telephotometer (ERT) are manually directed to look dead ahead and parallel to the aircraft flight axis. The aircraft is put into a nose-high climb attitude and it maintains this condition while the three forward-looking telephotometers simultaneously measure the radiance of the sky directly ahead of the aircraft.

By aiming the aircraft at a reasonably uniform portion of the sky in a direction away from the sun, one obtains a data set representing the simultaneous in-flight measurement of a common scene by three different radiometer systems. These data are automatically processed to validate or, if necessary, to evaluate a potential update of the system calibration constants prior to final data processing.

A summary of the upper and lower hemisphere scanner cross-calibration data is presented in Table 3-6. These ratios are not corrected or adjusted and thus represent direct in-flight absolute radiance measurements. The ratios indicate a moderate spectral mismatch between the two scanners, illustrated by the drift from 0.95 in the blue filter to 0.86 in the red. They also indicate a moderate mismatch in absolute level, i.e., all average values are less than 1.0. However, since this was an initial attempt at this flight procedure and since a major portion of the ratios fall within our anticipated ± 5 percent overall accuracy for each system, no calibration updates were made to the METRO data on the basis of the X-CAL ratios.

Table 3-6

UHS/LHS Radiance Ratios from X-CAL Sequences

Flight No.	Average Radiance Ratio: UHS/LHS		
	Filter 2 (Blue)	Filter 4 (Pseudo-Photopic)	Filter 3 (Red)
C-180	0.82	0.77	0.75
C-181	0.81	0.83	0.80
C-182A & B	1.02	0.95	0.91
C-183A & B	1.12	0.93	0.91
C-185A & B	0.94	0.82	0.74
C-186A & B	0.91	0.88	0.86
C-187A & B	0.96	0.94	0.91
C-188A & B	0.95	0.91	0.88
Overall	0.95	0.89	0.86

3.6 STANDARD RESPONSE CHARACTERISTICS FOR BROAD BAND SENSORS

All the radiometric instruments both ground-based and airborne used by the Atmospheric Visibility Branch are equipped with automatic filter changing assemblies. Thus, any one of five different spectral filters can be interposed into each instrument's optical path. The combination of the sensor sensitivity S_λ and the filter transmittance T_λ is the resultant sensitivity of the filtered phototube $S_\lambda T_\lambda$. The standard responses which each individual optical system attempts to duplicate are indicated as $\overline{S_\lambda T_\lambda}$.

PEAK WAVELENGTH

The peak or maximum value of the standard sensor response $\overline{S_\lambda T_\lambda}$ is used to normalize the response values. The wavelength of the maximum value of the standard response is called the "peak wavelength".

MEAN WAVELENGTH

The mean wavelength $\bar{\lambda}$ is defined as

$$\bar{\lambda} = \frac{\int_0^{\infty} \lambda \overline{S_\lambda T_\lambda} \Delta \lambda}{\int_0^{\infty} \overline{S_\lambda T_\lambda} \Delta \lambda}$$

The λ is the wavelength of the relative spectral response $\overline{S_\lambda T_\lambda}$.

RESPONSE AREA

The response area is the area under the normalized relative spectral response curve. It is equal to the width of the passband of a rectangular filter of equivalent area; hence, it is designated as $\delta\lambda$ and defined by $\delta\lambda = \int \overline{S_\lambda T_\lambda} \Delta \lambda$. The radiometric units of watts/m²μm are obtained from units of watts/m² by dividing by the response area $\delta\lambda$, in appropriate units.

A summary of the response characteristics of the standards for Project METRO is presented in Table 3-7. The first four columns give filter code, peak wavelength, mean wavelength, and response area. The values for inherent solar properties are in columns 5, 6, and 7 and the Rayleigh limits are in columns 8, 9, and 10. The table was produced by Program RAYLIMIT.

Table 3-7

Spectral Characteristics Summary for Project METRO

Spectral Characteristics for Project METRO				Inherent Sun Properties (Johnson)			Rayleigh Atmosphere Properties (15°C)		
Filter Code No.	Peak Wavelength (nm)	Mean Wavelength (nm)	Response Area (nm)	Irradiance (w/m ² μm)	Radiance (w/Ωm ² μm)		Attenuation Length (m)	Total Scattering Coefficient (Per m)	Vertical Beam Transmittance
					Average	Center			
2	475	478	19.9	2.14E+03	3.13E+07	4.07E+07	4.84E+04	2.07E-05	0.839
3	660	664	30.2	1.57E+03	2.30E+07	2.75E+07	1.86E+05	5.41E-06	0.955
5	750	765	50.4	1.23E+03	1.80E+07	2.10E+07	3.28E+05	3.03E-06	0.974
4	550	557	78.5	1.90E+03	2.78E+07	3.47E+07	8.93E+04	1.15E-05	0.907
6	440	532	183.5	1.91E+03	2.80E+07	3.55E+07	7.22E+04	1.64E-05	0.867
9	555	560	106.9	1.89E+03	2.77E+07	3.45E+07	9.22E+04	1.15E-05	0.907

RELATIVE SPECTRAL RESPONSE OF STANDARDS

The relative spectral response of a standard $S_{\lambda}T_{\lambda}$ curve is obtained by normalizing the curve values so that the maximum relative response is 1. Program RAYLIMIT checks to see if the input standard spectral response curve is normalized and renormalizes if necessary. It also interpolates to wavelength increments of 5 nanometers if the standard has been specified for only 10-nanometer increments. It is more reasonable to interpolate the relatively smooth response values than to ignore the fine spectral structure of the sun irradiance out of the atmosphere.

A graph of the relative spectral response of the standards used in Project METRO is presented in Fig. 1-5 and 3-5. In Fig. 3-5, which is the computer-generated plot from Program RAYLIMIT, a point is plotted for each 5 nanometers in wavelength, but an identifying symbol is printed on only every second point. The relative spectral response values are also presented in Table 3-8, from Program RAYLIMIT.

Fig. 3-5

Computer-Generated Plot of Standard Spectral Responses for Project METRO.

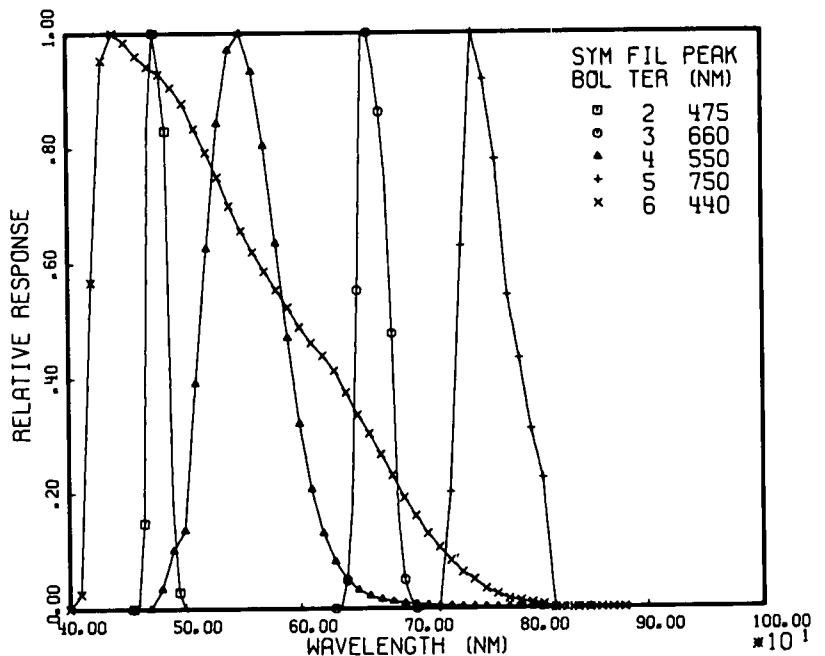


Table 3-8

Relative Spectral Response of Standards for Project METRO

Filter Identification and Mean Wavelength							Filter Identification and Mean Wavelength						
Wave-length (nm)	No. 2	No. 3	No. 4	No. 5	No. 6	No. 9	Wave-length (nm)	No. 2	No. 3	No. 4	No. 5	No. 6	No. 9
	Blue 478nm	Red 664nm	Pseudo- Photopic 557nm	NIR 765nm	S-20 532nm	True Photopic 560nm		Blue 478nm	Red 664nm	Pseudo- Photopic 557nm	NIR 765nm	S-20 532nm	True Photopic 560nm
400	0	0	0	0	0	0.0004	615	0	0	0.1680	0	0.4500	0.4412
405	0	0	0	0	0.0129	0.0006	620	0	0	0.1300	0	0.4390	0.3810
410	0	0	0	0	0.0258	0.0012	625	0	0	0.1055	0	0.4260	0.3210
415	0	0	0	0	0.2969	0.0022	630	0	0	0.0810	0	0.4130	0.2650
420	0	0	0	0	0.5680	0.0040	635	0	0.0020	0.0657	0	0.3935	0.2170
425	0	0	0	0	0.7605	0.0073	640	0	0.0486	0.0504	0	0.3740	0.1750
430	0	0	0	0	0.9530	0.0116	645	0	0.1798	0.0411	0	0.3545	0.1382
435	0	0	0	0	0.9765	0.0168	650	0	0.5531	0.0318	0	0.3350	0.1070
440	0	0	0	0	1.0000	0.0230	655	0	0.9948	0.0268	0	0.3190	0.0816
445	0	0	0	0	0.9920	0.0298	660	0	1.0000	0.0218	0	0.3030	0.0610
450	0	0	0	0	0.9840	0.0380	665	0	0.9421	0.0188	0	0.2845	0.0446
455	0	0	0	0	0.9720	0.0480	670	0	0.8625	0.0157	0	0.2660	0.0320
460	0.0070	0	0	0	0.9600	0.0600	675	0	0.7482	0.0139	0	0.2480	0.0232
465	0.1487	0	0	0	0.9510	0.0739	680	0	0.4774	0.0120	0	0.2300	0.0170
470	0.8481	0	0	0	0.9420	0.0910	685	0	0.1585	0.0105	0	0.2105	0.0119
475	1.0000	0	0.0172	0	0.9355	0.1126	690	0	0.0495	0.0090	0	0.1910	0.0082
480	0.9329	0	0.0343	0	0.9290	0.1390	695	0	0.0166	0.0080	0	0.1755	0.0057
485	0.8304	0	0.0677	0	0.9175	0.1693	700	0	0	0.0070	0	0.1600	0.0041
490	0.1790	0	0.1010	0	0.9060	0.2080	705	0	0	0.0061	0	0.1445	0.0029
495	0.0292	0	0.1185	0	0.8920	0.2586	710	0	0	0.0053	0	0.1290	0.0021
500	0	0	0.1360	0	0.8780	0.3230	715	0	0	0.0048	0	0.1170	0.0015
505	0	0	0.2635	0	0.8560	0.4073	720	0	0	0.0042	0	0.1050	0.0010
510	0	0	0.3910	0	0.8340	0.5030	725	0	0	0.0038	0.1005	0.0938	0.0007
515	0	0	0.5085	0	0.8135	0.6082	730	0	0	0.0033	0.2010	0.0826	0.0005
520	0	0	0.6260	0	0.7930	0.7100	735	0	0	0.0030	0.4155	0.0723	0.0004
525	0	0	0.7345	0	0.7715	0.7932	740	0	0	0.0026	0.6300	0.0619	0.0003
530	0	0	0.8430	0	0.7500	0.8620	745	0	0	0.0025	0.8150	0.0558	0.0002
535	0	0	0.9065	0	0.7250	0.9149	750	0	0	0.0023	1.0000	0.0497	0.0001
540	0	0	0.9700	0	0.7000	0.9540	755	0	0	0.0020	0.9595	0.0416	0.0001
545	0	0	0.9850	0	0.6785	0.9803	760	0	0	0.0018	0.9190	0.0335	0.0001
550	0	0	1.0000	0	0.6570	0.9950	765	0	0	0.0017	0.8495	0.0292	0
555	0	0	0.9665	0	0.6385	1.0002	770	0	0	0.0016	0.7800	0.0249	0
560	0	0	0.9330	0	0.6200	0.9950	775	0	0	0.0014	0.6620	0.0206	0
565	0	0	0.8685	0	0.6030	0.9786	780	0	0	0.0013	0.5440	0.0162	0
570	0	0	0.8040	0	0.5860	0.9520	785	0	0	0.0012	0.4890	0.0144	0
575	0	0	0.7195	0	0.5700	0.9154	790	0	0	0.0012	0.4340	0.0125	0
580	0	0	0.6350	0	0.5540	0.8700	795	0	0	0.0012	0.3720	0.0107	0
585	0	0	0.5525	0	0.5385	0.8163	800	0	0	0.0011	0.3100	0.0088	0
590	0	0	0.4700	0	0.5230	0.7570	805	0	0	0.0005	0.2675	0.0075	0
595	0	0	0.3950	0	0.5060	0.6949	810	0	0	0	0.2250	0.0062	0
600	0	0	0.3200	0	0.4890	0.6310	815	0	0	0	0.1125	0.0031	0
605	0	0	0.2630	0	0.4750	0.5668	820	0	0	0	0	0	0
610	0	0	0.2060	0	0.4610	0.5030							

4. DATA COLLECTION METHODS

During Project METRO, two independent activities were maintained simultaneously. The operation of the airborne instrument system was one activity and that of the ground-based instrument system was the other. The procedural routine was for each system to run full data collection sequences at every opportunity, on a daily schedule.

4.1 AIRBORNE SYSTEM

The data collection sequence for the airborne system was broken into five standardized elements: (1) preflight warmup and calibration check, (2) straight and level sequences, (3) vertical profile sequences, (4) in-flight calibration checks, and (5) post-flight calibration check.

The airborne data collection was accomplished through the use of an instrumented C-130A aircraft in a manner similar to that reported in AFCRL-70-0137, Duntley *et al.* (1970) and AFCRL-72-0593, Duntley *et al.* (1972c). During each data collection flight, the aircraft flew a predetermined pattern within the specified test area. An illustration of a typical flight pattern is shown in Fig. 4-1. In this stylized pattern, two basic elements, the straight and level and the vertical profile, are combined to yield the total mission flight plan. These two primary elements are summarized in the following paragraphs.

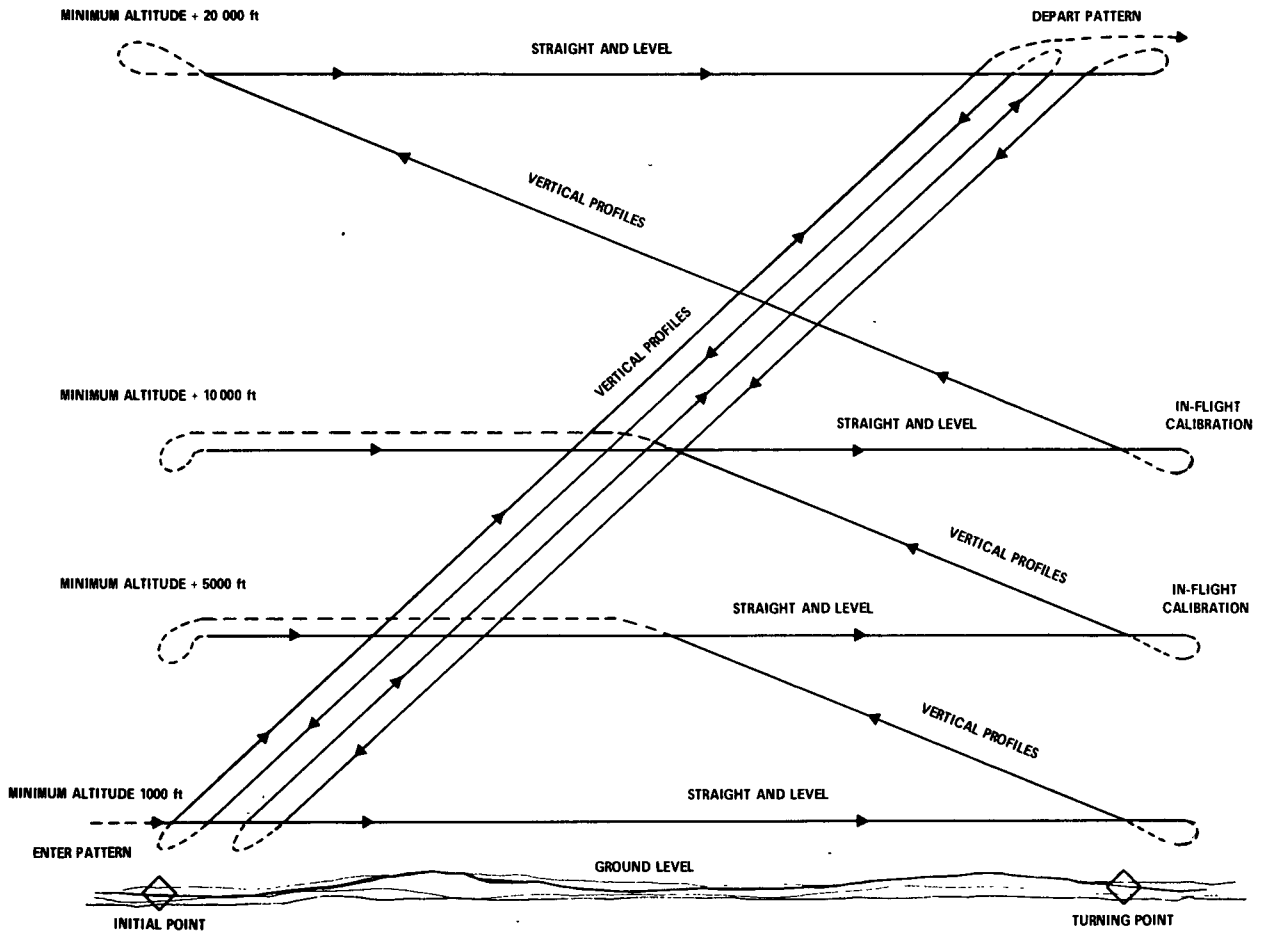


Fig. 4-1. Typical Visibility Laboratory Flight Profile.

STRAIGHT AND LEVEL SEQUENCE

During each straight and level element of the data collection sequence, the pilot maintains a straight and level flight attitude at a maximum indicated airspeed of 150 knots. If weather and terrain permit, the aircraft heading is established crosswind. The ideal pattern for the straight and level sequences would result in all four ground tracks falling on a single line between the initial point and the turn point. See Fig. 1-4. The four straight and level elements are actually stacked in a vertical slab of atmosphere approximately 45 miles long, 0.5 mile wide, and 4 miles high.

VERTICAL PROFILE SEQUENCE

During each vertical profile element of the data collection sequence, the pilot maintains an approximately level attitude, a straight heading, a maximum indicated airspeed of 150 knots, and an average rate of descent or ascent of 1000 feet per minute. Up to five vertical profile elements are run during each data collection sequence. These elements are conducted in the same vertical slab of atmosphere that was defined by the preceding four straight and level elements.

For Project METRO the typical flight profile illustrated in Fig. 4-1 was modified to include only three straight and level sequences. These three straight and levels were run at indicated altitudes of 1500, 5500, and 9500 feet above mean sea level (460, 1680, and 2900 meters MSL).

However, in order to sample the optical atmospheric properties both upwind and downwind of the city during the same flight, dual missions were flown. That is, a three filter/three level profile was run on a track upwind of the city, and then the aircraft ferried directly to a downwind track, where the same three filter/three level profile was repeated. The total elapsed flight time for these dual missions was approximately 5 hours, and they were scheduled to occur between 0930 and 1430 hours local civil time.

DATA COLLECTION SEQUENCE

During each mission, top priority is given to those systems essential for the recovery of beam transmission and path radiance data. Thus, the primary systems are the integrating nephelometer and the upper and lower hemisphere scanners. All other systems are either peripheral or backup and are therefore subject to cannibalization or abandonment in the event of any malfunction which affects a primary system.

At the conclusion of each mission, the data which have been recorded and stored on magnetic tape are returned to the Laboratory for computer reduction and analysis.

4.2 GROUND-BASED SYSTEM

The ground-based data collection sequence was designed to supplement the airborne data whenever the aircraft was operating in the immediate vicinity. However, it is also complete enough to stand alone when the aircraft mission is diverted or aborted.

The ground-based instrument system has several operational responsibilities. First, it must supply a ground-level data base to allow interpolation of various measurements between ground altitude and the lowest attainable aircraft altitude. Second, it must supply long term temporal sampling of those meteorological and radiometric quantities which relate to the project task. Third, the ground system serves as a spare parts and repair facility for the entire air/ground operation. In the event of a catastrophic failure in a primary airborne instrument or assembly, the equivalent piece of instrumentation is reassigned to the aircraft from the ground-based system. The aircraft can then return to service with a minimum of "down time" and repairs can be accomplished under the more convenient ground station conditions.

During Project METRO, the basic function of the ground station was to establish a data baseline against which the upwind and downwind airborne data could be judged. Thus, the ground station was left in one location, at Scott Air Force Base, during the entire deployment.

DATA COLLECTION SEQUENCE

The ground-based system was assigned three radiometer systems, three meteorological instruments, a Royco particle counter system, and communications equipment. The ground-based data collection sequence is not as automatic as the airborne sequence, but is otherwise quite similar. However, there is a basic difference in priorities. During each ground-based data sequence, top priority was given to those systems essential for the recovery of inherent background radiances and beam transmittance. Consequently, the primary systems were the automatic 2π scanner and the contrast reduction meter.

Ground-based data were collected in a fixed pattern on a repetitive basis during each designated data day. The Project METRO ground station data collection pattern consisted of the radiometric sequence listed below, plus a continuous Royco sampling at 10-minute accumulation intervals. A detailed description of each of these data collection sequences is presented in AFCRL-70-0137, Duntley *et al.* (1970), and thus is not repeated here.

1. Nephelometer Set, Σ , β_{30} , β_{150}
2. 2π Scanner Set, Vertical Plane Scan
3. Nephelometer Set, Σ only
4. Contrast Reduction Meter Set
5. Nephelometer Set, Σ , β_{30} , β_{150}
6. 2π Scanner Set, Upper Hemisphere Scan

As with the airborne data, all ground-based measurements were recorded in digital format on magnetic tape for computerized reduction and analysis upon return to the Laboratory. Unfortunately, subsequent to our return to the Laboratory, the calibration of the contrast reduction meter was found questionable. Thus our measurements of solar disk radiance have become irretrievable.

5. DATA PROCESSING

As in any reasonably complex, multi-input sample data system, there is a large amount of data-handling required before the scientific analyst ever sees the package. The degree of sophistication utilized for this portion of Project METRO data is illustrated in Fig. 5-1. In this generalized flow chart, the step-by-step processing of the raw field data is illustrated for the convenience of project organization and control and does not include the details of the actual computer programming. A description of each phase in the processing sequence is presented in fuller detail in AFCRL-72-0255, Duntley *et al.* (1972a), and AFCRL-72-0593, Duntley *et al.* (1972c).

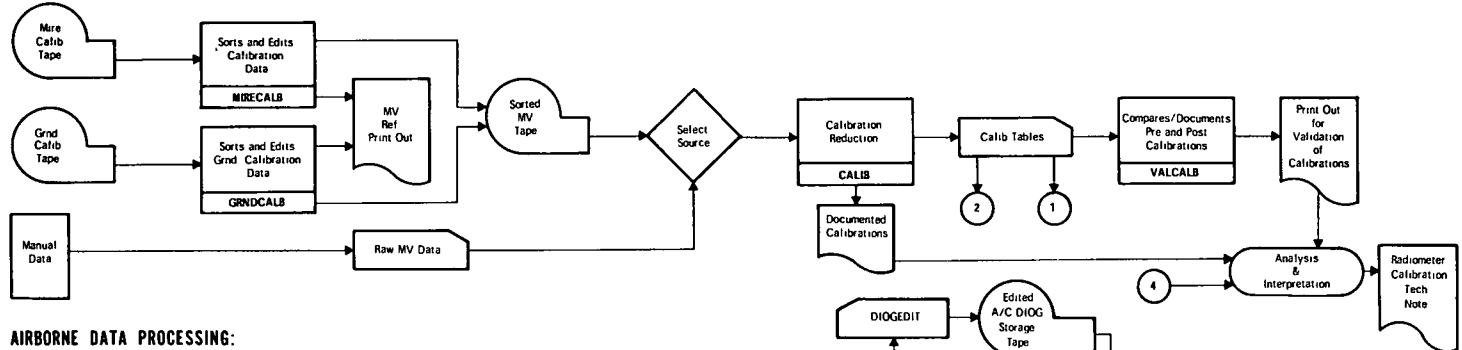
5.1 AIRBORNE DATA

As described in AFCRL-72-0255, Duntley *et al.* (1972a), several classes of data are recorded during an airborne data set: (1) radiometer outputs, (2) selector control codes, (3) transducer orientation and flight attitude signals, and (4) calibration voltages, etc. All systems, regardless of type, have been designed for an electrical output between 0 and ± 1 volt dc for full scale. The data logger has a least count of ± 1 millivolt and records in digital format at a multiplex rate of 240 samples per second and a tape rate of 3.56 inches per second at a recording density of 200 bits per inch.

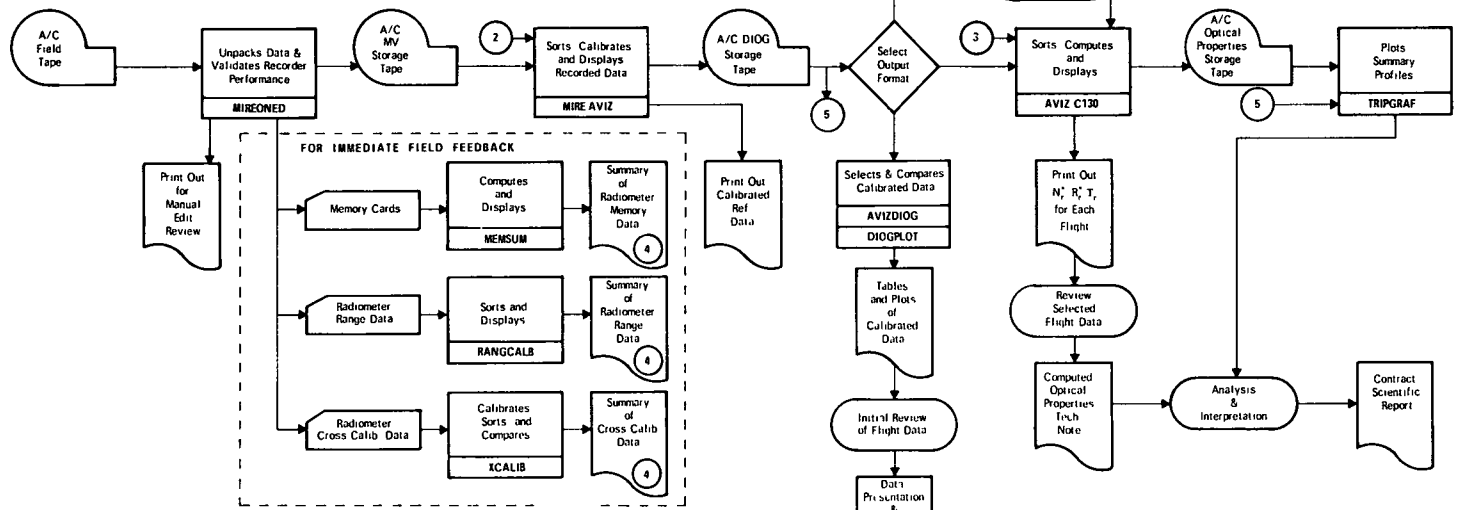
5.2 GROUND-BASED DATA

The data processing associated with the ground-based data set is similar in concept to that applied to the airborne data. The primary differences are the result of a different recording format between the two data loggers and the significantly lesser amount of data resulting from the ground station. As noted in AFCRL-72-0255, Duntley *et al.* (1972a), the same general classes of data are handled, but in much smaller quantities. Again, all systems, regardless of type, have been designed for an electrical output between 0 and ± 1 volt dc for full scale. The data logger is normally adjusted for a least count of ± 0.1 millivolt. It also records in digital format; however, the normal incremental sample rate is approximately only eight samples per second.

CALIBRATION DATA PROCESSING:



AIRBORNE DATA PROCESSING:



GROUND DATA PROCESSING:

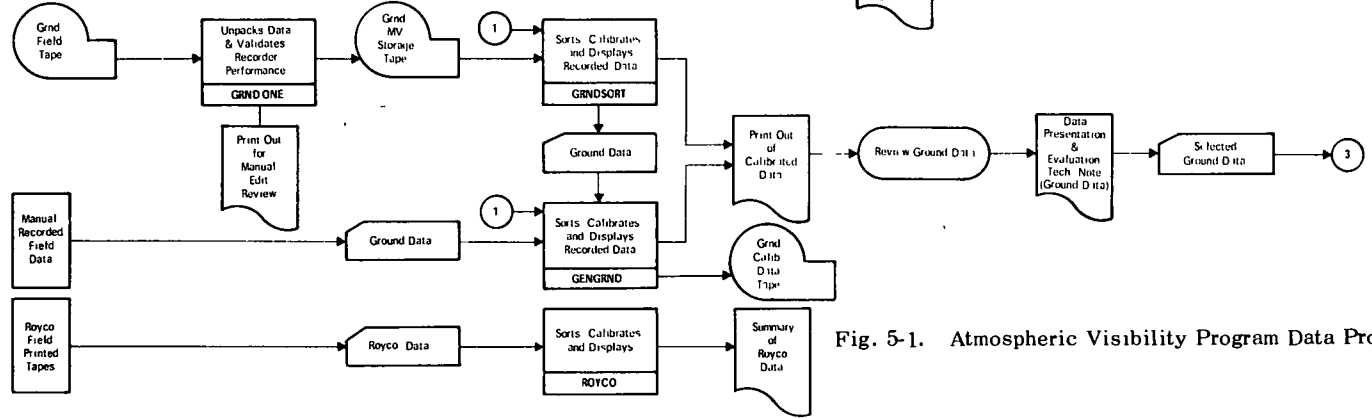


Fig. 5-1. Atmospheric Visibility Program Data Processing Schedule.

Since the recording format for the ground-based radiometer data is not as highly stylized as is the airborne format, efficient processing is best achieved by converting to card format. This conversion is accomplished by Program GRNDSORT. See Fig. 5-1. The insertion of manually recorded peripheral data into the basic data deck is also optimized through the use of this card format.

The punched card format is established to accept data from any radiometer system, plus selected identification and control information. Each radiometer measurement in each spectral band is recorded on a separate card along with the value of its "memory" reading and identification code. This one-card format was selected for conciseness and to facilitate maximum flexibility within the processing procedures.

As illustrated in Fig. 5-1, the card data are processed by the generalized program GENGRND. This program is suitable for use with all ground-based radiometer systems, i.e., CRM, UHS, and NEPH. It not only sorts and calibrates the input data, but also performs selected computations from among those illustrated in Section 2.2.

The results from Program GENGRND are available both as printer output for use in preliminary data evaluation and as a storage tape for use in further automatic data processing and manipulation.

5.3 CALIBRATION DATA

The calibration data are the heart of the data processing system in that any data processed are only as good as the calibrations applied to them. The calibration data are presently being recorded on tape to help eliminate the human bias in the system and are being handled in a phased procedure similar to that used in the general data processing technique. The data can be recorded on either the airborne or the ground data logging system. In an initial procedure, these data go through Program MIRECALB or GRNDCALB, according to the recording system used, to verify the electrical quality of the radiometer data and associated monitored parameters. The data are sorted and stored in set fashion for final processing.

Program CALIB performs this processing by generating documentation printouts and standard radiometer calibration card decks which can be used by any of the system's programs for calibrating field data. These card decks are also used by Program VALCALB which, in its documentation mode, was used to generate printout describing Project METRO radiometer calibrations. This program also has a comparison mode which is used to compare pre- and post-deployment calibration sets. This mode is a particularly useful tool in calibration verification and is the source of the preferred calibration data illustrated in Table 3-2.

5.4 DATA TAPES

The data processing sequences discussed in the previous paragraphs produce output tapes containing a broad catalog of calibrated data. These tapes are useable as data inputs to a multiplicity of diverse problems requiring a knowledge of atmospheric optical properties. Thus, the data tape numbers and the in-house descriptions of the data and the computed properties reported herein are summarized in Tables 5-1 and 5-2 to simplify future retrieval.

Table 5-1

Processed Data Tapes

METRO Flight No.	MIREAVIZ*	Data Presentation No.	AVIZC130**	Computed Properties No.
	Tape No. VL-301D File No.		Tape No. VL-346D File No.	
C-180	19	60	11	78
C-181	2	61	6	73
C-182A	4	62	2	74
C-182B	14	62	1	74
C-183A	16	63	9	79
C-183B	7	63	***	79
C-185A	6	64	10	80
C-185B	8	64	***	80
C-186A	9	65	3	75
C-186B	10	65	7	75
C-187A	11	66	8	76
C-187B	12	66	***	76
C-188A	17	67	4	77
C-188B	18	67	5	77

* Duplicate of VL-384

** Duplicate of VL-371C

*** No AVIZC130 Output Tape

Table 5-2

Processed Data Tapes for METRO Ground-Based Data.
(Data Presentation No. 108.)

Ground Data Set	Date (1971)	GENGRND	GRNDSCAN
		Tape No. VL-335D File No.	Tape No. VL-329C File No.
MET-01	12 August	1	1
MET-02	13 August	1	2
MET-03	13 August	1	3
MET-04	14 August	1	4
MET-05	18 August	1	5
MET-06	19 August	1	6
MET-07	19 August	1	7
MET-08	23 August	1	8
MET-09	23 August	1	9
MET-10	24 August	1	10
MET-11	24 August	1	11

6. WEATHER SUMMARY

6.1 SUMMARY

Meteorological data available for analysis included daily surface and 500-millibar charts prepared by the U. S. Department of Commerce, National Oceanic and Atmospheric Administration, Environmental Data Service. The surface charts were for 7:00 A.M., E.S.T. (1200 GMT). Portions of these charts have been copied and are presented as Fig. 6-1. The 500-millibar charts were also for 7:00 A.M., E.S.T. (1200 GMT). Also utilized were the 3-hourly facsimile charts issued by the National Meteorological Center and obtained from the Lindbergh Field NOAA office. The 500-millibar facsimile charts were for 0000 GMT and 1200 GMT daily. Used but not described were various other facsimile charts. Also available for days when the flights were conducted were the hourly and special reports made by the weather office at Scott Air Force Base.

This section includes a discussion of the surface and 500-millibar charts for only the days on which flight data were taken and are reported herein. For daily continuity, the reader is referred to AFCRL-TR-73-0422, Duntley *et al.* (1973). Listed in tabular form are the hourly and special reports made by the observers at Scott Air Force Base. The meteorological data taken by the Visibility Laboratory ground station (located on the base) are in agreement with these observations.

Also included in Section 6 are graphical representations of ambient temperature profiles measured during each reported data flight (Fig. 6-2). These temperatures are measured continuously by an AN/AMQ-17 aerograph system described briefly in Duntley *et al.* (1970) and more completely in USNAF TP-133. The profile identification symbols used in Fig. 6-2 are related to the spectral filter sequence during which the temperature was measured; i.e., the temperature profile identified with the Filter 2 symbol was measured during the same time interval that the Filter 2 radiometric measurements were being made; the temperatures coded as Filter 3 were taken simultaneously with the Filter 3 radiometric measurements, etc. Users should be aware that these temperature profiles represent conditions appropriate to a specific flight track which may be from 50 to 100 miles away from the ground site at Scott Air Force Base.

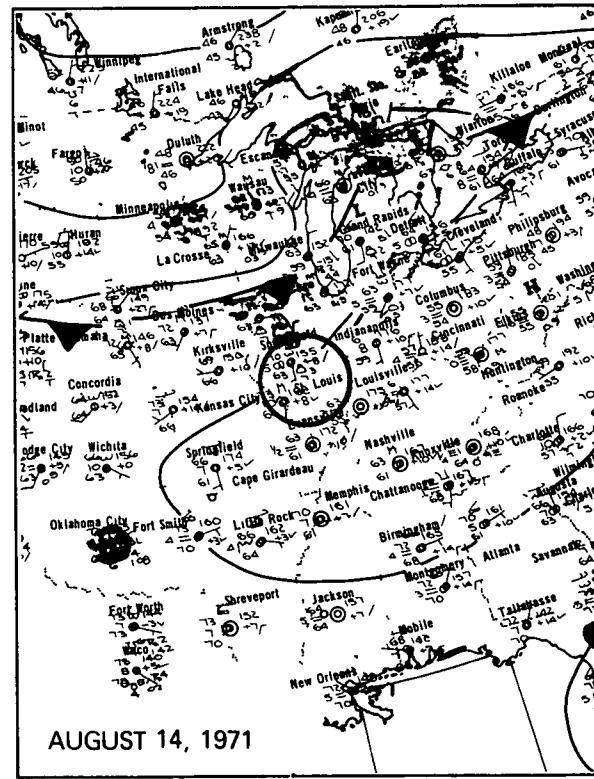
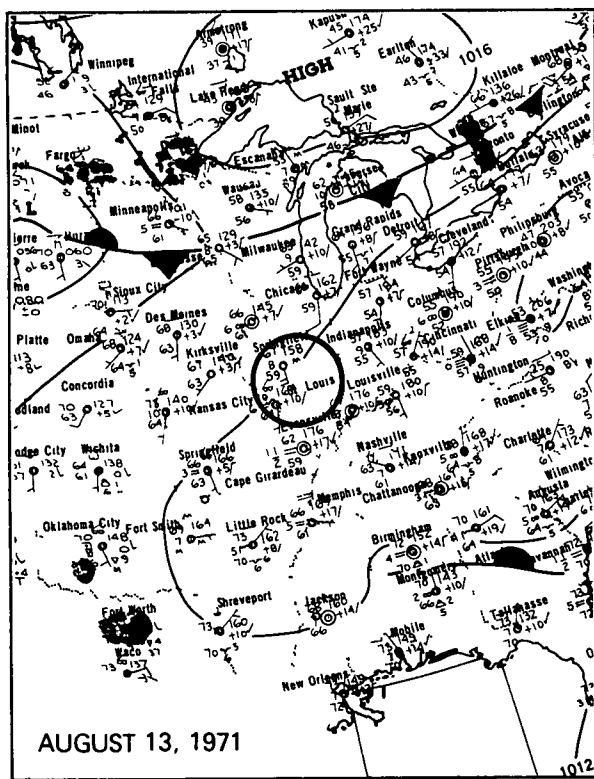
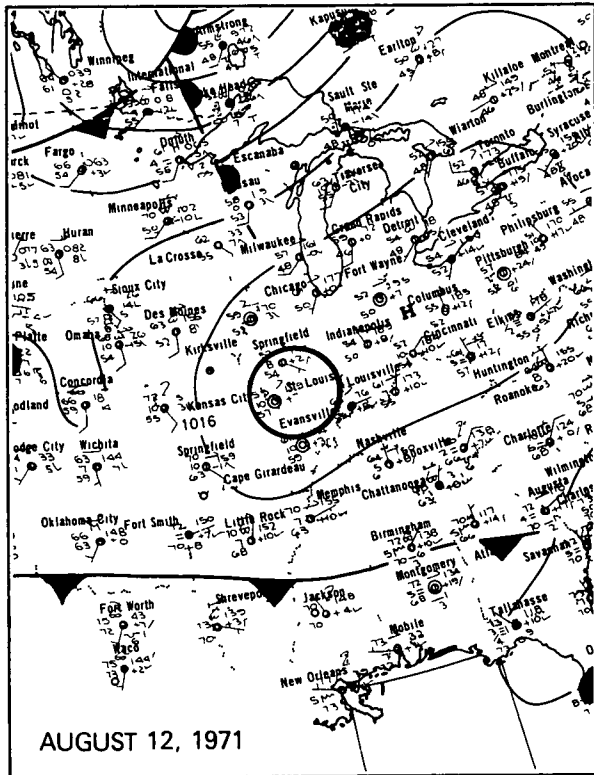
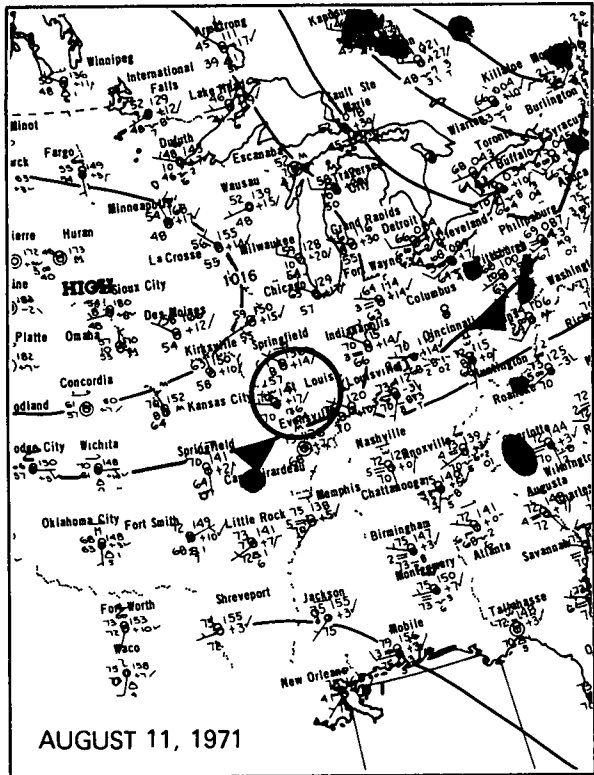


Fig. 6-1. Synoptic Charts of St. Louis Area During Project METRO.

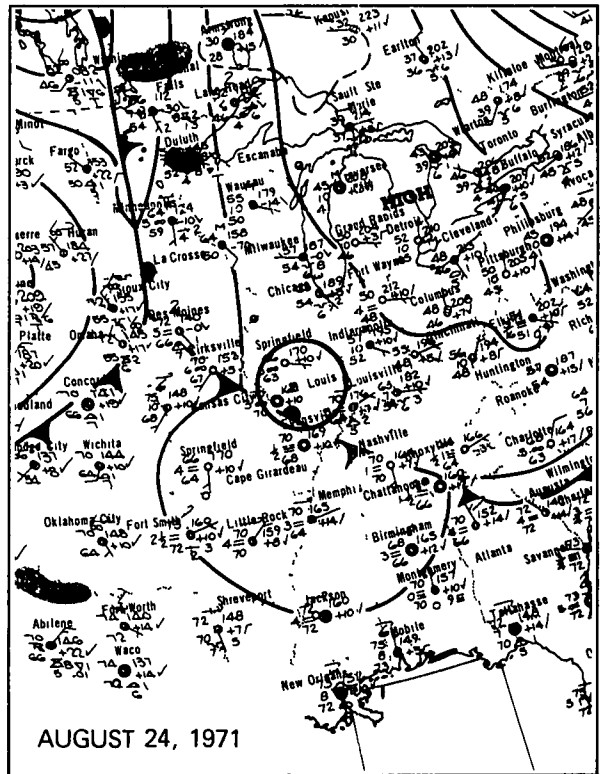
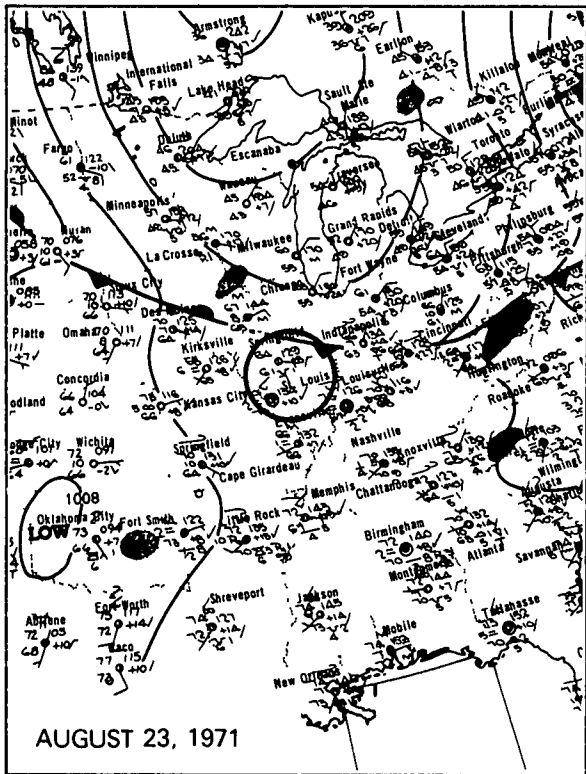
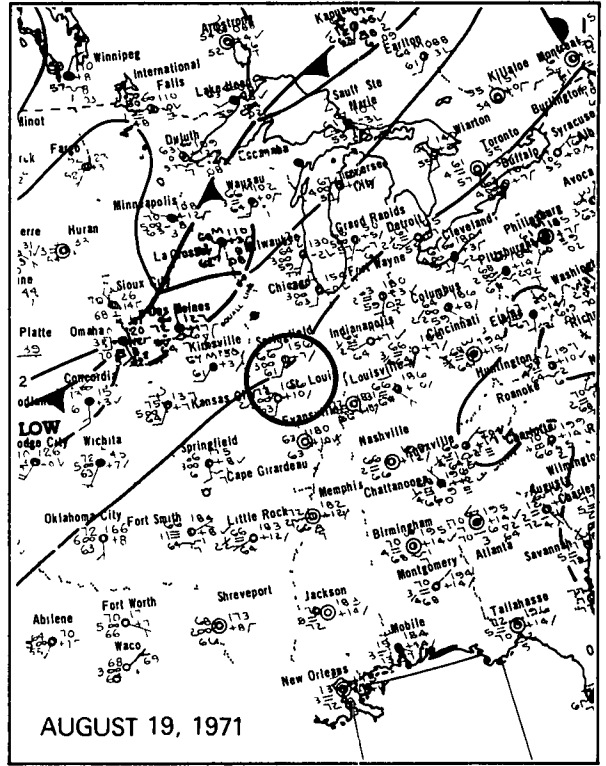
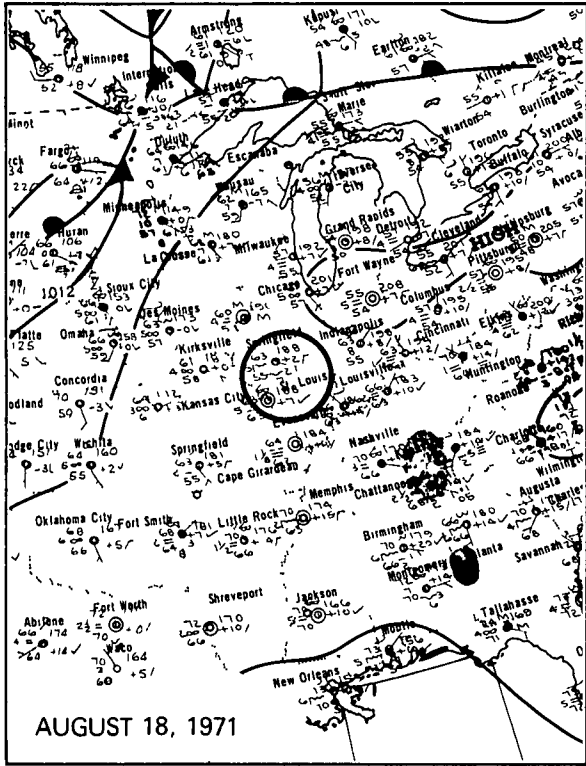
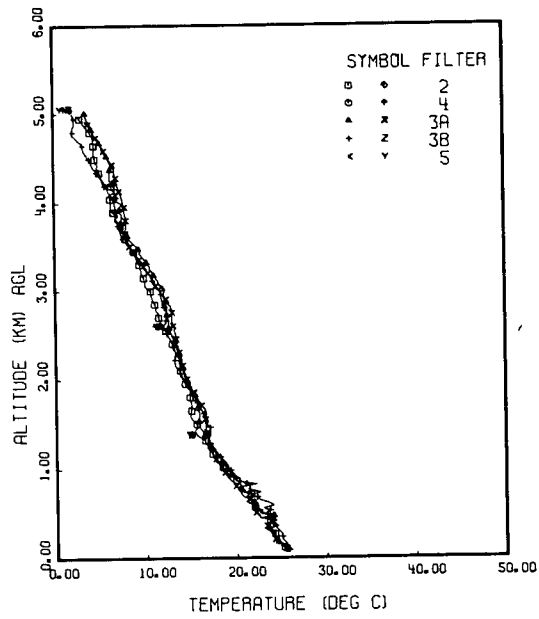
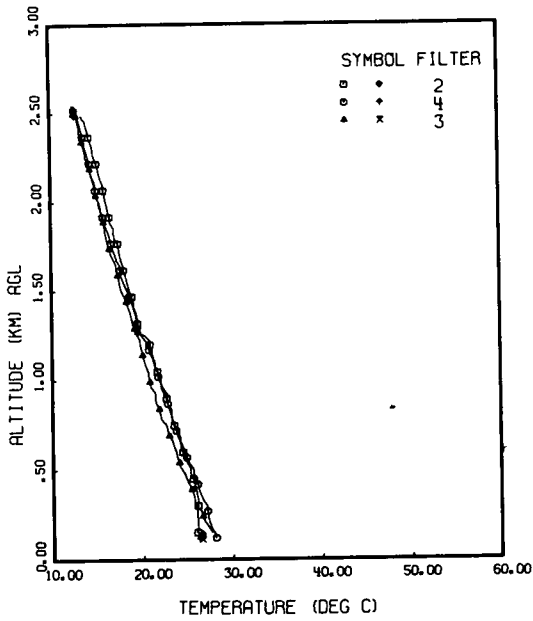


Fig. 6-1 (cont.). Synoptic Charts of St. Louis Area During Project METRO.

FLIGHT C-180



FLIGHT C-183A



FLIGHT C-183B

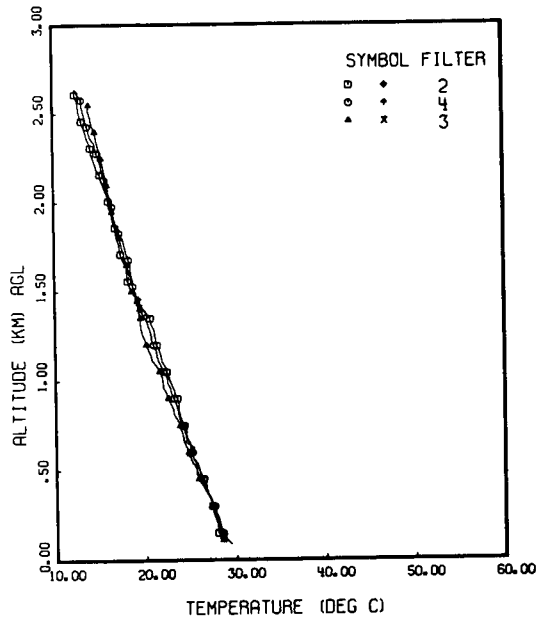
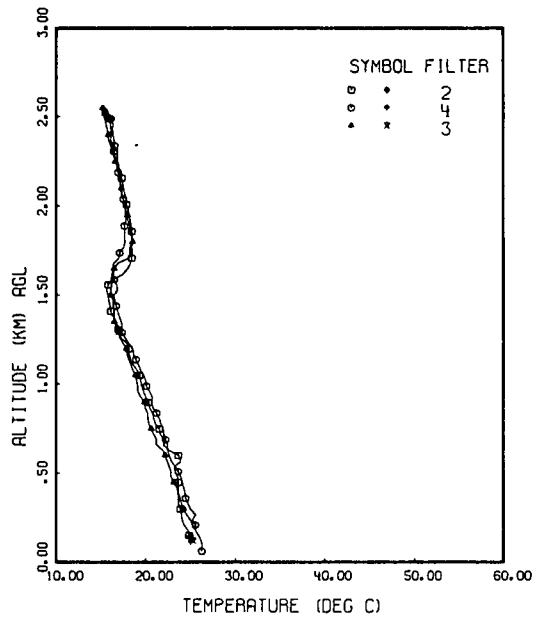
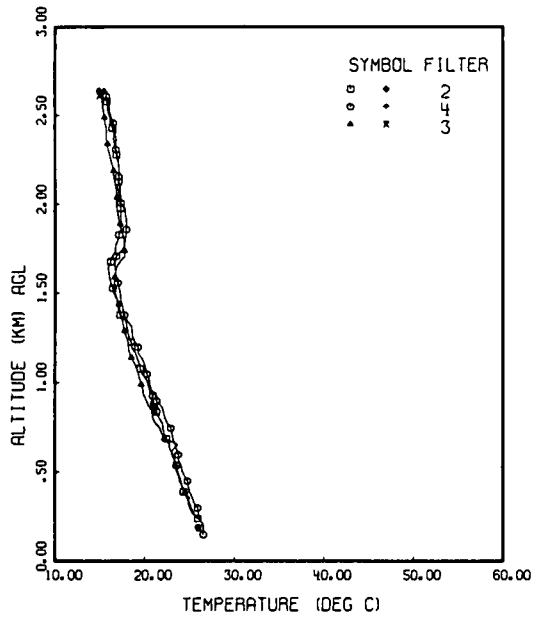


Fig. 6-2. Temperature Versus Altitude for Six Project METRO Flight Profiles.

FLIGHT C-185A



FLIGHT C-185B



FLIGHT C-187B

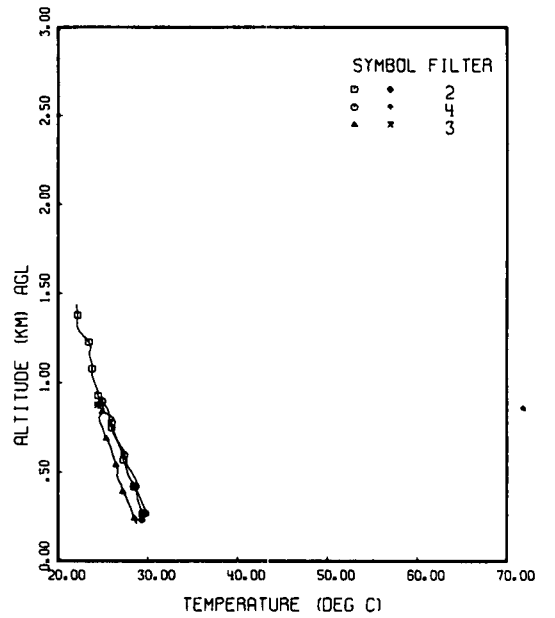


Fig. 6-2 Cont. Temperature Versus Altitude for Six Project METRO Flight Profiles.

6.2 SYNOPTIC CONDITIONS

During the period of deployment there were a few weak frontal passages which did little to alleviate the high temperatures and deposited very little precipitation. For the most part the synoptic situation was typically summer with weak gradients both at the surface and aloft.

FLIGHT C-180 ON 11 AUGUST 1971

The surface synoptic chart shows that there was a cold frontal passage accompanied by thunder-showers at about 0600 GMT. By 2100 GMT the front had moved to a line from Altoona to Bowling Green, then to northern Arkansas and Oklahoma, where it became stationary. A weak high existed over the middle half of the country with St. Louis on the leading edge. The 500-millibar chart shows a trough from Hudson Bay southward to Illinois. There was a low over the Texas Panhandle. Moderate westerly winds were present.

FLIGHTS C-183A AND B ON 14 AUGUST 1971

The surface chart shows that St. Louis was still on the rear of a high with its center near Pittsburgh. There was a cold front through Detroit, Davenport, and southern Nebraska which extended northwestward to British Columbia. Tropical storm "Beth" was off the Virginia coast. At 500 millibars there was a high area over Wyoming, Utah, Nevada, and California. Elsewhere there were very weak gradients.

FLIGHTS C-185A AND B ON 18 AUGUST 1971

The surface synoptic chart shows an extremely weak gradient. A low was centered in eastern South Dakota with a cold front extending southwestward. At 500 millibars there was a high extending from Illinois to Texas and westward to California. There was another area of high along and off the east coast extending from New Jersey to Florida. The flow over the St. Louis area was moderate northeasterly.

FLIGHT C-187B ON 23 AUGUST 1971

The surface chart shows a cold front extending south-southwestward from Maine to the DelMarVa* peninsula then westward to Evansville and northwestward to Springfield and Keokuk to a low in central North Dakota. At 500 millibars there was a high centered near Topeka and a trough from Ontario to Virginia. The gradient shows moderate northeasterly winds over the region.

6.3 TABULAR SUMMARY AND GLOSSARY

A summary of the daily meteorological observations taken at Scott Air Force Base on the days during which data flights were made is presented in Table 6-1. A glossary of the most often used symbols is also included. All Scott data were reported in local standard time (LST) but have been changed to central daylight time (CDT) to coincide with ground and flight logs.

* Indicates the Delaware/Maryland/Virginia peninsula between the Delaware and Chesapeake Bays.

METEOROLOGICAL GLOSSARY AND ABBREVIATIONS

SKY AND CEILING	VISIBILITY (VV)																								
<p>Sky cover symbols are in ascending order. Figures preceding symbols are heights in hundreds of feet above station. Sky cover symbols are:</p> <ul style="list-style-type: none"> ○ Clear: less than 0.1 sky cover ⊙ Scattered: 0.1 to less than 0.6 sky cover ⊕ Broken: 0.6 to 0.9 sky cover ⊖ Overcast: more than 0.9 sky cover - Thin (when prefixed); light (when suffixed) -- Very light (when suffixed) -X Partial obscuration: 0.1 to less than 1.0 sky hidden by precipitation or obstruction to vision (bases at surface) X Obscuration: 1.0 sky hidden by precipitation or obstruction to vision (bases at surface) <p>Letter preceding height of layer identifies ceiling layer and indicates how ceiling height was obtained. Thus:</p> <ul style="list-style-type: none"> A Aircraft B Balloon (pilot or ceiling) D Estimated height of cirriform clouds on basis of persistency E Estimated height of noncirriform clouds M Measured R Radiosonde balloon or radar U Height of cirriform ceiling layer unknown V Immediately following numerical value indicates a varying ceiling (also used with varying visibility) W Indefinite / Height of cirriform nonceiling layer unknown 	<p>Reported in statute miles.</p>																								
	WEATHER AND OBSTRUCTION TO VISION SYMBOLS																								
	<table style="width: 100%; border: none;"> <tr> <td style="width: 50%;">A Hail</td> <td style="width: 50%;">IF Ice fog</td> </tr> <tr> <td>AP Small hail</td> <td>K Smoke</td> </tr> <tr> <td>BD Blowing dust</td> <td>L Drizzle</td> </tr> <tr> <td>BN Blowing sand</td> <td>R Rain</td> </tr> <tr> <td>BS Blowing snow</td> <td>RW Rain showers</td> </tr> <tr> <td>D Dust</td> <td>S Snow</td> </tr> <tr> <td>E Sleet</td> <td>SG Snow grains</td> </tr> <tr> <td>EW Sleet showers</td> <td>SP Snow pellets</td> </tr> <tr> <td>F Fog</td> <td>SW Snow showers</td> </tr> <tr> <td>GF Ground fog</td> <td>T Thunderstorms</td> </tr> <tr> <td>H Haze</td> <td>ZL Freezing drizzle</td> </tr> <tr> <td>IC Ice crystals</td> <td>ZR Freezing rain</td> </tr> </table>	A Hail	IF Ice fog	AP Small hail	K Smoke	BD Blowing dust	L Drizzle	BN Blowing sand	R Rain	BS Blowing snow	RW Rain showers	D Dust	S Snow	E Sleet	SG Snow grains	EW Sleet showers	SP Snow pellets	F Fog	SW Snow showers	GF Ground fog	T Thunderstorms	H Haze	ZL Freezing drizzle	IC Ice crystals	ZR Freezing rain
A Hail	IF Ice fog																								
AP Small hail	K Smoke																								
BD Blowing dust	L Drizzle																								
BN Blowing sand	R Rain																								
BS Blowing snow	RW Rain showers																								
D Dust	S Snow																								
E Sleet	SG Snow grains																								
EW Sleet showers	SP Snow pellets																								
F Fog	SW Snow showers																								
GF Ground fog	T Thunderstorms																								
H Haze	ZL Freezing drizzle																								
IC Ice crystals	ZR Freezing rain																								
	CLOUD ABBREVIATIONS																								
	<table style="width: 100%; border: none;"> <tr> <td style="width: 50%;">Ac Altocumulus</td> <td style="width: 50%;">Cs Cirrostratus</td> </tr> <tr> <td>As Altostratus</td> <td>Cu Cumulus</td> </tr> <tr> <td>Cb Cumulonimbus</td> <td>Ns Nimbostratus</td> </tr> <tr> <td>Cc Cirrocumulus</td> <td>Sc Stratocumulus</td> </tr> <tr> <td>Ci Cirrus</td> <td>St Stratus</td> </tr> </table>	Ac Altocumulus	Cs Cirrostratus	As Altostratus	Cu Cumulus	Cb Cumulonimbus	Ns Nimbostratus	Cc Cirrocumulus	Sc Stratocumulus	Ci Cirrus	St Stratus														
Ac Altocumulus	Cs Cirrostratus																								
As Altostratus	Cu Cumulus																								
Cb Cumulonimbus	Ns Nimbostratus																								
Cc Cirrocumulus	Sc Stratocumulus																								
Ci Cirrus	St Stratus																								
	WIND																								
	<p>Direction in ten's of degrees from true north, speed in knots. A "0000" indicates calm. A "G" indicates gusty. A "Q" indicates squall. Peak speed of gusts, when reported, follows G or Q. The contraction WSHFT in remarks followed by time group (GMT) indicates wind shift and its time of occurrence.</p> <p>Examples: 0129 is 010 degrees, 29 knots.</p> <p style="text-align: right;">3627G40 is 360 degrees, 27 knots, peak speed in gusts of 40 knots.</p>																								
RELATIVE HUMIDITY (RH)																									
<p>Reported in percent and computed from temperature and dewpoint.</p>																									

Table 6-1

 STANDARD METEOROLOGICAL DATA SHEET
 11 August 1971

 Field Site: Scott Air Force Base
 Lat. 33°38' N — Long. 89°51' W — El. + 463 ft

 Data Source: Scott Air Force Base
 Flight No. C-180 Track 1

Time		Sky and Ceiling (Hundreds of Feet)	Visi- bility (miles)	Weather and Obstructions To Vision	Temp. (°F)	Dew- point (°F)	Rel. Hum. (%)	Wind		Cloud Type	Total Sky Cover	REMARKS
CDT	GMT							Direction (00-36)	Speed (Kt)			
0655	1155	40 ⊕ E80 ⊕ 250 ⊕	10		72	64	72	33	04	CuAcCi	0.9	
0756	1256	40 ⊕ E80 ⊕ 330 ⊕	15		73	64	69	35	07	CuAcCi	0.9	
0855	1355	40 ⊕ 80 ⊕ 300- ⊕	15		74	60	58	36	07	CuAcCi	1.0	
0956	1456	40 ⊕ 300- ⊕	15		76	57	52	36	07	CuCi	0.8	
1056	1556	300- ⊕	15		80	54	41	26	06	Ci	0.8	
1157	1657	300 ⊕	15		84	57	40	35	06	Ci	0.1	
1257	1757	300 ⊕	15		83	56	42	01	07	Ci	0.1	Cu East South & West, Wind 330 V 050
1359	1859	300 ⊕	12		83	54	37	01	07+18	Ci	0.1	Cu All Quadrants, Wind 340 V 040
1456	1956	50 ⊕	12		85	55	36	33	07	Ci	0.2	Wind 300 V 360
1555	2055	50 ⊕	12		84	55	37	36	10	Cu	0.1	
1655	2155	50 ⊕	15		84	54	35	35	14+20	Cu	0.1	Wind 330 V 030
1755	2255	300- ⊕	15		82	53	37	36	12+17	Ci	0.3	Cu Northeast to Southwest & West to Northwest, Wind 340 V 030
1855	2355	300- ⊕	15		79	55	44	01	07	Cs	0.7	
1955	0055	300- ⊕	15		75	54	48	02	03	Cs	0.7	

Table 6-1 (cont)

STANDARD METEOROLOGICAL DATA SHEET

14 August 1971

Data Source Scott Air Force Base
Flight No C-183A & B Tracks 7 and 4Field Site Scott Air Force Base
Lat 33°38' N – Long 89°51' W – El +463 ft

Time		Sky and Ceiling (Hundreds of Feet)	Visi- bility (miles)	Weather and Obstructions To Vision	Temp (°F)	Dew point (°F)	Rel Hum (%)	Wind		Cloud Type	Total Sky Cover	REMARKS
CDT	GMT							Direction (00-36)	Speed (Kt)			
0658	1155	E35 ☉	5	GF H	69	60	72	00	00	Cu	0 6	Moderate Cu All Quadrants
0759	1259	35 ☉	6	GF	72	62	70	18	04	Cu	0 5	
0857	1357	35 ☉	8		79	63	58	18	04	Cu	0 2	Haze All Quadrants
0957	1457	35 ☉ 150 ☉	8		83	64	53	24	06	CuAc	0 2	Haze All Quadrants
1057	1557	50 ☉ 100 ☉	8		85	65	51	23	05	CuAc	0 5	Cb 25 Northwest – 25 North, Movement Un- known, Haze All Quadrants
1157	1657	50 ☉ 250- ☉	12		87	63	44	21	05	CuCi	0 8	Cb 25 Northwest – 25 North, Movement Un- known, Wind Direction Variable
1257	1757	50 ☉ R70 ☉ 310 ☉	12		80	65	60	03	17G23	CbAcCi	0 9	Cb All Quadrants Moving South
1310	1810	50 ☉ E70 ☉ 310 ☉	12	T				01	12G24	CbAcCi	0 9	T Northwest Moving South, Occasional Lightning Cloud to Ground Northwest
1322	1822	50 ☉ E70 ☉ 310 ☉	8	T RW -				36	20G26	CbAcCi	0 9	T Overhead Moving South, Occasional Lightning Cloud to Ground North to Northwest
1357	1857	50 ☉ E70 ☉	8	T RW -	71	65	81	36	05	CbAc	1 0	Thunder Overhead and West Moving South, Occasional Lightning Cloud to Ground Southwest to West
1403	1903	50 ☉ E70 ☉	12	T RW - -				09	02			Thunder Overhead and West Moving South, Occasional Lightning Cloud to Ground All Quadrants, Wind Direction Variable
1448	1948	50 ☉ E70 ☉ 310 ☉	12	RW - -				28	03			T Ended 1447 Moved South, Wind Direction Variable

Table 6-1 (cont.)

STANDARD METEOROLOGICAL DATA SHEET
18 August 1971

Data Source: Scott Air Force Base
Flight No. C-185A & B Tracks 7 and 3

Field Site: Scott Air Force Base
Lat. 33°38' N – Long. 89°51' W – El. +463 ft

Time		Sky and Ceiling (Hundreds of Feet)	Visi- bility (miles)	Weather and Obstructions To Vision	Temp. (°F)	Dew- point (°F)	Rel. Hum. (%)	Wind		Cloud Type	Total Sky Cover	REMARKS
CDT	GMT							Dirac- tion (00-36)	Speed (Kt)			
0658	1158	200 ☉	5	GF H	62	58	86	00	00	Cs	0.2	
0757	1257	60 ☉ 200 ☉	4	H GF	66	59	78	00	00	AcCs	0.3	
0858	1358	200-☉	4	H	72	60	66	11	01	Cs	0.7	Ac North
0958	1458	200-☉	5	H	77	62	60	15	02	Cs	0.9	Wind Direction Variable
1057	1557	○	5	H	81	62	52	18	02		0	In-Flight Visibility 3, Wind Direction Variable
1155	1655	40 ☉	6	H	84	57	40	29	06	Cu	0.1	Wind Direction Variable
1256	1756	40 ☉	6	H	85	55	37	23	09	Cu	0.1	Wind Direction Variable
1355	1855	40 ☉	6	H	86	56	36	25	04	Cu	0.1	Wind Direction Variable
1455	1955	45 ☉	6	H	88	55	32	19	08	Cu	0.1	Wind 070 V 250
1558	2058	○	6	H	88	56	34	18	04	Sc	0	Sc All Quadrants
1655	2155	○	5	H	88	57	35	17	09	Sc	0	Sc All Quadrants

Table 6-1 (cont.)

STANDARD METEOROLOGICAL DATA SHEET
23 August 1971Data Source: Scott Air Force Base
Flight No. C-1878 Track 4Field Site: Scott Air Force Base
Lat. 33°38' N - Long. 87°51' W - El. +463 ft

Time		Sky and Ceiling (Hundreds of Feet)	Visi- bility (miles)	Weather and Obstructions To Vision	Temp. (°F)	Dew- point (°F)	Rel. Hum. (%)	Wind		Cloud Type	Total Sky Cover	REMARKS
CDT	GMT							Direc- tion (00-36)	Speed (Kt)			
0655	1155	-X320-⊕	1-1/4	H	70	65	84	00	00	Ci	0.8	
0711	1211	-X320-⊕	1-1/2	GF H				23	02			Visibility Northwest 2
0742	1242	320-⊕	2	GF H				22	02			Visibility Northwest 2-1/2
0757	1257	320-⊕	2-1/2	H	73	67	81	24	05	Cs	0.9	
0827	1327	320-⊕	3	H				24	06			
0855	1355	300-⊕	4	H	79	70	74	24	05	Cs	0.7	
0955	1455	300-⊕	5	H	85	69	58	26	05	Cs	0.7	Wind Direction Variable
1055	1555		6	H	90	67	46	31	07	Cs	0.1	Wind 250 V 340
1155	1655	○	12		91	67	46	34	03		0	Few Cu All Quads, Thin Ci North, Wind Direction Variable
1257	1757	○	15		89	66	47	36	05		0	Cu South-West ○ V ⊕, Wind Direction Variable
1355	1855	40 ⊕	12		93	65	40	03	03	Cu	0.1	Wind Direction Variable
1455	1955	40 ⊕ 300-⊕	12		93	65	40	03	05	CuCi	0.3	Wind Direction Variable
1555	2055	40 ⊕ 300-⊕	12		94	64	38	06	02	CuCi	0.6	Wind Direction Variable
1656	2156	40 ⊕ 100 ⊕ 300-⊕	12		93	63	37	03	03	CuAcCi	0.7	

6.4 ANALYSIS OF RADIOMETRIC AND METEOROLOGICAL RELATIONSHIPS

A continuing goal of the Visibility Laboratory's measurement program is the accumulation of a body of data appropriate for direct application to the interpretation of the relationship between the optical properties of the atmosphere and the meteorological specifications of that atmosphere.

During the METRO deployment, the airmass characteristics were not well-defined. Despite the passage of a few weak fronts, there were no changes apparent in the airmass character but they were rather diffuse. Thus, there are no clear-cut comparisons by airmass discrimination that can realistically be made, as in Edgerton (1967). Consequently, the METRO data will become a subset for comparison with other data subsets from subsequent deployments.

7. DATA PRESENTATION

7.1 AIRBORNE DATA AND FLIGHT SUMMARY

Between 11 and 24 August 1971, eight flights resulting in 14 data profiles were made in southern Illinois and eastern Missouri. A ninth flight, C-184, was attempted, but bad weather caused the flight to be terminated without obtaining any data. Eight of the data profiles were reported in Duntley *et al.* (1973). Data for the remaining six data profiles from four flights are included in this report.

The flights were conducted in the vicinity of St. Louis, Missouri, in order to conveniently sample the optical properties both upwind and downwind of a major inland city. (See Fig. 1-4). Only five of the nine designated track locations surrounding the city were used during the field trip. The latitude and longitude coordinates, average elevation above sea level, location relative to St. Louis, and basic terrain description for each of these five flight tracks are given in Table 7-1.

PHOTOGRAPHIC DOCUMENTATION

The sky and terrain conditions encountered during each of the data flights were documented photographically during each straight and level flight sequence. These documentary photographs were made simultaneously with the measurements of sky and terrain radiance at each of three designated altitudes.

There are six profiles for which the pictures show skies clear at all altitudes, except for a few horizon clouds, and with no clouds appearing in the lower hemisphere. All these flight profiles were reported in Duntley *et al.* (1973). Pictures for an additional five profiles show skies clear at the top altitude, but with scattered clouds appearing in the lower hemisphere. Thus, at the lower altitudes these five profiles show skies containing scattered clouds in addition to the horizon clouds. Three of these profiles, C-180, C-183A, and C-185A, are reported herein, while the other two were included in Duntley *et al.* (1973). Photographs from the three remaining flight profiles, C-183B, C-185B, and C-187B, illustrate cloud conditions so severe or unstable that these profiles were processed for only scattering coefficient, equivalent attenuation length, and beam transmittance. They are, however, also reported here.

Table 7-1

Location and Description of METRO Flight Tracks

Track	Site Reference	Latitude (N)	Longitude (W)	Ground Elevation (m)	Flights	Direction from St. Louis	Terrain Description
1	Quincy/ Capitol	39.9°	90.3°	192	180	N	Cultivated farm area
3	Vandalia	39.4°	88.8°	183	181,182B,185B, 186B	NE	Flat, highly cultivated farmland with multiple small fields
4	Centralia	38.4°	89.1°	153	183B,187B,188B	ESE	Flat, highly cultivated farmland and small bodies of water
7	Maples	37.8°	91.5°	305	182A,183A,185A, 186A,187A	SW	Heavily wooded, rolling hills
9	Hallsville	39.1°	91.6°	244	188A	NW	Cultivated farm area with small fields and woodlands

Photographs illustrating typical sky and terrain conditions during four of the six data collection profiles reported herein are shown in Fig. 7-1 and 7-2. In each instance, the picture on the left represents the sky (upper hemisphere) as seen through a 180-degree lens, and the picture on the right represents the terrain (lower hemisphere). The photographs are taken from both the highest and lowest flight altitudes for each of the four flight profiles. The pictures representing flight profiles C-183A and C-185A illustrate cloud conditions typical for those profiles having clear skies at only the top altitude. Those representing C-183B and C-185B illustrate the more severe cloud conditions as well as terrain characteristics of two additional tracks.

RADIOMETRIC DOCUMENTATION

Table 7-2 contains a summary of pertinent descriptive information on the six flight profiles for which radiometric data are reported herein. The flight numbers are sequential. The times under the Total Time of Data-Taking column are Greenwich mean time (GMT) and central daylight time (CDT). CDT is equal to GMT-5. The sun zenith angles are tabulated for the time when sky radiance data-taking began, at the time of sun transit (minimum sun zenith angle), and at the conclusion of the sky radiance data-taking. The average sun zenith angles in column 12 were used in Eq. 2.6, 2.22, and 2.36 during the calculations leading to the derivation of path radiance and path reflectance. The maximum flight altitude is noted in column 13.

Table 7-2

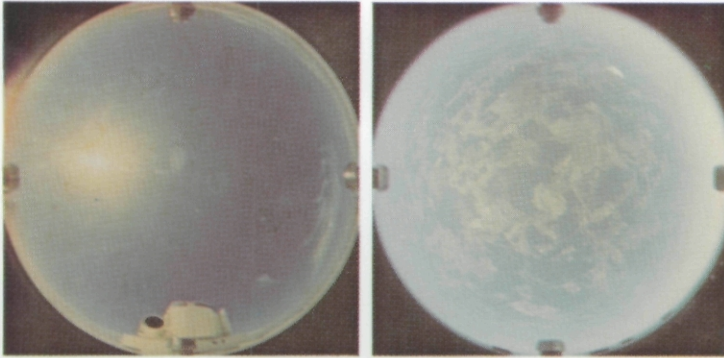
METRO Flight Data Summary

		Total Time of Data-Taking						Sun Zenith Angle (degrees)				Maximum Flight Altitude
		Start		End				Start	Transit	End	Average	
Flight No.	Date (1971)	GMT	CDT	GMT	CDT	Track	Filters					
C-180	11 August	1933	1433	2321	1821	1	2,3,4	31.1	-	51.9	40.5	5064
C-183A	14 August	1502	1002	1635	1135	7	2,3,4	47.5	-	37.8	42.6	2550
C-183B	14 August	1731	1231	1848	1348	4	2,3,4	24.8	24.0	24.0	24.3	2550
C-185A	18 August	1522	1022	1700	1200	7	2,3,4	44.6	-	35.2	39.8	2550
C-185B	18 August	1746	1246	1913	1413	3	2,3,4	26.3	26.2	28.0	26.8	2640
C-187B	23 August	1942	1442	2024	1524	4	2,3,4	35.5	-	39.8	37.6	1440

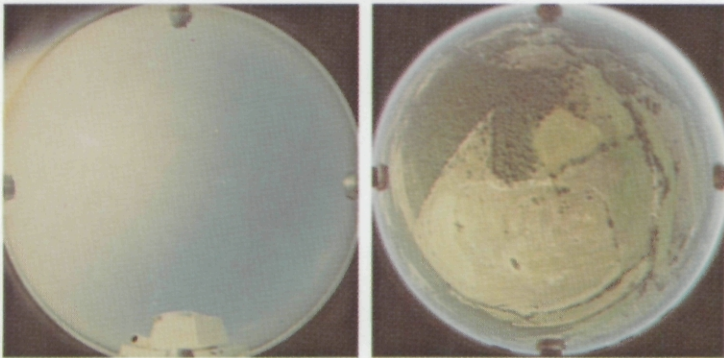
Radiometric data for the four flights representing six separate profiles are presented tabularly and graphically in Section 7.3 in sets by flight number. The six profiles consist of three with clear skies at only the top altitude, C-180, C-183A, and C-185A, plus the limited data available for C-183B, C-185B, and C-187B. A detailed description and report of weather characteristics are given as the introductory page of each data set. For the cloudy-day profiles only total scattering coefficient, equivalent attenuation length, and beam transmittance are presented.

The beam transmittance is extrapolated from space to the highest altitude of flight as described in Section 2.1. The results of this extrapolation are not included in the standard sets of data tables by flight. These extrapolations and the resultant space-to-ground beam transmittance, when combined with the beam transmittance based on the total scattering coefficient profile, are presented for the three relatively clear-day flight profiles in Table 7-3.

FLIGHT C-183A



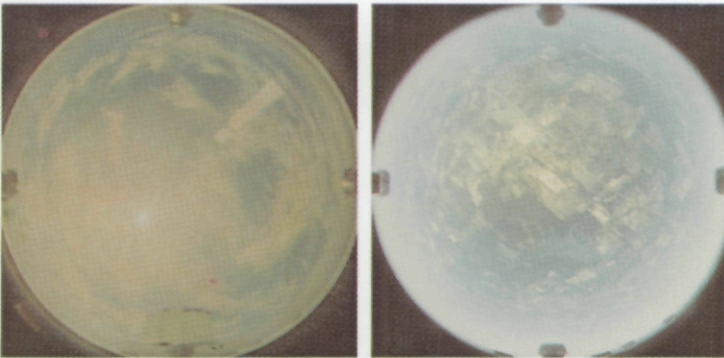
Upper and Lower Hemisphere
2509m AGL 1552 GMT Track 7.



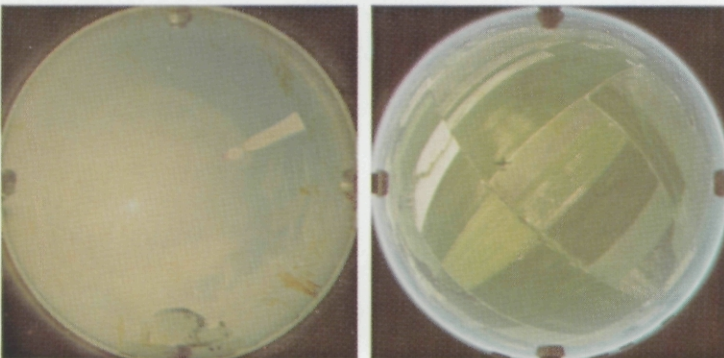
Upper and Lower Hemisphere
125m AGL 1505 GMT Track 7.

Fig. 7-1. Typical Sky and Terrain Photographs for Flight C-183.

FLIGHT C-183B



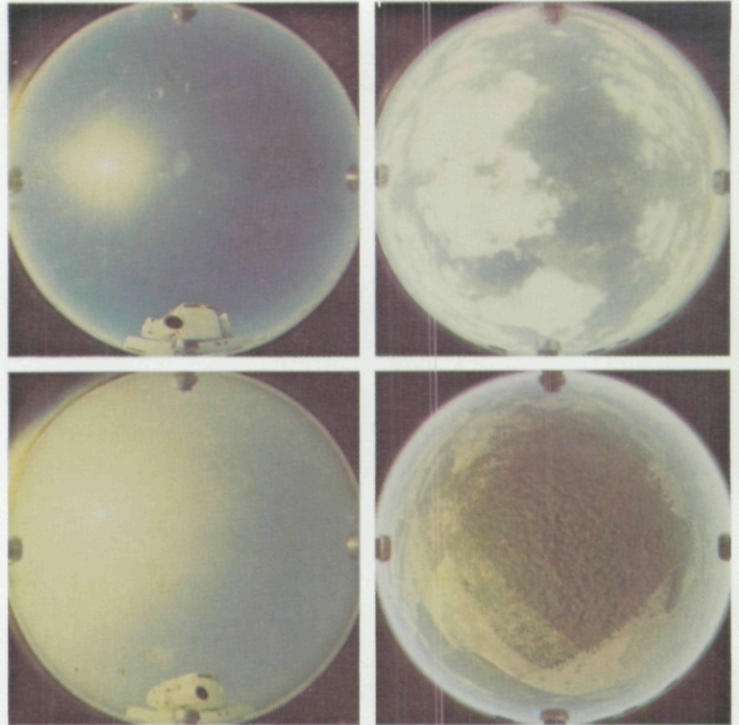
Upper and Lower Hemisphere
1434m AGL 1757 GMT Track 4.



Upper and Lower Hemisphere
115m AGL 1731 GMT Track 4.

FLIGHT C-185A

Upper and Lower Hemisphere
2525m AGL 1610 GMT Track 7.

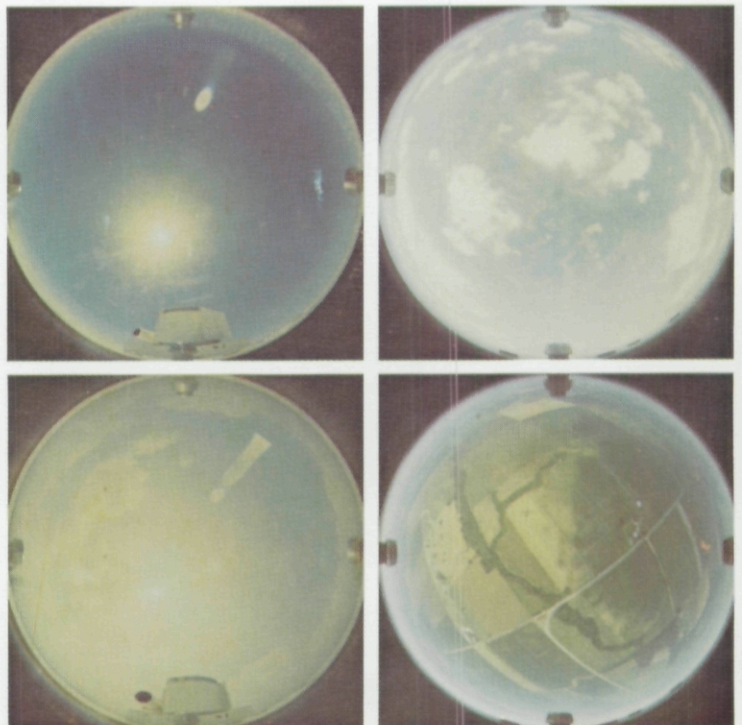


Upper and Lower Hemisphere
125m AGL 1525 GMT Track 7.

Fig. 7-2. Typical Sky and Terrain Photographs for Flight C-185.

FLIGHT C-185B

Upper and Lower Hemisphere
2626m AGL 1838 GMT Track 3.



Upper and Lower Hemisphere
188m AGL 1749 GMT Track 3.

Table 7-3

Vertical Beam Transmittance, Space to Sensor and Space to Ground

Flight No.	Date (1971)	Sensor Altitude (meters AGL)	Space-to-Sensor Beam Transmittance			Space-to-Ground Beam Transmittance		
			Filter 2	Filter 4	Filter 3	Filter 2	Filter 4	Filter 3
C-180	11 August	5100	0.885	0.704	0.950	0.485	0.505	0.711
C-183A	14 August	3000	0.886	0.943	0.934	0.494	0.616	0.690
C-185A	18 August	3000	0.860	0.915	0.926	0.335	0.456	0.562

7.2 DESCRIPTION OF AIRBORNE DATA TABLES AND GRAPHS

DATA TABLES

Data are presented in tables of:

- Irradiance
- Directional Reflectance of Terrain
- Total Scattering Coefficient
- Equivalent Attenuation Length from Ground to Altitude
- Beam Transmittance from Ground to Altitude
- Path Radiance from Ground to Altitude
- Directional Path Reflectance from Ground to Altitude

Each optical property is tabulated in the tables as a function of altitude above ground level except for the directional reflectance of terrain which is tabulated as a function of zenith angle. The data are further divided by optical filters which are given in order of increasing wavelength. The tables of directional reflectance of terrain, path radiance from ground to altitude, and directional path reflectance from ground to altitude are presented in four sets of four azimuths, with respect to the sun, of 0, 90, 180, and 270 degrees.

Irradiance. The downwelling irradiances $H(z,d)$ and upwelling irradiances $H(z,u)$, albedos $H(z,u)/H(z,d)$, scalar irradiances $h_s(z)$, $h_k(z,d)$, $h(z,u)$, and $h(z)$, and scalar albedos $h(z,u)/h(z,d)$ are presented in columnar form as a function of altitude. The irradiances are computed from measurements of sky and terrain radiance made by the airborne 2π scanner system at each of the flight profile level altitudes.

The altitudes are given in meters above ground level for the altitudes of flight. There are four tables of irradiance for each flight, one table for each optical filter. The dimensions and units for the irradiances are " $\text{wm}^{-2}\mu\text{m}^{-1}$ ". Albedos are, of course, dimensionless.

The irradiances for Filter Code Number 4 can be converted to illuminance values in units of lumens per square meter by multiplying each irradiance by the factor $72.0 \text{ lu}\mu\text{m}/\text{w}$.

Directional Reflectance of Terrain. The directional terrain reflectance $R_o(z,\theta,\phi)$ is tabulated by zenith angle in four columns for the optical filters. A table is presented for each of the four azimuthal points. Reflectance is dimensionless. These reflectances are based on the apparent terrain radiance and the downwelling irradiance measured at the minimum aircraft altitude.

It should be stressed again that the reflectances presented in this section are typical of the average terrain beneath the flight path. The lower hemisphere scanner has a 5-degree circular field of view and, during the data-taking interval, the aircraft is traveling at approximately 150 knots. Both of these characteristics contribute to the optical smearing of the measurement area and the attendant radiometric averaging.

The background reflectance required as input to a contrast transmittance computation must represent the actual background at the immediate boundary of the target object. This will not necessarily be the same as the average reflectance of the surrounding area.

Inherent and Apparent Terrain Radiances. The terrain radiance is not included in these tables. The inherent radiance of the terrain $N_o(z_t,\theta,\phi)$ immediately surrounding the target may be computed from the directional reflectance of the terrain $R_o(0,\theta,\phi)$ and the downwelling irradiance $H(z_t,d)$:

$$N_o(z_t,\theta,\phi) = \frac{1}{\pi} R_o(z_t,\theta,\phi) H(z_t,d) . \quad (7.1)$$

The downwelling irradiance at the lowest flight altitude for each filter may be used as the ground-level irradiance with reasonable accuracy (Duntley *et al.* (1970), p. 7-25). The apparent terrain radiance $N_r(z,\theta,\phi)$ at the sensor altitude z can be computed as follows:

$$N_r(z,\theta,\phi) = N_o(z_t,\theta,\phi) T_r(z,\theta) + N_r^*(z,\theta,\phi) . \quad (7.2)$$

The beam transmittances $T_r(z,\theta)$ and the path radiances $N_r^*(z,\theta,\phi)$ from ground to altitude are given in the tables to be described later.

The terrain radiances for Filter Code Number 4 may be converted to luminance values in units of $\text{lu}/\Omega\text{m}^2$ by multiplying the radiance by the factor $72.0 \text{ lu}\mu\text{m}/\text{w}$.

Total Scattering Coefficient. The total volume scattering coefficient $s(z)$ is tabulated by altitude in three columns for the three optical filters. The altitude is given in meters, above ground level, at 30-meter (98.4-foot) increments. The dimension and unit for the total scattering coefficient is "m⁻¹".

At the bottom of the total scattering coefficient table are given the first and last data altitudes. This is the lowest and highest altitude of data measurements. When ground-based measurements of total scattering coefficient are available, the first data altitude is ground level.

The total scattering coefficient is used for the calculation of atmospheric beam transmittance in the next set of tables using the equations of the Theory, Section 2.

Equivalent Attenuation Length from Ground to Altitude. The equivalent attenuation length $\bar{L}(z)$ is a pseudo-attenuation length which, when combined with its altitude z , can be used directly in Eq. 2.12 to compute beam transmittance. The equivalent attenuation length permits easy calculation of the atmospheric beam transmittance between ground level and altitude z above ground level for a downward path of sight, or between altitude and ground level for the upward path of sight.

The equivalent attenuation length $\bar{L}(z)$ is tabulated by altitude for the path of sight between ground and the altitude shown in three columns for the three optical filters. The altitude is given in meters, above ground level, at 300-meter (984-foot) increments. The dimension and unit for the equivalent attenuation length is "km".

Beam Transmittance from Ground to Altitude. The atmospheric beam transmittance $T_r(z, \theta)$ is tabulated in two types of tables: one for the vertical path of sight and one for the slant paths of sight. Only the vertical path of sight table is given for the cloudy days.

The beam transmittance is tabulated for the vertical path of sight, between ground and the altitude shown, in three columns for the three optical filters. The altitude is given in meters, above ground level, at 300-meter (984-foot) increments. This property is dimensionless.

The atmospheric beam transmittance for the relatively clear days is tabulated for the slant paths of sight, between ground and the altitude shown, for the six zenith angles from 95 to 180 degrees. There are three tables, one for each optical filter. This property is dimensionless.

The beam transmittance is computed from measurements of total scattering coefficient. The assumption is made that there is no significant atmospheric absorption in the pass bands of the measurements, whence the atmospheric attenuation coefficient $\alpha(z)$ is assumed equivalent to the scattering coefficient $s(z)$.

Path Radiance from Ground to Altitude. Path radiance $N_r^*(z, \theta, \phi)$ is tabulated for the slant paths of sight, between ground and the altitude shown, for the six zenith angles from 95 to 180 degrees. The path radiance is computed from measurements of total scattering coefficient, measurements of sky and terrain radiances, and a catalog of proportional directional scattering coefficients based upon the work of Barteneva (1960).

There are four sets of data tables, one set for each of the four cardinal azimuths from the sun, 0, 90, 180, and 270 degrees. Each set is listed on a single sheet and contains three tables, one for each spectral filter. The dimensions and units are " $w\Omega^{-1}m^{-2}\mu m^{-1}$ ".

The path radiance values for Filter 4 may be converted to path luminance values with units of $lu/\Omega m^2$ by multiplying the radiance by the factor $72.0 lu\mu m/w$.

Directional Path Reflectance from Ground to Altitude. Directional path reflectance $R_r^*(z,\theta,\phi)$ is also tabulated for the downward-looking slant paths of sight, between ground and the altitude shown, for the six zenith angles from 95 to 180 degrees. The directional path reflectance is computed from the previously derived values of path radiance, beam transmittance, and total downwelling irradiance.

There are four sets of data tables, one set for each of the four cardinal azimuths from the sun, 0, 90, 180, and 270 degrees. Each set is listed on a single sheet and contains three tables, one for each spectral filter. This property is dimensionless.

Contrast Transmittance. Contrast transmittance ${}_b\tau_t(z,\theta,\phi)$ is not tabulated. This optical property is a function of the directional path reflectance and the directional background reflectance against which an object is viewed. The directional terrain reflectance reported herein is measured by the airborne radiometer. Thus, it is the average reflectance of many individual areas integrated into one value by the 5-degree circular field of the radiometer. The background reflectance against which the object is viewed will probably never be the same as the reflectance of the average terrain. If the area of the background is sufficiently small, its reflectance will have no appreciable effect on the path reflectance. In such cases, decoupling exists between the object background area and the atmospheric path reflectance and the contrast transmittance may be calculated by Eq. 3 of Duntley (1969) repeated below:

$${}_b\tau_t(z,\theta,\phi) = \left\{ 1 + [R_r^*(z,\theta,\phi) / {}_bR_o(z,\theta,\phi)] \right\}^{-1} \quad (7.3)$$

DATA GRAPHS

Data are also presented in graphs of:

- Downwelling Irradiance
- Total Scattering Coefficient
- Equivalent Attenuation Length from Ground to Altitude
- Vertical Beam Transmittance from Ground to Altitude
- Path Radiance from Ground to Altitude
- Directional Path Reflectance from Ground to Altitude.

Downwelling Irradiance. The downwelling irradiance $H(z,d)$ is graphed as a function of altitude AGL. These irradiances are from column 2 of the irradiance table. They are computed from the sky measurements and the sun irradiance at each of the flight profile level altitudes.

Total Scattering Coefficient. The total volume scattering coefficient $s(z)$ in m^{-1} is graphed using a single average value for each 30-meter change in altitude. Identifying symbols for the spectral filters appear at every fifth data point, or at 150-meter intervals. These same data were tabulated in the total scattering coefficient table.

Equivalent Attenuation Length from Ground to Altitude. The equivalent attenuation length $\bar{L}(z)$ in kilometers, for the path between ground and altitude, is graphed for each 30-meter change in altitude. Spectral identifying symbols appear at 150-meter intervals or every fifth data point.

Vertical Beam Transmittance from Ground to Altitude. The vertical beam transmittance $T_r(0,0)$ or $T_r(z,180)$ between ground and altitude is graphed for each 30-meter interval. Spectral identifying symbols appear at 150-meter intervals or every fifth data point. This represents smaller altitude increments than in the tabular display of beam transmittance.

Path Radiance from Ground to Altitude. The path radiance $N_r^*(z,\theta,\phi)$ is graphed for downward-looking slant paths between ground and the altitude shown. Each graph is for one path of sight for all three optical filters. The first graph is for the vertical downward path of sight, the second and third are for zenith angles 120 and 100 degrees toward the azimuth of the sun. These are data selected from the path radiance tables.

Directional Path Reflectance from Ground to Altitude. The directional path reflectance $R_r^*(z,\theta,\phi)$ is also graphed for downward-looking slant paths between ground and the altitude shown. Each graph is for one path of sight and three optical filters. The first graph is for the vertical downward path of sight, the second and third are for zenith angles 120 and 100 degrees toward the azimuth of the sun. These selected paths of sight are the same as for the path radiance graphs. The data were selected from the many paths of sight tabulated in the directional path reflectance tables.

7.3 PRESENTATION OF AIRBORNE DATA

Tabular listings and graphical displays of the data discussed in Section 7.2 are presented in the pages immediately following. Users should be aware that regardless of the display format, the data values are valid to, at best, only three significant figures. The tables of beam transmittance and directional reflectance of the terrain, in particular, should be rounded off to two digits prior to further application.

It should also be remembered that all values in the data tables except scattering coefficient are computed values based upon the measured values of upper and lower hemisphere radiances. All other direct radiometric measurements made by the airborne data systems are used only for corroboration and cross-checking.

All altitudes presented in the data tables, in the flight description, and in the graphs are given as above ground level (AGL) unless otherwise specified. The flight log entries have two altitudes specified: (1) the altitude of flight in meters AGL at the time of the observation and (2) the estimated altitude in feet mean sea level (MSL) of the observed cloud or haze feature.

FLIGHT C-180 – 11 AUGUST 1971 – TRACK 1 – DESCRIPTION OF FLIGHT AND WEATHER CHARACTERISTICS

It was a sunlit afternoon. There were scattered cumulus clouds during the flight. These cumulus dissipated, and a layer of thin cirrostratus formed by the end of the flight. The flight was conducted over farmlands and a river north of St. Louis. The typical terrain was cultivated farmlands. The data-taking started at 1933 GMT (1433 CDT) and continued until 2321 GMT (1821 CDT). The sun zenith angle during sky radiance data-taking for Filters 2, 3, and 4 was 31.1 degrees at the beginning and 51.9 degrees at the end. The maximum altitude for the flight was 5064 meters. Average terrain elevation along this track was 192 meters.

At the beginning of data-taking, Scott Air Force Base was reporting 0.2 cumulus clouds at 5000 feet (1500 meters) with a visibility of 12 miles (19 kilometers).

The ground station, located at Scott 51 miles (82 kilometers) from the center of the flight path, recorded no data since it did not operate on this day.

During the flight, the aircrew made the following observations, which have been extracted from the flight log and summarized. Metric altitudes have been added editorially.

FLIGHT LOG ENTRY

Time (GMT)	Altitude (m AGL)	Aircrew Observations
1955	1470	Cumulus bases at approximately 5500 ft (1670 m) MSL
1959	1470	Below top of haze layer 5500 ft (1670 m) MSL
2047	2670	On top. Moderate haze below and scattered cumulus on the horizons.
2111	5070	Clear overhead

At the end of data-taking, Scott was reporting 0.7 thin cirrostratus at 30 000 feet (9000 meters) and a visibility of 15 miles (24 kilometers).

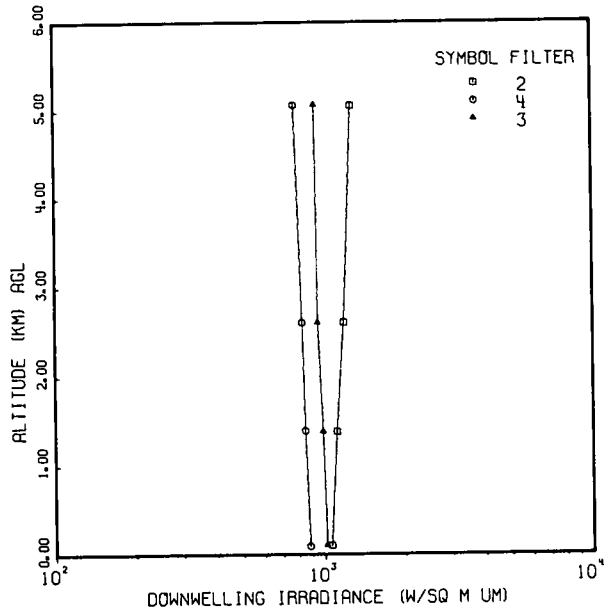
The surface synoptic chart shows that there was a cold frontal passage accompanied by thunder-showers at about 0600 GMT. By 2100 GMT the front had moved to a line from Altoona, to Bowling Green, and then to northern Arkansas and Oklahoma where it became stationary. A weak high existed over the middle half of the country with St. Louis on the leading edge.

At 500 millibars there was a trough from Hudson Bay southward to Illinois. There was a low over the Texas Panhandle. Moderate westerly winds were present.

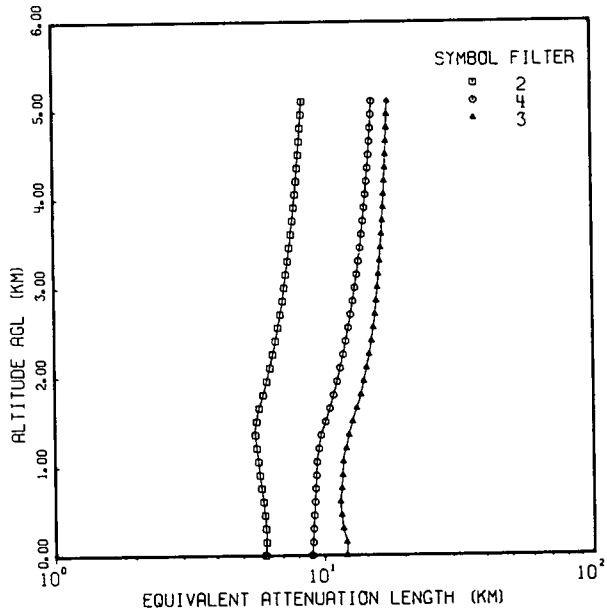
These data were taken from the 3-hourly facsimile charts issued by the National Meteorological Center (NMC) and obtained from Lindbergh Field NOAA office. The 500-millibar charts are for 0000 GMT and 1200 GMT daily.

FLIGHT NO. C-180

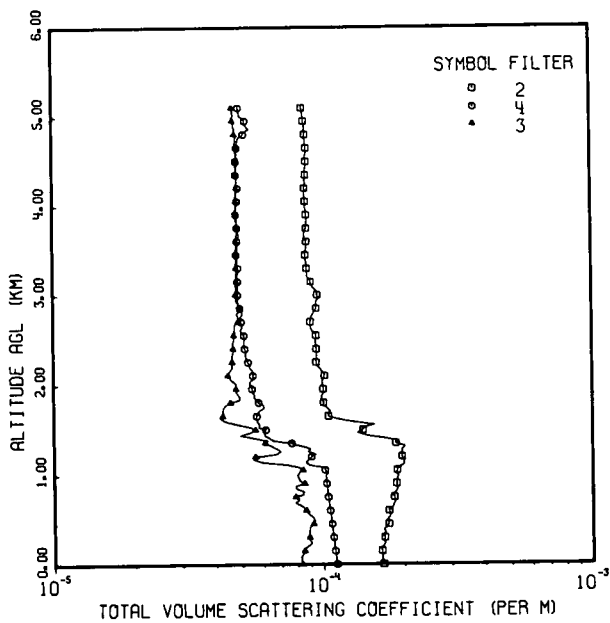
FLIGHT C-180



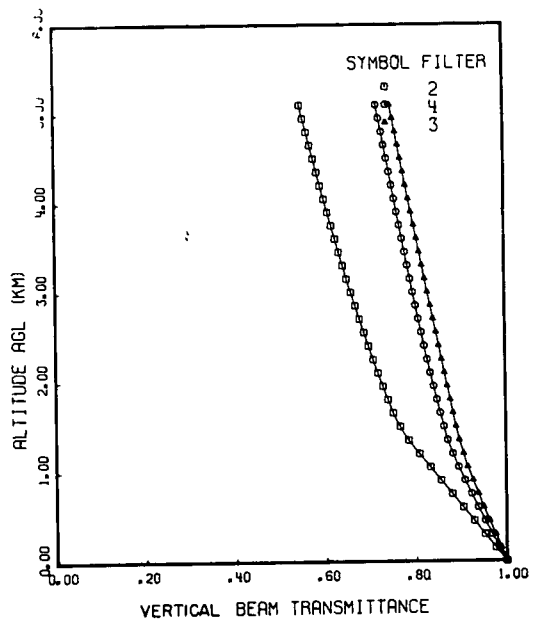
FLIGHT C-180



FLIGHT C-180

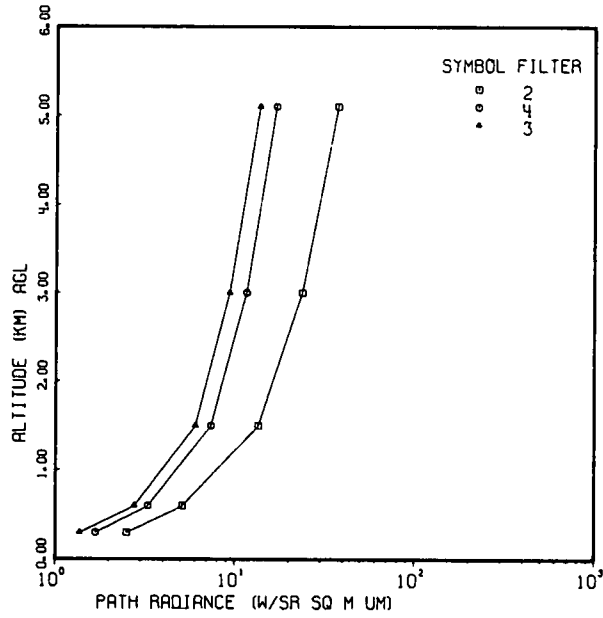


FLIGHT C-180

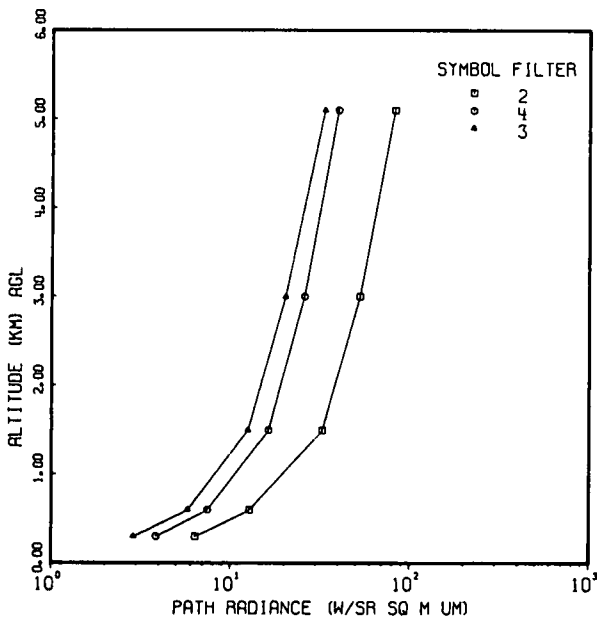


FLIGHT NO. C-180

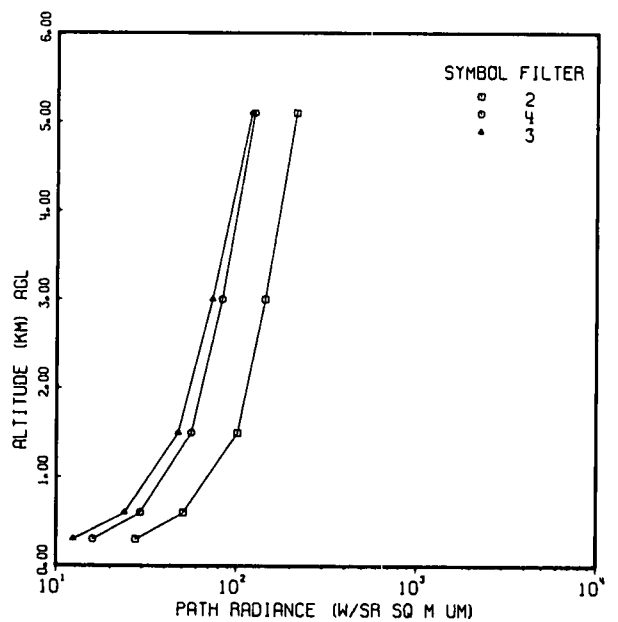
FLIGHT C-180 ZENITH ANGLE 180
AZIMUTH 0



FLIGHT C-180 ZENITH ANGLE 120
AZIMUTH 0

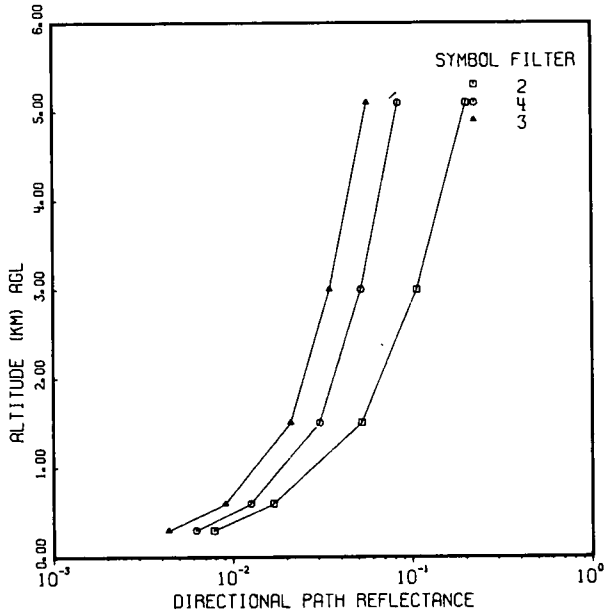


FLIGHT C-180 ZENITH ANGLE 100
AZIMUTH 0

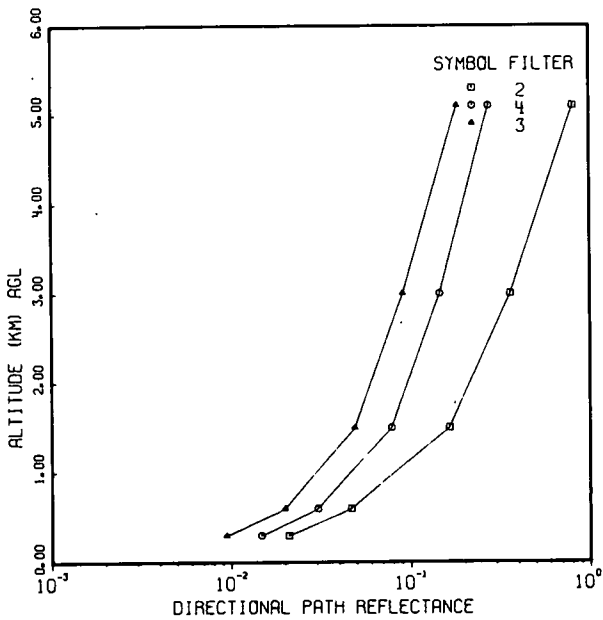


FLIGHT NO. C-180

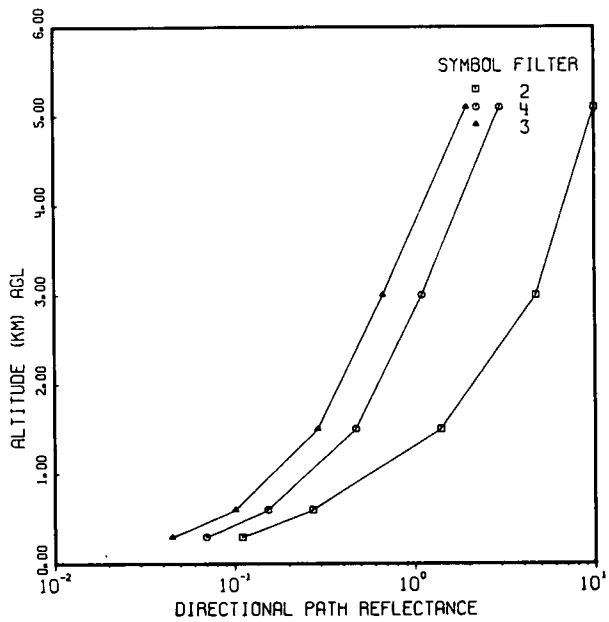
FLIGHT C-180 ZENITH ANGLE 180
AZIMUTH 0



FLIGHT C-180 ZENITH ANGLE 120
AZIMUTH 0



FLIGHT C-180 ZENITH ANGLE 100
AZIMUTH 0



FLIGHT NO. C-180

IRRADIANCE

(JOB 5786 DATE 03/18/74)
 FLIGHT NO. C-180 FILTER NO. 2 SUN ZENITH ANGLE 40.5
 IRRADIANCE (W/SQ M UP)

ALTITUDE (METERS)	DOWN-WELLING	UP-WELLING	ALBEDO	SCALAR SUN	SCALAR SKY	SCALAR UPWELLING	SCALAR TOTAL	SCALAR ALBEDO
102	1.06E 03	4.94E 01	.046	8.22E 02	7.32E 02	1.24E 02	1.68E 03	.080
1384	1.11E 03	1.02E 02	.092	1.12E 03	4.86E 02	2.92E 02	1.89E 03	.182
2604	1.19E 03	1.11E 02	.093	1.33E 03	4.81E 02	3.25E 02	2.14E 03	.180
5056	1.28E 03	1.36E 02	.107	1.77E 03	4.20E 02	4.11E 02	2.60E 03	.187

FLIGHT NO. C-180 FILTER NO. 4 SUN ZENITH ANGLE 40.5
 IRRADIANCE (W/SQ M UP)

ALTITUDE (METERS)	DOWN-WELLING	UP-WELLING	ALBEDO	SCALAR SUN	SCALAR SKY	SCALAR UPWELLING	SCALAR TOTAL	SCALAR ALBEDO
93	8.77E 02	9.07E 01	.092	7.65E 02	4.79E 02	1.75E 02	1.42E 03	.140
1391	8.48E 02	1.03E 02	.121	9.08E 02	2.83E 02	2.54E 02	1.45E 03	.213
2603	8.30E 02	1.05E 02	.127	9.93E 02	2.55E 02	2.81E 02	1.53E 03	.225
5059	7.82E 02	1.11E 02	.142	1.16E 03	1.93E 02	3.16E 02	1.67E 03	.233

FLIGHT NO. C-180 FILTER NO. 3 SUN ZENITH ANGLE 40.5
 IRRADIANCE (W/SQ M UP)

ALTITUDE (METERS)	DOWN-WELLING	UP-WELLING	ALBEDO	SCALAR SUN	SCALAR SKY	SCALAR UPWELLING	SCALAR TOTAL	SCALAR ALBEDO
106	1.01E 03	5.15E 01	.051	9.90E 02	3.51E 02	1.06E 02	1.45E 03	.079
1383	9.87E 02	5.90E 01	.060	1.13E 03	1.61E 02	1.51E 02	1.44E 03	.117
2603	9.50E 02	6.42E 01	.068	1.22E 03	1.27E 02	1.70E 02	1.52E 03	.126
5064	9.34E 02	6.40E 01	.069	1.43E 03	1.14E 02	1.91E 02	1.73E 03	.124

FLIGHT NO. C-180

DIRECTIONAL REFLECTANCE OF TERRAIN

(JOB 5786 DATE 03/18/74)
 FLIGHT NO. C-180
 AZIMUTH OF PATH OF SIGHT = 0
 DIRECTIONAL REFLECTANCE OF TERRAIN
 FILTERS

ZENITH ANGLE	2	4	3
95	.1388	.1547	.0485
100	.0672	.1082	.0525
105	.0662	.0863	.0409
120	.0290	.0800	.0601
150	.0590	.0500	.0336
180	.0426	.0735	.0359

FLIGHT NO. C-180
 AZIMUTH OF PATH OF SIGHT = 90
 DIRECTIONAL REFLECTANCE OF TERRAIN
 FILTERS

ZENITH ANGLE	2	4	3
95	.0879	.1154	.0449
100	.0717	.0995	.0409
105	.0536	.0861	.0465
120	.0571	.0735	.0371
150	.0211	.0502	.0733
180	.0426	.0735	.0359

FLIGHT NO. C-180
 AZIMUTH OF PATH OF SIGHT = 180
 DIRECTIONAL REFLECTANCE OF TERRAIN
 FILTERS

ZENITH ANGLE	2	4	3
95	.1014	.1182	.0795
100	.0626	.1021	.0606
105	.0528	.1113	.0596
120	.0757	.1691	.0445
150	.0709	.0824	.1675
180	.0426	.0735	.0359

FLIGHT NO. C-180
 AZIMUTH OF PATH OF SIGHT = 270
 DIRECTIONAL REFLECTANCE OF TERRAIN
 FILTERS

ZENITH ANGLE	2	4	3
95	.1425	.1168	.0604
100	.0626	.0964	.0609
105	.0402	.1002	.0822
120	.0316	.0747	.0426
150	.0286	.1027	.0438
180	.0426	.0735	.0359

FLIGHT NO. C-180

TOTAL VOLUME SCATTERING COEFFICIENT

(JOB 5786 DATE 03/18/74)
 DATE 81171 FLIGHT NO. C-180 GROUND LEVEL ALTITUDE (M)= 183

ALTITUDE (M)	TOTAL VOLUME SCATTERING COEFFICIENT (PER M)		
	FILTERS	2	4
0	1.66E-04	1.12E-04	8.30E-05
30	1.65E-04	1.11E-04	8.25E-05
60	1.65E-04	1.11E-04	8.23E-05
90	1.64E-04	1.10E-04	8.21E-05
120	1.64E-04	1.10E-04	8.35E-05
150	1.64E-04	1.10E-04	8.47E-05
180	1.63E-04	1.10E-04	8.51E-05
210	1.67E-04	1.09E-04	8.78E-05
240	1.68E-04	1.09E-04	9.02E-05
270	1.66E-04	1.09E-04	8.94E-05
300	1.68E-04	1.08E-04	8.84E-05
330	1.65E-04	1.08E-04	8.80E-05
360	1.70E-04	1.08E-04	8.83E-05
390	1.67E-04	1.08E-04	8.86E-05
420	1.69E-04	1.07E-04	8.86E-05
450	1.74E-04	1.07E-04	9.15E-05
480	1.75E-04	1.07E-04	9.26E-05
510	1.72E-04	1.06E-04	9.20E-05
540	1.76E-04	1.06E-04	8.97E-05
570	1.76E-04	1.06E-04	8.73E-05
600	1.74E-04	1.05E-04	8.61E-05
630	1.80E-04	1.05E-04	8.46E-05
660	1.82E-04	1.05E-04	8.20E-05
690	1.83E-04	1.05E-04	7.83E-05
720	1.83E-04	1.04E-04	8.13E-05
750	1.83E-04	1.04E-04	7.87E-05
780	1.80E-04	1.04E-04	8.42E-05
810	1.85E-04	1.03E-04	8.44E-05
840	1.88E-04	1.03E-04	7.92E-05
870	1.87E-04	1.03E-04	7.87E-05
900	1.86E-04	1.02E-04	8.51E-05
930	1.88E-04	1.02E-04	8.14E-05
960	1.88E-04	1.02E-04	8.07E-05
990	1.89E-04	1.02E-04	7.99E-05
1020	1.86E-04	1.04E-04	8.10E-05
1050	1.88E-04	1.01E-04	8.39E-05
1080	1.90E-04	1.01E-04	8.12E-05
1110	1.98E-04	8.82E-05	7.35E-05
1140	1.99E-04	8.63E-05	5.92E-05
1170	1.99E-04	8.79E-05	5.49E-05
1200	1.96E-04	9.02E-05	5.60E-05
1230	1.95E-04	9.39E-05	6.69E-05
1260	1.96E-04	8.77E-05	6.98E-05
1290	1.97E-04	8.97E-05	6.70E-05
1320	2.01E-04	8.31E-05	6.41E-05
1350	1.85E-04	7.63E-05	6.08E-05
1380	1.90E-04	6.52E-05	6.24E-05
1410	1.67E-04	6.28E-05	5.50E-05
1440	1.45E-04	6.02E-05	4.91E-05
1470	1.34E-04	6.03E-05	5.35E-05
1500	1.41E-04	6.11E-05	5.62E-05

FLIGHT NO. C-180
TOTAL VOLUME SCATTERING COEFFICIENT

(JOB 5786 DATE 03/13/74)
 DATE 81171 FLIGHT NO. C-180 GROUND LEVEL ALTITUDE (M)= 183

ALTITUDE (M)	TOTAL VOLUME SCATTERING COEFFICIENT (PER M)			
	FILTERS	2	4	3
1530		1.42E-04	5.75E-05	5.35E-05
1560		1.55E-04	5.80E-05	4.84E-05
1590		1.30E-04	5.71E-05	4.39E-05
1620		1.15E-04	5.65E-05	4.18E-05
1650		1.05E-04	5.65E-05	4.25E-05
1680		1.05E-04	5.75E-05	4.26E-05
1710		1.06E-04	5.79E-05	4.27E-05
1740		1.04E-04	6.03E-05	4.27E-05
1770		1.00E-04	6.03E-05	4.35E-05
1800		1.00E-04	5.77E-05	4.55E-05
1830		9.96E-05	5.66E-05	4.91E-05
1860		9.85E-05	5.55E-05	4.92E-05
1890		9.94E-05	5.55E-05	4.83E-05
1920		1.01E-04	5.49E-05	4.76E-05
1950		1.00E-04	5.46E-05	4.76E-05
1980		1.00E-04	5.51E-05	4.78E-05
2010		9.93E-05	5.44E-05	4.77E-05
2040		9.92E-05	5.39E-05	4.62E-05
2070		1.00E-04	5.48E-05	4.52E-05
2100		1.01E-04	5.40E-05	4.45E-05
2130		1.01E-04	5.41E-05	4.48E-05
2160		9.90E-05	5.49E-05	4.55E-05
2190		9.69E-05	5.46E-05	4.61E-05
2220		9.54E-05	5.47E-05	4.61E-05
2250		9.46E-05	5.49E-05	4.62E-05
2280		9.52E-05	5.41E-05	4.61E-05
2310		9.50E-05	5.19E-05	4.63E-05
2340		9.50E-05	5.18E-05	4.64E-05
2370		9.50E-05	5.18E-05	4.55E-05
2400		9.47E-05	5.15E-05	4.67E-05
2430		9.47E-05	5.10E-05	4.67E-05
2460		9.44E-05	5.13E-05	4.66E-05
2490		9.42E-05	5.12E-05	4.68E-05
2520		9.49E-05	5.16E-05	4.69E-05
2550		9.48E-05	5.12E-05	4.70E-05
2580		9.41E-05	5.04E-05	4.74E-05
2610		9.10E-05	4.96E-05	4.73E-05
2640		9.04E-05	5.3E-05	4.73E-05
2670		9.04E-05	5.17E-05	4.73E-05
2700		9.04E-05	5.00E-05	4.88E-05
2730		9.00E-05	4.98E-05	4.91E-05
2760		9.10E-05	4.79E-05	4.86E-05
2790		9.23E-05	5.06E-05	4.82E-05
2820		9.37E-05	5.03E-05	4.93E-05
2850		9.50E-05	4.95E-05	4.95E-05
2880		9.52E-05	4.99E-05	4.89E-05
2910		9.49E-05	4.79E-05	4.85E-05
2940		9.53E-05	4.16E-05	4.79E-05
2970		9.72E-05	4.99E-05	4.81E-05
3000		9.58E-05	4.17E-05	4.78E-05

FLIGHT NO. C-180
TOTAL VOLUME SCATTERING COEFFICIENT

(JOB 5786 DATE 03/18/74)
 DATE 81171 FLIGHT NO. C-180 GROUND LEVEL ALTITUDE (M)= 183

ALTITUDE (M)	FILTERS	TOTAL VOLUME SCATTERING COEFFICIENT (PER M)		
		2	4	3
3030	9.59E-05	4.88E-05	4.80E-05	
3060	9.46E-05	4.88E-05	4.80E-05	
3090	9.20E-05	4.85E-05	4.78E-05	
3120	9.07E-05	4.89E-05	4.79E-05	
3150	9.06E-05	4.87E-05	4.82E-05	
3180	8.96E-05	4.86E-05	4.81E-05	
3210	8.79E-05	4.85E-05	4.83E-05	
3240	8.80E-05	4.88E-05	4.82E-05	
3270	8.82E-05	4.88E-05	4.84E-05	
3300	8.78E-05	4.88E-05	4.80E-05	
3330	8.83E-05	4.86E-05	4.80E-05	
3360	8.78E-05	4.86E-05	4.82E-05	
3390	8.71E-05	4.86E-05	4.82E-05	
3420	8.70E-05	4.84E-05	4.81E-05	
3450	8.69E-05	4.83E-05	4.82E-05	
3480	8.66E-05	4.85E-05	4.83E-05	
3510	8.76E-05	4.87E-05	4.81E-05	
3540	8.77E-05	4.88E-05	4.82E-05	
3570	8.74E-05	4.87E-05	4.84E-05	
3600	8.77E-05	4.86E-05	4.81E-05	
3630	8.63E-05	4.91E-05	4.91E-05	
3660	8.63E-05	4.95E-05	4.84E-05	
3690	8.64E-05	4.91E-05	4.86E-05	
3720	8.63E-05	4.92E-05	4.90E-05	
3750	8.77E-05	4.86E-05	4.88E-05	
3780	8.83E-05	4.85E-05	4.88E-05	
3810	8.81E-05	4.86E-05	4.87E-05	
3840	8.83E-05	4.88E-05	4.79E-05	
3870	8.78E-05	4.79E-05	4.83E-05	
3900	8.78E-05	4.81E-05	4.82E-05	
3930	8.79E-05	4.87E-05	4.81E-05	
3960	8.77E-05	4.84E-05	4.82E-05	
3990	8.68E-05	4.85E-05	4.82E-05	
4020	8.76E-05	4.87E-05	4.84E-05	
4050	8.72E-05	4.87E-05	4.82E-05	
4080	8.72E-05	4.86E-05	4.86E-05	
4110	8.70E-05	4.80E-05	4.86E-05	
4140	8.68E-05	4.85E-05	4.83E-05	
4170	8.70E-05	4.84E-05	4.85E-05	
4200	8.65E-05	4.89E-05	4.85E-05	
4230	8.75E-05	4.85E-05	4.85E-05	
4260	8.75E-05	4.86E-05	4.86E-05	
4290	8.67E-05	4.87E-05	4.85E-05	
4320	8.74E-05	4.86E-05	4.88E-05	
4350	8.75E-05	4.83E-05	4.86E-05	
4380	8.72E-05	4.85E-05	4.87E-05	
4410	8.75E-05	4.84E-05	4.86E-05	
4440	8.77E-05	4.88E-05	4.83E-05	
4470	8.78E-05	4.80E-05	4.89E-05	
4500	8.79E-05	4.82E-05	4.87E-05	

FLIGHT NO. C-180
TOTAL VOLUME SCATTERING COEFFICIENT

(JOB 5786 DATE 03/18/74)
 DATE 81171 FLIGHT NO. C-180 GROUND LEVEL ALTITUDE (M)= 183

ALTITUDE (M)	FILTERS	TOTAL VOLUME SCATTERING COEFFICIENT (PER M)		
		2	4	3
4530	8.73E-05	4.74E-05	4.87E-05	
4560	8.74E-05	4.86E-05	4.85E-05	
4590	8.80E-05	4.88E-05	4.84E-05	
4620	8.80E-05	4.81E-05	4.85E-05	
4650	8.80E-05	4.89E-05	4.85E-05	
4680	8.79E-05	4.41E-05	4.82E-05	
4710	8.74E-05	4.92E-05	4.82E-05	
4740	8.74E-05	4.94E-05	4.84E-05	
4770	8.67E-05	4.98E-05	4.84E-05	
4800	8.73E-05	5.17E-05	4.79E-05	
4830	8.67E-05	5.22E-05	4.78E-05	
4860	8.71E-05	5.44E-05	4.80E-05	
4890	8.70E-05	5.32E-05	4.75E-05	
4920	8.66E-05	5.22E-05	4.75E-05	
4950	8.62E-05	5.24E-05	4.71E-05	
4980	8.62E-05	5.17E-05	4.68E-05	
5010	8.59E-05	5.00E-05	4.74E-05	
5040	8.57E-05	4.98E-05	4.73E-05	
5070	8.54E-05	4.97E-05	4.71E-05	
5100	8.51E-05	4.95E-05	4.70E-05	
FIRST DATA ALT	120	930	90	
LAST DATA ALT	4980	5010	5010	

FLIGHT NO. C-180
EQUIVALENT ATTENUATION LENGTH

(JOB 5786 DATE 03/18/74)
DATE 81171 FLIGHT NO. C-180 GROUND LEVEL ALTITUDE (M)= 183

ALTITUDE (M)	EQUIVALENT ATTENUATION LENGTH (KM)		
	FILTERS 2	4	3
0	6.02E 00	8.97E 00	1.21E 01
300	6.05E 00	9.13E 00	1.17E 01
600	5.94E 00	9.22E 00	1.15E 01
900	5.77E 00	9.35E 00	1.17E 01
1200	5.62E 00	9.57E 00	1.21E 01
1500	5.62E 00	1.01E 01	1.28E 01
1800	5.95E 00	1.03E 01	1.37E 01
2100	6.32E 00	1.13E 01	1.45E 01
2400	6.64E 00	1.21E 01	1.51E 01
2700	5.94E 00	1.27E 01	1.56E 01
3000	7.19E 00	1.32E 01	1.60E 01
3300	7.42E 00	1.36E 01	1.63E 01
3600	7.65E 00	1.40E 01	1.66E 01
3900	7.85E 00	1.43E 01	1.69E 01
4200	8.03E 00	1.47E 01	1.71E 01
4500	8.19E 00	1.50E 01	1.73E 01
4800	8.34E 00	1.52E 01	1.75E 01
5100	8.48E 00	1.54E 01	1.76E 01

FLIGHT NO. C-180
VERTICAL BEAM TRANSMITTANCE FROM GROUND TO ALTITUDE

ALTITUDE (M)	VERTICAL BEAM TRANSMITTANCE FROM GROUND TO ALTITUDE		
	FILTERS 2	4	3
0	1.00E 00	1.00E 00	1.00E 00
300	9.52E-01	9.58E-01	9.75E-01
600	9.04E-01	9.37E-01	9.49E-01
900	8.56E-01	9.09E-01	9.26E-01
1200	8.08E-01	8.82E-01	9.05E-01
1500	7.60E-01	8.62E-01	8.89E-01
1800	7.39E-01	8.47E-01	8.77E-01
2100	7.17E-01	8.34E-01	8.65E-01
2400	6.97E-01	8.20E-01	8.53E-01
2700	6.78E-01	8.08E-01	8.41E-01
3000	6.59E-01	7.95E-01	8.29E-01
3300	6.41E-01	7.85E-01	8.17E-01
3600	6.25E-01	7.73E-01	8.05E-01
3900	6.08E-01	7.62E-01	7.94E-01
4200	5.93E-01	7.51E-01	7.82E-01
4500	5.77E-01	7.40E-01	7.71E-01
4800	5.62E-01	7.29E-01	7.60E-01
5100	5.48E-01	7.18E-01	7.49E-01

FLIGHT NO. C-180

BEAM TRANSMITTANCE FROM GROUND TO ALTITUDE

(JOB 5786 DATE 03/13/74)

ALTITUDE M	FLIGHT NO. C-180					FILTER NO. 2	180
	BEAM TRANSMITTANCE FROM GROUND TO ALTITUDE						
	ZENITH ANGLE OF PATH OF SIGHT (DEG)						
	95	100	105	120	150		
300	5.65E-01	7.52E-01	8.26E-01	9.06E-01	9.44E-01	9.52E-01	9.52E-01
600	3.17E-01	5.59E-01	6.77E-01	8.17E-01	8.90E-01	9.04E-01	9.04E-01
1500	4.49E-02	2.15E-01	3.57E-01	5.86E-01	7.35E-01	7.66E-01	7.66E-01
3000	7.11E-03	9.04E-02	1.99E-01	4.34E-01	6.18E-01	6.59E-01	6.59E-01
5100	6.67E-04	3.13E-02	9.79E-02	3.00E-01	4.99E-01	5.48E-01	5.48E-01

ALTITUDE M	FLIGHT NO. C-180					FILTER NO. 4	180
	BEAM TRANSMITTANCE FROM GROUND TO ALTITUDE						
	ZENITH ANGLE OF PATH OF SIGHT (DEG)						
	95	100	105	120	150		
300	6.84E-01	8.27E-01	8.80E-01	9.36E-01	9.63E-01	9.68E-01	9.68E-01
600	4.72E-01	6.98E-01	7.78E-01	8.78E-01	9.28E-01	9.37E-01	9.37E-01
1500	1.78E-01	4.26E-01	5.64E-01	7.44E-01	8.43E-01	8.62E-01	8.62E-01
3000	6.68E-02	2.69E-01	4.14E-01	6.34E-01	7.68E-01	7.96E-01	7.96E-01
5100	1.76E-02	1.49E-01	2.78E-01	5.16E-01	6.82E-01	7.18E-01	7.18E-01

ALTITUDE M	FLIGHT NO. C-180					FILTER NO. 3	180
	BEAM TRANSMITTANCE FROM GROUND TO ALTITUDE						
	ZENITH ANGLE OF PATH OF SIGHT (DEG)						
	95	100	105	120	150		
300	7.45E-01	8.63E-01	9.06E-01	9.50E-01	9.71E-01	9.75E-01	9.75E-01
600	5.46E-01	7.40E-01	8.17E-01	9.01E-01	9.41E-01	9.49E-01	9.49E-01
1500	2.55E-01	5.09E-01	6.35E-01	7.91E-01	8.73E-01	8.89E-01	8.89E-01
3000	1.08E-01	3.39E-01	4.84E-01	6.87E-01	8.05E-01	8.29E-01	8.29E-01
5100	3.00E-02	1.89E-01	3.27E-01	5.61E-01	7.16E-01	7.49E-01	7.49E-01

FLIGHT NO. C-180
PATH RADIANCE FROM GROUND TO ALTITUDE
AZIMUTH OF PATH OF SIGHT = 0

(JOB 5786 DATE 03/18/74)

AZIMUTH OF PATH OF SIGHT = 0

ALTITUDE M	FLIGHT NO. C-180 FILTER NO. 2					
	PATH RADIANCE FROM GROUND TO ALTITUDE (W/SR SQ M UM)					
	ZENITH ANGLE OF PATH OF SIGHT (DEG)					
	95	100	105	120	150	180
300	6.03E 01	2.77E 01	1.69E 01	6.36E 00	2.71E 00	2.51E 00
600	9.64E 01	5.09E 01	3.75E 01	1.28E 01	5.54E 00	5.11E 00
1500	1.46E 02	1.01E 02	7.20E 01	3.25E 01	1.47E 01	1.35E 01
3000	1.94E 02	1.44E 02	1.08E 02	5.27E 01	2.51E 01	2.36E 01
5100	2.88E 02	2.13E 02	1.63E 02	8.19E 01	3.95E 01	3.72E 01

ALTITUDE M	FLIGHT NO. C-180 FILTER NO. 4					
	PATH RADIANCE FROM GROUND TO ALTITUDE (W/SR SQ M UM)					
	ZENITH ANGLE OF PATH OF SIGHT (DEG)					
	95	100	105	120	150	180
300	3.62E 01	1.60E 01	9.76E 00	3.84E 00	1.79E 00	1.68E 00
600	5.03E 01	2.93E 01	1.84E 01	7.46E 00	3.51E 00	3.29E 00
1500	9.55E 01	5.62E 01	3.75E 01	1.63E 01	7.83E 00	7.34E 00
3000	1.29E 02	8.29E 01	5.72E 01	2.58E 01	1.23E 01	1.15E 01
5100	1.85E 02	1.24E 02	8.77E 01	3.96E 01	1.82E 01	1.68E 01

ALTITUDE M	FLIGHT NO. C-180 FILTER NO. 3					
	PATH RADIANCE FROM GROUND TO ALTITUDE (W/SR SQ M UM)					
	ZENITH ANGLE OF PATH OF SIGHT (DEG)					
	95	100	105	120	150	180
300	2.94E 01	1.25E 01	7.49E 00	2.87E 00	1.35E 00	1.37E 00
600	5.22E 01	2.41E 01	1.48E 01	5.79E 00	2.72E 00	2.77E 00
1500	8.76E 01	4.75E 01	3.04E 01	1.25E 01	5.86E 00	6.02E 00
3000	1.23E 02	7.34E 01	4.83E 01	2.02E 01	9.28E 00	9.30E 00
5100	1.92E 02	1.20E 02	8.10E 01	3.32E 01	1.43E 01	1.36E 01

FLIGHT NO. C-180
PATH RADIANCE FROM GROUND TO ALTITUDE
AZIMUTH OF PATH OF SIGHT = 90

(JOB 5786 DATE 03/18/74)

AZIMUTH OF PATH OF SIGHT = 90

ALTITUDE M	FLIGHT NO. C-180 FILTER NO. 2					
	PATH RADIANCE FROM GROUND TO ALTITUDE (W/SR SQ M UM)					
	ZENITH ANGLE OF PATH OF SIGHT (DEG)					
	95	100	105	120	150	180
300	3.74E 01	1.85E 01	1.21E 01	5.54E 00	2.86E 00	2.51E 00
600	5.93E 01	3.38E 01	2.31E 01	1.11E 01	5.83E 00	5.11E 00
1500	8.68E 01	6.58E 01	5.06E 01	2.78E 01	1.53E 01	1.35E 01
3000	1.05E 02	8.80E 01	7.25E 01	4.42E 01	2.63E 01	2.36E 01
5100	1.23E 02	1.10E 02	9.58E 01	6.46E 01	4.10E 01	3.72E 01

ALTITUDE M	FLIGHT NO. C-180 FILTER NO. 4					
	PATH RADIANCE FROM GROUND TO ALTITUDE (W/SR SQ M UM)					
	ZENITH ANGLE OF PATH OF SIGHT (DEG)					
	95	100	105	120	150	180
300	2.26E 01	1.08E 01	7.11E 00	3.36E 00	1.84E 00	1.68E 00
600	3.71E 01	1.97E 01	1.33E 01	6.51E 00	3.61E 00	3.29E 00
1500	5.63E 01	3.67E 01	2.68E 01	1.42E 01	8.07E 00	7.34E 00
3000	6.66E 01	4.95E 01	3.81E 01	2.17E 01	1.27E 01	1.15E 01
5100	7.47E 01	6.17E 01	5.02E 01	3.08E 01	1.86E 01	1.68E 01

ALTITUDE M	FLIGHT NO. C-180 FILTER NO. 3					
	PATH RADIANCE FROM GROUND TO ALTITUDE (W/SR SQ M UM)					
	ZENITH ANGLE OF PATH OF SIGHT (DEG)					
	95	100	105	120	150	180
300	1.61E 01	7.58E 00	4.99E 00	2.43E 00	1.47E 00	1.37E 00
600	2.79E 01	1.44E 01	9.70E 00	4.85E 00	2.96E 00	2.77E 00
1500	4.35E 01	2.68E 01	1.92E 01	1.03E 01	6.38E 00	6.02E 00
3000	5.14E 01	3.64E 01	2.76E 01	1.57E 01	9.94E 00	9.30E 00
5100	5.88E 01	4.72E 01	3.78E 01	2.31E 01	1.48E 01	1.36E 01

FLIGHT NO. C-180
PATH RADIANCE FROM GROUND TO ALTITUDE
AZIMUTH OF PATH OF SIGHT = 180

(JOB 5786 DATE 03/18/74)

AZIMUTH OF PATH OF SIGHT = 180

ALTITUDE M	FLIGHT NO. C-180 FILTER NO. 2					
	PATH RADIANCE FROM GROUND TO ALTITUDE (W/SR SQ M UM)					
	ZENITH ANGLE OF PATH OF SIGHT (DEG)					
	95	100	105	120	150	180
300	3.40E C1	1.75E C1	1.19E 01	6.07E 00	3.50E 00	2.51E 00
600	5.44E C1	3.21E 01	2.28E 01	1.22E 01	7.14E C0	5.11E 00
1500	8.20E 01	6.39E 01	5.07E 01	3.09E 01	1.88E C1	1.35E 01
3000	1.11E C2	9.38E 01	7.93E 01	5.39E 01	3.39E 01	2.36E 01
5100	1.40E C2	1.28E 02	1.15E 02	8.71E 01	5.44E 01	3.72E 01

ALTITUDE M	FLIGHT NO. C-180 FILTER NO. 4					
	PATH RADIANCE FROM GROUND TO ALTITUDE (W/SR SQ M UM)					
	ZENITH ANGLE OF PATH OF SIGHT (DEG)					
	95	100	105	120	150	180
300	2.12E 01	1.07E J1	7.34E C0	3.92E 00	2.32E C0	1.68E C0
600	3.52E 01	1.95E 01	1.38E 01	7.60E 00	4.53E C0	3.29E 00
1500	5.51E C1	3.72E 01	2.81E 01	1.66E 01	1.01E 01	7.34E 00
3000	6.90E 01	5.24E 01	4.16E 01	2.62E 01	1.60E C1	1.15E 01
5100	8.19E 01	6.90E 01	5.79E 01	3.91E 01	2.36E C1	1.68E 01

ALTITUDE M	FLIGHT NO. C-180 FILTER NO. 3					
	PATH RADIANCE FROM GROUND TO ALTITUDE (W/SR SQ M UM)					
	ZENITH ANGLE OF PATH OF SIGHT (DEG)					
	95	100	105	120	150	180
300	1.52E C1	7.56E C0	5.26E 00	2.92E 00	1.96E C0	1.37E 00
600	2.65E C1	1.44E 01	1.03E 01	5.88E 00	3.96E C0	2.77E 00
1500	4.18E 01	3.72E 01	2.07E 01	1.26E 01	8.57E C0	6.02E 00
3000	5.21E 01	3.88E 01	3.09E 01	2.01E 01	1.34E 01	9.30E 00
5100	6.35E C1	5.29E 01	4.46E 01	3.13E 01	2.00E 01	1.36E 01

FLIGHT NO. C-180
PATH RADIANCE FROM GROUND TO ALTITUDE
AZIMUTH OF PATH OF SIGHT = 270

(JOB 5786 DATE 03/18/74)

AZIMUTH OF PATH OF SIGHT = 270

ALTITUDE M	FLIGHT NO. C-180 FILTER NO. 2					
	PATH RADIANCE FROM GROUND TO ALTITUDE (W/SR SQ M UM)					
	ZENITH ANGLE OF PATH OF SIGHT (DEG)					
	95	100	105	120	150	180
300	3.93E 01	1.93E 01	1.25E 01	5.61E 00	2.88E 00	2.51E 00
600	6.15E 01	3.49E 01	2.37E 01	1.12E 01	5.86E 00	5.11E 00
1500	8.63E 01	6.56E 01	5.04E 01	2.76E 01	1.54E 01	1.35E 01
3000	1.04E 02	8.70E 01	7.18E 01	4.40E 01	2.65E 01	2.36E 01
5100	1.22E 02	1.09E 02	9.52E 01	6.45E 01	4.14E 01	3.72E 01

ALTITUDE M	FLIGHT NO. C-180 FILTER NO. 4					
	PATH RADIANCE FROM GROUND TO ALTITUDE (W/SR SQ M UM)					
	ZENITH ANGLE OF PATH OF SIGHT (DEG)					
	95	100	105	120	150	180
300	2.25E 01	1.09E 01	7.18E 00	3.48E 00	1.96E 00	1.68E 00
600	3.70E 01	1.97E 01	1.34E 01	6.71E 00	3.82E 00	3.29E 00
1500	5.56E 01	3.65E 01	2.67E 01	1.45E 01	8.49E 00	7.34E 00
3000	6.49E 01	4.85E 01	3.76E 01	2.19E 01	1.32E 01	1.15E 01
5100	7.32E 01	6.06E 01	4.96E 01	3.09E 01	1.92E 01	1.68E 01

ALTITUDE M	FLIGHT NO. C-180 FILTER NO. 3					
	PATH RADIANCE FROM GROUND TO ALTITUDE (W/SR SQ M UM)					
	ZENITH ANGLE OF PATH OF SIGHT (DEG)					
	95	100	105	120	150	180
300	1.66E 01	7.83E 00	5.17E 00	2.51E 00	1.48E 00	1.35E 00
600	2.86E 01	1.47E 01	9.98E 00	4.99E 00	2.98E 00	2.73E 00
1500	4.35E 01	2.69E 01	1.94E 01	1.04E 01	6.41E 00	5.89E 00
3000	5.14E 01	3.66E 01	2.78E 01	1.59E 01	1.00E 01	9.19E 00
5100	5.89E 01	4.73E 01	3.80E 01	2.33E 01	1.49E 01	1.37E 01

FLIGHT NO. C-180
DIRECTIONAL PATH REFLECTANCE FROM GROUND TO ALTITUDE
AZIMUTH OF PATH OF SIGHT = 0

(JOB 5786 DATE 03/18/74)

AZIMUTH OF PATH OF SIGHT = 0

ALTITUDE M	FLIGHT NO. C-180 FILTER NO. 2					
	DIRECTIONAL PATH REFLECTANCE FROM GROUND TO ALTITUDE					
	ZENITH ANGLE OF PATH OF SIGHT (DEG)					
	95	100	105	120	150	180
300	3.17E-C1	1.09E-01	6.10E-02	2.09E-02	8.54E-C3	7.83E-03
600	9.19E-01	2.70E-01	1.43E-01	4.66E-02	1.85E-02	1.68E-02
1500	9.65E C0	1.40E 00	6.00E-01	1.65E-01	5.94E-02	5.24E-02
3000	8.12E C1	4.73E 00	1.60E 00	3.61E-01	1.21E-C1	1.06E-01
5100	1.29E 03	2.02E 01	4.96E 00	8.11E-01	2.35E-C1	2.02E-01

ALTITUDE M	FLIGHT NO. C-180 FILTER NO. 4					
	DIRECTIONAL PATH REFLECTANCE FROM GROUND TO ALTITUDE					
	ZENITH ANGLE OF PATH OF SIGHT (DEG)					
	95	100	105	120	150	180
300	1.89E-C1	6.93E-02	3.97E-02	1.47E-02	6.67E-03	6.22E-03
600	4.58E-C1	1.53E-01	8.47E-02	3.04E-02	1.35E-C2	1.26E-02
1500	1.92E 00	4.72E-01	2.38E-01	7.86E-02	3.33E-C2	3.05E-02
3000	6.91E 00	1.10E 00	4.95E-01	1.46E-01	5.73E-02	5.19E-02
5100	3.73E C1	3.00E 00	1.13E 00	2.75E-01	9.56E-02	8.40E-02

ALTITUDE M	FLIGHT NO. C-180 FILTER NO. 3					
	DIRECTIONAL PATH REFLECTANCE FROM GROUND TO ALTITUDE					
	ZENITH ANGLE OF PATH OF SIGHT (DEG)					
	95	100	105	120	150	180
300	1.22E-01	4.47E-02	2.56E-02	9.38E-03	4.31E-C3	4.36E-03
600	2.96E-01	1.01E-01	5.01E-02	1.99E-02	8.97E-03	9.06E-03
1500	1.07E 00	2.90E-01	1.49E-01	4.90E-02	2.09E-C2	2.10E-02
3000	3.53E C0	6.70E-01	3.09E-01	9.11E-02	3.57E-C2	3.48E-02
5100	1.98E 01	1.97E 00	7.66E-01	1.83E-01	6.17E-C2	5.64E-02

FLIGHT NO. C-180
DIRECTIONAL PATH REFLECTANCE FROM GROUND TO ALTITUDE
AZIMUTH OF PATH OF SIGHT = 90

(JOB 5786 DATE 03/18/74)

AZIMUTH OF PATH OF SIGHT = 90

ALTITUDE M	FLIGHT NO. C-180 FILTER NO. 2					
	DIRECTIONAL PATH REFLECTANCE FROM GROUND TO ALTITUDE					
	ZENITH ANGLE OF PATH OF SIGHT (DEG)					
	95	100	105	120	150	180
300	1.97E-01	7.33E-02	4.37E-02	1.82E-02	9.00E-03	7.83E-03
600	5.65E-01	1.80E-01	1.02E-01	4.04E-02	1.95E-02	1.68E-02
1500	5.75E 00	9.09E-01	4.22E-01	1.41E-01	6.21E-02	5.24E-02
3000	4.40E 01	7.89E 00	1.08E 00	3.03E-01	1.27E-01	1.06E-01
5100	5.48E 02	1.04E 01	2.91E 00	6.39E-01	2.44E-01	2.02E-01

ALTITUDE M	FLIGHT NO. C-180 FILTER NO. 4					
	DIRECTIONAL PATH REFLECTANCE FROM GROUND TO ALTITUDE					
	ZENITH ANGLE OF PATH OF SIGHT (DEG)					
	95	100	105	120	150	180
300	1.18E-01	4.69E-02	2.89E-02	1.29E-02	6.85E-03	6.22E-03
600	2.82E-01	1.03E-01	6.14E-02	2.66E-02	1.39E-02	1.26E-02
1500	1.13E 00	3.09E-01	1.70E-01	6.84E-02	3.43E-02	3.05E-02
3000	3.57E 00	6.59E-01	3.30E-01	1.23E-01	5.93E-02	5.19E-02
5100	1.50E 01	1.49E 00	6.47E-01	2.14E-01	9.78E-02	8.40E-02

ALTITUDE M	FLIGHT NO. C-180 FILTER NO. 3					
	DIRECTIONAL PATH REFLECTANCE FROM GROUND TO ALTITUDE					
	ZENITH ANGLE OF PATH OF SIGHT (DEG)					
	95	100	105	120	150	180
300	6.69E-02	2.72E-02	1.71E-02	7.92E-03	4.70E-03	4.36E-03
600	1.58E-01	6.02E-02	3.68E-02	1.67E-02	9.76E-03	9.06E-03
1500	5.29E-01	1.63E-01	9.37E-02	4.03E-02	2.26E-02	2.10E-02
3000	1.48E 00	3.33E-01	1.77E-01	7.10E-02	3.83E-02	3.48E-02
5100	6.07E 00	7.72E-01	3.58E-01	1.28E-01	6.42E-02	5.64E-02

FLIGHT NO. C-180
DIRECTIONAL PATH REFLECTANCE FROM GROUND TO ALTITUDE
AZIMUTH OF PATH OF SIGHT = 180

(JOB 5786 DATE 03/18/74)
 AZIMUTH OF PATH OF SIGHT = 180

ALTITUDE M	FLIGHT NO. C-180 FILTER NO. 2					
	DIRECTIONAL PATH REFLECTANCE FROM GROUND TO ALTITUDE					
	ZENITH ANGLE OF PATH OF SIGHT (DEG)					
	95	100	105	120	150	180
300	1.74E-01	5.93E-02	4.28E-02	1.99E-02	1.10E-02	7.83E-03
600	5.19E-01	1.71E-01	1.00E-01	4.44E-02	2.38E-02	1.68E-02
1500	5.43E 00	8.83E-01	4.23E-01	1.56E-01	7.60E-02	5.24E-02
3000	4.64E C1	3.08E C0	1.18E 00	3.69E-01	1.63E-C1	1.06E-01
5100	6.25E C2	1.21E 01	3.50E C0	8.62E-01	3.24E-C1	2.02E-01

ALTITUDE M	FLIGHT NO. C-180 FILTER NO. 4					
	DIRECTIONAL PATH REFLECTANCE FROM GROUND TO ALTITUDE					
	ZENITH ANGLE OF PATH OF SIGHT (DEG)					
	95	100	105	120	150	180
300	1.11E-01	4.62E-02	2.99E-02	1.50E-02	8.63E-03	6.22E-03
600	2.67E-01	1.02E-01	6.36E-02	3.10E-02	1.75E-02	1.26E-02
1500	1.11E 00	5.13E-01	1.78E-01	7.98E-02	4.30E-02	3.05E-02
3000	3.70E C0	6.98E-01	3.60E-01	1.48E-01	7.47E-02	5.19E-02
5100	1.65E 01	1.66E 00	7.46E-01	2.71E-01	1.24E-C1	8.40E-02

ALTITUDE M	FLIGHT NO. C-180 FILTER NO. 3					
	DIRECTIONAL PATH REFLECTANCE FROM GROUND TO ALTITUDE					
	ZENITH ANGLE OF PATH OF SIGHT (DEG)					
	95	100	105	120	150	180
300	6.32E-02	2.72E-02	1.30E-02	9.54E-03	6.25E-03	4.36E-03
600	1.65E-01	4.03E-02	3.90E-02	2.07E-02	1.30E-02	9.06E-03
1500	5.08E-01	1.66E-01	1.01E-01	4.95E-02	3.04E-02	2.10E-02
3000	1.50E C0	3.54E-01	1.98E-01	9.09E-02	5.18E-02	3.48E-02
5100	6.55E C0	8.66E-01	4.22E-01	1.73E-01	9.66E-02	5.64E-02

FLIGHT NO. C-180
DIRECTIONAL PATH REFLECTANCE FROM GROUND TO ALTITUDE
AZIMUTH OF PATH OF SIGHT = 270

(JOB 5786 DATE 03/18/74)
 AZIMUTH OF PATH OF SIGHT = 270

FLIGHT NO. C-180 FILTER NO. 2
 DIRECTIONAL PATH REFLECTANCE FROM GROUND TO ALTITUDE
 ZENITH ANGLE OF PATH OF SIGHT (DEG)

ALTITUDE	95	100	105	120	150	180
M						
300	2.07E-C1	7.64E-02	4.52E-02	1.84E-02	9.06E-03	7.83E-03
600	5.87E-C1	1.85E-01	1.04E-01	4.07E-02	1.96E-02	1.68E-02
1500	5.71E 00	9.06E-01	4.20E-01	1.40E-01	6.23E-02	5.24E-02
3000	4.34E 01	2.86E 00	1.07E 00	3.01E-01	1.27E-01	1.06E-01
5100	5.44E 02	1.04E 01	2.89E 00	6.38E-01	2.46E-01	2.02E-01

FLIGHT NO. C-180 FILTER NO. 4
 DIRECTIONAL PATH REFLECTANCE FROM GROUND TO ALTITUDE
 ZENITH ANGLE OF PATH OF SIGHT (DEG)

ALTITUDE	95	100	105	120	150	180
M						
300	1.18E-01	4.70E-02	2.92E-02	1.33E-02	7.28E-03	6.22E-03
600	2.80E-01	1.03E-01	6.18E-02	2.74E-02	1.48E-02	1.26E-02
1500	1.12E 00	3.06E-01	1.70E-01	6.99E-02	3.61E-02	3.05E-02
3000	3.48E 00	6.46E-01	3.25E-01	1.24E-01	6.16E-02	5.19E-02
5100	1.47E 01	1.46E 00	6.38E-01	2.15E-01	1.01E-01	8.40E-02

FLIGHT NO. C-180 FILTER NO. 3
 DIRECTIONAL PATH REFLECTANCE FROM GROUND TO ALTITUDE
 ZENITH ANGLE OF PATH OF SIGHT (DEG)

ALTITUDE	95	100	105	120	150	180
M						
300	6.90E-C2	2.81E-02	1.77E-02	8.20E-03	4.73E-03	4.31E-03
600	1.02E-C1	6.18E-02	3.79E-02	1.72E-02	9.82E-C3	8.93E-03
1500	5.30E-01	1.64E-01	9.46E-02	4.08E-02	2.28E-C2	2.05E-02
3000	1.48E 00	3.34E-01	1.78E-01	7.17E-02	3.85E-02	3.44E-02
5100	6.08E 00	7.74E-C1	3.60E-01	1.29E-01	6.46E-C2	5.65E-02

FLIGHT C-183A – 14 AUGUST 1971 – TRACK 7 – DESCRIPTION OF FLIGHT AND WEATHER CHARACTERISTICS

It was a sunlit morning. At the beginning of the flight there were scattered cumulus and altocumulus clouds. Cumulonimbus developed north of the station during the period of the flight. The flight was conducted over rolling hills southwest of St. Louis. The typical terrain was heavily wooded. The data-taking started at 1502 GMT (1002 CDT) and continued until 1635 GMT (1135 CDT). The sun zenith angle during sky radiance data-taking for Filters 2, 3, and 4 was 47.5 degrees at the beginning and 37.8 degrees at the end. The maximum altitude for the flight was 2550 meters. Average terrain elevation was 305 meters.

At the beginning of data-taking, Scott Air Force Base was reporting 0.2 cloud cover with scattered cumulus at 3500 feet (1050 meters) and scattered altocumulus at 15 000 feet (4500 meters). Visibility was 8 miles (13 kilometers) but there was haze all quadrants of the horizon.

The ground station located at Scott, 85 miles (137 kilometers) from the center of the flight path, recorded mostly clear, heavy cumulus buildup northern horizon.

During the flight, the aircrew made the following observations, which have been extracted from the flight log and summarized. Metric altitudes have been added editorially.

FLIGHT LOG ENTRY

Time (GMT)	Altitude (m AGL)	Aircrew Observations
-	-	Moderate to heavy haze, clear overhead
1510	-	Entering smoky area, sharply reduced visibility
1529	1345	Hazy at south end of track at 5500 ft (1670 m) MSL
1540	2545	On top of haze at 9500 ft (2900 m) MSL, basic layer appears to be about 7500 ft (2300 m) MSL thinning with a new layer from 9500 to 10 500 feet (2900 m to 3200 m) MSL
1633	1945	Large cloud buildup below and to the east

At the end of data-taking, Scott was reporting 0.8 cloud cover with scattered cumulus at 5000 feet (1500 meters) and thin broken cirrus at 25 000 feet (7500 meters). Visibility was 12 miles (19 kilometers). There were cumulonimbus clouds northwest and north of the station; their movements were unknown.

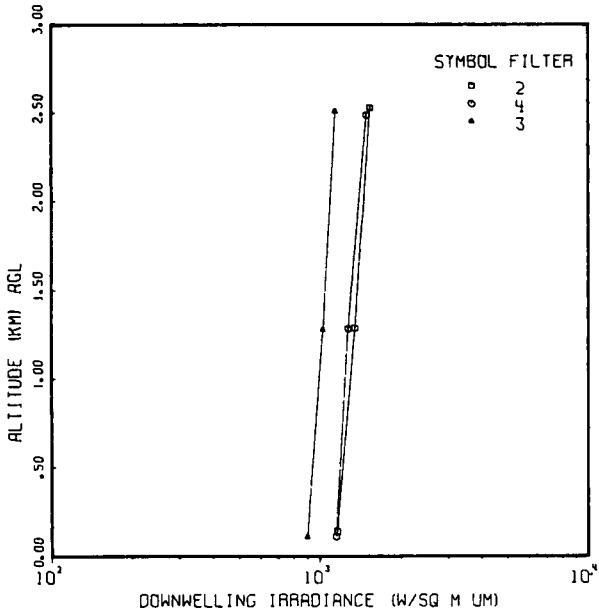
The surface synoptic chart shows that St. Louis was still on the rear of a high with its center near Pittsburgh. There was a cold front through Detroit, Davenport, and southern Nebraska, which extended northwestward to British Columbia. Tropical storm "Beth" was off the Virginia coast.

At 500 millibars there was a high area over Wyoming, Utah, Nevada, and California. Elsewhere there were very weak gradients.

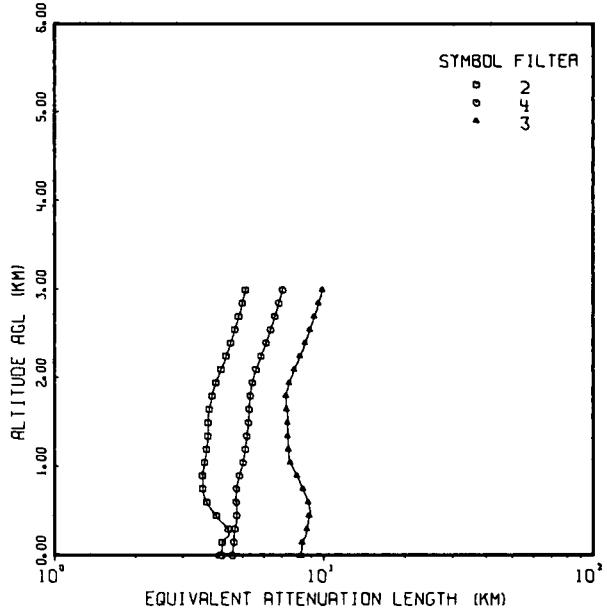
These data were taken from the 3-hourly facsimile charts issued by the NMC and obtained from Lindbergh Field NOAA office. The 500-millibar charts are for 0000 GMT and 1200 GMT daily.

FLIGHT NO. C-183A

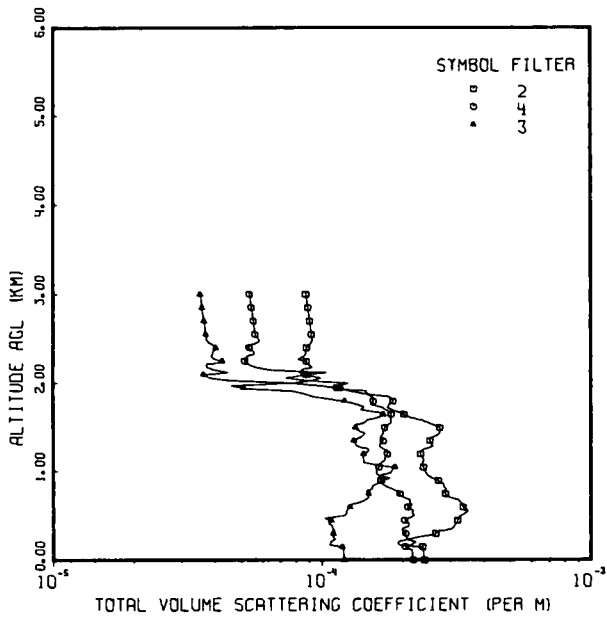
FLIGHT C-183A



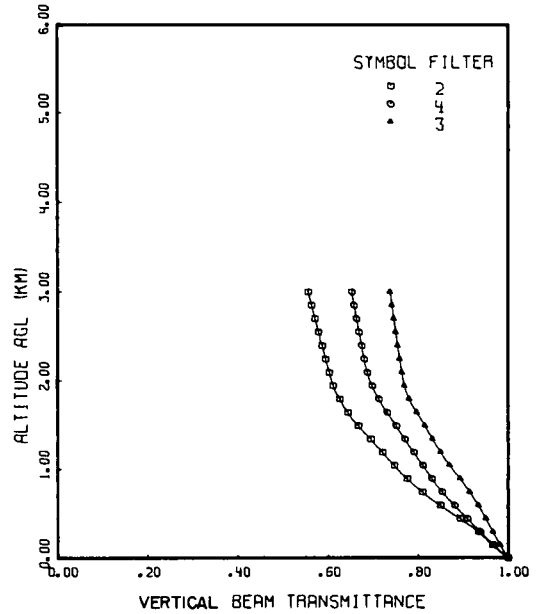
FLIGHT C-183A



FLIGHT C-183A

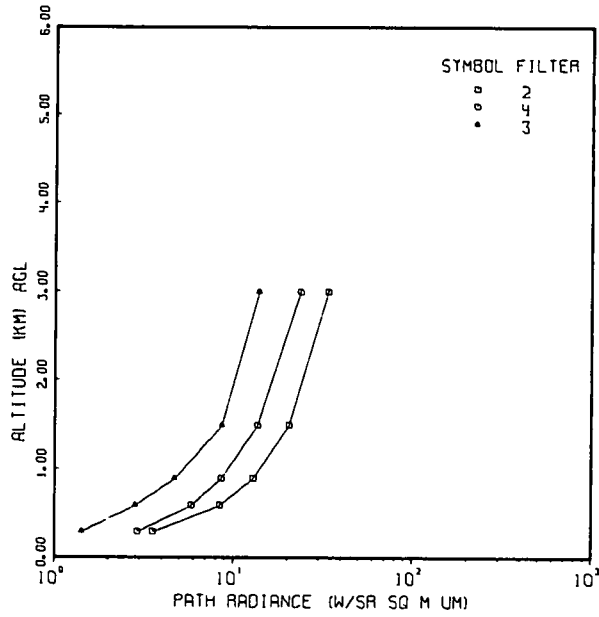


FLIGHT C-183A

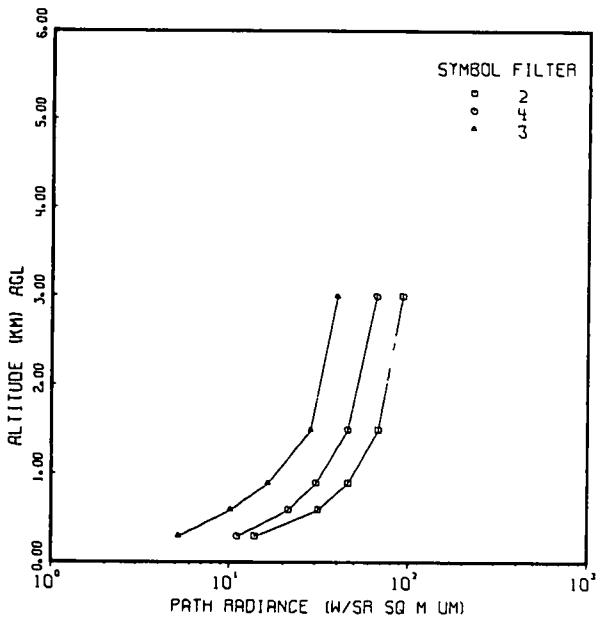


FLIGHT NO. C-183A

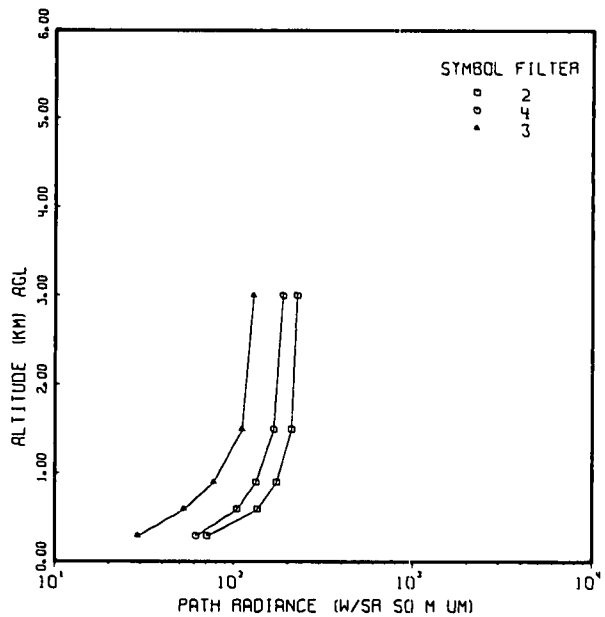
FLIGHT C-183A ZENITH ANGLE 180
AZIMUTH 0



FLIGHT C-183A ZENITH ANGLE 120
AZIMUTH 0

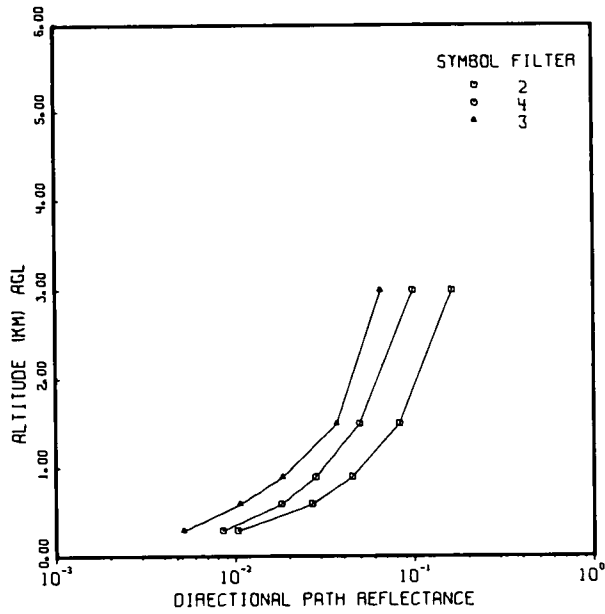


FLIGHT C-183A ZENITH ANGLE 100
AZIMUTH 0

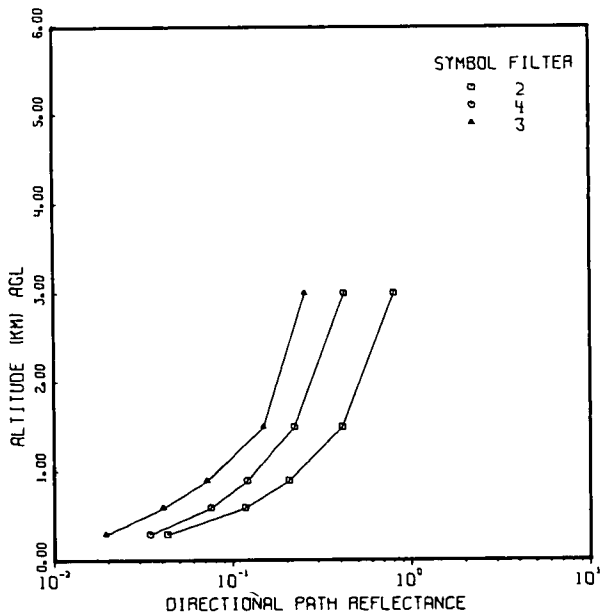


FLIGHT NO. C-183A

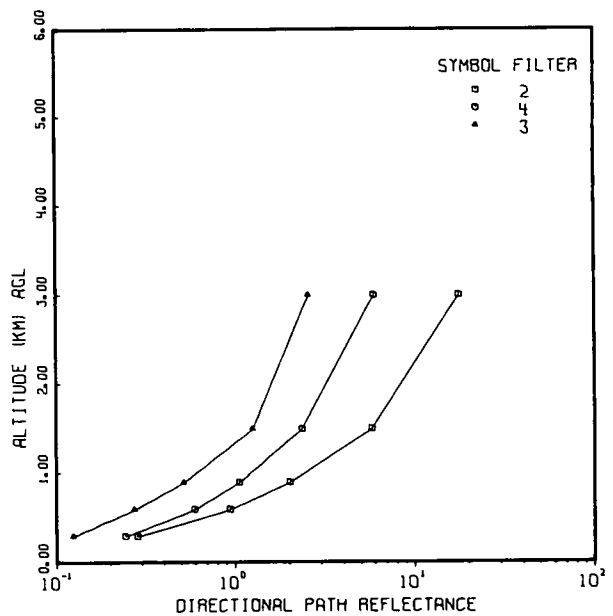
FLIGHT C-183A ZENITH ANGLE 180
AZIMUTH 0



FLIGHT C-183A ZENITH ANGLE 120
AZIMUTH 0



FLIGHT C-183A ZENITH ANGLE 100
AZIMUTH 0



FLIGHT NO. C-183A IRRADIANCE

(JOB 5627 DATE 04/25/73) FLIGHT NO. C-183A FILTER NO. 2 SUN ZENITH ANGLE 42.6

IRRADIANCE (W/SQ M UM)

ALTITUDE (METERS)	DCWN- WELLING	LP- WELLING	ALBEDO	SCALAR SUN	SCALAR SKY	SCALAR UPWELLING	SCALAR TOTAL	SCALAR ALBEDO
143	1.16E 03	4.3CE C1	.C37	8.41E 02	1.19E 03	1.32E 02	2.16E 03	.065
1288	1.35E 03	1.23E C2	.C91	1.28E 03	8.82E 02	3.73E 02	2.54E 03	.172
2530	1.54E 03	1.68E C2	.1C9	1.67E 03	5.84E 02	4.76E 02	2.73E 03	.211

FLIGHT NO. C-183A FILTER NO. 4 SUN ZENITH ANGLE 42.6

IRRADIANCE (W/SQ M UM)

ALTITUDE (METERS)	DOWN- WELLING	LP- WELLING	ALBEDO	SCALAR SUN	SCALAR SKY	SCALAR UPWELLING	SCALAR TOTAL	SCALAR ALBEDO
114	1.15E 03	5.12E C1	.C45	9.95E 02	9.45E 02	1.31E 02	2.07E 03	.068
1284	1.27E 03	1.15E C2	.C9C	1.35E 03	6.10E 02	3.34E 02	2.29E 03	.170
2488	1.49E 03	1.51E 02	.1C1	1.65E 03	4.26E 02	4.03E 02	2.48E 03	.195

FLIGHT NO. C-183A FILTER NO. 3 SUN ZENITH ANGLE 42.6

IRRADIANCE (W/SQ M UM)

ALTITUDE (METERS)	DCWN- WELLING	LP- WELLING	ALBEDO	SCALAR SUN	SCALAR SKY	SCALAR UPWELLING	SCALAR TOTAL	SCALAR ALBEDO
113	8.98E 02	4.68E C1	.C52	9.43E 02	5.46E 02	1.12E 02	1.60E 03	.075
1279	1.03E 03	7.91E C1	.C77	1.17E 03	3.65E 02	2.20E 02	1.76E 03	.143
2510	1.14E 03	1.03E C2	.C9C	1.36E 03	1.82E 02	2.66E 02	1.81E 03	.173

FLIGHT NO. C-183A

DIRECTIONAL REFLECTANCE OF TERRAIN

(JOB 5627 DATE 04/25/73)
 FLIGHT NO. C-183A
 AZIMUTH OF PATH OF SIGHT = 0
 DIRECTIONAL REFLECTANCE OF TERRAIN

ZENITH ANGLE	FILTERS		
	2	4	3
95	.2399	.1927	.1926
100	.1355	.1108	.0878
105	.0882	.0758	.0772
120	.0456	.0348	.0784
150	.0138	.0291	.0515
180	.0209	.0344	.0304

FLIGHT NO. C-183A

AZIMUTH OF PATH OF SIGHT = 90
 DIRECTIONAL REFLECTANCE OF TERRAIN

ZENITH ANGLE	FILTERS		
	2	4	3
95	.0881	.0831	.0853
100	.0739	.0618	.0673
105	.0593	.0545	.0360
120	.0411	.0339	.0610
150	.0135	.0312	.0432
180	.0209	.0344	.0304

FLIGHT NO. C-183A

AZIMUTH OF PATH OF SIGHT = 180
 DIRECTIONAL REFLECTANCE OF TERRAIN

ZENITH ANGLE	FILTERS		
	2	4	3
95	.0898	.0806	.0806
100	.0729	.0736	.0903
105	.0620	.0735	.1064
120	.0638	.0598	.0534
150	.0202	.0470	.0814
180	.0209	.0344	.0304

FLIGHT NO. C-183A

AZIMUTH OF PATH OF SIGHT = 270
 DIRECTIONAL REFLECTANCE OF TERRAIN

ZENITH ANGLE	FILTERS		
	2	4	3
95	.1154	.0820	.0809
100	.0760	.0680	.0668
105	.0508	.0543	.0541
120	.0583	.0394	.0415
150	.0166	.0381	.0636
180	.0209	.0344	.0304

FLIGHT NO. C-183A
TOTAL VOLUME SCATTERING COEFFICIENT

(JOB 5627 DATE 04/25/73)
 DATE 81471 FLIGHT NO. C-183A GROUND LEVEL ALTITUDE (M)= 305

ALTITUDE (M)	TOTAL VOLUME SCATTERING COEFFICIENT (PER M)			
	FILTERS	2	4	3
C		2.40E-04	2.18E-04	1.21E-04
30		2.39E-04	2.17E-04	1.21E-04
60		2.39E-04	2.17E-04	1.20E-04
90		2.38E-04	2.16E-04	1.20E-04
120		2.38E-04	2.16E-04	1.20E-04
150		2.37E-04	2.04E-04	1.19E-04
180		1.93E-04	2.16E-04	1.06E-04
210		1.92E-04	2.25E-04	1.08E-04
240		2.09E-04	2.06E-04	1.12E-04
270		2.30E-04	2.05E-04	1.09E-04
300		2.64E-04	2.05E-04	1.10E-04
330		2.73E-04	1.99E-04	1.11E-04
360		3.05E-04	1.98E-04	1.10E-04
390		3.11E-04	2.11E-04	1.09E-04
420		3.14E-04	2.11E-04	1.06E-04
450		3.20E-04	2.03E-04	1.08E-04
480		3.23E-04	2.11E-04	1.02E-04
510		3.29E-04	2.21E-04	1.21E-04
540		3.42E-04	2.17E-04	1.23E-04
570		3.51E-04	2.18E-04	1.23E-04
600		3.35E-04	2.08E-04	1.27E-04
630		3.34E-04	2.18E-04	1.29E-04
660		3.29E-04	2.11E-04	1.39E-04
690		3.22E-04	2.13E-04	1.46E-04
720		2.98E-04	1.99E-04	1.49E-04
750		2.88E-04	1.95E-04	1.49E-04
780		2.88E-04	1.91E-04	1.46E-04
810		2.90E-04	1.83E-04	1.54E-04
840		2.84E-04	1.74E-04	1.55E-04
870		2.83E-04	1.67E-04	1.61E-04
900		2.71E-04	1.65E-04	1.68E-04
930		2.59E-04	1.64E-04	1.79E-04
960		2.49E-04	1.63E-04	1.63E-04
990		2.45E-04	1.59E-04	1.80E-04
1020		2.40E-04	1.59E-04	1.83E-04
1050		2.39E-04	1.63E-04	1.87E-04
1080		2.36E-04	1.65E-04	1.62E-04
1110		2.36E-04	1.68E-04	1.43E-04
1140		2.39E-04	1.72E-04	1.43E-04
1170		2.37E-04	1.73E-04	1.42E-04
1200		2.32E-04	1.75E-04	1.43E-04
1230		2.34E-04	1.77E-04	1.49E-04
1260		2.40E-04	1.71E-04	1.49E-04
1290		2.59E-04	1.64E-04	1.36E-04
1320		2.57E-04	1.65E-04	1.33E-04
1350		2.52E-04	1.64E-04	1.32E-04
1380		2.52E-04	1.66E-04	1.36E-04
1410		2.64E-04	1.66E-04	1.42E-04
1440		2.75E-04	1.69E-04	1.45E-04
1470		2.73E-04	1.69E-04	1.37E-04
1500		2.74E-04	1.71E-04	1.34E-04

FLIGHT NO. C-183A
TOTAL VOLUME SCATTERING COEFFICIENT

(JOB 5627 DATE 04/25/73)
 DATE 81471 FLIGHT NO. C-183A GROUND LEVEL ALTITUDE (M)= 305

ALTITUDE (M)	TOTAL VOLUME SCATTERING COEFFICIENT (PER M)			
	FILTERS	2	4	3
1530		2.64E-04	1.76E-04	1.33E-04
1560		2.50E-04	1.81E-04	1.44E-04
1590		2.37E-04	1.81E-04	1.47E-04
1620		2.15E-04	1.80E-04	1.62E-04
1650		2.02E-04	1.81E-04	1.69E-04
1680		1.95E-04	1.79E-04	1.62E-04
1710		1.81E-04	1.73E-04	1.39E-04
1740		1.75E-04	1.65E-04	1.44E-04
1770		1.78E-04	1.51E-04	1.35E-04
1800		1.84E-04	1.55E-04	1.22E-04
1830		1.82E-04	1.56E-04	1.06E-04
1860		1.77E-04	1.53E-04	9.21E-05
1890		1.48E-04	1.46E-04	8.57E-05
1920		1.46E-04	1.28E-04	7.78E-05
1950		1.14E-04	1.16E-04	5.12E-05
1980		1.00E-04	1.18E-04	4.59E-05
2010		7.78E-05	1.25E-04	7.87E-05
2040		9.22E-05	8.69E-05	4.53E-05
2070		9.90E-05	7.34E-05	3.83E-05
2100		8.82E-05	8.65E-05	3.64E-05
2130		8.23E-05	1.04E-04	4.49E-05
2160		8.46E-05	6.39E-05	3.97E-05
2190		9.25E-05	5.69E-05	3.73E-05
2220		8.87E-05	5.34E-05	3.72E-05
2250		8.74E-05	5.16E-05	4.27E-05
2280		8.14E-05	5.32E-05	3.59E-05
2310		8.58E-05	5.23E-05	3.87E-05
2340		8.75E-05	5.61E-05	3.92E-05
2370		8.75E-05	5.57E-05	3.94E-05
2400		8.76E-05	5.36E-05	4.04E-05
2430		8.94E-05	5.23E-05	3.97E-05
2460		9.14E-05	5.72E-05	3.83E-05
2490		9.20E-05	5.87E-05	3.73E-05
2520		9.17E-05	5.75E-05	3.72E-05
2550		9.14E-05	5.64E-05	3.71E-05
2580		9.11E-05	5.63E-05	3.69E-05
2610		9.09E-05	5.61E-05	3.68E-05
2640		9.06E-05	5.59E-05	3.67E-05
2670		9.03E-05	5.57E-05	3.66E-05
2700		9.00E-05	5.56E-05	3.65E-05
2730		8.97E-05	5.54E-05	3.64E-05
2760		8.94E-05	5.52E-05	3.63E-05
2790		8.92E-05	5.50E-05	3.61E-05
2820		8.89E-05	5.49E-05	3.60E-05
2850		8.86E-05	5.47E-05	3.59E-05
2880		8.83E-05	5.45E-05	3.58E-05
2910		8.80E-05	5.43E-05	3.57E-05
2940		8.78E-05	5.42E-05	3.56E-05
2970		8.75E-05	5.40E-05	3.55E-05
3000		8.72E-05	5.38E-05	3.54E-05
FIRST DATA ALT		150	120	150
LAST DATA ALT		2490	2550	2490

FLIGHT NO. C-183A
EQUIVALENT ATTENUATION LENGTH

(JOB 5627 DATE 04/25/73)
 DATE 01471 FLIGHT NO. C-183A GROUND LEVEL ALTITUDE (M)= 305

ALTITUDE (M)	EQUIVALENT ATTENUATION LENGTH (KM)		
	FILTERS 2	4	3
0	4.16E CC	4.58E CC	8.25E CC
300	4.41E CC	4.69E CC	8.68E CC
600	3.68E CC	4.73E CC	8.76E CC
900	3.55E CC	4.87E CC	7.98E CC
1200	3.68E CC	5.11E CC	7.41E CC
1500	3.72E CC	5.26E CC	7.36E CC
1800	3.85E CC	5.34E CC	7.26E CC
2100	4.16E CC	5.62E CC	7.81E CC
2400	4.52E CC	6.12E CC	8.55E CC
2700	4.84E CC	6.60E CC	9.25E CC
3000	5.13E CC	7.05E CC	9.91E CC

FLIGHT NO. C-183A
VERTICAL BEAM TRANSMITTANCE FROM GROUND TO ALTITUDE

ALTITUDE (M)	VERTICAL BEAM TRANSMITTANCE FROM GROUND TO ALTITUDE		
	FILTERS 2	4	3
0	1.00E CC	1.00E CC	1.00E CC
300	9.34E-C1	9.38E-C1	9.66E-01
600	8.50E-C1	8.81E-C1	9.34E-01
900	7.76E-C1	8.31E-C1	8.93E-01
1200	7.21E-C1	7.91E-C1	8.51E-01
1500	6.68E-01	7.52E-C1	8.16E-01
1800	6.27E-C1	7.14E-C1	7.81E-01
2100	5.83E-C1	6.88E-C1	7.64E-01
2400	5.88E-C1	6.75E-C1	7.55E-01
2700	5.72E-C1	6.64E-C1	7.47E-01
3000	5.57E-C1	6.53E-C1	7.39E-01

FLIGHT NO. C-183A
BEAM TRANSMITTANCE FROM GROUND TO ALTITUDE

(JOB 5627 DATE 04/25/73)

ALTITUDE M	FLIGHT NO. C-183A FILTER NO. 2					180
	BEAM TRANSMITTANCE FROM GROUND TO ALTITUDE					
	ZENITH ANGLE OF PATH OF SIGHT (DEG)					
	95	100	105	120	150	
300	4.57E-C1	6.76E-C1	7.69E-C1	8.73E-01	9.25E-C1	9.34E-01
600	1.53E-01	3.91E-C1	5.33E-01	7.22E-01	8.28E-01	8.50E-01
900	5.33E-C2	2.32E-C1	3.75E-01	6.02E-01	7.46E-C1	7.76E-01
1500	9.17E-C3	9.81E-C2	2.11E-01	4.46E-01	6.28E-C1	6.68E-01
3000	6.60E-C4	3.45E-C2	1.04E-01	3.10E-C1	5.09E-C1	5.57E-01

ALTITUDE M	FLIGHT NO. C-183A FILTER NO. 4					180
	BEAM TRANSMITTANCE FROM GROUND TO ALTITUDE					
	ZENITH ANGLE OF PATH OF SIGHT (DEG)					
	95	100	105	120	150	
300	4.79E-C1	6.92E-C1	7.81E-01	8.80E-C1	9.29E-C1	9.38E-01
600	2.31E-C1	4.82E-C1	6.13E-01	7.76E-01	8.64E-01	8.81E-01
900	1.18E-C1	3.45E-C1	4.89E-01	6.91E-01	8.08E-01	8.31E-01
1500	3.61E-C2	1.93E-C1	3.32E-01	5.65E-01	7.19E-01	7.52E-01
3000	6.35E-C3	8.62E-C2	1.93E-01	4.27E-01	6.12E-C1	6.53E-01

ALTITUDE M	FLIGHT NO. C-183A FILTER NO. 3					180
	BEAM TRANSMITTANCE FROM GROUND TO ALTITUDE					
	ZENITH ANGLE OF PATH OF SIGHT (DEG)					
	95	100	105	120	150	
300	6.72E-C1	8.20E-C1	8.75E-C1	9.33E-01	9.61E-C1	9.66E-01
600	4.54E-C1	6.74E-C1	7.67E-C1	8.72E-C1	9.24E-01	9.34E-01
900	2.71E-C1	5.22E-C1	6.47E-C1	7.98E-01	8.78E-01	8.93E-01
1500	9.35E-C2	3.09E-C1	4.59E-C1	6.65E-01	7.90E-C1	8.16E-01
3000	2.75E-C2	1.75E-C1	3.10E-01	5.46E-01	7.05E-01	7.39E-01

FLIGHT NO. C-183A
PATH RADIANCE FROM GROUND TO ALTITUDE
AZIMUTH OF PATH OF SIGHT = 0

(JOB 5627 DATE 04/25/73)
 AZIMUTH OF PATH OF SIGHT = 0

ALTITUDE M	FLIGHT NO. C-183A FILTER NO. 2					
	PATH RADIANCE FROM GROUND TO ALTITUDE (W/SR SQ M CM)					
	ZENITH ANGLE OF PATH OF SIGHT (DEG)					
	95	100	105	120	150	180
300	1.49E C2	7.09E C1	4.19E 01	1.38E 01	4.38E 00	3.55E 00
600	2.30E C2	1.35E 02	8.65E 01	3.12E 01	1.03E 01	8.40E 00
900	2.57E C2	1.73E C2	1.18E 02	4.6CE 01	1.58E 01	1.29E 01
1500	2.73E C2	2.10E 02	1.54E 02	6.77E 01	2.48E 01	2.04E 01
3000	2.66E C2	2.25E C2	1.81E 02	9.19E 01	3.87E 01	3.37E 01

ALTITUDE M	FLIGHT NO. C-183A FILTER NO. 4					
	PATH RADIANCE FROM GROUND TO ALTITUDE (W/SR SQ M CM)					
	ZENITH ANGLE OF PATH OF SIGHT (DEG)					
	95	100	105	120	150	180
300	1.32E C2	6.14E 01	3.53E 01	1.10E 01	3.45E 00	2.91E 00
600	1.92E C2	1.04E C2	6.34E 01	2.13E 01	6.91E 00	5.81E 00
900	2.19E C2	1.33E 02	8.51E 01	3.04E 01	1.02E 01	8.55E 00
1500	2.39E C2	1.67E C2	1.15E 02	4.58E 01	1.62E 01	1.36E 01
3000	2.35E 02	1.88E C2	1.42E C2	6.58E 01	2.68E 01	2.36E 01

ALTITUDE M	FLIGHT NO. C-183A FILTER NO. 3					
	PATH RADIANCE FROM GROUND TO ALTITUDE (W/SR SQ M CM)					
	ZENITH ANGLE OF PATH OF SIGHT (DEG)					
	95	100	105	120	150	180
300	6.76E C1	2.91E C1	1.65E C1	5.19E 00	1.69E 00	1.42E 00
600	1.11E C2	5.26E 01	3.08E 01	1.01E 01	3.39E 00	2.84E 00
900	1.45E C2	7.71E 01	4.67E 01	1.64E 01	5.64E 00	4.70E 00
1500	1.76E C2	1.11E C2	7.21E 01	2.83E 01	1.03E 01	8.61E 00
3000	1.76E C2	1.25E C2	9.13E 01	3.97E 01	1.60E 01	1.38E 01

FLIGHT NO. C-183A
PATH RADIANCE FROM GROUND TO ALTITUDE
AZIMUTH OF PATH OF SIGHT = 90

(JOB 5627 DATE 04/25/73)

AZIMUTH OF PATH OF SIGHT = 90

ALTITUDE M	FLIGHT NO. C-183A FILTER NO. 2					
	PATH RADIANCE FROM GROUND TO ALTITUDE (W/SR SQ M UM)					
	ZENITH ANGLE OF PATH OF SIGHT (DEG)					
	95	100	105	120	150	180
300	5.95E 01	3.15E 01	2.06E 01	9.05E 00	4.25E 00	3.55E 00
600	9.44E 01	6.13E 01	4.32E 01	2.07E 01	1.00E 01	8.40E 00
900	1.08E 02	8.00E 01	5.99E 01	3.07E 01	1.54E 01	1.29E 01
1500	1.21E 02	1.01E 02	8.15E 01	4.62E 01	2.42E 01	2.04E 01
3000	1.29E 02	1.23E 02	1.06E 02	6.73E 01	3.89E 01	3.37E 01

ALTITUDE M	FLIGHT NO. C-183A FILTER NO. 4					
	PATH RADIANCE FROM GROUND TO ALTITUDE (W/SR SQ M UM)					
	ZENITH ANGLE OF PATH OF SIGHT (DEG)					
	95	100	105	120	150	180
300	4.78E 01	2.47E 01	1.59E 01	6.83E 00	3.32E 00	2.91E 00
600	7.17E 01	4.31E 01	2.93E 01	1.34E 01	6.65E 00	5.81E 00
900	8.43E 01	5.64E 01	4.02E 01	1.94E 01	9.80E 00	8.55E 00
1500	9.81E 01	7.48E 01	5.70E 01	2.99E 01	1.56E 01	1.36E 01
3000	1.13E 02	9.54E 01	7.83E 01	4.65E 01	2.66E 01	2.36E 01

ALTITUDE M	FLIGHT NO. C-183A FILTER NO. 3					
	PATH RADIANCE FROM GROUND TO ALTITUDE (W/SR SQ M UM)					
	ZENITH ANGLE OF PATH OF SIGHT (DEG)					
	95	100	105	120	150	180
300	2.22E 01	1.09E 01	7.05E 00	3.20E 00	1.65E 00	1.42E 00
600	3.72E 01	2.01E 01	1.34E 01	6.30E 00	3.30E 00	2.84E 00
900	5.02E 01	3.02E 01	2.10E 01	1.03E 01	5.47E 00	4.70E 00
1500	6.44E 01	4.58E 01	3.41E 01	1.81E 01	1.00E 01	8.61E 00
3000	7.26E 01	5.80E 01	4.60E 01	2.68E 01	1.57E 01	1.38E 01

FLIGHT NO. C-183A
PATH RADIANCE FROM GROUND TO ALTITUDE
AZIMUTH OF PATH OF SIGHT = 180

(JOB 5627 DATE 04/25/73)

AZIMUTH OF PATH OF SIGHT = 180

ALTITUDE M	FLIGHT NO. C-183A FILTER NO. 2					
	PATH RADIANCE FROM GROUND TO ALTITUDE (W/SR SQ M LM)					
	ZENITH ANGLE OF PATH OF SIGHT (DEG)					
	95	100	105	120	150	180
300	4.54E C1	2.77E C1	1.92E 01	1.01E 01	5.04E C0	3.55E 00
600	7.87E C1	5.35E C1	4.03E C1	2.28E 01	1.19E C1	8.40E C0
900	9.06E C1	7.04E C1	5.57E 01	3.36E 01	1.82E C1	1.29E 01
1500	1.03E C2	8.93E C1	7.56E C1	4.99E 01	2.86E 01	2.04E 01
3000	1.30E C2	1.17E C2	1.04E C2	7.47E 01	4.67E 01	3.37E 01

ALTITUDE M	FLIGHT NO. C-183A FILTER NO. 4					
	PATH RADIANCE FROM GROUND TO ALTITUDE (W/SR SQ M LM)					
	ZENITH ANGLE OF PATH OF SIGHT (DEG)					
	95	100	105	120	150	180
300	3.77E C1	2.10E C1	1.46E C1	7.77E C0	4.06E C0	2.91E 00
600	5.67E C1	3.66E C1	2.68E C1	1.50E C1	8.10E C0	5.81E 00
900	6.71E C1	4.79E C1	3.66E C1	2.15E 01	1.19E 01	8.55E C0
1500	7.93E C1	6.37E C1	5.16E 01	3.26E 01	1.89E 01	1.36E 01
3000	1.02E C2	8.79E C1	7.54E C1	5.21E 01	3.27E 01	2.36E 01

ALTITUDE M	FLIGHT NO. C-183A FILTER NO. 3					
	PATH RADIANCE FROM GROUND TO ALTITUDE (W/SR SQ M LM)					
	ZENITH ANGLE OF PATH OF SIGHT (DEG)					
	95	100	105	120	150	180
300	1.50E C1	1.00E C1	6.94E C0	3.79E C0	2.01E C0	1.42E C0
600	3.17E C1	1.84E C1	1.31E 01	7.40E 00	4.00E C0	2.84E C0
900	4.25E C1	2.74E C1	2.03E 01	1.19E 01	6.61E C0	4.70E C0
1500	5.43E C1	4.11E C1	3.26E 01	2.07E 01	1.20E C1	8.61E C0
3000	6.50E C1	5.42E C1	4.54E C1	3.10E 01	1.93E C1	1.38E 01

FLIGHT NO. C-183A
PATH RADIANCE FROM GROUND TO ALTITUDE
AZIMUTH OF PATH OF SIGHT = 270

(JCB 5627 DATE C4/25/73)

AZIMUTH OF PATH OF SIGHT = 270

ALTITUDE M	FLIGHT NO. C-183A FILTER NO. 2					
	PATH RADIANCE FROM GROUND TO ALTITUDE (W/SR SQ M CM)					
	ZENITH ANGLE OF PATH OF SIGHT (DEG)					
	95	100	105	120	150	180
300	5.43E C1	2.91E C1	1.93E 01	8.83E 00	4.29E C0	3.55E 00
600	8.61E C1	5.66E C1	4.04E C1	2.00E 01	1.01E C1	8.40E 00
900	9.86E C1	7.38E C1	5.58E 01	2.96E 01	1.54E C1	1.29E 01
1500	1.11E C2	9.25E C1	7.56E C1	4.42E 01	2.42E C1	2.04E C1
3000	1.29E C2	1.14E 02	9.86E 01	6.43E 01	3.87E 01	3.37E C1

ALTITUDE M	FLIGHT NO. C-183A FILTER NO. 4					
	PATH RADIANCE FROM GROUND TO ALTITUDE (W/SR SQ M CM)					
	ZENITH ANGLE OF PATH OF SIGHT (DEG)					
	95	100	105	120	150	180
300	4.15E C1	2.19E C1	1.44E 01	6.58E 00	3.41E C0	2.91E 00
600	6.24E C1	3.81E C1	2.64E 01	1.29E 01	6.82E C0	5.81E C0
900	7.36E C1	5.00E C1	3.63E C1	1.86E 01	1.00E C1	8.55E C0
1500	8.64E C1	6.65E C1	5.14E 01	2.86E 01	1.60E C1	1.36E C1
3000	1.04E C2	8.75E C1	7.23E 01	4.47E 01	2.70E C1	2.36E 01

ALTITUDE M	FLIGHT NO. C-183A FILTER NO. 3					
	PATH RADIANCE FROM GROUND TO ALTITUDE (W/SR SQ M CM)					
	ZENITH ANGLE OF PATH OF SIGHT (DEG)					
	95	100	105	120	150	180
300	2.05E C1	1.01E C1	6.59E C0	3.04E 00	1.63E 00	1.42E 00
600	3.41E C1	1.86E C1	1.25E 01	5.99E 00	3.25E 00	2.84E 00
900	4.58E C1	2.78E C1	1.94E 01	9.72E C0	5.36E C0	4.70E C0
1500	5.83E C1	4.19E C1	3.14E 01	1.70E 01	9.72E C0	8.61E C0
3000	6.70E C1	5.36E C1	4.27E 01	2.54E 01	1.54E 01	1.38E 01

FLIGHT NO. C-183A
DIRECTIONAL PATH REFLECTANCE FROM GROUND TO ALTITUDE
AZIMUTH OF PATH OF SIGHT = 0

(JCB 5627 DATE 04/25/73)

AZIMUTH OF PATH OF SIGHT = C

ALTITUDE M	FLIGHT NO. C-183A FILTER NO. 2					
	DIRECTIONAL PATH REFLECTANCE FROM GROUND TO ALTITUDE					
	ZENITH ANGLE OF PATH OF SIGHT (DEG)					
	95	100	105	120	150	180
300	8.80E-C1	2.84E-C1	1.48E-C1	4.29E-02	1.28E-02	1.03E-02
600	4.08E C0	5.37E-C1	4.40E-C1	1.17E-01	3.37E-C2	2.68E-02
900	1.31E C1	2.02E C0	8.49E-01	2.07E-01	5.73E-02	4.50E-02
1500	8.05E C1	5.78E C0	1.98E C0	4.11E-01	1.07E-01	8.27E-02
3000	7.51E C2	1.77E C1	4.68E CC	8.02E-01	2.06E-01	1.64E-01

ALTITUDE M	FLIGHT NO. C-183A FILTER NO. 4					
	DIRECTIONAL PATH REFLECTANCE FROM GROUND TO ALTITUDE					
	ZENITH ANGLE OF PATH OF SIGHT (DEG)					
	95	100	105	120	150	180
300	7.53E-C1	2.43E-C1	1.24E-C1	3.43E-02	1.02E-C2	8.49E-03
600	2.27E C0	5.92E-C1	2.84E-01	7.52E-02	2.19E-02	1.81E-02
900	5.10E CC	1.06E CC	4.76E-C1	1.21E-01	3.45E-02	2.82E-02
1500	1.81E C1	2.36E CC	9.51E-01	2.22E-01	6.17E-C2	4.95E-02
3000	1.01E C2	5.96E CC	2.02E CC	4.22E-01	1.20E-01	9.89E-02

ALTITUDE M	FLIGHT NO. C-183A FILTER NO. 3					
	DIRECTIONAL PATH REFLECTANCE FROM GROUND TO ALTITUDE					
	ZENITH ANGLE OF PATH OF SIGHT (DEG)					
	95	100	105	120	150	180
300	3.52E-C1	1.24E-C1	6.61E-C2	1.95E-02	6.16E-C3	5.14E-03
600	8.54E-C1	2.73E-C1	1.40E-01	4.07E-02	1.28E-02	1.06E-02
900	1.87E CC	5.16E-C1	2.53E-01	7.18E-02	2.25E-C2	1.84E-02
1500	6.58E C0	1.26E CC	5.55E-01	1.49E-01	4.57E-02	3.69E-02
3000	2.25E C1	2.58E CC	1.03E CC	2.55E-01	7.93E-C2	6.55E-02

FLIGHT NO. C-183A
DIRECTIONAL PATH REFLECTANCE FROM GROUND TO ALTITUDE
AZIMUTH OF PATH OF SIGHT = 90

(JOB 5627 DATE 04/25/73)
 AZIMUTH OF PATH OF SIGHT = 90

ALTITUDE M	FLIGHT NO. C-183A FILTER NO. 2					
	DIRECTIONAL PATH REFLECTANCE FROM GROUND TO ALTITUDE					
	ZENITH ANGLE OF PATH OF SIGHT (DEG)					
	95	100	105	120	150	180
300	3.52E-C1	1.26E-01	7.24E-02	2.81E-02	1.24E-02	1.03E-02
600	1.67E C0	4.24E-C1	2.20E-01	7.75E-02	3.28E-02	2.68E-02
900	5.50E C0	9.33E-C1	4.32E-01	1.38E-01	5.58E-02	4.50E-02
1500	3.58E C1	2.79E CC	1.05E C0	2.80E-01	1.04E-01	8.27E-02
3000	3.91E C2	9.67E CC	2.74E CC	5.87E-01	2.07E-01	1.64E-01

ALTITUDE M	FLIGHT NO. C-183A FILTER NO. 4					
	DIRECTIONAL PATH REFLECTANCE FROM GROUND TO ALTITUDE					
	ZENITH ANGLE OF PATH OF SIGHT (DEG)					
	95	100	105	120	150	180
300	2.73E-C1	9.79E-C2	5.57E-02	2.12E-02	9.79E-03	8.49E-03
600	8.48E-C1	2.45E-C1	1.31E-01	4.72E-02	2.11E-02	1.81E-02
900	1.96E C0	4.48E-C1	2.25E-01	7.68E-02	3.32E-C2	2.82E-02
1500	7.45E C0	1.06E CC	4.70E-01	1.45E-01	5.94E-02	4.95E-02
3000	4.86E C1	3.03E CC	1.11E CC	2.98E-01	1.19E-01	9.89E-02

ALTITUDE M	FLIGHT NO. C-183A FILTER NO. 3					
	DIRECTIONAL PATH REFLECTANCE FROM GROUND TO ALTITUDE					
	ZENITH ANGLE OF PATH OF SIGHT (DEG)					
	95	100	105	120	150	180
300	1.16E-C1	4.67E-C2	2.82E-02	1.20E-02	6.01E-03	5.14E-03
600	2.87E-C1	1.05E-C1	6.12E-02	2.53E-02	1.25E-02	1.06E-02
900	6.47E-C1	2.03E-C1	1.13E-01	4.51E-02	2.18E-02	1.84E-02
1500	2.41E C0	5.18E-C1	2.62E-C1	9.53E-02	4.43E-02	3.69E-02
3000	9.25E C0	1.16E CC	5.19E-01	1.72E-01	7.80E-02	6.55E-02

FLIGHT NO. C-183A
DIRECTIONAL PATH REFLECTANCE FROM GROUND TO ALTITUDE
AZIMUTH OF PATH OF SIGHT = 180

(JCB 5627 DATE 04/25/73)

AZIMUTH OF PATH OF SIGHT = 180

ALTITUDE M	FLIGHT NO. C-183A FILTER NO. 2					
	DIRECTIONAL PATH REFLECTANCE FROM GROUND TO ALTITUDE					
	ZENITH ANGLE OF PATH OF SIGHT (DEG)					
	95	100	105	120	150	180
300	2.52E-C1	1.11E-C1	6.77E-C2	3.13E-02	1.48E-C2	1.03E-02
600	1.40E C0	3.73E-C1	2.05E-01	8.57E-02	3.88E-C2	2.68E-02
900	4.60E CC	8.21E-C1	4.01E-C1	1.51E-01	6.59E-02	4.50E-02
1500	3.04E C1	2.47E CC	9.73E-C1	3.03E-C1	1.23E-C1	8.27E-02
3000	3.67E C2	9.21E CC	2.69E CC	6.52E-01	2.48E-C1	1.64E-01

ALTITUDE M	FLIGHT NO. C-183A FILTER NO. 4					
	DIRECTIONAL PATH REFLECTANCE FROM GROUND TO ALTITUDE					
	ZENITH ANGLE OF PATH OF SIGHT (DEG)					
	95	100	105	120	150	180
300	2.15E-C1	8.32E-C2	5.13E-C2	2.42E-C2	1.20E-C2	8.49E-03
600	6.71E-C1	2.08E-C1	1.20E-C1	5.30E-02	2.57E-02	1.81E-C2
900	1.56E CC	3.80E-C1	2.05E-01	8.52E-02	4.03E-C2	2.82E-02
1500	6.02E CC	9.01E-C1	4.25E-C1	1.58E-01	7.18E-C2	4.95E-02
3000	4.38E C1	2.79E CC	1.07E CC	3.34E-01	1.46E-C1	9.89E-02

ALTITUDE M	FLIGHT NO. C-183A FILTER NO. 3					
	DIRECTIONAL PATH REFLECTANCE FROM GROUND TO ALTITUDE					
	ZENITH ANGLE OF PATH OF SIGHT (DEG)					
	95	100	105	120	150	180
300	9.89E-C2	4.28E-C2	2.77E-02	1.42E-02	7.30E-C3	5.14E-03
600	2.44E-C1	9.53E-C2	5.98E-C2	2.97E-02	1.51E-02	1.06E-02
900	5.48E-C1	1.83E-C1	1.10E-C1	5.23E-02	2.63E-C2	1.84E-02
1500	2.03E CC	4.65E-C1	2.51E-C1	1.09E-01	5.32E-C2	3.69E-02
3000	8.28E CC	1.08E CC	5.12E-C1	1.98E-01	9.56E-C2	6.55E-C2

FLIGHT NO. C-183A
DIRECTIONAL PATH REFLECTANCE FROM GROUND TO ALTITUDE
AZIMUTH OF PATH OF SIGHT = 270

(JOB 5627 DATE 04/25/73)

AZIMUTH OF PATH OF SIGHT = 270

FLIGHT NO. C-183A FILTER NO. 2

DIRECTIONAL PATH REFLECTANCE FROM GROUND TO ALTITUDE

ZENITH ANGLE OF PATH OF SIGHT (DEG)

ALTITUDE M	95	100	105	120	150	180
300	3.21E-C1	1.17E-C1	6.79E-02	2.74E-02	1.26E-02	1.03E-02
600	1.53E C0	3.92E-C1	2.05E-01	7.52E-02	3.30E-C2	2.68E-02
900	5.02E C0	8.60E-C1	4.02E-C1	1.33E-01	5.60E-C2	4.50E-02
1500	3.27E C1	2.57E C0	9.71E-01	2.68E-01	1.04E-01	8.27E-02
3000	3.63E C2	8.98E C0	2.56E CC	5.61E-01	2.06E-01	1.64E-01

FLIGHT NO. C-183A FILTER NO. 4

DIRECTIONAL PATH REFLECTANCE FROM GROUND TO ALTITUDE

ZENITH ANGLE OF PATH OF SIGHT (DEG)

ALTITUDE M	95	100	105	120	150	180
300	2.37E-C1	8.66E-C2	5.04E-02	2.05E-02	1.01E-C2	8.49E-03
600	7.38E-C1	2.17E-C1	1.18E-01	4.54E-02	2.16E-C2	1.81E-02
900	1.71E C0	3.97E-C1	2.03E-01	7.36E-02	3.40E-C2	2.82E-02
1500	6.55E C0	9.41E-C1	4.24E-C1	1.32E-01	6.08E-02	4.95E-02
3000	4.48E C1	2.78E CC	1.02E CC	2.87E-01	1.21E-01	9.89E-02

FLIGHT NO. C-183A FILTER NO. 3

DIRECTIONAL PATH REFLECTANCE FROM GROUND TO ALTITUDE

ZENITH ANGLE OF PATH OF SIGHT (DEG)

ALTITUDE M	95	100	105	120	150	180
300	1.07E-C1	4.33E-C2	2.63E-C2	1.14E-02	5.95E-C3	5.14E-03
600	2.63E-C1	5.66E-C2	5.69E-02	2.40E-02	1.23E-02	1.06E-02
900	5.90E-C1	1.86E-C1	1.05E-01	4.26E-02	2.14E-02	1.84E-02
1500	2.18E C0	4.74E-C1	2.41E-01	8.96E-02	4.30E-02	3.69E-02
3000	8.54E C0	1.07E CC	4.82E-C1	1.62E-01	7.64E-C2	6.55E-02

FLIGHT C-183B – 14 AUGUST 1971 – TRACK 4 – DESCRIPTION OF FLIGHT AND WEATHER CHARACTERISTICS

It was a sunlit afternoon. At the beginning of the flight there were scattered cumulus clouds and thin broken cirrus clouds. There were also some cumulonimbus north of the station. During the flight and at its termination there were thundershowers at the station. The flight was conducted over cultivated farmlands eastsoutheast of St. Louis. The typical terrain was flat, highly cultivated farmland. The data-taking started at 1731 GMT (1231 CDT) and continued until 1848 GMT (1348 CDT). The sun zenith angle during sky radiance data-taking for Filters 2, 3, and 4 was 24.8 degrees at the beginning and 24.0 degrees at the end. The maximum altitude for the flight was 2550 meters. Average terrain elevation along this track was 153 meters.

At the beginning of data-taking, Scott Air Force Base was reporting 0.8 cloud cover with scattered cumulus at 5000 feet (1500 meters) and thin broken cirrus at 25 000 feet (7500 meters). Visibility was 12 miles (19 kilometers). There were cumulonimbus clouds northwest and north of the station; their movements were unknown.

The ground station located at Scott, 39 miles (63 kilometers) from the center of the flight path, recorded mostly clear, heavy cumulus buildups northern horizon. The ground station ceased data collection when the rain started.

During the flight, the aircrew made the following observations, which have been extracted from the flight log and summarized. Metric altitudes have been added editorially.

FLIGHT LOG ENTRY

Time (GMT)	Altitude (m AGL)	Aircrew Observations
1727	-	Bumpy ride at low altitude
1748	-	Scattered to broken thin cirrus
1815	-	Abort 9500-ft (2900 m) MSL straight and level due to heavy weather buildup, rain in track area and at field

At the end of data-taking, Scott was reporting 1.0 cloud cover with scattered clouds at 5000 feet (1500 meters) and overcast at 7000 feet (2100 meters). Visibility was 8 miles (13 kilometers) in a light thundershower. There was thunder overhead and west moving south. There was occasional lightning cloud to ground southwest to west.

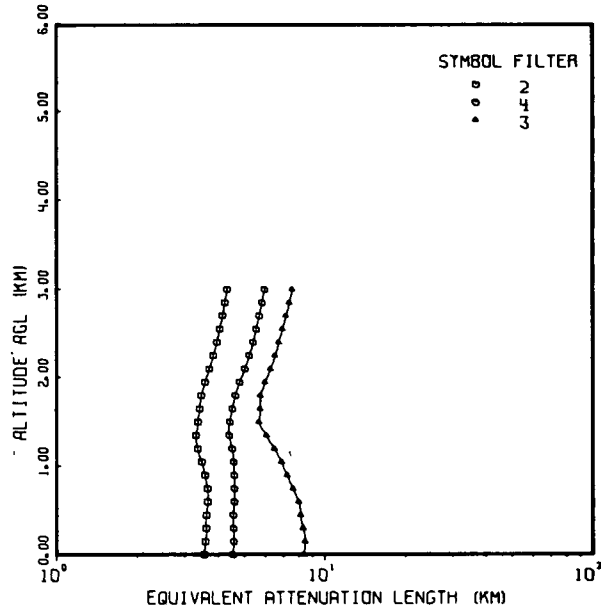
The surface synoptic chart shows that St. Louis was still on the rear of a high with its center near Pittsburgh. There was a cold front through Detroit and southern Nebraska, which extended northwestward into British Columbia. Tropical storm "Beth" was off the Virginia coast.

At 500 millibars there was a high over Wyoming, Utah, Nevada, and California. Elsewhere there were very weak gradients.

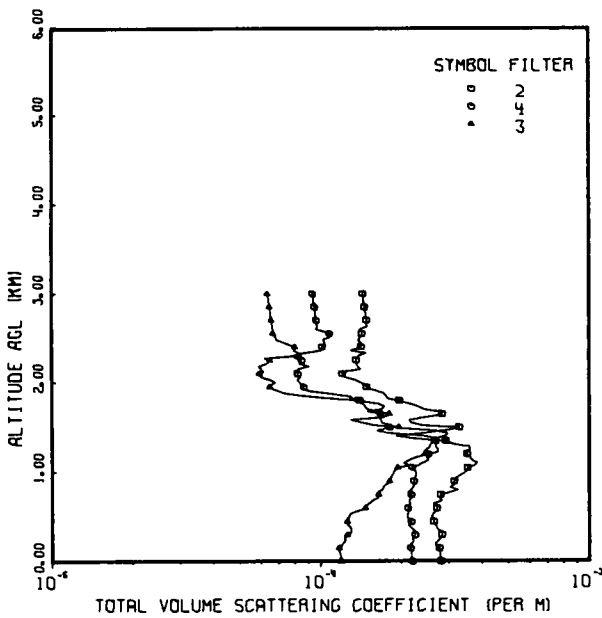
These data were taken from the 3-hourly facsimile charts issued by the NMC and obtained from Lindbergh Field NOAA office. The 500-millibar charts are for 0000 GMT and 1200 GMT daily.

FLIGHT NO. C-183B

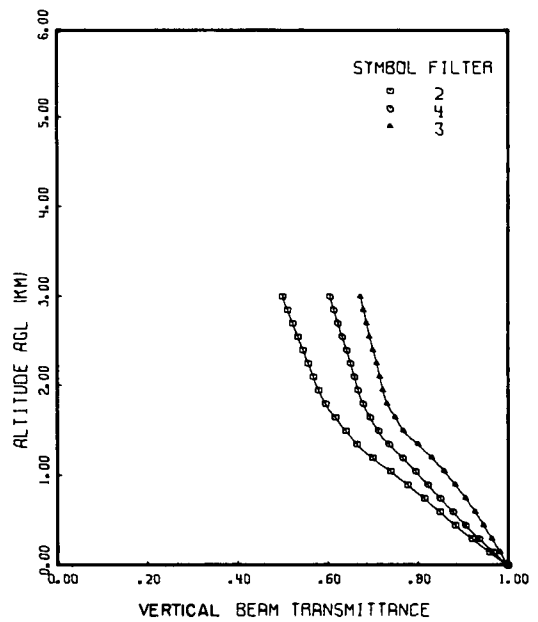
FLIGHT C-183B



FLIGHT C-183B



FLIGHT C-183B



FLIGHT NO. C-183B
TOTAL VOLUME SCATTERING COEFFICIENT

(JCB 5666 DATE 04/26/73)
 DATE 81471 FLIGHT NO. C-183B GROUND LEVEL ALTITUDE (M)= 152

ALTITUDE (M)	TOTAL VOLUME SCATTERING COEFFICIENT (PER M)			
	FILTERS	2	4	3
0		2.81E-04	2.20E-04	1.19E-04
30		2.80E-04	2.19E-04	1.19E-04
60		2.79E-04	2.18E-04	1.19E-04
90		2.78E-04	2.18E-04	1.18E-04
120		2.78E-04	2.17E-04	1.17E-04
150		2.77E-04	2.17E-04	1.17E-04
180		2.70E-04	2.15E-04	1.20E-04
210		2.67E-04	2.19E-04	1.22E-04
240		2.75E-04	2.23E-04	1.24E-04
270		2.80E-04	2.19E-04	1.23E-04
300		2.83E-04	2.25E-04	1.26E-04
330		2.85E-04	2.24E-04	1.31E-04
360		2.77E-04	2.23E-04	1.30E-04
390		2.71E-04	2.17E-04	1.29E-04
420		2.68E-04	2.12E-04	1.26E-04
450		2.64E-04	2.18E-04	1.26E-04
480		2.63E-04	2.12E-04	1.26E-04
510		2.60E-04	2.10E-04	1.28E-04
540		2.62E-04	2.11E-04	1.29E-04
570		2.69E-04	2.12E-04	1.37E-04
600		2.71E-04	2.12E-04	1.47E-04
630		2.75E-04	2.15E-04	1.49E-04
660		2.63E-04	2.17E-04	1.52E-04
690		2.84E-04	2.14E-04	1.57E-04
720		2.79E-04	2.17E-04	1.64E-04
750		2.80E-04	2.18E-04	1.65E-04
780		3.02E-04	2.13E-04	1.64E-04
810		3.25E-04	2.18E-04	1.71E-04
840		3.03E-04	2.21E-04	1.72E-04
870		3.17E-04	2.25E-04	1.76E-04
900		3.15E-04	2.23E-04	1.82E-04
930		3.19E-04	2.23E-04	1.83E-04
960		3.27E-04	2.27E-04	1.83E-04
990		3.39E-04	2.27E-04	1.87E-04
1020		3.51E-04	2.26E-04	1.89E-04
1050		3.53E-04	2.19E-04	1.94E-04
1080		3.74E-04	2.31E-04	2.14E-04
1110		3.85E-04	2.40E-04	2.04E-04
1140		3.68E-04	2.53E-04	2.14E-04
1170		3.61E-04	2.50E-04	2.27E-04
1200		3.52E-04	2.52E-04	2.47E-04
1230		3.45E-04	2.74E-04	2.45E-04
1260		3.62E-04	2.75E-04	2.48E-04
1290		3.59E-04	2.69E-04	2.57E-04
1320		3.14E-04	2.69E-04	2.57E-04
1350		2.93E-04	2.69E-04	2.66E-04
1380		2.28E-04	2.72E-04	2.72E-04
1410		1.93E-04	2.41E-04	2.91E-04
1440		2.38E-04	1.85E-04	2.98E-04
1470		2.84E-04	1.62E-04	2.69E-04
1500		3.24E-04	1.81E-04	1.97E-04

FLIGHT NO. C-183B

TOTAL VOLUME SCATTERING COEFFICIENT

(JOB 5666 DATE 04/26/73)
 DATE 81471 FLIGHT NO. C-183B GROUND LEVEL ALTITUDE (M)= 152

ALTITUDE (M)	TOTAL VOLUME SCATTERING COEFFICIENT (PER M)		
	FILTERS 2	4	3
1530	2.40E-04	1.78E-04	1.58E-04
1560	2.17E-04	1.70E-04	1.42E-04
1590	2.15E-04	1.68E-04	1.30E-04
1620	2.44E-04	1.66E-04	1.72E-04
1650	2.84E-04	1.67E-04	1.81E-04
1680	2.83E-04	1.65E-04	1.50E-04
1710	2.44E-04	1.49E-04	1.69E-04
1740	2.32E-04	1.47E-04	1.73E-04
1770	2.18E-04	1.44E-04	1.65E-04
1800	1.97E-04	1.38E-04	1.43E-04
1830	1.78E-04	1.31E-04	1.10E-04
1860	1.76E-04	1.26E-04	8.69E-05
1890	1.72E-04	1.06E-04	7.34E-05
1920	1.61E-04	8.9CE-05	6.93E-05
1950	1.49E-04	8.68E-05	6.49E-05
1980	1.46E-04	8.49E-05	6.59E-05
2010	1.42E-04	8.38E-05	6.83E-05
2040	1.35E-04	8.22E-05	6.51E-05
2070	1.23E-04	8.47E-05	6.01E-05
2100	1.21E-04	8.23E-05	5.94E-05
2130	1.22E-04	8.15E-05	6.18E-05
2160	1.41E-04	8.34E-05	6.04E-05
2190	1.38E-04	9.09E-05	5.88E-05
2220	1.36E-04	8.34E-05	6.32E-05
2250	1.36E-04	8.53E-05	6.52E-05
2280	1.37E-04	8.17E-05	6.20E-05
2310	1.39E-04	7.9CE-05	8.47E-05
2340	1.48E-04	8.75E-05	8.26E-05
2370	1.30E-04	1.01E-04	7.95E-05
2400	1.42E-04	1.02E-04	8.05E-05
2430	1.41E-04	1.05E-04	7.70E-05
2460	1.42E-04	1.04E-04	7.28E-05
2490	1.38E-04	1.02E-04	6.87E-05
2520	1.41E-04	1.09E-04	6.81E-05
2550	1.43E-04	1.09E-04	6.68E-05
2580	1.43E-04	1.04E-04	6.66E-05
2610	1.41E-04	9.59E-05	6.64E-05
2640	1.50E-04	9.73E-05	6.62E-05
2670	1.49E-04	9.70E-05	6.60E-05
2700	1.49E-04	9.67E-05	6.58E-05
2730	1.48E-04	9.64E-05	6.56E-05
2760	1.48E-04	9.61E-05	6.54E-05
2790	1.47E-04	9.58E-05	6.52E-05
2820	1.47E-04	9.55E-05	6.50E-05
2850	1.46E-04	9.52E-05	6.48E-05
2880	1.46E-04	9.49E-05	6.46E-05
2910	1.45E-04	9.46E-05	6.44E-05
2940	1.45E-04	9.43E-05	6.42E-05
2970	1.44E-04	9.40E-05	6.40E-05
3000	1.44E-04	9.37E-05	6.38E-05

FIRST DATA ALT	150	150	90
LAST DATA ALT	2640	2640	2550

FLIGHT NO. C-183B
EQUIVALENT ATTENUATION LENGTH

(JOB 5666 DATE 04/26/73)
 DATE 81471 FLIGHT NO. C-1938 GROUND LEVEL ALTITUDE (M)= 152

ALTITUDE (M)	EQUIVALENT ATTENUATION LENGTH (KM)		
	FILTERS 2	4	3
0	3.56E CC	4.54E CC	8.37E CC
300	3.62E CC	4.57E CC	8.33E CC
600	3.66E CC	4.60E CC	8.00E CC
900	3.58E CC	4.60E CC	7.26E CC
1200	3.36E CC	4.52E CC	6.51E CC
1500	3.37E CC	4.43E CC	5.70E CC
1800	3.47E CC	4.65E CC	5.78E CC
2100	3.72E CC	5.04E CC	6.28E CC
2400	3.96E CC	5.42E CC	6.76E CC
2700	4.16E CC	5.71E CC	7.19E CC
3000	4.33E CC	5.98E CC	7.59E CC

FLIGHT NO. C-183B
VERTICAL BEAM TRANSMITTANCE FROM GROUND TO ALTITUDE

ALTITUDE (M)	VERTICAL BEAM TRANSMITTANCE FROM GROUND TO ALTITUDE		
	FILTERS 2	4	3
0	1.00E CC	1.00E CC	1.00E CC
300	9.20E-01	9.36E-01	9.65E-01
600	8.49E-01	8.78E-01	9.28E-01
900	7.79E-01	8.22E-01	8.83E-01
1200	7.00E-01	7.67E-01	8.32E-01
1500	6.41E-01	7.13E-01	7.69E-01
1800	5.95E-01	6.79E-01	7.32E-01
2100	5.68E-01	6.59E-01	7.16E-01
2400	5.46E-01	6.42E-01	7.01E-01
2700	5.23E-01	6.23E-01	6.87E-01
3000	5.00E-01	6.05E-01	6.74E-01

FLIGHT C-185A—18 AUGUST 1971—TRACK 7—DESCRIPTION OF FLIGHT AND WEATHER CHARACTERISTICS

It was a sunlit morning. At the beginning of data-taking there were 0.8 thin cirrostratus clouds which dissipated by the end of data-taking. The flight was conducted over rolling hills southwest of St. Louis. The typical terrain was heavily wooded. The data-taking started at 1522 GMT (1022 CDT) and continued until 1700 GMT (1200 CDT). The sun zenith angle during sky radiance data-taking for Filters 2, 3, and 4 was 44.6 degrees at the beginning and 35.2 degrees at the end. The maximum altitude for the flight was 2550 meters. Average terrain elevation on this track was 305 meters.

At the beginning of data-taking, Scott Air Force Base was reporting 0.8 cirrostratus at 20 000 feet (6000 meters), with 5-mile (8-kilometer) visibility in haze.

The ground station located at Scott, 85 miles (137 kilometers) from the center of the flight path, recorded clear with moderate haze.

During the flight, the aircrew made the following observations, which have been extracted from the flight log and summarized. Metric altitudes have been added editorially.

FLIGHT LOG ENTRY

Time (GMT)	Altitude (m AGL)	Aircrew Observations
1535	1650	Haze layer top approximately 6500 ft (1980 m) MSL
1558	1500	On top of haze, blue sky overhead Haze downsun is gray-black, upsun is white
1610	2550	Heavy cloud buildup at south end of track; heavy broken clouds below 9500 ft (2900 m) MSL, broken above
1626	1800	Top of cloud deck approximately 7000 ft (2130 m) MSL
1630	1500	Inside the haze at 6000 ft (1830 m) MSL
1651	2550	Hazy at 9500 ft (2900 m) MSL, broken clouds above

At the end of data-taking, Scott was reporting clear skies with 5-mile (8-kilometer) visibility in haze. They also reported an in-flight visibility of 3 miles (4.8 kilometers).

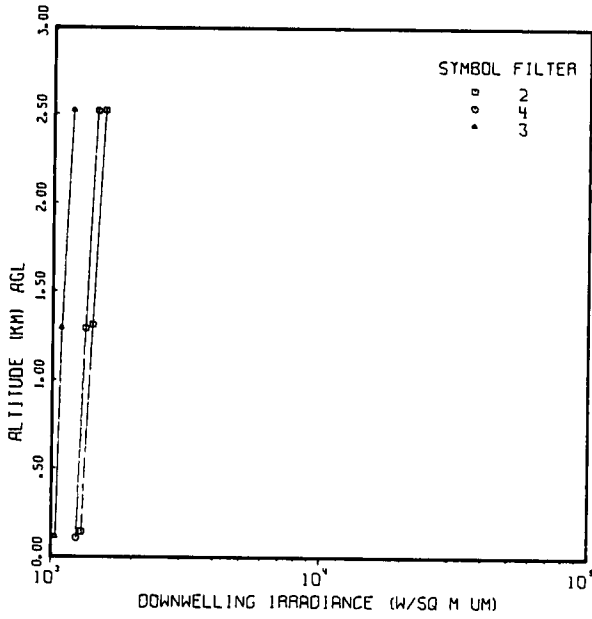
The surface synoptic chart shows an extremely weak gradient. A low was centered in eastern South Dakota with a cold front extending southwestward.

At 500 millibars there was a small low center over Tennessee. A trough of low extended southwestward from Pennsylvania to Louisiana.

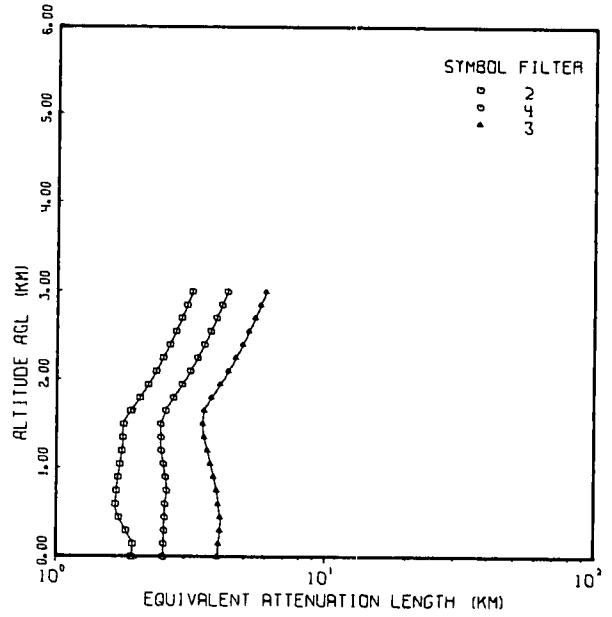
These data were taken from the 3-hourly facsimile charts issued by the NMC and obtained from Lindbergh Field NOAA office. The 500-millibar charts are for 0000 GMT and 1200 GMT daily.

FLIGHT NO. C-185A

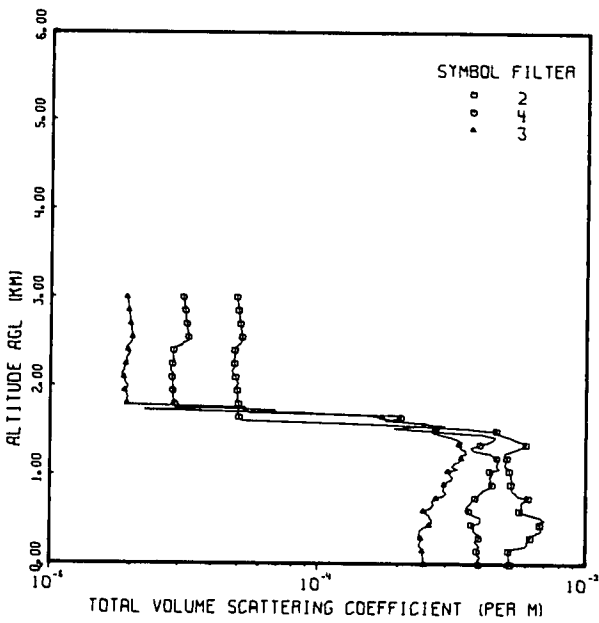
FLIGHT C-185A



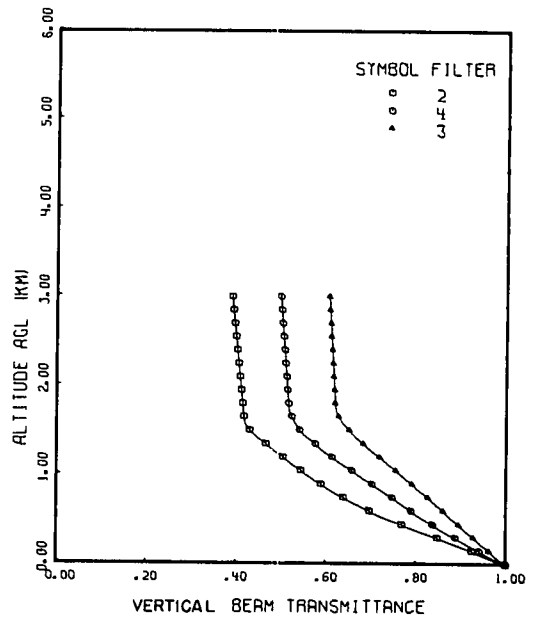
FLIGHT C-185A



FLIGHT C-185A

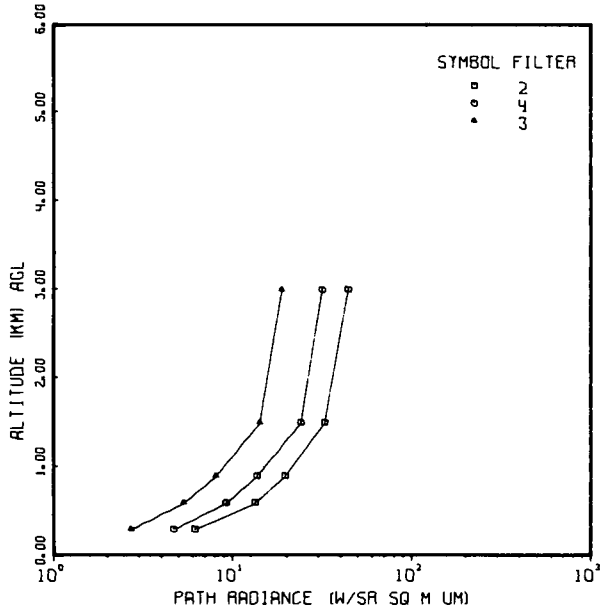


FLIGHT C-185A

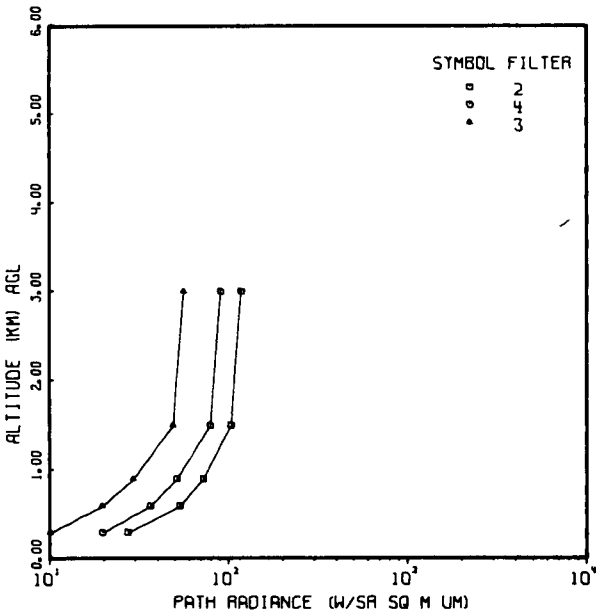


FLIGHT NO. C-185A

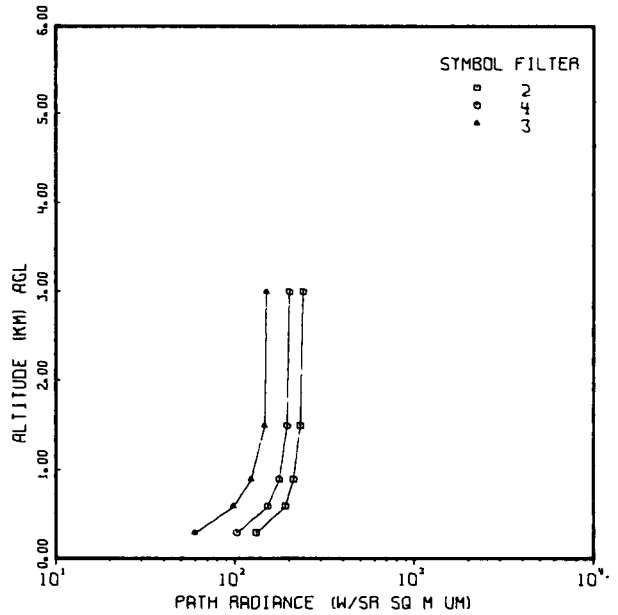
FLIGHT C-185A ZENITH ANGLE 180
AZIMUTH 0



FLIGHT C-185A ZENITH ANGLE 120
AZIMUTH 0

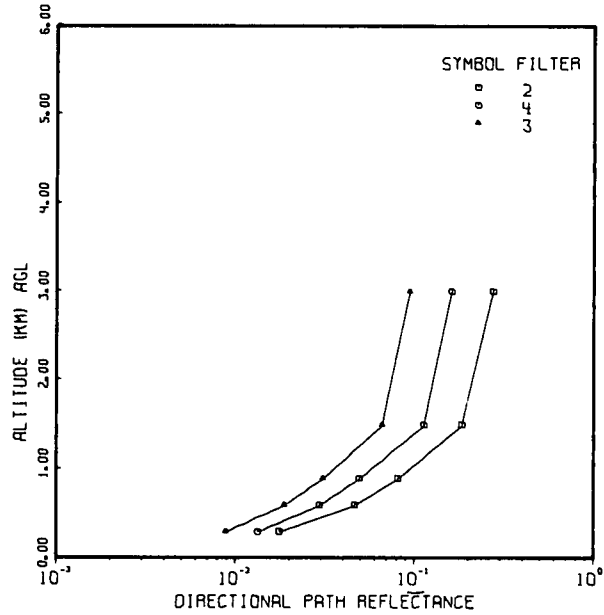


FLIGHT C-185A ZENITH ANGLE 100
AZIMUTH 0

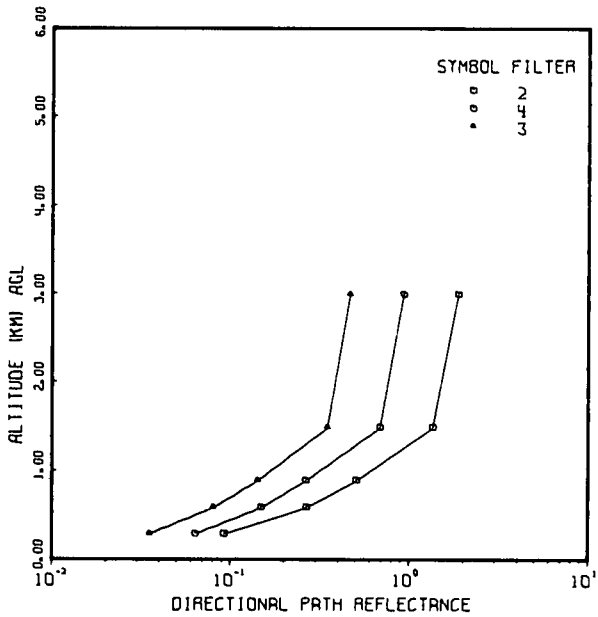


FLIGHT NO. C-185A

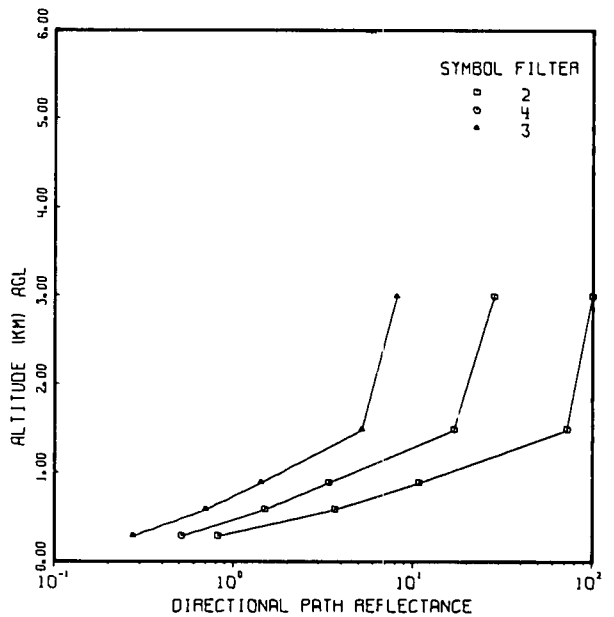
FLIGHT C-185A ZENITH ANGLE 180
AZIMUTH 0



FLIGHT C-185A ZENITH ANGLE 120
AZIMUTH 0



FLIGHT C-185A ZENITH ANGLE 100
AZIMUTH 0



FLIGHT NO. C-185A IRRADIANCE

(JCB 5712 DATE 04/27/73)

		FLIGHT NO. C-185A		FILTER NO. 2		SUN ZENITH ANGLE 39.8			
		IRRADIANCE (W/SQ M UM)							
ALTITUDE (METERS)	DOWN- WELLING	UP- WELLING	ALBEDO	SCALAR SUN	SCALAR SKY	SCALAR UPWELLING	SCALAR TOTAL	SCALAR ALBEDO	
146	1.30E 03	6.08E 01	.047	5.58E 02	1.65E 03	1.91E 02	2.40E 03	.086	
1315	1.41E 03	1.85E 02	.131	1.33E 03	8.43E 02	5.25E 02	2.70E 03	.241	
2526	1.56E 03	4.27E 02	.274	1.66E 03	5.66E 02	1.04E 03	3.27E 03	.466	

		FLIGHT NO. C-185A		FILTER NO. 4		SUN ZENITH ANGLE 39.8			
		IRRADIANCE (W/SQ M UM)							
ALTITUDE (METERS)	DOWN- WELLING	UP- WELLING	ALBEDO	SCALAR SUN	SCALAR SKY	SCALAR UPWELLING	SCALAR TOTAL	SCALAR ALBEDO	
111	1.24E 03	6.56E 01	.053	7.10E 02	1.37E 03	1.94E 02	2.27E 03	.093	
1295	1.33E 03	1.75E 02	.132	1.33E 03	6.17E 02	4.65E 02	2.41E 03	.239	
2523	1.46E 03	3.44E 02	.236	1.62E 03	3.46E 02	8.65E 02	2.83E 03	.440	

		FLIGHT NO. C-185A		FILTER NO. 3		SUN ZENITH ANGLE 39.8			
		IRRADIANCE (W/SQ M UM)							
ALTITUDE (METERS)	DOWN- WELLING	UP- WELLING	ALBEDO	SCALAR SUN	SCALAR SKY	SCALAR UPWELLING	SCALAR TOTAL	SCALAR ALBEDO	
118	1.04E 03	5.51E 01	.053	7.53E 02	9.68E 02	1.46E 02	1.87E 03	.085	
1296	1.08E 03	1.23E 02	.114	1.16E 03	3.97E 02	3.31E 02	1.88E 03	.213	
2527	1.19E 03	2.32E 02	.195	1.37E 03	1.72E 02	5.99E 02	2.14E 03	.388	

FLIGHT NO. C-185A
DIRECTIONAL REFLECTANCE OF TERRAIN

(JOB 5712 DATE 04/27/73)
 FLIGHT NO. C-185A
 AZIMUTH OF PATH OF SIGHT = 0
 DIRECTIONAL REFLECTANCE OF TERRAIN

ZENITH ANGLE	FILTERS		
	2	4	3
95	.2574	.3507	.3224
100	.1970	.2011	.1516
105	.1360	.1329	.0925
120	.0647	.0524	.0400
150	.0209	.0347	.0713
180	.0286	.0660	.0440

FLIGHT NO. C-185A
 AZIMUTH OF PATH OF SIGHT = 90
 DIRECTIONAL REFLECTANCE OF TERRAIN

ZENITH ANGLE	FILTERS		
	2	4	3
95	.1251	.1381	.1369
100	.0888	.0889	.0934
105	.0705	.0756	.0838
120	.0444	.0433	.0252
150	.0185	.0367	.0749
180	.0286	.0660	.0440

FLIGHT NO. C-185A
 AZIMUTH OF PATH OF SIGHT = 180
 DIRECTIONAL REFLECTANCE OF TERRAIN

ZENITH ANGLE	FILTERS		
	2	4	3
95	.1531	.1157	.1116
100	.0963	.0937	.1093
105	.0725	.0778	.1227
120	.0893	.0638	.0543
150	.0288	.0526	.0634
180	.0286	.0660	.0440

FLIGHT NO. C-185A
 AZIMUTH OF PATH OF SIGHT = 270
 DIRECTIONAL REFLECTANCE OF TERRAIN

ZENITH ANGLE	FILTERS		
	2	4	3
95	.1618	.1299	.1072
100	.1068	.0923	.0841
105	.0802	.0746	.0566
120	.0741	.0438	.0327
150	.0192	.0414	.0985
180	.0286	.0660	.0440

FLIGHT NO. C-185A
TOTAL VOLUME SCATTERING COEFFICIENT

(JOB 5712 DATE 04/27/73)
 DATE 81871 FLIGHT NO. C-185A GROUND LEVEL ALTITUDE (M)= 305

ALTITUDE (M)	TOTAL VOLUME SCATTERING COEFFICIENT (PER M)			
	FILTERS	2	4	3
0		5.22E-04	3.99E-04	2.50E-04
30		5.20E-04	3.97E-04	2.49E-04
60		5.19E-04	3.96E-04	2.48E-04
90		5.17E-04	4.05E-04	2.48E-04
120		5.16E-04	3.94E-04	2.47E-04
150		5.15E-04	3.93E-04	2.46E-04
180		5.35E-04	3.96E-04	2.46E-04
210		5.93E-04	4.03E-04	2.39E-04
240		6.05E-04	3.95E-04	2.39E-04
270		6.04E-04	3.85E-04	2.43E-04
300		6.21E-04	4.00E-04	2.44E-04
330		6.06E-04	4.07E-04	2.38E-04
360		6.49E-04	3.95E-04	2.40E-04
390		6.81E-04	3.80E-04	2.41E-04
420		6.79E-04	3.81E-04	2.48E-04
450		6.74E-04	3.74E-04	2.61E-04
480		6.53E-04	4.04E-04	2.66E-04
510		7.03E-04	4.04E-04	2.66E-04
540		6.73E-04	4.02E-04	2.62E-04
570		6.20E-04	3.76E-04	2.58E-04
600		5.65E-04	3.66E-04	2.48E-04
630		5.77E-04	3.57E-04	2.60E-04
660		5.79E-04	3.60E-04	2.68E-04
690		5.77E-04	3.70E-04	2.71E-04
720		5.80E-04	3.75E-04	2.66E-04
750		6.11E-04	3.86E-04	2.77E-04
780		5.56E-04	3.98E-04	2.94E-04
810		5.48E-04	4.03E-04	3.02E-04
840		5.31E-04	4.14E-04	2.93E-04
870		5.27E-04	4.31E-04	2.93E-04
900		5.25E-04	4.47E-04	2.96E-04
930		5.30E-04	4.36E-04	3.02E-04
960		5.28E-04	4.41E-04	3.16E-04
990		5.25E-04	4.37E-04	3.17E-04
1020		5.24E-04	4.46E-04	3.10E-04
1050		5.17E-04	4.38E-04	3.06E-04
1080		5.17E-04	4.77E-04	3.33E-04
1110		4.99E-04	4.63E-04	3.15E-04
1140		5.00E-04	4.64E-04	3.21E-04
1170		5.01E-04	4.69E-04	3.37E-04
1200		5.07E-04	4.64E-04	3.43E-04
1230		5.01E-04	4.53E-04	3.37E-04
1260		4.96E-04	4.38E-04	3.59E-04
1290		5.30E-04	3.83E-04	3.56E-04
1320		5.63E-04	3.71E-04	3.39E-04
1350		5.96E-04	4.03E-04	3.36E-04
1380		5.85E-04	4.33E-04	3.47E-04
1410		5.46E-04	4.50E-04	3.33E-04
1440		5.21E-04	4.59E-04	3.11E-04
1470		4.79E-04	4.13E-04	2.81E-04
1500		4.62E-04	2.74E-04	2.73E-04

FLIGHT NO. C-185A
TOTAL VOLUME SCATTERING COEFFICIENT

{JOB 5712 DATE 04/27/73}
 DATE 81871 FLIGHT NO. C-185A GROUND LEVEL ALTITUDE (M)= 305

ALTITUDE (M)	TOTAL VOLUME SCATTERING COEFFICIENT (PER M)			
	FILTERS	2	4	3
1530		3.65E-04	1.93E-04	2.80E-04
1560		2.33E-04	2.43E-04	2.97E-04
1590		1.19E-04	2.52E-04	2.37E-04
1620		5.20E-05	1.78E-04	1.93E-04
1650		5.05E-05	2.03E-04	1.74E-04
1680		5.03E-05	1.94E-04	1.54E-04
1710		5.00E-05	5.50E-05	8.85E-05
1740		5.01E-05	6.88E-05	2.26E-05
1770		5.05E-05	2.93E-05	5.34E-05
1800		5.02E-05	2.91E-05	1.93E-05
1830		4.99E-05	2.88E-05	1.94E-05
1860		4.96E-05	2.86E-05	1.92E-05
1890		4.99E-05	2.86E-05	1.93E-05
1920		4.96E-05	2.85E-05	1.92E-05
1950		4.96E-05	2.85E-05	1.89E-05
1980		4.94E-05	2.83E-05	1.93E-05
2010		4.94E-05	2.87E-05	1.95E-05
2040		5.01E-05	2.85E-05	1.91E-05
2070		4.93E-05	2.86E-05	1.88E-05
2100		4.89E-05	2.83E-05	1.88E-05
2130		4.86E-05	2.87E-05	1.84E-05
2160		4.75E-05	2.85E-05	1.85E-05
2190		4.75E-05	2.79E-05	1.88E-05
2220		4.84E-05	2.81E-05	1.89E-05
2250		4.86E-05	2.84E-05	1.91E-05
2280		4.81E-05	2.87E-05	1.93E-05
2310		4.83E-05	2.88E-05	1.92E-05
2340		4.85E-05	2.86E-05	1.93E-05
2370		4.87E-05	2.86E-05	1.98E-05
2400		4.85E-05	2.87E-05	1.95E-05
2430		4.88E-05	2.87E-05	1.91E-05
2460		5.00E-05	3.05E-05	1.94E-05
2490		5.12E-05	3.13E-05	1.99E-05
2520		5.19E-05	3.27E-05	2.01E-05
2550		5.17E-05	3.26E-05	2.02E-05
2580		5.15E-05	3.25E-05	2.01E-05
2610		5.14E-05	3.24E-05	2.01E-05
2640		5.12E-05	3.23E-05	2.00E-05
2670		5.10E-05	3.22E-05	1.99E-05
2700		5.09E-05	3.21E-05	1.99E-05
2730		5.07E-05	3.20E-05	1.98E-05
2760		5.06E-05	3.19E-05	1.97E-05
2790		5.04E-05	3.18E-05	1.97E-05
2820		5.03E-05	3.17E-05	1.96E-05
2850		5.01E-05	3.16E-05	1.96E-05
2880		4.99E-05	3.15E-05	1.95E-05
2910		4.98E-05	3.14E-05	1.94E-05
2940		4.96E-05	3.13E-05	1.94E-05
2970		4.95E-05	3.12E-05	1.93E-05
3000		4.93E-05	3.11E-05	1.93E-05
FIRST DATA ALT		150	60	180
LAST DATA ALT		2520	2520	2550

FLIGHT NO. C-185A
EQUIVALENT ATTENUATION LENGTH

{JOB 5712 DATE 04/27/73}
 DATE 81871 FLIGHT NO. C-185A GROUND LEVEL ALTITUDE (M)= 305

ALTITUDE (M)	EQUIVALENT ATTENUATION LENGTH (KM)		
	FILTERS 2	4	3
0	1.91E 00	2.51E 00	4.00E 00
300	1.82E 00	2.52E 00	4.08E 00
600	1.66E 00	2.54E 00	4.02E 00
900	1.70E 00	2.55E 00	3.86E 00
1200	1.75E 00	2.45E 00	3.65E 00
1500	1.78E 00	2.44E 00	3.51E 00
1800	2.04E 00	2.72E 00	3.77E 00
2100	2.34E 00	3.14E 00	4.35E 00
2400	2.63E 00	3.54E 00	4.91E 00
2700	2.91E 00	3.93E 00	5.46E 00
3000	3.19E 00	4.30E 00	5.99E 00

FLIGHT NO. C-185A
VERTICAL BEAM TRANSMITTANCE FROM GROUND TO ALTITUDE

ALTITUDE (M)	VERTICAL BEAM TRANSMITTANCE FROM GROUND TO ALTITUDE		
	FILTERS 2	4	3
0	1.00E 00	1.00E 00	1.00E 00
300	8.48E-01	8.88E-01	9.29E-01
600	6.97E-01	7.90E-01	8.61E-01
900	5.89E-01	7.03E-01	7.92E-01
1200	5.04E-01	6.13E-01	7.20E-01
1500	4.30E-01	5.41E-01	6.52E-01
1800	4.14E-01	5.16E-01	6.21E-01
2100	4.08E-01	5.12E-01	6.17E-01
2400	4.02E-01	5.08E-01	6.13E-01
2700	3.96E-01	5.03E-01	6.10E-01
3000	3.90E-01	4.98E-01	6.06E-01

FLIGHT NO. C-185A
BEAM TRANSMITTANCE FROM GROUND TO ALTITUDE

(JGB 5712 DATE 04/27/73)

ALTITUDE #	FLIGHT NO. C-185A FILTER NO. 2					
	BEAM TRANSMITTANCE FROM GROUND TO ALTITUDE					
	ZENITH ANGLE OF PATH OF SIGHT (DEG)					
	95	100	105	120	150	180
300	1.50E-01	3.87E-C1	5.29E-01	7.19E-01	8.27E-01	8.48E-01
600	1.56E-C2	1.25E-01	2.48E-01	4.86E-01	6.59E-01	6.97E-01
900	2.18E-03	4.73E-C2	1.29E-01	3.47E-01	5.42E-C1	5.89E-01
1500	5.45E-C5	7.77E-03	3.84E-02	1.85E-01	3.78E-C1	4.30E-01
3000	1.30E-C5	4.42E-C3	2.63E-02	1.52E-01	3.37E-01	3.90E-01

ALTITUDE #	FLIGHT NO. C-185A FILTER NO. 4					
	BEAM TRANSMITTANCE FROM GROUND TO ALTITUDE					
	ZENITH ANGLE OF PATH OF SIGHT (DEG)					
	95	100	105	120	150	180
300	2.55E-C1	5.04E-C1	6.32E-01	7.88E-01	8.72E-01	8.88E-01
600	6.57E-C2	2.57E-C1	4.02E-01	6.24E-01	7.61E-01	7.90E-01
900	1.68E-02	1.31E-C1	2.56E-01	4.94E-01	6.65E-01	7.03E-01
1500	7.91E-C4	2.91E-C2	9.33E-02	2.93E-01	4.92E-01	5.41E-01
3000	2.43E-C4	1.80E-C2	6.76E-02	2.48E-01	4.47E-01	4.98E-01

ALTITUDE #	FLIGHT NO. C-185A FILTER NO. 3					
	BEAM TRANSMITTANCE FROM GROUND TO ALTITUDE					
	ZENITH ANGLE OF PATH OF SIGHT (DEG)					
	95	100	105	120	150	180
300	4.29E-01	6.55E-C1	7.53E-01	8.63E-01	9.19E-01	9.29E-01
600	1.79E-C1	4.23E-C1	5.62E-01	7.42E-01	8.42E-01	8.61E-01
900	6.73E-C2	2.61E-C1	4.06E-01	6.27E-01	7.64E-01	7.92E-01
1500	6.92E-C3	8.51E-C2	1.92E-01	4.25E-01	6.10E-01	6.52E-01
3000	2.56E-C3	5.60E-C2	1.45E-01	3.68E-01	5.61E-01	6.06E-01

FLIGHT NO. C-185A
PATH RADIANCE FROM GROUND TO ALTITUDE
AZIMUTH OF PATH OF SIGHT = 0

(JOB 5712 DATE 04/27/73)

AZIMUTH OF PATH OF SIGHT = C

FLIGHT NO. C-185A FILTER NO. 2
 PATH RADIANCE FROM GROUND TO ALTITUDE (W/SR SQ M UM)

ALTITUDE M	ZENITH ANGLE OF PATH OF SIGHT (DEG)					
	95	100	105	120	150	180
300	2.26E 02	1.31E 02	8.12E 01	2.74E 01	7.97E 00	6.16E 00
600	2.60E 02	1.91E 02	1.34E 02	5.35E 01	1.72E 01	1.34E 01
900	2.66E 02	2.12E 02	1.62E 02	7.25E 01	2.51E 01	1.97E 01
1500	2.72E 02	2.32E 02	1.94E 02	1.04E 02	4.09E 01	3.27E 01
3000	2.76E 02	2.41E 02	2.06E 02	1.18E 02	5.18E 01	4.43E 01

FLIGHT NO. C-185A FILTER NO. 4
 PATH RADIANCE FROM GROUND TO ALTITUDE (W/SR SQ M UM)

ALTITUDE M	ZENITH ANGLE OF PATH OF SIGHT (DEG)					
	95	100	105	120	150	180
300	1.91E 02	1.02E 02	6.13E 01	1.98E 01	5.88E 00	4.69E 00
600	2.32E 02	1.52E 02	1.01E 02	3.67E 01	1.16E 01	9.22E 00
900	2.37E 02	1.77E 02	1.27E 02	5.15E 01	1.74E 01	1.37E 01
1500	2.30E 02	1.95E 02	1.59E 02	7.95E 01	3.06E 01	2.42E 01
3000	2.32E 02	2.02E 02	1.69E 02	9.10E 01	3.86E 01	3.17E 01

FLIGHT NO. C-185A FILTER NO. 3
 PATH RADIANCE FROM GROUND TO ALTITUDE (W/SR SQ M UM)

ALTITUDE M	ZENITH ANGLE OF PATH OF SIGHT (DEG)					
	95	100	105	120	150	180
300	1.26E 02	5.95E 01	3.38E 01	1.01E 01	3.18E 00	2.72E 00
600	1.73E 02	9.80E 01	6.00E 01	1.97E 01	6.37E 00	5.36E 00
900	1.88E 02	1.23E 02	8.15E 01	2.94E 01	9.79E 00	8.10E 00
1500	1.84E 02	1.47E 02	1.12E 02	4.91E 01	1.76E 01	1.43E 01
3000	1.81E 02	1.51E 02	1.19E 02	5.66E 01	2.21E 01	1.89E 01

FLIGHT NO. C-185A
PATH RADIANCE FROM GROUND TO ALTITUDE
AZIMUTH OF PATH OF SIGHT = 90

(JOB 5712 DATE 04/27/73)

AZIMUTH OF PATH OF SIGHT = 90

ALTITUDE M	FLIGHT NO. C-185A FILTER NO. 2					
	PATH RADIANCE FROM GROUND TO ALTITUDE (W/SR SQ M UM)					
	ZENITH ANGLE OF PATH OF SIGHT (DEG)					
	95	100	105	120	150	180
300	9.61E C1	6.05E C1	4.12E C1	1.81E 01	7.62E 00	6.16E 00
600	1.16E 02	9.18E C1	7.07E 01	3.62E 01	1.64E 01	1.34E 01
900	1.24E 02	1.07E 02	8.80E C1	5.01E 01	2.41E C1	1.97E 01
1500	1.40E C2	1.28E 02	1.14E 02	7.49E C1	3.95E 01	3.27E 01
3000	1.68E 02	1.45E 02	1.32E 02	8.99E 01	5.13E 01	4.43E 01

ALTITUDE M	FLIGHT NO. C-185A FILTER NO. 4					
	PATH RADIANCE FROM GROUND TO ALTITUDE (W/SR SQ M UM)					
	ZENITH ANGLE OF PATH OF SIGHT (DEG)					
	95	100	105	120	150	180
300	7.81E C1	4.53E 01	3.00E 01	1.27E 01	5.56E 00	4.69E 00
600	9.78E C1	6.97E C1	5.05E C1	2.37E 01	1.09E 01	9.22E 00
900	1.04E C2	8.41E C1	6.55E 01	3.39E 01	1.62E 01	1.37E 01
1500	1.12E C2	1.02E C2	8.87E 01	5.42E 01	2.82E 01	2.42E 01
3000	1.35E C2	1.18E C2	1.03E 02	6.59E 01	3.65E 01	3.17E 01

ALTITUDE M	FLIGHT NO. C-185A FILTER NO. 3					
	PATH RADIANCE FROM GROUND TO ALTITUDE (W/SR SQ M UM)					
	ZENITH ANGLE OF PATH OF SIGHT (DEG)					
	95	100	105	120	150	180
300	4.37E C1	2.29E C1	1.46E 01	5.95E 00	2.96E 00	2.72E 00
600	6.20E C1	3.88E 01	2.66E 01	1.18E 01	5.91E 00	5.36E 00
900	6.98E C1	5.07E C1	3.72E 01	1.79E 01	5.08E 00	8.10E 00
1500	7.58E C1	6.62E C1	5.47E C1	3.12E 01	1.63E 01	1.43E 01
3000	8.62E C1	7.45E C1	6.32E 01	3.81E 01	2.11E 01	1.89E 01

FLIGHT NO. C-185A
PATH RADIANCE FROM GROUND TO ALTITUDE
AZIMUTH OF PATH OF SIGHT = 180

(JOB 5712 DATE 04/27/73)

AZIMUTH OF PATH OF SIGHT = 180

ALTITUDE M	FLIGHT NO. C-185A		FILTER NO. 2		PATH RADIANCE FROM GROUND TO ALTITUDE (W/SR SQ M UM)		
	ZENITH ANGLE OF PATH OF SIGHT (DEG)						
	95	100	105	120	150	180	
300	7.48E 01	4.95E 01	3.56E 01	1.82E 01	8.70E 00	6.16E 00	
600	9.05E 01	7.50E 01	6.06E 01	3.58E 01	1.86E 01	1.34E 01	
900	9.68E 01	8.69E 01	7.49E 01	4.88E 01	2.69E 01	1.97E 01	
1500	1.14E 02	1.07E 02	9.78E 01	7.23E 01	4.40E 01	3.27E 01	
3000	1.67E 02	1.43E 02	1.28E 02	9.55E 01	6.12E 01	4.43E 01	

ALTITUDE M	FLIGHT NO. C-185A		FILTER NO. 4		PATH RADIANCE FROM GROUND TO ALTITUDE (W/SR SQ M UM)		
	ZENITH ANGLE OF PATH OF SIGHT (DEG)						
	95	100	105	120	150	180	
300	5.59E 01	3.45E 01	2.44E 01	1.25E 01	6.39E 00	4.69E 00	
600	7.00E 01	5.28E 01	4.07E 01	2.29E 01	1.24E 01	9.22E 00	
900	7.46E 01	6.34E 01	5.22E 01	3.21E 01	1.81E 01	1.37E 01	
1500	8.45E 01	7.86E 01	7.08E 01	5.03E 01	3.10E 01	2.42E 01	
3000	1.20E 02	1.02E 02	9.04E 01	6.47E 01	4.09E 01	3.17E 01	

ALTITUDE M	FLIGHT NO. C-185A		FILTER NO. 3		PATH RADIANCE FROM GROUND TO ALTITUDE (W/SR SQ M UM)		
	ZENITH ANGLE OF PATH OF SIGHT (DEG)						
	95	100	105	120	150	180	
300	3.15E 01	1.79E 01	1.23E 01	6.18E 00	3.41E 00	2.72E 00	
600	4.42E 01	2.99E 01	2.20E 01	1.19E 01	6.72E 00	5.36E 00	
900	4.93E 01	3.83E 01	3.01E 01	1.76E 01	1.02E 01	8.10E 00	
1500	5.50E 01	4.98E 01	4.35E 01	2.95E 01	1.80E 01	1.43E 01	
3000	7.58E 01	6.43E 01	5.59E 01	3.88E 01	2.44E 01	1.89E 01	

FLIGHT NO. C-185A
PATH RADIANCE FROM GROUND TO ALTITUDE
AZIMUTH OF PATH OF SIGHT = 270

(JOB 5712 DATE 04/27/73)

AZIMUTH OF PATH OF SIGHT = 270

ALTITUDE M	FLIGHT NO. C-185A FILTER NO. 2					
	PATH RADIANCE FROM GROUND TO ALTITUDE (W/SR SQ M UM)					
	ZENITH ANGLE OF PATH OF SIGHT (DEG)					
	95	100	105	120	150	180
300	8.72E 01	5.56E 01	3.84E 01	1.75E 01	7.72E 00	6.16E 00
600	1.04E 02	8.33E 01	6.48E 01	3.44E 01	1.65E 01	1.34E 01
900	1.09E 02	9.54E 01	7.95E 01	4.68E 01	2.39E 01	1.97E 01
1500	1.23E 02	1.13E 02	1.01E 02	6.83E 01	3.86E 01	3.27E 01
3000	1.58E 02	1.37E 02	1.21E 02	8.43E 01	5.11E 01	4.43E 01

ALTITUDE M	FLIGHT NO. C-185A FILTER NO. 4					
	PATH RADIANCE FROM GROUND TO ALTITUDE (W/SR SQ M UM)					
	ZENITH ANGLE OF PATH OF SIGHT (DEG)					
	95	100	105	120	150	180
300	6.53E 01	3.85E 01	2.60E 01	1.17E 01	5.65E 00	4.69E 00
600	8.12E 01	5.88E 01	4.33E 01	2.17E 01	1.10E 01	9.22E 00
900	8.56E 01	7.02E 01	5.56E 01	3.06E 01	1.63E 01	1.37E 01
1500	9.21E 01	8.43E 01	7.39E 01	4.80E 01	2.81E 01	2.42E 01
3000	1.14E 02	9.93E 01	8.69E 01	5.83E 01	3.59E 01	3.17E 01

ALTITUDE M	FLIGHT NO. C-185A FILTER NO. 3					
	PATH RADIANCE FROM GROUND TO ALTITUDE (W/SR SQ M UM)					
	ZENITH ANGLE OF PATH OF SIGHT (DEG)					
	95	100	105	120	150	180
300	3.83E 01	2.02E 01	1.31E 01	5.67E 00	3.05E 00	2.72E 00
600	5.36E 01	3.39E 01	2.35E 01	1.11E 01	6.04E 00	5.36E 00
900	5.95E 01	4.37E 01	3.24E 01	1.66E 01	9.17E 00	8.10E 00
1500	6.39E 01	5.61E 01	4.69E 01	2.82E 01	1.62E 01	1.43E 01
3000	7.81E 01	6.65E 01	5.63E 01	3.52E 01	2.11E 01	1.89E 01

FLIGHT NO. C-185A
DIRECTIONAL PATH REFLECTANCE FROM GROUND TO ALTITUDE
AZIMUTH OF PATH OF SIGHT = 0

(JOB 5712 DATE 04/27/73)

AZIMUTH OF PATH OF SIGHT = 0

FLIGHT NO. C-185A FILTER NO. 2
DIRECTIONAL PATH REFLECTANCE FROM GROUND TO ALTITUDE

ALTITUDE M	ZENITH ANGLE OF PATH OF SIGHT (DEG)					
	95	100	105	120	150	180
300	3.64E 00	8.20E-01	3.72E-01	9.22E-02	2.34E-02	1.76E-02
600	4.05E 01	3.69E 00	1.31E 00	2.67E-01	6.31E-02	4.66E-02
900	2.96E 02	1.09E 01	3.03E 00	5.06E-01	1.12E-01	8.10E-02
1500	1.21E 04	7.22E 01	1.22E 01	1.36E 00	2.62E-01	1.84E-01
3000	5.12E 04	1.32E 02	1.90E 01	1.88E 00	3.72E-01	2.75E-01

FLIGHT NO. C-185A FILTER NO. 4
DIRECTIONAL PATH REFLECTANCE FROM GROUND TO ALTITUDE

ALTITUDE M	ZENITH ANGLE OF PATH OF SIGHT (DEG)					
	95	100	105	120	150	180
300	1.90E 00	5.12E-01	2.46E-01	6.37E-02	1.71E-02	1.34E-02
600	8.55E 00	1.50E 00	6.35E-01	1.49E-01	3.87E-02	2.96E-02
900	3.57E 01	3.42E 00	1.26E 00	2.65E-01	6.62E-02	4.94E-02
1500	7.36E 02	1.70E 01	4.33E 00	6.88E-01	1.57E-01	1.13E-01
3000	2.42E 03	2.83E 01	6.33E 00	9.29E-01	2.19E-01	1.61E-01

FLIGHT NO. C-185A FILTER NO. 3
DIRECTIONAL PATH REFLECTANCE FROM GROUND TO ALTITUDE

ALTITUDE M	ZENITH ANGLE OF PATH OF SIGHT (DEG)					
	95	100	105	120	150	180
300	8.87E-01	2.75E-01	1.36E-01	3.54E-02	1.05E-02	8.86E-03
600	2.94E 00	7.02E-01	3.24E-01	8.03E-02	2.29E-02	1.88E-02
900	8.45E 00	1.43E 00	6.08E-01	1.42E-01	3.88E-02	3.10E-02
1500	8.03E 01	5.21E 00	1.77E 00	3.50E-01	8.72E-02	6.63E-02
3000	2.14E 02	8.14E 00	2.50E 00	4.66E-01	1.19E-01	9.44E-02

FLIGHT NO. C-185A
DIRECTIONAL PATH REFLECTANCE FROM GROUND TO ALTITUDE
AZIMUTH OF PATH OF SIGHT = 90

(JOB 5712 DATE 04/27/73)

AZIMUTH OF PATH OF SIGHT = 90

FLIGHT NO. C-185A FILTER NO. 2

DIRECTIONAL PATH REFLECTANCE FROM GROUND TO ALTITUDE

ZENITH ANGLE OF PATH OF SIGHT (DEG)

ALTITUDE M	95	100	105	120	150	180
300	1.55E C0	3.75E-C1	1.89E-C1	6.10E-02	2.23E-02	1.76E-02
600	1.80E C1	1.78E CC	6.91E-01	1.81E-01	6.05E-02	4.66E-02
900	1.37E C2	5.46E CC	1.65E CC	3.50E-01	1.07E-01	8.10E-02
1500	6.21E C3	4.00E C1	7.18E C0	9.80E-01	2.53E-01	1.84E-01
3000	3.12E C4	8.14E C1	1.22E 01	1.43E C0	3.69E-C1	2.75E-01

FLIGHT NO. C-185A FILTER NO. 4

DIRECTIONAL PATH REFLECTANCE FROM GROUND TO ALTITUDE

ZENITH ANGLE OF PATH OF SIGHT (DEG)

ALTITUDE M	95	100	105	120	150	180
300	7.77E-C1	2.28E-C1	1.20E-01	4.07E-02	1.62E-02	1.34E-02
600	3.77E C0	6.88E-C1	3.18E-01	9.64E-02	3.63E-02	2.96E-02
900	1.56E C1	1.63E C0	6.49E-01	1.74E-01	6.16E-02	4.94E-02
1500	3.60E C2	8.91E CC	2.41E CC	4.69E-01	1.45E-C1	1.13E-01
3000	1.41E C3	1.66E C1	3.87E CC	6.73E-01	2.07E-01	1.61E-01

FLIGHT NO. C-185A FILTER NO. 3

DIRECTIONAL PATH REFLECTANCE FROM GROUND TO ALTITUDE

ZENITH ANGLE OF PATH OF SIGHT (DEG)

ALTITUDE M	95	100	105	120	150	180
300	3.09E-C1	1.06E-C1	5.88E-02	2.09E-02	9.77E-03	8.86E-03
600	1.05E C0	2.78E-C1	1.43E-01	4.81E-02	2.13E-C2	1.88E-02
900	3.14E C0	5.88E-C1	2.77E-C1	8.66E-02	3.60E-C2	3.10E-02
1500	3.32E C1	2.36E CC	8.65E-C1	2.22E-01	8.09E-C2	6.63E-02
3000	1.02E C2	4.05E CC	1.32E CC	3.14E-01	1.14E-01	9.44E-02

FLIGHT NO. C-185A
DIRECTIONAL PATH REFLECTANCE FROM GROUND TO ALTITUDE
AZIMUTH OF PATH OF SIGHT = 180

(JOB 5712 DATE 04/27/73)
 AZIMUTH OF PATH OF SIGHT = 180

ALTITUDE M	FLIGHT NO. C-185A FILTER NO. 2					
	DIRECTIONAL PATH REFLECTANCE FROM GROUND TO ALTITUDE					
	ZENITH ANGLE OF PATH OF SIGHT (DEG)					
	95	100	105	120	150	180
300	1.21E C0	3.10E-01	1.63E-01	6.12E-02	2.55E-02	1.76E-02
600	1.41E C1	1.45E C0	5.92E-01	1.78E-01	6.82E-02	4.66E-02
900	1.08E C2	4.45E C0	1.41E C0	3.41E-01	1.20E-01	8.10E-02
1500	5.09E C3	3.32E 01	6.17E C0	9.47E-01	2.82E-01	1.84E-01
3000	3.10E C4	7.83E 01	1.18E 01	1.52E 00	4.40E-01	2.75E-01

ALTITUDE M	FLIGHT NO. C-185A FILTER NO. 4					
	DIRECTIONAL PATH REFLECTANCE FROM GROUND TO ALTITUDE					
	ZENITH ANGLE OF PATH OF SIGHT (DEG)					
	95	100	105	120	150	180
300	5.56E-01	1.73E-01	9.77E-02	4.00E-02	1.86E-02	1.34E-02
600	2.70E C0	5.21E-01	2.57E-01	9.32E-02	4.12E-02	2.96E-02
900	1.12E C1	1.23E 00	5.18E-01	1.65E-01	6.89E-02	4.94E-02
1500	2.71E C2	6.84E C0	1.92E 00	4.35E-01	1.59E-01	1.13E-01
3000	1.25E C3	1.44E C1	3.39E C0	6.61E-01	2.32E-01	1.61E-01

ALTITUDE M	FLIGHT NO. C-185A FILTER NO. 3					
	DIRECTIONAL PATH REFLECTANCE FROM GROUND TO ALTITUDE					
	ZENITH ANGLE OF PATH OF SIGHT (DEG)					
	95	100	105	120	150	180
300	2.22E-01	8.26E-02	4.97E-02	2.17E-02	1.12E-02	8.86E-03
600	7.51E-01	2.14E-01	1.19E-01	4.86E-02	2.42E-02	1.88E-02
900	2.22E C0	4.44E-01	2.25E-01	8.49E-02	4.03E-02	3.10E-02
1500	2.41E C1	1.77E 00	6.88E-01	2.10E-01	8.94E-02	6.63E-02
3000	8.98E C1	3.48E C0	1.17E C0	3.20E-01	1.32E-01	9.44E-02

FLIGHT NO. C-185A
DIRECTIONAL PATH REFLECTANCE FROM GROUND TO ALTITUDE
AZIMUTH OF PATH OF SIGHT = 270

(JOB 5712 DATE 04/27/73)

AZIMUTH OF PATH OF SIGHT = 270

FLIGHT NO. C-185A FILTER NO. 2

DIRECTIONAL PATH REFLECTANCE FROM GROUND TO ALTITUDE

ALTITUDE M	ZENITH ANGLE OF PATH OF SIGHT (DEG)					
	95	100	105	120	150	180
300	1.41E C0	3.48E-01	1.76E-01	5.89E-02	2.26E-02	1.76E-02
600	1.61E C1	1.61E C0	6.33E-01	1.71E-01	6.05E-02	4.66E-02
900	1.22E C2	4.88E C0	1.49E C0	3.27E-01	1.07E-01	8.10E-02
1500	5.46E C3	3.51E C1	6.35E C0	8.94E-01	2.48E-01	1.84E-01
3000	2.94E C4	7.51E C1	1.12E C1	1.34E C0	3.67E-01	2.75E-01

FLIGHT NO. C-185A FILTER NO. 4

DIRECTIONAL PATH REFLECTANCE FROM GROUND TO ALTITUDE

ALTITUDE M	ZENITH ANGLE OF PATH OF SIGHT (DEG)					
	95	100	105	120	150	180
300	6.50E-01	1.94E-01	1.04E-01	3.77E-02	1.64E-02	1.34E-02
600	3.13E C0	5.80E-01	2.73E-01	8.83E-02	3.67E-02	7.96E-02
900	1.29E C1	1.76E C0	5.51E-01	1.57E-01	6.20E-02	4.94E-02
1500	2.95E C2	7.33E C0	2.01E C0	4.15E-01	1.45E-01	1.13E-01
3000	1.19E C3	1.39E C1	3.26E C0	5.96E-01	2.03E-01	1.61E-01

FLIGHT NO. C-185A FILTER NO. 3

DIRECTIONAL PATH REFLECTANCE FROM GROUND TO ALTITUDE

ALTITUDE M	ZENITH ANGLE OF PATH OF SIGHT (DEG)					
	95	100	105	120	150	180
300	2.70E-01	9.37E-02	5.27E-02	1.99E-02	1.01E-02	8.86E-03
600	9.10E-01	7.43E-01	1.27E-01	4.52E-02	2.17E-02	1.88E-02
900	2.68E C0	5.07E-01	2.42E-01	8.00E-02	3.64E-02	3.10E-02
1500	2.79E C1	2.00E C0	7.42E-01	2.01E-01	8.04E-02	6.63E-02
3000	9.26E C1	3.60E C0	1.18E C0	2.90E-01	1.14E-01	9.44E-02

FLIGHT C-185B – 18 AUGUST 1971 – TRACK 3 – DESCRIPTION OF FLIGHT AND WEATHER CHARACTERISTICS

It was a sunlit afternoon. There were scattered cumulus clouds and surface haze during the flight. The flight was conducted over multiple small fields northeast of St. Louis. The typical terrain was flat, highly cultivated farmland. The data-taking started at 1746 GMT (1246 CDT) and continued until 1913 GMT (1413 CDT). The sun zenith angle during sky radiance data-taking for Filters 2, 3, and 4 was 26.3 degrees at the beginning and 28.0 degrees at the end. The maximum altitude for the flight was 2640 meters. Average terrain elevation along this track was 183 meters.

At the beginning of data-taking, Scott Air Force Base was reporting 0.1 cumulus clouds at 4000 feet (1200 meters) and 6-mile (9.6-kilometer) visibility in haze.

The ground station located at Scott, 70 miles (110 kilometers) from the center of the flight path, recorded scattered cumulus clouds and moderate haze.

During the flight, the aircrew made the following observations, which have been extracted from the flight log and summarized. Metric altitudes have been added editorially.

FLIGHT LOG ENTRY

Time (GMT)	Altitude (m AGL)	Aircrew Observations
1746	1950	Haze top at 7500 ft (2280 m) MSL
1800	840	Just below cloud base, second straight and level run in the top of the haze
1823	1560	On top of haze at 6200 ft (1890 m) MSL, clear overhead
1831	2550	Cloud deck sitting on top of haze

At the end of data-taking, Scott was reporting 0.1 cumulus cloud at 4500 feet (1350 meters) and a visibility of 6 miles (9.6 kilometers) in haze.

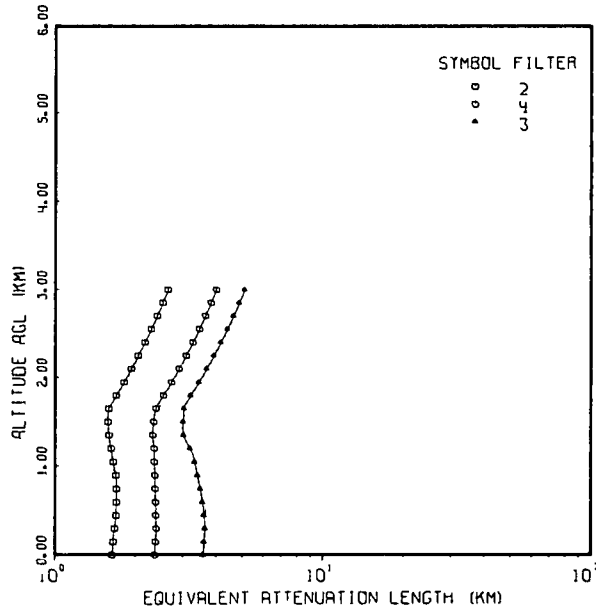
The surface synoptic chart shows an extremely weak gradient. There was a low centered in eastern South Dakota with a cold front extending southwestward.

At 500 millibars there was high extending from Illinois to Texas and westward to California. There was another area of high along and off the east coast extending from New Jersey to Florida. The flow over the St. Louis area was moderate northeasterly.

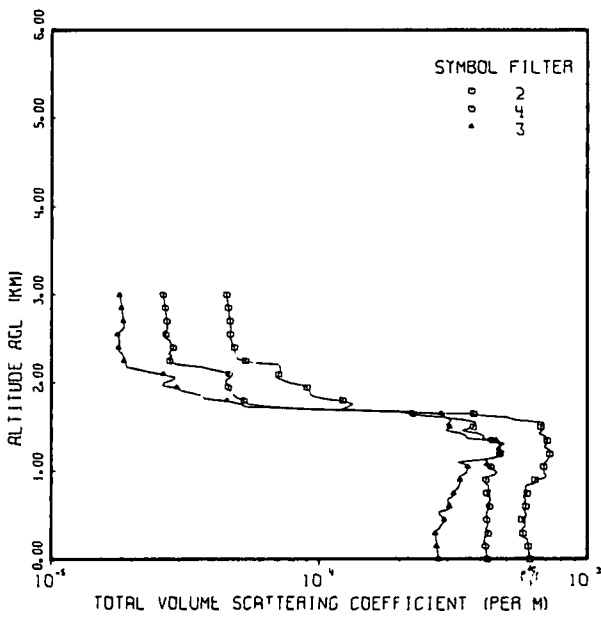
These data were taken from the 3-hourly facsimile charts issued by the NMC and obtained from Lindbergh Field NOAA office. The 500-millibar charts are for 0000 GMT and 1200 GMT daily.

FLIGHT NO. C-185B

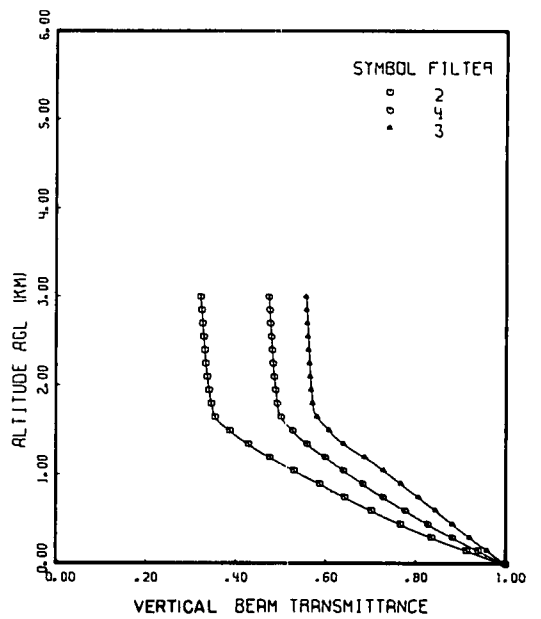
FLIGHT C-185B



FLIGHT C-185B



FLIGHT C-185B



FLIGHT NO. C-185B
TOTAL VOLUME SCATTERING COEFFICIENT

(JOB 5732 DATE 04/28/73)
 DATE 81871 FLIGHT NO. C-185B GROUND LEVEL ALTITUDE (M)= 183

ALTITUDE (M)	TOTAL VOLUME SCATTERING COEFFICIENT (PER M) FILTERS			
		2	4	3
0	6.11E-04	4.24E-04	2.79E-04	
30	6.08E-04	4.22E-04	2.78E-04	
60	6.07E-04	4.21E-04	2.77E-04	
90	6.05E-04	4.20E-04	2.77E-04	
120	6.04E-04	4.19E-04	2.76E-04	
150	6.02E-04	4.18E-04	2.75E-04	
180	6.01E-04	4.19E-04	2.74E-04	
210	5.99E-04	4.11E-04	2.74E-04	
240	5.98E-04	4.15E-04	2.73E-04	
270	5.70E-04	4.16E-04	2.72E-04	
300	5.75E-04	4.28E-04	2.72E-04	
330	5.73E-04	4.23E-04	2.74E-04	
360	5.71E-04	4.18E-04	2.81E-04	
390	5.86E-04	4.23E-04	2.84E-04	
420	5.85E-04	4.27E-04	2.89E-04	
450	5.69E-04	4.22E-04	2.93E-04	
480	5.89E-04	4.22E-04	2.88E-04	
510	5.91E-04	4.20E-04	2.83E-04	
540	5.88E-04	4.21E-04	2.79E-04	
570	5.82E-04	4.26E-04	3.03E-04	
600	5.90E-04	4.32E-04	3.07E-04	
630	5.92E-04	4.25E-04	3.10E-04	
660	5.83E-04	4.31E-04	3.01E-04	
690	5.89E-04	4.34E-04	3.03E-04	
720	5.77E-04	4.33E-04	3.15E-04	
750	5.97E-04	4.22E-04	3.18E-04	
780	5.89E-04	4.38E-04	3.22E-04	
810	5.89E-04	4.27E-04	3.29E-04	
840	5.90E-04	4.29E-04	3.32E-04	
870	6.39E-04	4.15E-04	3.36E-04	
900	6.39E-04	4.19E-04	3.36E-04	
930	6.99E-04	4.23E-04	3.31E-04	
960	7.00E-04	4.47E-04	3.43E-04	
990	6.89E-04	4.63E-04	3.55E-04	
1020	6.88E-04	4.46E-04	3.57E-04	
1050	6.88E-04	4.37E-04	3.60E-04	
1080	6.96E-04	4.09E-04	3.50E-04	
1110	6.96E-04	4.26E-04	3.29E-04	
1140	7.11E-04	4.19E-04	4.06E-04	
1170	7.21E-04	4.61E-04	4.60E-04	
1200	7.24E-04	4.72E-04	4.74E-04	
1230	7.31E-04	4.77E-04	4.90E-04	
1260	7.15E-04	4.72E-04	4.55E-04	
1290	6.89E-04	4.72E-04	4.68E-04	
1320	7.04E-04	4.73E-04	4.91E-04	
1350	7.09E-04	4.41E-04	4.59E-04	
1380	6.98E-04	4.06E-04	3.59E-04	
1410	6.95E-04	4.11E-04	3.52E-04	
1440	6.59E-04	3.87E-04	3.36E-04	
1470	6.77E-04	3.40E-04	2.95E-04	
1500	6.71E-04	3.75E-04	3.08E-04	

FLIGHT NO. C-185B
TOTAL VOLUME SCATTERING COEFFICIENT

(JOB 5732 DATE 04/28/73)
 DATE 81871 FLIGHT NO. C-185B GROUND LEVEL ALTITUDE (M)= 183

ALTITUDE (M)	TOTAL VOLUME SCATTERING COEFFICIENT (PER M)			
	FILTERS	2	4	3
1530		6.92E-04	3.80E-04	2.97E-04
1560		6.84E-04	3.84E-04	3.06E-04
1590		5.38E-04	3.45E-04	3.11E-04
1620		5.01E-04	2.91E-04	2.94E-04
1650		3.77E-04	2.23E-04	2.86E-04
1680		1.85E-04	2.00E-04	2.14E-04
1710		1.21E-04	9.19E-05	1.01E-04
1740		1.28E-04	6.61E-05	5.30E-05
1770		1.34E-04	5.42E-05	5.09E-05
1800		1.22E-04	5.24E-05	4.54E-05
1830		1.04E-04	4.99E-05	3.72E-05
1860		9.41E-05	4.81E-05	3.69E-05
1890		9.25E-05	4.76E-05	3.38E-05
1920		9.17E-05	4.64E-05	3.05E-05
1950		8.98E-05	4.57E-05	2.95E-05
1980		8.70E-05	4.57E-05	2.58E-05
2010		7.76E-05	4.44E-05	2.66E-05
2040		7.32E-05	4.48E-05	2.83E-05
2070		6.90E-05	4.68E-05	2.92E-05
2100		7.05E-05	4.61E-05	2.63E-05
2130		7.17E-05	4.42E-05	2.34E-05
2160		7.16E-05	3.99E-05	2.12E-05
2190		7.15E-05	3.63E-05	1.90E-05
2220		7.02E-05	2.94E-05	1.90E-05
2250		5.30E-05	2.76E-05	1.87E-05
2280		4.96E-05	2.74E-05	1.88E-05
2310		4.89E-05	2.84E-05	1.86E-05
2340		4.86E-05	2.74E-05	1.83E-05
2370		4.81E-05	2.77E-05	1.78E-05
2400		4.82E-05	2.85E-05	1.79E-05
2430		4.74E-05	2.84E-05	1.79E-05
2460		4.72E-05	2.78E-05	1.79E-05
2490		4.69E-05	2.76E-05	1.79E-05
2520		4.64E-05	2.66E-05	1.78E-05
2550		4.65E-05	2.67E-05	1.77E-05
2580		4.64E-05	2.61E-05	1.80E-05
2610		4.68E-05	2.72E-05	1.84E-05
2640		4.67E-05	2.71E-05	1.87E-05
2670		4.66E-05	2.70E-05	1.86E-05
2700		4.64E-05	2.70E-05	1.86E-05
2730		4.63E-05	2.69E-05	1.85E-05
2760		4.61E-05	2.68E-05	1.85E-05
2790		4.60E-05	2.67E-05	1.84E-05
2820		4.58E-05	2.66E-05	1.83E-05
2850		4.57E-05	2.65E-05	1.83E-05
2880		4.55E-05	2.65E-05	1.82E-05
2910		4.54E-05	2.64E-05	1.82E-05
2940		4.53E-05	2.63E-05	1.81E-05
2970		4.51E-05	2.62E-05	1.81E-05
3000		4.50E-05	2.61E-05	1.80E-05
FIRST DATA ALT	240	150	270	
LAST DATA ALT	2610	2610	2640	

FLIGHT NO. C-185B
EQUIVALENT ATTENUATION LENGTH

(JOB 5732 DATE 04/28/73)
 UATE 81871 FLIGHT NO. C-185B GROUND LEVEL ALTITUDE (M)= 183

ALTITUDE (M)	EQUIVALENT ATTENUATION LENGTH (KM)		
	FILTERS 2	4	3
0	1.64E 00	2.36E 00	3.58E 00
300	1.67E 00	2.39E 00	3.63E 00
600	1.69E 00	2.38E 00	3.56E 00
900	1.69E 00	2.36E 00	3.41E 00
1200	1.62E 00	2.34E 00	3.20E 00
1500	1.58E 00	2.34E 00	3.01E 00
1800	1.69E 00	2.54E 00	3.21E 00
2100	1.93E 00	2.90E 00	3.68E 00
2400	2.17E 00	3.28E 00	4.17E 00
2700	2.41E 00	3.64E 00	4.64E 00
3000	2.64E 00	4.01E 00	5.11E 00

FLIGHT NO. C-185B
VERTICAL BEAM TRANSMITTANCE FROM GROUND TO ALTITUDE

ALTITUDE (M)	VERTICAL BEAM TRANSMITTANCE FROM GROUND TO ALTITUDE		
	FILTERS 2	4	3
0	1.00E 00	1.00E 00	1.00E 00
300	8.36E-01	8.82E-01	9.21E-01
600	7.02E-01	7.77E-01	8.45E-01
900	5.67E-01	6.82E-01	7.68E-01
1200	4.76E-01	5.95E-01	6.87E-01
1500	3.86E-01	5.27E-01	6.08E-01
1800	3.45E-01	4.92E-01	5.71E-01
2100	3.36E-01	4.85E-01	5.66E-01
2400	3.30E-01	4.81E-01	5.62E-01
2700	3.26E-01	4.77E-01	5.59E-01
3000	3.21E-01	4.73E-01	5.56E-01

FLIGHT C-187B – 23 AUGUST 1971 – TRACK 4 – DESCRIPTION OF FLIGHT AND WEATHER CHARACTERISTICS

It was a sunlit afternoon. At the beginning of data-taking there were two layers of scattered clouds reported. By the end of data-taking the higher layer had increased to broken. The flight was conducted over cultivated farmland eastsoutheast of St. Louis. The typical terrain was cultivated lands and small bodies of water. The data-taking started at 1942 GMT (1442 CDT) and continued until 2024 GMT (1524 CDT). The sun zenith angle during sky radiance data-taking for Filters 2, 3, and 4 was 35.5 degrees at the beginning and 39.8 degrees at the end. The maximum altitude for the flight was 1440 meters. Average terrain elevation for this track was 153 meters.

At the beginning of data-taking, Scott Air Force Base was reporting 0.3 cloud cover with scattered cumulus at 4000 feet (1200 meters) and thin scattered cirrus at 30 000 feet (9000 meters). Visibility was 12 miles (19 kilometers).

The ground station located at Scott, 39 miles (63 kilometers) from the center of the flight path, recorded scattered small cumulus and moderate haze.

During the flight, the aircrew made the following observations, which have been extracted from the flight log and summarized. Metric altitudes have been added editorially.

FLIGHT LOG ENTRY

Time (GMT)	Altitude (m AGL)	Aircrew Observations
-	-	There were heavy cloud buildups in all northeastern tracks
1945	1037	Light to moderate haze at 1800 ft (550 m) MSL, scattered clouds above, hazy blue zenith sky
1957		Passing through cloud layer at 5000 ft (1525 m) MSL
2004	915	Running below cloud base at 3500 ft (1070 m) MSL in heavy haze

At the end of data-taking, Scott was reporting 0.6 cloud cover with scattered cumulus clouds at 4000 feet (1200 meters) and thin broken cirrus at 30 000 feet (9000 meters). Visibility was 12 miles (19 kilometers).

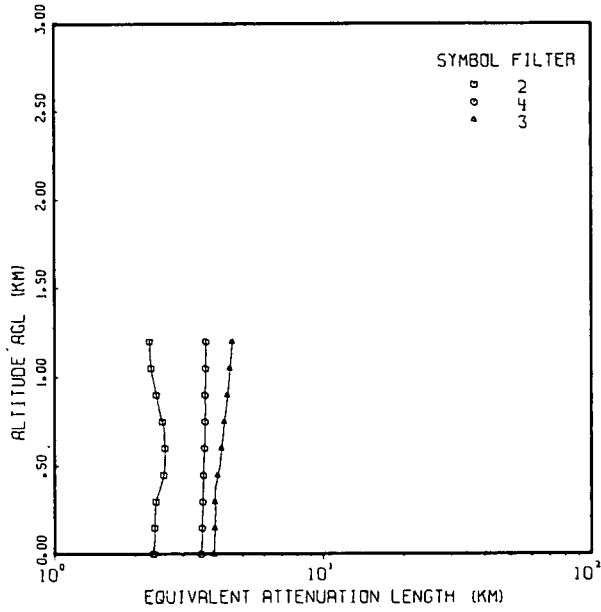
The surface synoptic chart shows a cold front extending south-southwestward from Maine to the DelMarVa peninsula, then westward to Evansville and northwestward to Springfield and Keokuk to a low in central North Dakota.

At 500 millibars there was a high centered near Topeka and a trough from Ontario to Virginia. The gradient shows moderate northeasterly winds over the region.

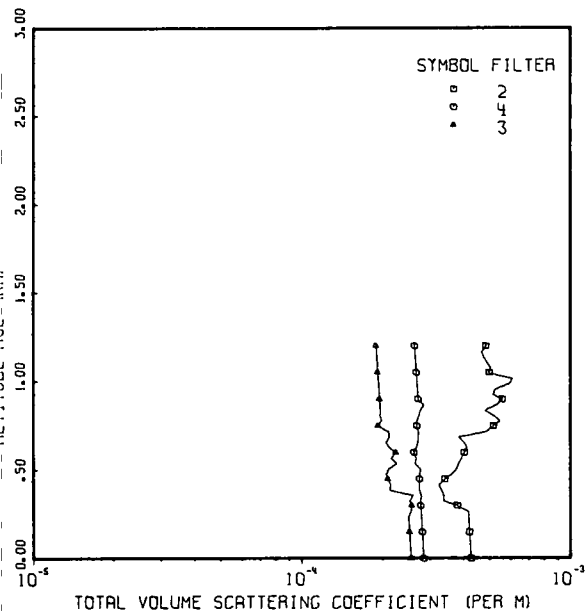
These data were taken from the 3-hourly facsimile charts issued by the NMC and obtained from Lindbergh Field NOAA office. The 500-millibar charts are for 0000 GMT and 1200 GMT daily.

FLIGHT NO. C-187B

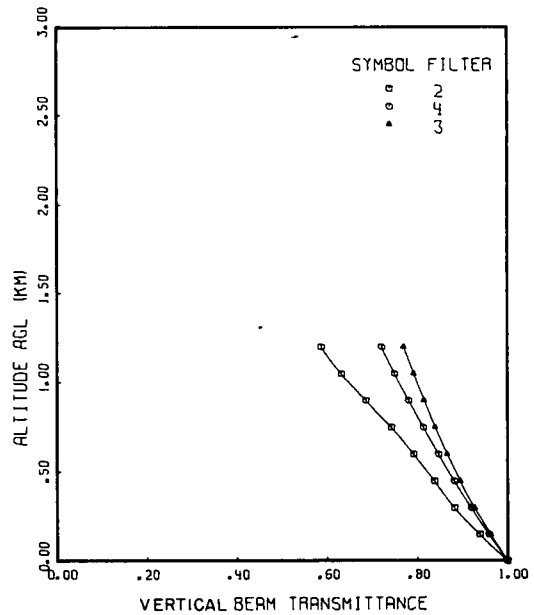
FLIGHT C-187B



FLIGHT C-187B



FLIGHT C-187B



FLIGHT NO. C-187B
TOTAL VOLUME SCATTERING COEFFICIENT

(JOB 5594 DATE 04/25/73)
 DATE 82371 FLIGHT NO. C-187B GROUND LEVEL ALTITUDE (M)= 152

ALTITUDE (M)	TOTAL VOLUME SCATTERING COEFFICIENT (PER M)		
	FILTERS 2	4	3
0	4.28E-04	2.85E-04	2.55E-04
30	4.25E-04	2.83E-04	2.54E-04
60	4.24E-04	2.83E-04	2.53E-04
90	4.23E-04	2.82E-04	2.53E-04
120	4.22E-04	2.81E-04	2.52E-04
150	4.21E-04	2.81E-04	2.52E-04
180	4.20E-04	2.80E-04	2.51E-04
210	4.19E-04	2.79E-04	2.50E-04
240	4.18E-04	2.78E-04	2.49E-04
270	4.17E-04	2.78E-04	2.55E-04
300	3.80E-04	2.77E-04	2.57E-04
330	3.37E-04	2.78E-04	2.52E-04
360	3.38E-04	2.78E-04	2.60E-04
390	3.31E-04	2.73E-04	2.12E-04
420	3.24E-04	2.73E-04	2.14E-04
450	3.41E-04	2.74E-04	2.09E-04
480	3.62E-04	2.75E-04	2.05E-04
510	3.77E-04	2.76E-04	2.11E-04
540	3.82E-04	2.64E-04	2.26E-04
570	3.93E-04	2.67E-04	2.14E-04
600	4.03E-04	2.61E-04	2.23E-04
630	4.13E-04	2.68E-04	2.11E-04
660	4.01E-04	2.70E-04	2.05E-04
690	3.84E-04	2.71E-04	2.12E-04
720	4.85E-04	2.72E-04	2.10E-04
750	5.17E-04	2.68E-04	1.92E-04
780	5.49E-04	2.68E-04	1.98E-04
810	5.19E-04	2.73E-04	1.95E-04
840	4.81E-04	2.76E-04	1.96E-04
870	5.30E-04	2.84E-04	1.95E-04
900	5.59E-04	2.71E-04	1.94E-04
930	5.14E-04	2.70E-04	1.94E-04
960	5.27E-04	2.69E-04	1.93E-04
990	5.94E-04	2.68E-04	1.93E-04
1020	6.10E-04	2.67E-04	1.92E-04
1050	4.99E-04	2.67E-04	1.92E-04
1080	5.06E-04	2.66E-04	1.91E-04
1110	4.89E-04	2.65E-04	1.90E-04
1140	4.76E-04	2.64E-04	1.90E-04
1170	4.66E-04	2.63E-04	1.89E-04
1200	4.84E-04	2.63E-04	1.89E-04
FIRST DATA ALT	270	270	210
LAST DATA ALT	1200	900	840

FLIGHT NO. C-187B
EQUIVALENT ATTENUATION LENGTH

(JOB 5594 DATE 04/25/73)
 DATE 82371 FLIGHT NO. C-187B GROUND LEVEL ALTITUDE (M)= 152

ALTITUDE (M)	EQUIVALENT ATTENUATION LENGTH (KM)			
	FILTERS	2	4	3
0		2.34E 00	3.51E CC	3.92E 00
300		2.38E 00	3.56E CC	3.96E 00
600		2.57E 00	3.62E CC	4.19E 00
900		2.39E 00	3.64E CC	4.42E 00
1200		2.26E 00	3.67E CC	4.59E 00

FLIGHT NO. C-187B
VERTICAL BEAM TRANSMITTANCE FROM GROUND TO ALTITUDE

ALTITUDE (M)	VERTICAL BEAM TRANSMITTANCE FROM GROUND TO ALTITUDE			
	FILTERS	2	4	3
0		1.00E 00	1.00E 00	1.00E 00
300		8.82E-C1	9.19E-C1	9.27E-01
600		7.92E-C1	8.47E-C1	8.67E-01
900		6.87E-C1	7.81E-C1	8.16E-01
1200		5.87E-01	7.21E-C1	7.70E-01

7.4 GROUND-BASED DATA SUMMARY

The threefold purpose of the ground station was to (1) provide measurements of inherent terrain radiance and reflectance appropriate for use with airborne measurements, (2) provide continuity of measurement by establishing ground-level values of downwelling irradiance and total scattering coefficient, and (3) establish earth-to-space beam transmittance, path radiance, and path reflectance for the vertically downward path of sight for comparison with the partial path transmittance, path radiance, and path reflectance derived from airborne measurements.

Unfortunately, the calibration of the contrast reduction meter optical collector for the solar disk radiance is questionable. Thus the third purpose, that of establishing values of earth-to-space beam transmittance, path radiance, and path reflectance, was not achieved.

Figure 1-4 presented St. Louis and the surrounding area in detail and the locations of the various flight tracks. Also indicated on Fig. 1-4 is Scott Air Force Base, latitude 38.55°N, longitude 89.85°W, altitude 138 meters MSL, where the ground station was located throughout the METRO deployment.

A summary of all the ground station data sets for METRO is presented in Table 7-4. The numbering is sequential. The times under the Total Time of Data-Taking column are Greenwich mean time (GMT) and central daylight time (CDT). CDT is equal to GMT-5. The sun zenith angles are tabulated for the time when data-taking began, at the time of sun transit (minimum sun zenith angle), and at the conclusion of data-taking. The coding for data modes indicated in columns 10 and 11 is explained in Table 7-5. The final column indicates the numbers for the flights which were concurrent with the period of the ground-based data-taking.

During the automatic data modes the irradiance $H(0,d)$, as measured by the contrast reduction meter and the sky scanner, and the total scattering coefficient $s(0)$ were monitored continuously. Thus these three measurements are available during each data mode in addition to the data indicated under the Basic Data Type column in Table 7-5. The scanner during Mode 2 is oriented so that the scanner zenith moves 90 degrees in elevation to a position on the horizon, which is 90 degrees in azimuth from the azimuth of the sun. Thus, the instrument's hemispherical scan includes all the terrain and sky radiances in the azimuths 0 degrees to 180 degrees from the sun.

The manual data modes were designed to provide data in case the automatic data logging system failed. Since the automatic data system operated properly, the manual data were not reduced.

DESCRIPTION OF WEATHER CHARACTERISTICS

MET-01 12 August 1971

It was a sunlit afternoon. The weather was hot and clear with some high cirrus. The data-taking started at 1857 GMT (1357 CDT) and continued until 2107 GMT (1607 CDT). The sun zenith angle during data-taking was 26.2 degrees at the beginning and 46.4 degrees at the end.

Table 7-4

METRO Ground-Based Data Summary

Ground Data Set	Date (1971)	Total Time of Data-Taking				Sun Zenith Angle (Deg)			Data Modes		Concurrent Flight No.
		Start		End		Start	Transit	End	Automatic	Manual *	
		GMT	CDT	GMT	CDT						
MET 01	12 Aug	1857	1357	2107	1607	26.2	-	46.4	1-2-3-4-1-5		C-181
MET 02	13 Aug	1509	1009	1705	1205	45.2	-	27.2	1-2-3-4-1-5		C-182A
MET 03	13 Aug	1859	1359	1923	1423	26.7	-	29.5	3-4		
MET 04	14 Aug	1613	1113	1623	1123	34.4	-	32.8	1		C-183A
MET 05	18 Aug	1609	1109	1851	1351	35.8	25.2	27.5	1-2-3-4-1-5	21-24	C-185A C-185B
MET 06	19 Aug	1554	1054	1741	1241	38.4	-	26.2	1-4-3-2-1-5	21-24	C-186A
MET 07	19 Aug	1912	1412	1946	1446	29.9	-	34.4	1-4-1		
MET 08	23 Aug	1749	1249	1948	1448	27.2	26.8	35.9	1-4-2-3-5-1	21	C-187A
MET 09	23 Aug	2032	1532	2040	1540	42.9	-	44.3	1		
MET 10	24 Aug	1312	812	1510	1010	69.4	-	47.0	1-2-3-4-1-5	21	C-188A
MET 11	24 Aug	1553	1053	1658	1158	39.6	-	30.9	1-2-3-4-1	21	C-188B

* Data not reduced

Table 7-5

Data Mode Explanation

Mode Code	Primary Instrument	Basic Data Type
1 (Automatic)	Nephelometer	$s(o), \sigma(30,0), \sigma(150,0)$
2 (Automatic)	Scanner	sky and terrain radiance, $H(0,d)$
3 (Automatic)	Nephelometer	$s(o)$
4 (Automatic)	CRM	$T_{\infty}(0,0), N_{\infty}^*(\infty,180), H(0,d)$
5 (Automatic)	Scanner	sky radiance, $H(0,d)$
21 (Manual)	Nephelometer	$s(o), \sigma(30,0), \sigma(150,0)$
24 (Manual)	CRM	$T_{\infty}(0,0), N_{\infty}^*(\infty,180), H(0,d)$

MET-02 13 August 1971

It was a sunlit morning. It was clear with moderate to heavy haze. The data-taking started at 1509 GMT (1009 CDT) and continued until 1705 GMT (1205 CDT). The sun zenith angle during data-taking was 45.2 degrees at the beginning and 27.2 degrees at the end.

MET-03 13 August 1971

It was a sunlit afternoon. It was clear with moderate to heavy haze. The data-taking started at 1859 GMT (1359 CDT) and continued until 1923 GMT (1423 CDT). The sun zenith angle during data-taking was 26.7 degrees at the beginning and 29.5 degrees at the end.

MET-04 14 August 1971

It was a partly cloudy morning. It was mostly clear with a heavy cumulus buildup on the northern horizon. The data-taking started at 1613 GMT (1113 CDT) and continued until 1623 GMT (1123 CDT). The sun zenith angle during data-taking was 34.4 degrees at the beginning and 32.8 degrees at the end.

MET-04 LOG ENTRY

Time (GMT)	Data Mode	Ground Crew Observations
1625	1	Heavy cumulus moved from northern horizon to overhead

MET-05 18 August 1971

It was variable, clear then cloudy, late morning through noon. The morning began clear with moderate haze. The data-taking started at 1609 GMT (1109 CDT) and continued until 1851 GMT (1351 CDT). The sun zenith angle during data-taking was 35.8 degrees at the beginning, 25.2 degrees during transit, and 27.5 degrees at the end.

MET-05 LOG ENTRY

Time (GMT)	Data Mode	Ground Crew Observations
1619	2	Small cumulus cloud on western horizon
1625	2	More small cumulus forming in western hemisphere but moving
1633	2	Large cumulus cloud occults sun. Large cumulus buildup very fast.
1830	5	Scattered small cumulus but sun clear. Thick haze.

MET-06 19 August 1971

It was a sunlit morning. It was clear with moderate haze. The data-taking started at 1554 GMT (1054 CDT) and continued until 1741 GMT (1241 CDT). The sun zenith angle during data-taking was 38.4 degrees at the beginning and 26.2 degrees at the end.

MET-07 19 August 1971

It was a sunlit afternoon. It was clear with moderate haze at the start with some cumulus later. The data-taking started at 1912 GMT (1412 CDT) and continued until 1946 GMT (1446 CDT). The sun zenith angle during data-taking was 29.9 degrees at the start and 34.4 degrees at the end.

MET-07 LOG ENTRY

Time (GMT)	Data Mode	Ground Crew Observations
1935	4	Cumulus cloud drifted over sun

MET-08 23 August 1971

It was variably cloudy late morning through afternoon. There were scattered small cumulus and a moderate haze at the beginning. The data-taking started at 1749 GMT (1249 CDT) and continued until 1948 GMT (1448 CDT). The sun zenith angle during data-taking was 27.2 degrees at the start, 26.8 degrees during transit, and 35.9 degrees at the end.

MET-08 LOG ENTRY

Time (GMT)	Data Mode	Ground Crew Observations
1749	1	Heavy cumulus buildup on western horizon, sun occulted
1810	4	Small cirrus cloud over sun
1817	2	Fast-moving cumulus randomly occulting sun during this mode
1916	5	Heavy fast-moving cumulus during this mode

MET-09 23 August 1971

It was a cloudy afternoon. The heavy cumulus was fast-moving. The data-taking started at 2032 GMT (1532 CDT) and continued until 2040 GMT (1540 CDT). The sun zenith angle during data-taking was 42.9 degrees at the start and 44.3 degrees at the end.

MET-10 24 August 1971

It was a sunlit morning. It was clear with moderate haze. The data-taking started at 1312 GMT (812 CDT) and ended at 1510 GMT (1010 CDT). The sun zenith angle during data-taking was 69.4 degrees at the start and 47.0 degrees at the end.

MET-11 24 August 1971

It was a sunlit late morning. It was clear with moderate haze. The data-taking started at 1553 GMT (1053 CDT) and ended at 1658 GMT (1158 CDT). The sun zenith angle during data-taking was 39.6 degrees at the start and 30.9 degrees at the end.

7.5 DESCRIPTION AND PRESENTATION OF GROUND-BASED DATA TABLES

Data are presented in tables of:

Irradiance

Directional Reflectance of Terrain

Total Scattering Coefficient

Proportional Directional Scattering Function at 30 Degrees

Proportional Directional Scattering Function at 150 Degrees

In each table, the data are presented by filter, with the filters in order of increasing mean wavelength. Note that data for Filter 6, a broad band optical filter with a mean wavelength of 532 nanometers, and Filter 5, a narrow band filter with mean wavelength of 765 nanometers, have been included although airborne data were limited to Filters 2, 3, and 4. (Refer to Fig. 1-5 for further details on the spectral responses of the filters).

Users should be aware that regardless of the display format, the data values are valid to, at best, only three significant figures. The tables of directional reflectance of the terrain, in particular, should be rounded off to two digits prior to further application.

IRRADIANCE

The downwelling irradiance $H(0,d)$ measured by the scanner with an irradiance cap attachment is presented in Table 7-6. The data are presented chronologically. The dimensions and units for the irradiances are " $\text{w m}^{-2} \mu\text{m}^{-1}$ "

DIRECTIONAL REFLECTANCE OF TERRAIN

The terrain reflectance $R_o(0,\theta,\phi)$ is tabulated for six dates and times in six tables, 7-7, 7-8, 7-9, 7-10, 7-11, and 7-12. The directional terrain reflectance is tabulated by zenith angle and azimuth in five columns for the five optical filters. These reflectances are based upon the inherent terrain radiance and the downwelling irradiance measured with the scanner. Reflectance is dimensionless.

The appearance of the terrain at the ground station site is depicted in Fig. 3-2. The terrain here was mowed grass, dry and browning.

TOTAL SCATTERING COEFFICIENT

The total volume scattering coefficient $s(0)$ measured by the ground-based integrating nephelometer is presented chronologically in Table 7-13. The dimension and unit for the total scattering coefficient is " m^{-1} ".

PROPORTIONAL DIRECTIONAL SCATTERING FUNCTION AT 30 DEGREES

The proportional directional scattering function at an angle 30 degrees from the light source $\sigma(0,30^\circ)/s(0)$ measured by the ground-based nephelometer is presented chronologically in Table 7-14. The dimension and unit for the proportional directional scattering function is " Ω^{-1} ".

PROPORTIONAL DIRECTIONAL SCATTERING FUNCTION AT 150 DEGREES

The proportional directional scattering function at 150 degrees from the light source $\sigma(0,150^\circ)/s(0)$ measured by the ground-based nephelometer is presented chronologically in Table 7-15. The dimension and unit for the proportional directional scattering function is " Ω^{-1} ".

Table 7-6

Irradiance

GSNTABLE JOB 2225 (05/24/74)
GRNDSCAN JCB 5127 (04/18/74)

DOWNWELLING IRRADIANCE MEASURED BY GROUND BASED SCANNER FOR
GROUND LEVEL ALTITUDE (141 M) DURING PROJECT METRO AT SCOTT AFB

IRRADIANCE (W/SQ M UM)								
DATE	TIME GMT	SUN ZENITH ANGLE	FILTER 2	FILTER 6	FILTER 4	FILTER 3	FILTER 5	PKG-NO
8/12/71								MET-01
	1857	26.2	1.65E C3	9.64E C2	1.36E C3	1.13E C3	9.19E C2	
	1913	28.0	1.64E C3	9.58E C2	1.35E C3	1.12E C3	9.12E C2	
	1919	28.7	1.57E C3	9.29E C2	1.31E C3	1.08E C3	8.86E C2	
	1945	32.3	1.48E C3	8.72E C2	1.26E C3	1.04E C3	8.58E C2	
	1950	33.1	1.47E C3	8.71E C2	1.26E C3	1.04E C3	8.49E C2	
	1956	34.0	1.45E C3	8.56E C2	1.23E C3	1.02E C3	8.37E C2	
	2002	35.0	1.44E C3	8.32E C2	1.21E C3	1.00E C3	8.19E C2	
	2024	38.7	1.34E C3	7.93E C2	1.13E C3	9.42E C2	7.71E C2	
	2032	40.1	1.32E C3	7.90E C2	1.13E C3	9.32E C2	7.53E C2	
	2042	41.8	1.30E C3	7.62E C2	1.10E C3	9.02E C2	7.40E C2	
	2047	42.8	1.27E C3	7.34E C2	1.06E C3	8.80E C2	7.13E C2	
	2107	46.4	1.19E C3	6.97E C2	1.02E C3	8.28E C2	6.89E C2	
8/13/71								MET-02
	1509	45.7	1.15E C3	6.85E C2	9.71E C2	7.96E C2	6.65E C2	
	1519	43.4	1.19E C3	7.13E C2	1.02E C3	8.29E C2	6.99E C2	
	1523	42.7	1.21E C3	7.23E C2	1.03E C3	8.41E C2	7.04E C2	
	1558	36.6	1.36E C3	8.08E C2	1.17E C3	9.54E C2	7.98E C2	
	1605	35.4	1.42E C3	8.50E C2	1.22E C3	9.85E C2	8.31E C2	
	1609	34.8	1.46E C3	8.60E C2	1.24E C3	1.01E C3	8.48E C2	
	1613	34.2	1.46E C3	8.64E C2	1.25E C3	1.02E C3	8.45E C2	
	1630	31.6	1.51E C3	8.88E C2	1.28E C3	1.04E C3	8.68E C2	
	1634	31.0	1.52E C3	9.00E C2	1.29E C3	1.05E C3	8.75E C2	
	1643	29.8	1.53E C3	9.09E C2	1.31E C3	1.06E C3	8.81E C2	
	1647	29.3	1.56E C3	9.09E C2	1.33E C3	1.07E C3	8.91E C2	
	1705	27.2	1.56E C3	9.22E C2	1.33E C3	1.08E C3	8.95E C2	
8/13/71								MET-03
	1859	26.7	1.52E C3	8.87E C2	1.29E C3	1.04E C3	8.61E C2	
	1904	27.2	1.52E C3	8.74E C2	1.27E C3	1.04E C3	8.51E C2	
	1908	27.7	1.51E C3	8.76E C2	1.26E C3	1.03E C3	8.41E C2	
	1923	29.5	1.40E C3		1.24E C3	9.71E C2	8.27E C2	
8/14/71								MET-04
	1613	34.4	1.45E C3	8.58E C2	1.21E C3	1.02E C3	8.17E C2	
	1623	32.8	1.51E C3	8.51E C2	1.27E C3	1.11E C3	9.38E C2	
8/18/71								MET-05
	1609	35.8	1.33E C3	8.05E C2	1.12E C3	9.61E C2	7.74E C2	
	1615	34.9	1.37E C3	8.20E C2	1.15E C3	9.71E C2	7.95E C2	
	1620	34.2	1.37E C3	8.25E C2	1.16E C3	9.96E C2	8.15E C2	
	1645	30.7	1.24E C3	4.15E C2	1.10E C3	8.15E C2	4.62E C2	
	1649	30.3	6.11E C2	3.82E C2	4.93E C2	3.37E C2	3.03E C2	
	1653	29.8	1.32E C3	9.26E C2	1.28E C3	1.10E C3	9.53E C2	
	1731	26.4	1.57E C3	9.38E C2	1.31E C3	1.12E C3	9.32E C2	
	1815	25.5	1.74E C3	1.03E C3	1.47E C3	1.25E C3	1.03E C3	
	1819	25.6	1.67E C3	9.55E C2	1.38E C3	1.19E C3	1.68E C4	
	1826	25.9	1.60E C3	9.79E C2	1.38E C3	1.15E C3	9.68E C2	
	1831	26.1	1.61E C3	9.64E C2	1.40E C3	1.16E C3	1.00E C3	
	1851	27.5	1.59E C3	9.24E C2	1.39E C3	1.14E C3	9.68E C2	
8/19/71								MET-06
	1606	36.5	1.38E C3	8.26E C2	1.18E C3	9.71E C2	8.02E C2	
	1622	34.1	1.44E C3	8.57E C2	1.22E C3	1.00E C3	8.36E C2	
	1628	33.2	1.47E C3	8.62E C2	1.22E C3	1.02E C3	8.25E C2	

Table 7-6 (cont.)

Irradiance

GSNTABLE JCB 2225 (05/24/74)
GRNDSCAN JCB 5579 (04/19/74)

DOWNWELLING IRRADIANCE MEASURED BY GROUND BASED SCANNER FOR
GROUND LEVEL ALTITUDE (141 M) DURING PROJECT METRO AT SCOTT AFB

DATE	START TIME GMT	SUN ZENITH ANGLE	IRRADIANCE (W/SQ M UM)					PKG-NC
			FILTER 2	FILTER 6	FILTER 4	FILTER 3	FILTER 5	
8/19/71								MET-06
	1632	32.7	1.47E C3	8.78E C2	1.26E C3	1.03E C3	8.45E C2	
	1638	31.9	1.51E C3	8.64E C2	1.26E C3	1.05E C3	8.44E C2	
	1706	28.7	1.45E C3	8.48E C2	1.24E C3	1.01E C3	8.41E C2	
	1709	28.4	1.48E C3	8.75E C2	1.25E C3	1.01E C3	8.51E C2	
	1716	27.8	1.48E C3	8.71E C2	1.27E C3	1.02E C3	8.63E C2	
	1721	27.4	1.48E C3	8.77E C2	1.25E C3	1.02E C3	8.52E C2	
	1741	26.2	1.64E C3	9.38E C2	1.41E C3	1.15E C3	9.43E C2	
8/19/71								MET-07
	1912	29.9	1.51E C3	8.93E C2	1.29E C3	1.05E C3	8.81E C2	
	1920	30.9	1.45E C3	8.59E C2	1.24E C3	1.03E C3	8.51E C2	
	1923	31.3	1.50E C3	8.70E C2	1.26E C3	1.04E C3	8.57E C2	
	1935	32.8	1.39E C3	4.96E C2	1.22E C3	1.00E C3	5.69E C2	
	1939	33.4	1.21E C3	8.52E C2	1.19E C3	9.16E C2	8.51E C2	
	1946	34.4	C	8.81E C2	1.27E C3	1.05E C3	8.72E C2	
8/23/71								MET-08
	1749	27.2	1.37E C3	8.85E C2	1.23E C3	1.03E C3	8.81E C2	
	1756	27.1	1.33E C3	8.48E C2	1.18E C3	9.53E C2	8.45E C2	
	1801	27.1	1.36E C3	8.50E C2	1.20E C3	1.01E C3	8.47E C2	
	1813	27.2	1.33E C3	8.08E C2	1.18E C3	9.80E C2	8.07E C2	
	1817	27.3	1.31E C3	8.26E C2	1.16E C3	9.75E C2	8.25E C2	
	1902	30.2	9.35E C2	4.92E C2	6.32E C2	4.01E C2	3.07E C2	
	1909	30.9	7.37E C2	3.96E C2	5.60E C2	3.49E C2	2.82E C2	
	1912	31.2	1.35E C3	8.66E C2	1.23E C3	1.03E C3	9.06E C2	
	1916	31.7	1.30E C3	5.66E C2	1.14E C3	9.76E C2	7.18E C2	
	1935	34.1	5.37E C2	3.03E C2	4.24E C2	3.19E C2	2.43E C2	
	1941	34.9	6.49E C2	3.53E C2	8.19E C2	5.16E C2	3.08E C2	
	1948	35.9	6.26E C2	3.56E C2	5.02E C2	5.52E C2	2.86E C2	
8/23/71								MET-09
	2032	42.9	1.00E C3	6.33E C2	8.55E C2	7.53E C2	6.72E C2	
	2040	44.3	9.51E C2	5.66E C2	8.26E C2	6.76E C2	5.87E C2	
8/24/71								MET-10
	1312	69.4	4.01E C2	2.60E C2	3.53E C2	3.01E C2	2.52E C2	
	1347	62.6	6.13E C2	3.81E C2	5.34E C2	4.48E C2	3.73E C2	
	1350	62.0	6.46E C2	4.00E C2	5.62E C2	4.70E C2	3.91E C2	
	1414	57.4	7.62E C2	4.74E C2	6.78E C2	5.55E C2	4.80E C2	
	1418	56.6	8.09E C2	5.04E C2	7.32E C2	5.84E C2	5.14E C2	
	1421	56.0	8.27E C2	5.16E C2	7.44E C2	6.00E C2	5.25E C2	
	1425	55.3	8.41E C2	5.25E C2	7.57E C2	6.08E C2	5.34E C2	
	1438	52.8	9.25E C2	5.61E C2	8.20E C2	6.69E C2	5.69E C2	
	1442	52.1	9.34E C2	5.76E C2	8.28E C2	6.67E C2	5.82E C2	
	1449	50.8	9.83E C2	5.90E C2	8.61E C2	7.01E C2	6.03E C2	
	1453	50.0	9.95E C2	6.12E C2	9.07E C2	7.26E C2	6.27E C2	
	1510	47.0	1.07E C3	6.44E C2	9.25E C2	7.52E C2	6.31E C2	
8/24/71								MET-11
	1553	39.6	1.26E C3	7.27E C2	1.05E C3	8.75E C2	7.10E C2	
	1601	38.4	1.28E C3	7.72E C2	1.10E C3	9.03E C2	7.39E C2	
	1604	37.9	1.32E C3	7.86E C2	1.14E C3	9.26E C2	7.50E C2	
	1626	34.7	1.41E C3	8.27E C2	1.20E C3	9.52E C2	7.98E C2	
	1629	34.3	1.36E C3	8.25E C2	1.16E C3	9.62E C2	7.90E C2	
	1633	33.8	1.41E C3	8.37E C2	1.19E C3	9.85E C2	7.96E C2	

Table 7-6 (cont.)

Irradiance

GSNTABLE JOB 2225 (05/24/74)
GRNDSKAN JOB 5521 (04/23/74)

DOWNWELLING IRRADIANCE MEASURED BY GROUND BASED SCANNER FOR
GROUND LEVEL ALTITUDE (141 M) DURING PROJECT METRO AT SCOTT AFB

DATE	TIME GMT	SUN ZENITH ANGLE	IRRADIANCE (W/SQ M UM)					PKG-NO
			FILTER 2	FILTER 6	FILTER 4	FILTER 3	FILTER 5	
8/24/71								MET-11
	1636	33.4	1.42E 03	8.29E 02	1.18E 03	9.91E 02	8.05E 02	
	1647	32.1	1.42E 03	8.45E 02	1.21E 03	1.01E 03	8.14E 02	
	1651	31.6	1.42E 03	8.5CE 02	1.22E 03	1.01E 03	8.18E 02	
	1658	30.9	1.47E 03	8.8CE 02	1.26E 03	1.05E 03	8.43E 02	

Table 7-7

Directional Reflectance of Terrain at Scott Air Force Base on 12 August 1971

MET-01

Path of Sight		Directional Reflectance				
Azimuth	Zenith Angle	Filter 2 1925 GMT $\theta_s = 29.5^\circ$	Filter 6 1936 GMT $\theta_s = 31.0^\circ$	Filter 4 1930 GMT $\theta_s = 30.3^\circ$	Filter 3 1927 GMT $\theta_s = 29.9^\circ$	Filter 5 1933 GMT $\theta_s = 30.6^\circ$
0	100	-	-	-	-	-
	105	-	-	-	-	-
	120	-	-	-	-	-
	150	-	-	-	-	-
	180	-	-	-	-	-
90	100	.086	.141	.130	.145	.292
	105	.074	.131	.118	.133	.309
	120	.053	.107	.094	.106	.264
	150	.059	.109	.099	.119	.269
	180	-	-	-	-	-
180	100	.074	.131	.129	.139	.367
	105	.088	.159	.151	.173	.383
	120	.085	.157	.139	.174	.342
	150	.071	.129	.113	.147	.297
	180	-	-	-	-	-

Table 7-8

Directional Reflectance of Terrain at Scott Air Force Base on 13 August 1971

MET-02

Path of Sight		Directional Reflectance				
Azimuth	Zenith Angle	Filter 2	Filter 6	Filter 4	Filter 3	Filter 5
		-	1546 GMT $\theta_s = 38.6^\circ$	1541 GMT $\theta_s = 39.5^\circ$	1539 GMT $\theta_s = 39.9^\circ$	1544 GMT $\theta_s = 39.0^\circ$
0	100	-	.119	.107	.126	.307
	105	-	.102	.097	.113	.286
	120	-	.091	.083	.099	.252
	150	-	.098	-	-	-
	180	-	-	-	-	-
90	100	-	.140	-	.156	.325
	105	-	.130	.117	.151	.299
	120	-	.097	.088	.108	.247
	150	-	.092	.082	.102	.236
	180	-	-	-	-	-
180	100	-	.166	.144	.156	.323
	105	-	.144	.128	.154	.322
	120	-	-	-	-	-
	150	-	-	-	-	-
	180	-	-	-	-	-

Table 7-9

Directional Reflectance of Terrain at Scott Air Force Base on 18 August 1971

MET-05

Path of Sight		Directional Reflectance				
Azimuth	Zenith Angle	Filter 2 1625 GMT $\theta_s = 33.5^\circ$	Filter 6 1638 GMT $\theta_s = 31.7^\circ$	Filter 4 1630 GMT $\theta_s = 32.7^\circ$	Filter 3 1628 GMT $\theta_s = 33.1^\circ$	Filter 5 1635 GMT $\theta_s = 32.1^\circ$
0	100	.082	-	.120	.141	.199
	105	.066	-	.104	.123	.193
	120	.057	-	.095	.119	.180
	150	.070	-	.120	.143	.222
	180	-	-	-	-	-
90	100	.072	-	.111	.133	.274
	105	.064	-	.103	.125	.285
	120	.054	-	.092	.122	.234
	150	.054	-	.091	.125	.269
	180	-	-	-	-	-
180	100	.094	-	.139	.160	.286
	105	.079	-	.124	.155	.291
	120	.066	-	.113	.144	.235
	150	.052	-	.096	.123	.188
	180	-	-	-	-	-

Table 7-10

Directional Reflectance of Terrain at Scott Air Force Base on 19 August 1971

MET-06

Path of Sight		Directional Reflectance				
Azimuth	Zenith Angle	Filter 2 1642 GMT $\theta_s = 31.4^\circ$	Filter 6 1653 GMT $\theta_s = 30.1^\circ$	Filter 4 1648 GMT $\theta_s = 30.8^\circ$	Filter 3 1645 GMT $\theta_s = 31.1^\circ$	Filter 5 1650 GMT $\theta_s = 30.4^\circ$
0	100	.076	.119	.121	.143	.290
	105	.063	.112	.098	.126	.277
	120	.053	.098	.088	.110	.253
	150	-	-	-	-	-
	180	-	-	-	-	-
90	100	.080	.138	-	.154	.304
	105	.071	.127	-	.143	.292
	120	.055	.108	.095	.128	.256
	150	.058	.114	.096	.135	.265
	180	-	-	-	-	-
180	100	.100	.148	.137	.176	.295
	105	.074	.134	.123	.160	.307
	120	.058	.114	.100	.132	.275
	150	.062	.114	.108	.138	.307
	180	-	-	-	-	-

Table 7-11

Directional Reflectance of Terrain at Scott Air Force Base on 24 August 1971

MET-10

Path of Sight		Directional Reflectance				
Azimuth	Zenith Angle	Filter 2 1355 GMT $\theta_s = 61.1^\circ$	Filter 6 1405 GMT $\theta_s = 59.0^\circ$	Filter 4 1400 GMT $\theta_s = 60.1^\circ$	Filter 3 1358 GMT $\theta_s = 60.6^\circ$	Filter 5 1403 GMT $\theta_s = 59.5^\circ$
0	100	.086	.153	.161	.186	.344
	105	.073	.126	.119	.148	.322
	120	-	.099	.082	.100	.265
	150	-	.109	.090	.110	-
	180	-	-	-	-	-
90	100	.084	.158	.141	.173	.378
	105	.071	.142	.123	.160	.349
	120	.057	.120	.102	.135	.287
	150	.049	.102	.087	.103	.261
	180	-	-	-	-	-
180	100	.157	.238	.215	.248	.497
	105	.115	.220	.199	.249	.533
	120	-	-	-	-	-
	150	-	-	-	-	-
	180	-	-	-	-	-

Table 7-12

Directional Reflectance of Terrain at Scott Air Force Base on 24 August 1971

MET-11

Path of Sight		Directional Reflectance				
Azimuth	Zenith Angle	Filter 2 1608 GMT $\theta_s = 37.4^\circ$	Filter 6 1619 GMT $\theta_s = 35.8^\circ$	Filter 4 1613 GMT $\theta_s = 36.6^\circ$	Filter 3 1611 GMT $\theta_s = 37.0^\circ$	Filter 5 1616 GMT $\theta_s = 36.2^\circ$
0	100	.091	.107	.098	.112	.268
	105	.055	.098	.092	.108	.250
	120	.054	.097	.091	.108	.221
	150	.073	.133	.122	.147	.297
	180	.057	.103	.094	.122	.271
90	100	.078	.127	.117	.136	.263
	105	.065	.119	.109	.130	.275
	120	.050	.101	.091	.119	.231
	150	.052	.103	.094	.118	.251
	180	.057	.103	.094	.122	.271
180	100	.095	.147	.137	.152	.282
	105	.083	.125	.122	.155	.294
	120	.067	.127	.115	.145	.288
	150	.059	.125	.114	.147	.328
	180	.057	.103	.094	.122	.271

Table 7-13

Total Volume Scattering Coefficient

GNECTABLE JCB 5579 (C5/23/74)
GENGRNC JOB 5154 (04/02/74)

TOTAL VOLUME SCATTERING COEFFICIENT (PER M) FOR
GROUND LEVEL ALTITUDE (141 M) DURING PROJECT METRO AT SCCTT AFB

DATE	TIME GMT	TOTAL VOLUME SCATTERING COEFFICIENT (PER M)				
		FILTER 2	FILTER 6	FILTER 4	FILTER 3	FILTER 5
08/12/71	1901	2.26E-04	1.80E-04	1.56E-04	0	8.15E-05
08/12/71	1919	3.10E-04	2.43E-04	2.21E-04	1.49E-04	1.06E-04
08/12/71	1953	2.36E-04	1.92E-04	1.68E-04	1.18E-04	8.82E-05
08/12/71	2002	2.48E-04	2.03E-04	1.79E-04	1.23E-04	9.34E-05
08/12/71	2035	2.32E-04	2.21E-04	2.01E-04	1.10E-04	9.72E-05
08/12/71	2047	2.39E-04	1.88E-04	1.73E-04	1.17E-04	8.77E-05
08/13/71	1512	3.84E-04	2.82E-04	2.85E-04	1.88E-04	1.34E-04
08/13/71	1523	3.65E-04	2.93E-04	2.72E-04	1.85E-04	1.31E-04
08/13/71	1607	3.70E-04	2.90E-04	2.70E-04	1.84E-04	1.30E-04
08/13/71	1613	3.61E-04	2.87E-04	2.63E-04	1.81E-04	1.29E-04
08/13/71	1636	3.69E-04	2.82E-04	2.61E-04	1.76E-04	1.30E-04
08/13/71	1647	3.54E-04	2.78E-04	2.58E-04	1.76E-04	1.26E-04
08/13/71	1902	0	2.97E-04	2.74E-04	1.81E-04	1.27E-04
08/13/71	1908	3.69E-04	2.92E-04	2.70E-04	1.79E-04	0
08/14/71	1616	4.48E-04	3.49E-04	2.90E-04	2.09E-04	1.54E-04
08/18/71	1610	6.05E-04	4.81E-04	4.64E-04	3.21E-04	2.21E-04
08/18/71	1620	6.10E-04	4.85E-04	4.63E-04	3.18E-04	2.15E-04
08/18/71	1651	5.87E-04	4.70E-04	4.46E-04	3.11E-04	2.17E-04
08/18/71	1731	5.48E-04	4.58E-04	4.24E-04	2.96E-04	2.06E-04
08/18/71	1821	5.38E-04	4.40E-04	4.14E-04	2.88E-04	1.99E-04
08/18/71	1831	5.38E-04	4.40E-04	4.05E-04	2.82E-04	2.01E-04
08/19/71	1556	5.63E-04	4.57E-04	4.25E-04	3.13E-04	2.15E-04
08/19/71	1606	5.55E-04	4.53E-04	4.38E-04	3.07E-04	2.21E-04
08/19/71	1630	5.50E-04	4.53E-04	4.26E-04	3.07E-04	2.13E-04
08/19/71	1638	5.42E-04	4.55E-04	4.24E-04	3.01E-04	2.12E-04
08/19/71	1711	5.04E-04	4.15E-04	3.85E-04	2.70E-04	1.93E-04
08/19/71	1721	5.09E-04	4.13E-04	3.92E-04	2.78E-04	1.98E-04
08/19/71	1914	3.95E-04	3.34E-04	2.99E-04	0	1.51E-04
08/19/71	1923	3.71E-04	3.20E-04	2.83E-04	2.00E-04	1.43E-04
08/19/71	1941	4.03E-04	3.18E-04	3.20E-04	2.20E-04	1.53E-04
08/23/71	1751	4.41E-04	3.47E-04	3.44E-04	2.34E-04	1.64E-04
08/23/71	1801	4.30E-04	3.53E-04	3.21E-04	2.30E-04	1.61E-04
08/23/71	1817	4.08E-04	3.29E-04	3.09E-04	2.13E-04	1.49E-04
08/23/71	1910	4.45E-04	3.51E-04	3.30E-04	2.26E-04	1.60E-04
08/23/71	1916	4.31E-04	3.55E-04	3.26E-04	2.22E-04	1.59E-04
08/23/71	1942	5.34E-04	3.90E-04	3.89E-04	2.65E-04	1.82E-04
08/23/71	2035	4.61E-04	3.67E-04	3.44E-04	2.36E-04	1.65E-04
08/24/71	1342	4.30E-04	3.47E-04	3.30E-04	2.40E-04	1.66E-04
08/24/71	1350	4.48E-04	3.69E-04	3.51E-04	2.46E-04	1.71E-04
08/24/71	1419	4.04E-04	3.42E-04	3.17E-04	2.30E-04	1.63E-04
08/24/71	1425	4.12E-04	3.53E-04	3.30E-04	2.34E-04	1.72E-04
08/24/71	1444	4.27E-04	3.61E-04	3.51E-04	2.45E-04	1.76E-04
08/24/71	1453	4.17E-04	3.55E-04	3.47E-04	2.38E-04	1.79E-04
08/24/71	1554	4.21E-04	2.95E-04	3.15E-04	2.23E-04	1.61E-04
08/24/71	1604	3.59E-04	3.02E-04	2.81E-04	2.02E-04	1.46E-04
08/24/71	1631	3.06E-04	2.53E-04	2.30E-04	1.64E-04	1.20E-04
08/24/71	1636	3.14E-04	2.61E-04	2.42E-04	1.73E-04	1.31E-04
08/24/71	1653	3.14E-04	2.58E-04	2.44E-04	1.73E-04	1.28E-04

Table 7-14

Proportional Directional Scattering Function at 30 Degrees

GNDTABLE JCB 5579 (05/23/74)
 GENGRNC JOB 5154 (04/02/74)

PROPORTIONAL DIRECTIONAL SCATTERING FUNCTION AT 30 DEGREES FOR
 GROUND LEVEL ALTITUDE (141 M) DURING PROJECT METRO AT SCOTT AFB

PROPORTIONAL DIRECTIONAL SCATTERING FUNCTION AT 30 DEGREES						
DATE	TIME GMT	FILTER 2	FILTER 6	FILTER 4	FILTER 3	FILTER 5
08/12/71	1907	-C	2.83E-01	2.40E-01	0	2.23E-01
08/12/71	2035	2.74E-01	2.89E-01	2.51E-01	2.10E-01	2.35E-01
08/13/71	1512	3.37E-01	3.42E-01	2.74E-01	2.59E-01	2.63E-01
08/13/71	1637	3.34E-01	3.30E-01	2.80E-01	2.51E-01	2.61E-01
08/14/71	1617	3.52E-01	3.40E-01	3.07E-01	2.59E-01	2.60E-01
08/18/71	1611	3.96E-01	4.07E-01	3.42E-01	3.21E-01	3.37E-01
08/18/71	1821	4.01E-01	3.96E-01	3.47E-01	3.21E-01	3.36E-01
08/19/71	1556	4.04E-01	4.01E-01	3.45E-01	3.21E-01	3.53E-01
08/19/71	1711	3.95E-01	3.92E-01	3.35E-01	3.17E-01	3.35E-01
08/19/71	1914	3.73E-01	3.60E-01	3.12E-01	0	2.99E-01
08/19/71	1941	3.79E-01	-0	-C	2.94E-01	-C
08/23/71	1751	3.56E-01	3.56E-01	2.97E-01	2.84E-01	3.09E-01
08/23/71	1943	3.61E-01	3.75E-01	3.10E-01	3.01E-01	3.15E-01
08/23/71	2035	3.62E-01	3.60E-01	3.05E-01	2.85E-01	3.07E-01
08/24/71	1342	3.63E-01	3.80E-01	3.23E-01	3.06E-01	3.59E-01
08/24/71	1444	3.85E-01	3.75E-01	3.25E-01	3.26E-01	3.47E-01
08/24/71	1555	3.78E-01	3.98E-01	3.19E-01	3.05E-01	3.18E-01
08/24/71	1654	3.43E-01	3.40E-01	2.95E-01	2.63E-01	2.79E-01

** NOTE ** -0 MEANS SIGMA 30 DATA VALUE FOR THAT FILTER NOT AVAILABLE
 C MEANS S, CR BCTH DATA VALUE(S) FOR THAT FILTER NOT AVAILABLE

Table 7-15

Proportional Directional Scattering Function at 150 Degrees

GNDTABLE JCB 5579 (05/23/74)
 GENGRND JCB 5154 (04/02/74)

PROPORTIONAL DIRECTIONAL SCATTERING FUNCTION AT 150 DEGREES FOR
 GROUND LEVEL ALTITUDE (141 M) DURING PROJECT METRO AT SCOTT AFB

PROPORTIONAL DIRECTIONAL SCATTERING FUNCTION AT 150 DEGREES						
DATE	TIME GMT	FILTER 2	FILTER 6	FILTER 4	FILTER 3	FILTER 5

08/12/71	1908	-C	3.58E-C2	2.81E-C2	0	1.62E-02
08/12/71	2036	3.26E-02	3.41E-C2	2.67E-C2	3.01E-C2	2.13E-02
08/13/71	1513	2.67E-C2	3.12E-C2	2.33E-02	2.58E-C2	2.42E-02
08/13/71	1637	2.66E-C2	2.95E-02	2.47E-02	2.62E-C2	2.28E-02
08/14/71	1617	2.22E-C2	2.43E-C2	2.08E-02	2.17E-C2	2.04E-02
08/18/71	1611	2.02E-02	2.22E-02	1.76E-02	1.86E-C2	2.02E-02
08/18/71	1821	1.97E-02	2.12E-C2	1.64E-02	1.72E-C2	1.76E-02
08/19/71	1556	1.99E-02	2.13E-02	1.65E-02	1.63E-02	1.66E-02
08/19/71	1712	2.09E-02	2.17E-C2	1.73E-02	1.75E-02	1.65E-C2
08/19/71	1915	2.24E-02	2.34E-C2	1.82E-C2	C	-C
08/19/71	1942	2.31E-C2	2.35E-C2	-C	1.94E-02	1.67E-02
08/23/71	1752	2.62E-02	2.88E-C2	2.25E-02	2.34E-02	2.30E-02
08/23/71	1943	2.35E-02	2.73E-C2	2.09E-02	2.26E-02	2.30E-C2
08/23/71	2036	2.44E-02	2.64E-02	2.12E-02	2.24E-02	2.20E-02
08/24/71	1342	2.52E-02	2.75E-C2	2.09E-02	2.10E-02	2.12E-02
08/24/71	1445	2.53E-02	2.56E-C2	1.81E-02	2.02E-02	1.88E-02
08/24/71	1555	2.40E-C2	2.74E-C2	1.94E-02	1.80E-02	1.66E-02
08/24/71	1654	2.74E-02	2.87E-C2	2.23E-C2	2.26E-02	1.73E-02

** NOTE ** -C MEANS SIGMA 150 DATA VALUE FOR THAT FILTER NOT AVAILABLE
 0 MEANS S, OR BOTH DATA VALUE(S) FOR THAT FILTER NOT AVAILABLE

8. DATA INTERPRETATION AND EVALUATION

8.1 METEOROLOGICAL DATA

The basic discussion of meteorological conditions as presented in Section 6 and summarized with each flight description is based upon meteorological data reported for Scott Air Force Base. It should be remembered that the flight tracks were 32 to 108 miles from the Base so that the reports of visibility or cloud conditions often do not correspond to the conditions encountered along the flight tracks.

CLOUD CONDITIONS

The airborne pictures which documented the cloud conditions during the flights are summarized in Table 8-1. The descriptions are divided into five categories.

Table 8-1
Airborne Hemispherical Picture Summary

Category	Description	Flight Profiles
1	Upper and lower sky – clear	C-182B, C-188A, C-188B
2	Upper sky – horizon clouds; Lower sky – clear	C-181, C-186B, C-187A
3	Upper sky – horizon clouds; Lower sky – some clouds	C-183A, C-185A
4	Upper sky – some scattered clouds; Lower sky – variable, clouds or clear	C-180, C-182A, C-186A
5	Upper sky – considerable scattered clouds	C-183B, C-185B, C-187B

The sky radiance data for the flight profiles in categories 1 through 4 were sufficiently consistent that path radiance and path reflectance could be derived, but only the nephelometer data for the flights in category 5 could be utilized. Duntley *et al.* (1973) contains the data for the six clearest profiles, categories 1 and 2. In addition, in order to report as many double flights as possible, flight profiles for C-182A and C-186A from category 4 were included in that report, even though they represented somewhat variable cloud conditions. This report contains the data for the flights described in categories 3 and 5 and for the remaining flight, C-180, in category 4.

TEMPERATURE

During the METRO deployment, the AN/AMQ-17 system was linked with a -1 volt power supply to drive its temperature channel output signal. Inadvertently, a calibration curve for the +1 volt power supply was used for the METRO temperatures reported in Duntley *et al.* (1973). Thus, those temperatures are reported approximately 10 degrees Celsius too low. The two calibration curves, from which the earlier reported data can be corrected, are provided in Figure 8-1.

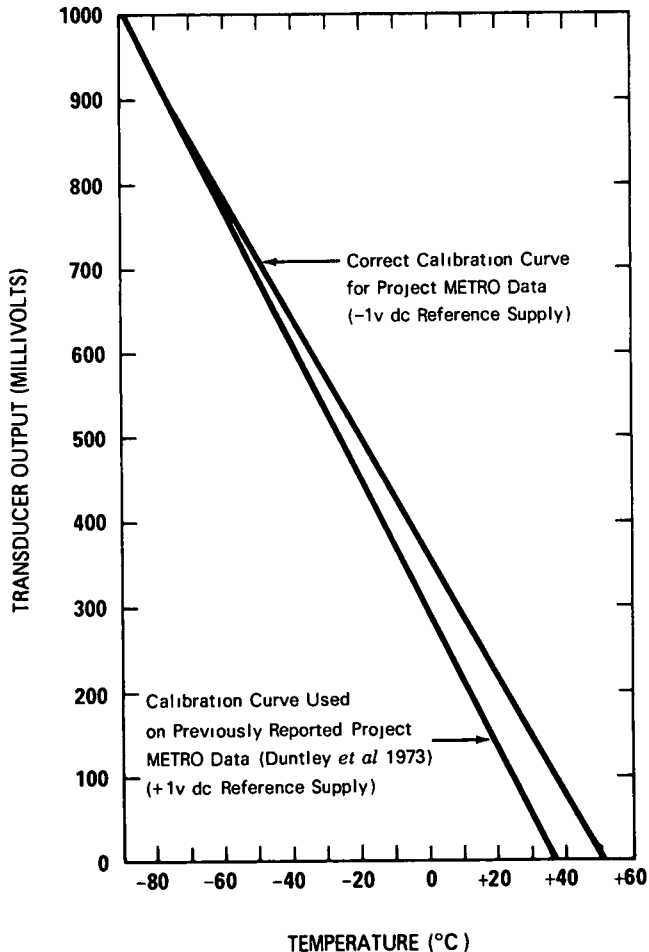


Fig. 8-1. AN/AMQ-17 Temperature Calibration Curves.

The flights were conducted during August at latitudes of 37.8°N to 39.9°N and therefore can be profitably compared to the U. S. Standard Atmosphere Supplements for latitudes 30°N and 45°N. To facilitate this comparison, the temperature profile (an average of the temperatures measured during the vertical profile sequences) of each of the six flights is superimposed on a graph of the temperature for July 30°N latitude and July 45°N latitude from the U. S. Standard Atmosphere Supplements. The temperatures for the six flight profiles reported herein from cloud categories 3 through 5 are depicted in Figure 8-2. Note that the altitude scale is above mean sea level. The ground level altitudes ranged between 153 and 305 meters.

The temperatures for the flights cluster around the curve for July 30°N. Since the curve for July 30°N is not an upper limit but an average, the measured temperatures appear to be reasonable in comparison to this average. There is also a general tendency toward either an inversion or a slight decrease in the lapse rate between 1 and 2 kilometers. The top of the primary haze layer tended to lie in this altitude range.

As reported in Duntley *et al.* (1973), there appears to be no significant difference between the temperature profiles for the clear flights and those for the flights with scattered clouds.

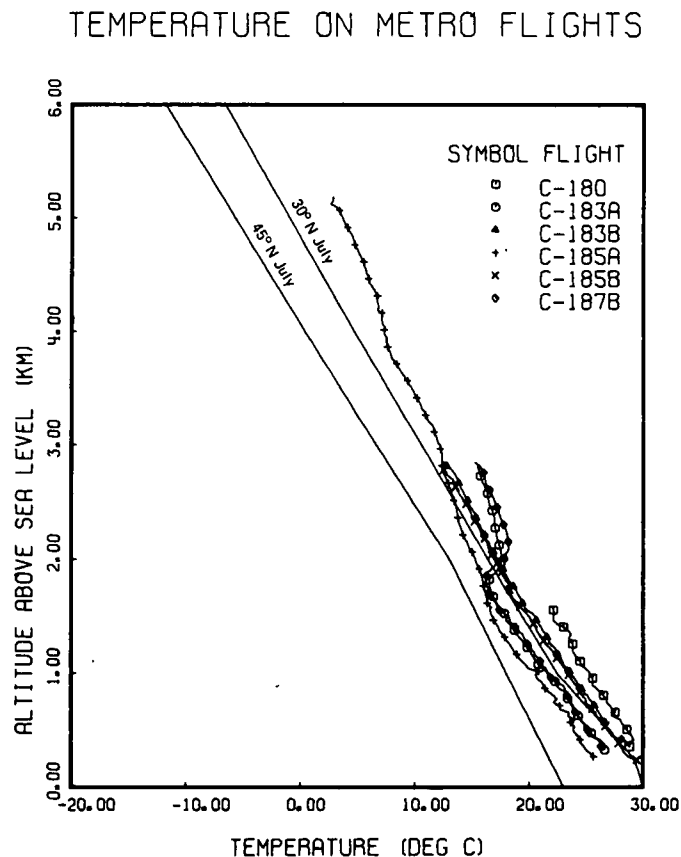


Fig. 8-2. Temperature for METRO Flights With Some Scattered Clouds Compared to 30°N July and 45°N July Temperatures from the U. S. Standard Atmosphere Supplements.

8.2 AIRBORNE RADIOMETRIC DATA

TOTAL VOLUME SCATTERING COEFFICIENT

The total volume scattering coefficients were measured during the vertical profile sequences. In all six profiles in this report, the vertical profile data for Filter 2 were taken during the segmented ascents made between the lowest and highest straight and level sequences. The vertical profile data for Filter 3 were taken during a continuous descent from the highest straight and level altitude, followed by a continuous ascent for measurements in Filter 4. For the flights with a maximum altitude of 2.6 kilometers, the average elapsed time between the start of the first and the end of the final vertical profile was 1 hour and 15 minutes. For Flight C-180 with a maximum altitude of 5 kilometers, the elapsed time was 2 hours and 19 minutes, whereas for the short flight, C-187B, with a maximum altitude of only 1.4 kilometers, the elapsed time was 30 minutes.

Six METRO flights with double profiles were designed to sample the optical properties upwind and downwind of the city. The ground-level wind information upon which the design was founded was from Scott Air Force Base. It was therefore assumed that wind directions and speeds were similar over the large area surrounding St. Louis. Three double flights and a profile from the fourth flight were reported in Duntley *et al.* (1973) with no clear correlation between haze and position upwind or downwind of the city. Similarly, Flights C-183 and C-185 show little difference in the two profiles for upwind and crosswind, or upwind and downwind in the latter case. Flight C-187B compared to C-187A from the earlier report indicates the crosswind C-187B profile has a heavier haze than the downwind C-187A profile. Thus the earlier conclusion still holds that more detailed spatial and chronological information on wind velocity near the flight tracks is necessary for a full understanding of the upwind/downwind haze characteristics.

For simultaneous data, the order of the scattering coefficient data by filter generally should be the inverse of the mean wavelength of the filters, i.e., $s(\text{Filter } 2) > s(4) > s(3)$. Parallel curves would then be an indication of optical stability during the period of measurement. As illustrated in the figures in Section 7.3, all six profiles show small areas of instability, most often at the edge of the haze layers.

In all cases except Flight C-180, Filter 4, it was possible to take airborne data down to at least 270 meters and sometimes as low as 60 meters. The low-altitude total scattering profile is consequently reasonably well-documented. The extrapolation to ground level is quite reasonable for five of the six profiles, but for C-183A the values at low altitude from the vertical profiles for Filters 2 and 3 were inconsistent, indicating optical instability. Thus, the extrapolations downward for these two filters for C-183A are based upon the total scattering coefficients measured during the low-altitude straight and level sequence.

During four of the six profiles, airborne data were generally taken up to 2.6 kilometers. Even so, extrapolations up to 3 kilometers appear reasonable, though some profiles indicate less optical stability around 2.5 kilometers.

In order to more easily compare the scattering characteristics of the six profiles, the Filter 4 (pseudophotopic) total volume scattering coefficients have been graphed in Figure 8-3. Although there is considerable variability in the six profiles, all indicate haze at low altitude, and the five with higher altitude data indicate clearer air above. The height of the haze layers, the sharpness of the haze edge, and the number

of haze layers vary appreciably. One of the flights, C-183A, has a denser haze below 0.5 kilometer and a second haze top around 1.6 kilometers.

There is no significant difference between the scattering for the eight profiles reported in Duntley *et al.* (1973) and the six profiles for partly cloudy days reported herein.

EQUIVALENT ATTENUATION LENGTH AND BEAM TRANSMITTANCE

At ground level the equivalent attenuation length is the reciprocal of the total scattering coefficient $s(z)$. As altitude increases, the equivalent attenuation length shows the cumulative effect of summing $s(z)$ from ground level to altitude z . The vertical beam transmittance starts at 1.0 and similarly shows the cumulative effect of the summation of the total scattering coefficient. For simultaneous data, the order by filter of the equivalent attenuation length \bar{L} and the beam transmittance should vary directly as the mean wavelength of the filters, i.e., $\bar{L}(\text{Filter 2}) < \bar{L}(4) < \bar{L}(3)$. All of the six profiles display this feature, indicating that the minor filter anomalies in the total scattering coefficient profiles have little affect when the total profile is summed.

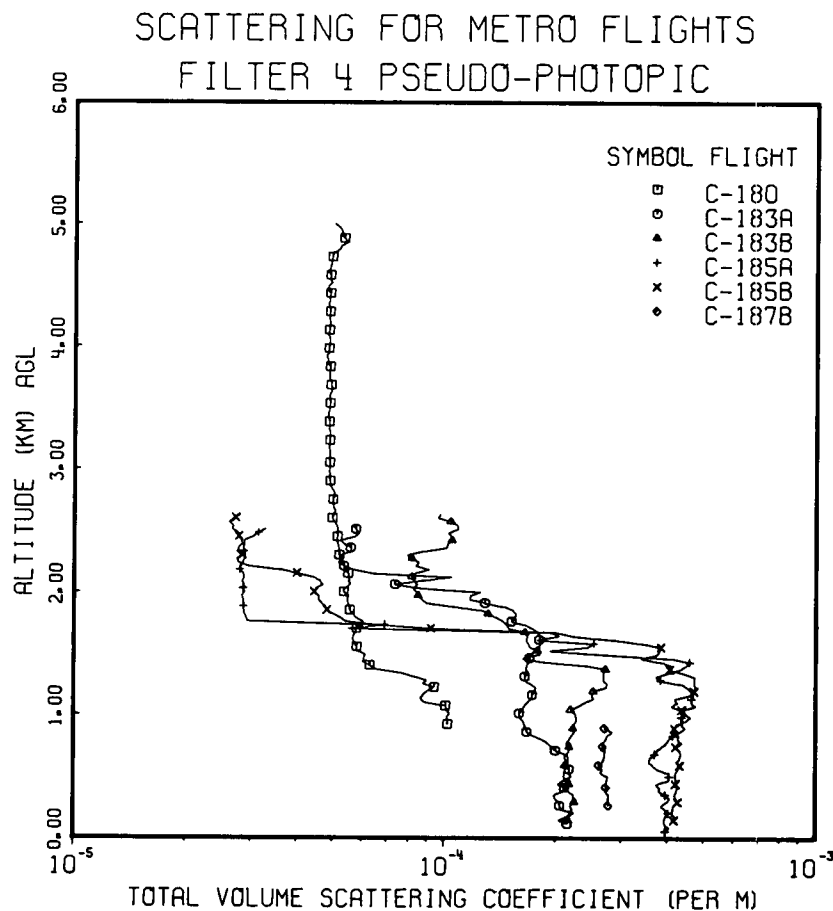


Fig. 8-3. Total Volume Scattering Coefficient for Filter 4 (Pseudo-Photopic) for Six METRO Flights.

IRRADIANCE

The downwelling irradiance at the lowest straight and level altitude is used as the irradiance for computing the directional reflectance of the terrain and the directional path reflectance. The low-altitude irradiance for photopic Filter 4 can be compared to the ground-level values of Brown (1952). The illuminance values of Brown for unobscured sun have been converted to irradiance units and are depicted in Figure 8-4. Superimposed on the same figure are the low-altitude downwelling irradiance values for Filter 4 for all the METRO profiles. The altitudes for the lowest straight and level sequence ranged between 88 and 241 meters above ground level. As would be expected, the irradiances cluster about the Brown curve for unobscured sun.

Also superimposed on Figure 8-4 is a curve for the photopic Rayleigh atmosphere with a scalar albedo of 0.10. (The range of the low-altitude scalar albedo for the METRO flights is 0.058 to 0.14.) The

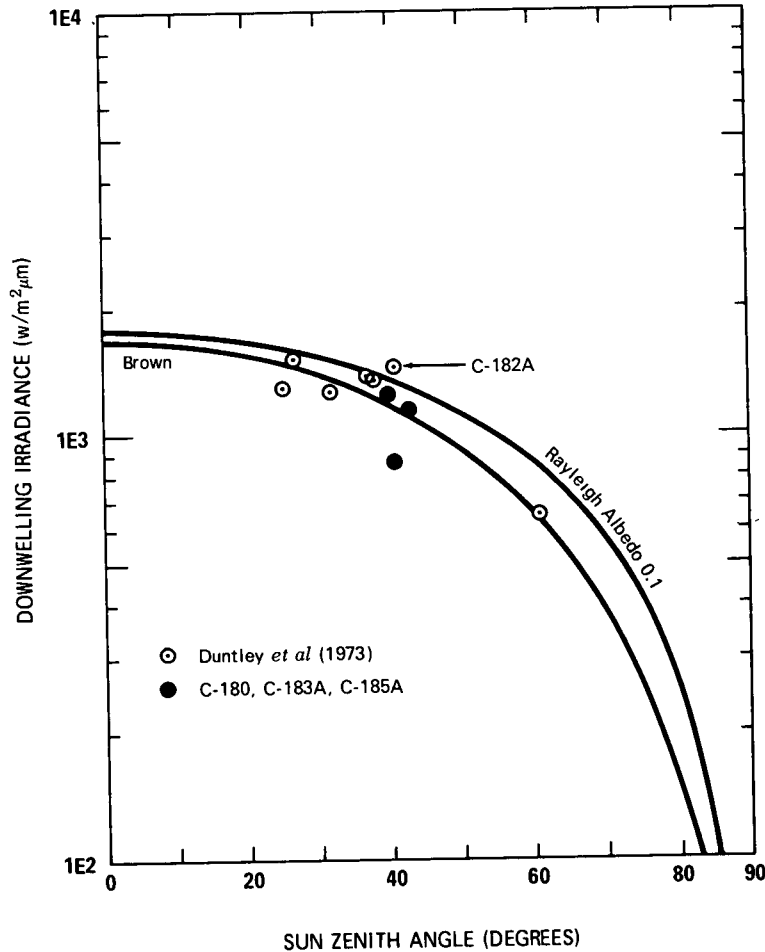


Fig. 8-4. Project METRO Low Altitude Downwelling Irradiance for Filter 4 (Pseudo-Photopic) Compared to Brown (1952) and a Rayleigh Atmosphere.

values, which represent an upper limit for a clear cloudless sky, were computed using the model atmosphere equations of Gordon (1969). The downwelling irradiance for Flight C-182A, albedo 0.058, is not totally unreasonable since the presence of highly-reflecting clouds can conceivably raise the total irradiance.

The graphs of downwelling irradiance versus altitude for all the METRO flights are generally more regular as a function of altitude and filter than the data from previous field trips. The irregularity of irradiance versus altitude in the previous data was difficult to explain and was the primary motivation for the improved techniques for handling sky radiance near the sun and apparent sun radiance, as described in Section 2. It is gratifying that the METRO data are much less anomalous. The new computational techniques and improved instruments are producing a more reliable and higher fidelity representation of the real world.

DIRECTIONAL REFLECTANCE OF TERRAIN

The tables of directional reflectance of the terrain presented with each flight are derived from data obtained with the lower hemisphere scanner at the lowest flight altitude. This instrument is a telephotometer with a 5-degree field of view. The tabular values of reflectance, therefore, relate to an average radiance throughout that field of view, and it is completely possible that no specific part of the terrain has that value of reflectance. In addition, objects of interest will almost certainly be located on a background having a different reflectance than that tabulated for the terrain. That is why ground-based measurements of directional reflectance of backgrounds are also made during the flight interval – to help provide appropriate values for generating contrast transmittance for a given problem. The affect of background reflectance on the contrast transmittance is not a trivial one. Care should be used in selecting the appropriate value for application to a specific problem.

Summary Table 8-2 presents all the METRO airborne data on terrain reflectance for the nadir path of sight. This summary groups the data into same or similar terrains and within each group presents the data in order by increasing sun zenith angle. For the nadir path of sight at the lowest altitude of all the flights, 92 meters, a 5-degree field would cover a circle 8 meters in diameter, whereas at the highest altitude of all the flights, 235 meters, a 5-degree field would cover a circle 20 meters in diameter. The nadir value is the average of the values obtained during one azimuthal revolution of the scanner (5 seconds). At the low-altitude flight speeds of 151 to 159 knots, the distance covered in 5 seconds is 389 to 409 meters. Thus, the tabulated nadir reflectances relate to an average radiance in an area 8 by 397 or 20 by 429 meters in size.

The seeming inconsistency of the reflectances filter to filter and flight to flight is probably a function of the patchiness of the terrain as illustrated in Figures 7-1 and 7-2. However, the reflectances are reasonable compared to the nadir reflectances of meadows, crops, and forests from the literature which were presented in Table 8-2 of Duntley *et al.* (1973). The range of these reflectances is indicated in the next-to-last row of data in Table 8-2.

EQUILIBRIUM RADIANCE

Equilibrium radiance (Eq. 2.22) is obtained by using an integrative method. An advantage of this method is the ability to handle highly variable data, variable in the sense of changing flux levels due to

Table 8-2

METRO Nadir Terrain Reflectances Based on Airborne Scanner Radiances

Track	Terrain Description	Date (1971)	Flight Profile No	Average Altitude (meters AGL)	Sun Zenith Angle (Degrees)	Nadir Reflectance		
						Filter 2	Filter 4	Filter 3
3	Flat, highly-cultivated farmland with multiple small fields	13 August	C-182B	92	25 0	0 060	0 057	0 131
		19 August	C-186B	202	27 2	0 031	-	0 041
		12 August	C-181	101	31 6	0 038	0 066	0 066
4	Flat, highly-cultivated farmland	24 August	C-188B	235	37 7	0 038	0 056	0 063
1	Cultivated farm area	11 August	C-180	100	40 5	0 043	0 074	0 036
9	Cultivated farm area with small fields and woodlands	24 August	C-188A	154	60 6	0 017	0 065	0 065
7	Heavily wooded, rolling hills	23 August	C-187A	200	26 6	0 017	0 040	0 054
		19 August	C-186A	148	36 8	0 024	0 056	0 032
		18 August	C-185A	125	39 8	0 029	0 066	0 044
		13 August	C-182A	135	40 6	0 015	0 057	0 050
		14 August	C-183A	123	42 6	0 021	0 034	0 030
	Range of values for meadows, crops, and forest [See Table 8-2, Duntley <i>et al.</i> (1973)]					0 013 to 0 082	0 032 to 0 14	0 027 to 0 21
Scott AFB	Mowed grass, dry and browning	24 August	MET-11	0		0 057	0 094	0 122

real changes occurring in space and/or time during the flight. Although the terrain over which a data flight takes place is chosen for its consistency of appearance, specific features vary in position relative to the aircraft as it flies the track. Anomalies in the sky-lighting distribution occur due to subtle changes in the weather. Also, the sun zenith angle increases or decreases in varying degrees due to changes in procedural elapsed times. These local occurrences contribute to the variability of the overall sky radiance flux level and directional radiance pattern, and these two properties plus the apparent sun radiance define the equilibrium radiance. The values of equilibrium radiance derived using the integrative method are directly descriptive of the real conditions encountered and measured during a flight, except for the average sun zenith angle used for obtaining the apparent sun radiances and the assumption that the sun, when unoccluded at the highest altitude, remains unoccluded. Thus the clouds when present contribute only to the variability of the sky irradiance at each altitude. This assumption of an unobscured sun is consistent with the real world case when checked against the scanner data arrays for the three flights containing scattered clouds in the upper sky.

Under comparatively stable clear-day conditions, equilibrium radiance tends to be relatively invariant with altitude. Several atmospheric models are based upon this tendency (Duntley (1948) and Gordon (1969)). The first model assumes an invariant particle-size distribution which decreases with increased altitude. The second model assumes both a clear day with no clouds and no absorption, and an invariant equilibrium radiance with altitude.

In contrast to these models, the entire eleven METRO flight profiles have equilibrium radiance functions which vary with altitude. The standard deviation of the equilibrium radiance from the average values varied from 1 to 93 percent, with the nadir path of sight often having standard deviations in the upper portion of that range. To illustrate this, the nadir equilibrium radiance for the Flight C-180 photopic response (Filter 4) is graphed in Figure 8-5. Flight C-180 was one of the more optically stable flights in terms of consistency in irradiance and total scattering coefficient, but the standard deviation for the nadir path equilibrium radiance varied from 3 to 34 percent for the three filters (Filter 4 standard deviation was 12 percent). Thus, the atmospheric models cited above appear inapplicable to the METRO flights.

There is a certain amount of consistency, however, in the equilibrium reflectance for the lowest altitude of the nadir path of sight. Equilibrium reflectance R_q is derived from the equilibrium radiance and the downwelling irradiance:

$$R_q(z, \theta, \phi) = N_q(z, \theta, \phi) \pi / H(z, d) \quad (8.1)$$

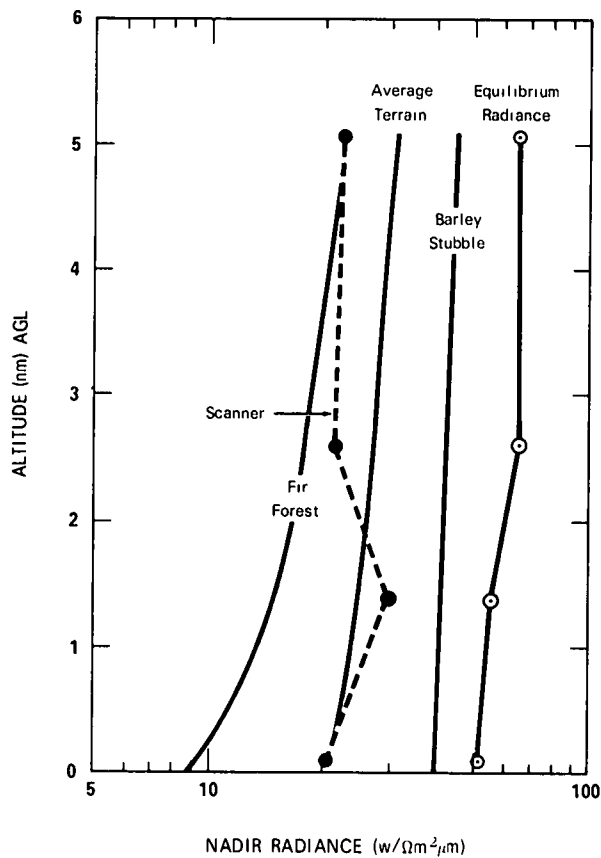


Fig. 8-5. Comparison of Equilibrium Nadir Radiance With Several Computed Apparent Nadir Terrain Radiances and the Measured Scanner Nadir Radiance from Flight C-180 Filter 4 (Pseudo-Photopic).

Since the apparent radiance of a terrain, background, or object tends to approach the equilibrium radiance, a look at the equilibrium reflectance at the lowest altitude will tell us whether a terrain will increase or decrease in radiance with altitude, at least initially. The nadir equilibrium reflectances for the 11 flight profiles are given in Table 8-3 in the same groupings as for Table 8-2. As can be seen, there is a rough overall consistency among the reflectances in a range of 0.10 to 0.25. However, all the nadir terrain reflectances (Table 8-2) are lower than the equilibrium reflectances for the same day, and, therefore, the apparent terrain radiance will increase with altitude, at least at the lower altitudes.

PATH RADIANCE

The path radiance is calculated from the values of equilibrium radiance for a given path of sight by means of Eq. 2.18 and 2.21. In this way, the path radiance combines the values of equilibrium radiance from each of the several altitudes. The required path radiance is essentially a scattered radiance in a given path at any one instant. The derived value, however, represents an averaging of the light conditions present during the entire flight (the use of integral Eq. 2.18 effectively combines the variable data into a crude average of the prevalent condition). The averaging, though, is progressive. The lowest altitude

Table 8-3
METRO Nadir Equilibrium Reflectance at Lowest Altitude

Track	Date (1971)	Flight Profile No.	Altitude (meters AGL)	Sun Zenith Angle (Degrees)	Nadir Equilibrium Reflectance		
					Filter 2	Filter 4	Filter 3
3	13 August	C-182B	92	25.0	0.14	0.16	0.16
3	19 August	C-186B	202	27.2	0.11	-	0.11
3	12 August	C-181	101	31.6	0.17	0.19	0.16
4	24 August	C-188B	235	37.7	0.11	0.12	0.12
1	11 August	C-180	100	40.5	0.15	0.18	0.17
9	24 August	C-188A	154	60.6	0.23	0.25	0.22
7	23 August	C-187A	200	26.6	0.13	0.13	0.11
7	19 August	C-186A	148	36.8	0.10	0.09	0.10
7	18 August	C-185A	125	39.8	0.096	0.10	0.12
7	13 August	C-182A	135	40.6	0.15	0.12	0.14
7	14 August	C-183A	123	42.6	0.14	0.13	0.14

value is derived solely from the low-altitude data, whereas the highest altitude value is an average of all the data. Thus, the path radiances represent neither the clearest nor the cloudiest portion of a flight, but a crude combination of the various segments.

The derived path radiance profiles are relatively smooth as a function of altitude due to the averaging process of the integration of Eq. 2.18. For simultaneous data, path radiance would be expected to decrease with increasing wavelength. The representative graphs of path radiance in Section 7.3 and in Duntley *et al.* (1973) indicate that this held for all 11 flight profiles.

The path radiances for both the ATOM and HAVEN VIEW field trips were less regular as a function of filter than for the METRO trip. The regularity of the METRO path radiances is a direct result of the improved methods of handling the sky radiance data near the sun, and of obtaining apparent sun radiance using the transmittance from sky radiance ratios and an average sun zenith angle. These new techniques are producing a more reliable and higher fidelity representation of the real world.

Path Radiance Applications. The path radiance enters into the equation for contrast transmittance, Eq. 2.2, into the equation for directional path reflectance, Eq. 2.4, and into the equation for computing apparent radiance, Eq. 7.2. By rearranging Eq. 7.2, we obtain an equation for predicting the inherent radiance of the terrain at ground level $N_o(0,\theta,\phi)$ from the apparent radiance, the beam transmittance, and the path radiance:

$$N_o(0,\theta,\phi) = [N_r(z,\theta,\phi) - N_r^*(z,\theta,\phi)]/T_r(z,\theta) \quad (8.2)$$

For example, the resultant inherent radiance for the nadir path of sight for Flight C-180, Filter 4 (photopic) is $20.2 \text{ w}/\Omega \text{ m}^2\mu\text{m}$. Then using Eq. 2.5, we obtain a reflectance of 0.072. This reflectance is indicative of the highly-cultivated farmland underlying the flight track. The measured scanner radiances and the extrapolated ground value have been graphed in Figure 8-5 and labeled as "scanner".

For conceptual purposes, we have computed the apparent nadir radiances for three types of terrains appropriate to Flight C-180, Filter 4 (photopic) using Eq. 7.2. The three terrains chosen were: highly cultivated farmland having a reflectance of 0.072 (the derived inherent terrain reflectance for the flight), a fir forest in late summer having a reflectance of 0.032, and barley stubble with a reflectance of 0.14. The latter two photopic reflectances are the minimum and maximum from the last row in Table 8-2 and illustrate high and low values for cultivated fields with woodlots. The computed radiances for these three terrains are graphed in Figure 8-5.

The computed farmland radiance closely follows the measured scanner radiance at low altitude, is lower than the scanner radiance at mid-altitude, and is higher than the scanner radiance at the upper altitudes. The low value of scanner radiance at high altitude is possibly due to an overall decrease in flux level with the larger sun zenith angle at the high altitude. The calculated value for the farmland shows the influence of the higher flux levels at the lower altitudes. The variability of the scanner radiance with altitude also is indicative of the patchiness of the terrain beneath the flight track.

Note how the computed terrain radiances tend to approach the equilibrium radiances. All the computed radiances increase with altitude since they are always less than the equilibrium radiance and tend to approach it.

CONTRAST TRANSMITTANCE

The contrast transmittance can be expressed as the beam transmittance times the ratio of the inherent to apparent background radiance:

$${}_b\tau_r(z,\theta,\phi) = T_r(z,\theta) {}_bN_o(0,\theta,\phi) / {}_bN_r(z,\theta,\phi) . \quad (8.3)$$

Thus, the contrast transmittance is a direct function of the background and the manner in which the background radiance changes with altitude. The contrast transmittance for items displayed against a background lower in reflectance than the equilibrium reflectance will always be less than the beam transmittance. This is true because the ratio of inherent to apparent background radiance is always less than 1, since apparent radiance increases with altitude as shown in Figure 8-5. This characteristic is illustrated in Figure 8-6. On the other hand, the contrast transmittance for a background higher in reflectance than the equilibrium reflectance will have a contrast transmittance greater than the beam transmittance.

The discussion above emphasizes the importance of selecting the appropriate terrain reflectance for use as background reflectance for computing valid contrast transmittance values. Photopic reflectances of many backgrounds are available for clear days with moderately high suns in Gordon (1964) and Gordon and Church (1966).

DIRECTIONAL PATH REFLECTANCE

Using the data from the two scanners to obtain both the path radiance $N_r^*(z,\theta,\phi)$ and the downwelling irradiance $H(z,d)$ adds to the reliability of the path reflectance $R_r^*(z,\theta,\phi)$ since these two quantities are ratioed in Eq. 2.4 to obtain path reflectance. In this manner, any absolute error in the calibration of the scanners or in the estimate of space-to-altitude transmittance is effectively minimized. Also, since both the path radiance and the downwelling irradiance are obtained by integration of a large number of radiance measurements, precision errors tend to cancel or average out.

For simultaneous data, the directional path reflectance should decrease with wavelength. All 11 flight profiles show this regularity in the representative graphs of path reflectance in Section 7.3 and in Duntley *et al.* (1973).

The path reflectances for both the ATOM and HAVEN VIEW field trips were less regular as a function of filter than those for METRO. The regularity of the METRO path reflectances is the result of the improved method of handling the sky radiance data near the sun and of obtaining the apparent sun radiance by using an average sun zenith angle and the transmittance from sky radiance ratios. These new techniques are producing a more reliable and higher fidelity representation of the real world.

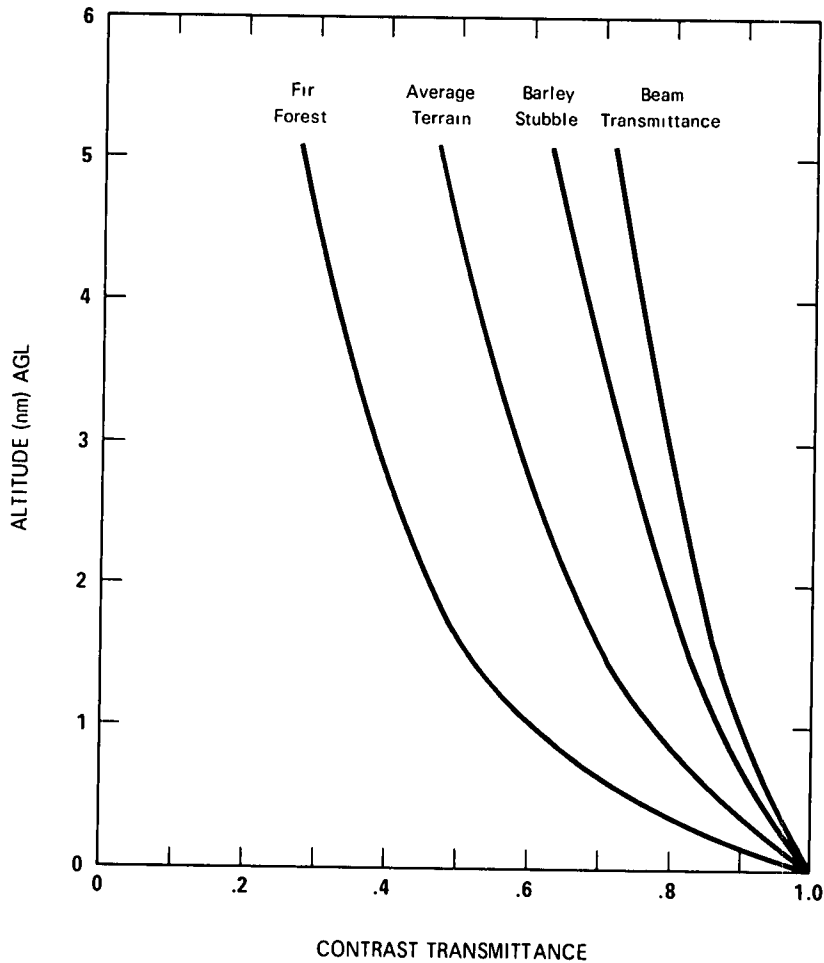


Fig. 8-6. Contrast Transmittance for Several Different Backgrounds and Beam Transmittance for Flight C-180 Filter 4 (Pseudo-Photopic) Nadir Path of Sight.

8.3 GROUND-BASED RADIOMETRIC DATA

The ground-based instruments were located at Scott Air Force Base (see Figure 1-4), which is closer to the center of St. Louis than any of the flight tracks. Various points of the flight tracks ranged between 30 miles and 110 miles from the ground station. The ground station, therefore, did not provide a ground point beneath any of the flights. Instead, it provided additional data on the optical properties of the atmosphere in the St. Louis region for comparison to the flight data.

TOTAL VOLUME SCATTERING COEFFICIENT

The order of the ground-based measurements of scattering coefficient by filter is the inverse of the mean wavelength of the filters expected for near simultaneous data.

To facilitate the comparison of airborne and ground-based measurements of scattering coefficient, the values for Filter 4 have been tabulated in Table 8-4. Column 5 contains the values from Section 7-3 obtained by extrapolating the airborne data to ground level. In column 6 are listed the ground-based measurements for the time nearest the airborne measurements at the lowest altitude. Flight tracks 3 and 4 were the shortest distance from Scott Air Force Base; the scattering coefficients measured on these tracks are relatively close to the ground-based values, with ground-based values being larger when the wind was not from the direction of the city. The closer proximity of Scott Air Force Base to the city might account for this.

Tracks 7 and 9 were farther from Scott Air Force Base, and the comparison is not as clear-cut. For four of the five cases where the wind was not from the city, the airborne scattering indicated clearer air than at Scott Air Force Base, but for the only flight where the wind was from the direction of St. Louis, C-187A, the airborne data indicated clearer air by a large factor. A more detailed knowledge of pollution sources in the area, etc. is necessary before comparisons of data taken 80 to 110 miles apart can be very meaningful.

The visibility "VV" reports in Section 6.3 of this report and in Duntley *et al.* (1973) from the weather office at Scott Air Force Base can be compared to the pseudo-photopic total scattering coefficient $s(\text{Filter } 4)$

Table 8-4

Ground-level Total Volume Scattering Coefficient $s(0)$ per Meter for Filter 4 (Pseudo-Photopic) Extrapolated from Airborne Measurements and Measured at Scott Air Force Base, and Visibilities Reported and Computed

Date (1971)	Airborne				Ground			Scott AFB Weather Office	
	Flight No	Track	Time (GMT)	$s(0)$ (per m)	$s(0)$ (per m)	Time (GMT)	Calculated Visibility (miles)	Reported Visibility (miles)	Time (GMT)
11 August	C-180	1	2236	1 12 E-4	-	-	-	15	2255
12 August	C-181	3	2032	1 39 E-4	2 01 E-4	2035	9	20	2056
13 August	C-182A	7	1632	1 51 E-4	2 61 E-4	1636	7	10	1655
13 August	C-182B	3	1849	2 99 E-4	2 74 E-4	1902	7	12	1855
14 August	C-183A	-	-	-	-	-	-	8	1557
14 August	C-183A	7	1628	2 18 E-4	2 90 E-4	1616	6	12	1657
14 August	C-183B	4	1840	2 20 E-4	-	-	-	8	1857
18 August	C-185A	7	1651	3 99 E-4	4 46 E-4	1651	4	6	1655
18 August	C-185B	3	1905	4 24 E-4	4 05 E-4	1831	5	6	1855
19 August	C-186A	7	1700	3 99 E-4	3 85 E-4	1711	5	6	1655
19 August	C-186B	3	-	-	2 99 E-4	1914	6	7	1855
23 August	C-187A	7	1853	1 17 E-4	3 30 E-4	1910	6	12	1855
23 August	C-187B	4	2022	2 85 E-4	3 44 E-4	2035	5	12	2055
24 August	C-188A	9	1454	8 08 E-5	3 47 E-4 ¹	1453	5	6	1455
24 August	C-188B	4	1649	3 09 E-4	2 44 E-4	1653	8	15	1655

by assuming no absorption. The visibility distance is considered roughly comparable to a 5-percent contrast transmittance range; thus when "s" and "VV" are in similar units,

$$s = \frac{3}{VV} \quad (8.4)$$

Values of visibility calculated from the measured s values in column 6 of Table 8-4 are tabulated in column 8. The estimated visibilities reported by the weather office are in column 9. The visibilities reported for Scott Air Force Base are always larger than the computed values, but the discrepancy is less when the visibilities are low. The tendency for reported visibilities to be higher than the calculated values was also noted during Project ATOM for data taken in central New Mexico (Duntley *et al.* (1972b)).

PROPORTIONAL DIRECTIONAL SCATTERING FUNCTION

The data on directional scattering are presented in the form of proportional directional scattering functions $\sigma(0,30^\circ)/s(0)$ and $\sigma(0,150^\circ)/s(0)$. This form is particularly useful since the integral of the proportional directional scattering function over 4π steradians is 1. The dimension of the proportional scattering function is per steradian. The values for the proportional scattering function at 30 degrees should be ≥ 0.1 , and the values for 150 degrees should be ≤ 0.1 . This evaluation comes from inspecting the catalog of proportional scattering functions published by Barteneva (1960). All the ground-based directional scattering data meet these criteria. In addition, the proportional directional scattering functions at 30 degrees and 150 degrees tend to decrease with wavelength but not monotonically. The values of proportional directional scattering functions may be converted to directional scattering coefficients in units of $\Omega^{-1}\text{m}^{-1}$ by multiplying by the total volume scattering coefficient.

The ratio of forward- to backscattering at 30 degrees and 150 degrees is a useful indication of the directionality of the scattering. The ratios for the ground-based data at Scott Air Force Base are given in Table 8-5. Similar ratios for the low-altitude airborne data are given in Table 8-6. The ranges of airborne and ground-based values are similar except for the large ratios for two flights, C-185A and C-186A, on Track 7. For both airborne and ground-based values the ratios sometimes increase and sometimes decrease with wavelength – they have no clear relationship with wavelength.

IRRADIANCE

The ground-based irradiances were measured using a cosine collector cap on the scanner, so these values are a direct measurement of total downwelling irradiance rather than computed values. The ground-based irradiances for Filter 4 (pseudo-photopic) can be compared to the ground-level values of Brown (1952). The illuminance values of Brown for unobscured sun, average cloud conditions, and black storm-cloud conditions have been converted to irradiance units and are depicted as solid curves in Figure 8-7. The ground-based irradiances measured by the scanner at Scott Air Force Base and coded by date are also depicted in Figure 8-7. All the ground-based values lie below or on the Brown curve for unobscured sun. Since moderate haze was generally noted at the ground station, it is reasonable for the irradiances to be slightly below the values for unobscured sun. In comparison, some of the low-altitude airborne irradiances

exceeded the Brown curve. In all but one case, Flight C-188B, these higher irradiances were measured on the flight tracks 80 to 110 miles from Scott Air Force Base. On these farther tracks, lower values of total scattering coefficient were also encountered.

On 2 days, 18 August 1971 and 23 August 1971, some of the downwelling irradiances cluster about the average cloud curve. The log entries for these 2 days indicate the presence of clouds at these times, with occasional obscuration of the sun.

Table 8-5

Ratio of Forward- to Backscattering at 30 Degrees and 150 Degrees for Ground-Based Data

Date (1971)	Time (GMT)	Ratio of Scattering at 30° to 150°				
		Filter 2	Filter 6	Filter 4	Filter 3	Filter 5
12 August	1907	-	7.91	8.52	7.82	13.8
12 August	2035	8.38	8.49	9.44	6.97	11.0
13 August	1512	12.6	11.0	11.8	10.1	10.9
13 August	1637	12.6	11.2	11.3	9.57	11.5
14 August	1617	15.8	14.0	14.7	12.0	12.8
18 August	1611	19.6	18.3	19.4	17.3	16.7
18 August	1821	20.4	18.7	21.1	18.7	19.1
19 August	1556	20.2	18.8	20.5	19.7	21.2
19 August	1711	18.9	18.1	19.3	18.1	20.3
19 August	1914	16.6	15.4	17.2	15.4	-
19 August	1941	16.3	-	-	15.2	-
23 August	1751	13.6	12.4	13.2	12.2	13.4
23 August	1943	15.4	13.8	14.8	13.3	13.7
23 August	2035	14.8	13.7	14.4	12.7	13.9
24 August	1342	14.4	13.8	15.4	12.5	16.9
24 August	1444	15.2	14.6	18.0	16.1	18.4
24 August	1555	15.7	14.5	16.5	17.0	19.2
24 August	1654	12.5	11.9	13.2	11.6	16.1

Table 8-6

Low-Altitude Airborne Values of the Ratio of Forward- to Backscattering at 30 degrees and 150 degrees

Flight	Date (1971)	Time (GMT)	Altitude (m)	Track	Ratio of Scattering at 30° to 150°		
					Filter 2	Filter 4	Filter 3
C-180	11 August	1933	99	1	9.85	10.1	10.1
C-181	12 August	1901	101	3	8.65	9.00	8.34
C-182A	13 August	1511	134	7	12.5	13.9	12.5
C-182B	13 August	1726	92	3	13.2	14.2	10.6
C-183A	14 August	1502	125	7	12.5	18.1	13.0
C-183B	14 August	1731	115	4	12.7	11.5	9.33
C-185A	18 August	1522	125	7	24.4	26.0	24.6
C-185B	18 August	1746	188	3	-	23.4	21.7
C-186A	19 August	1543	148	7	25.1	30.0	27.8
C-186B	19 August	1751	203	3	20.5	25.0	21.4
C-187A	23 August	1742	200	7	12.6	14.4	15.7
C-187B	23 August	1942	242	4	16.9	19.0	15.6
C-188A	24 August	1339	154	9	9.85	9.77	9.63
C-188B	24 August	1539	235	4	19.6	21.3	20.1

DIRECTIONAL REFLECTANCE OF TERRAIN

The measurements of dried and browning mowed grass were made by turning the scanner on its side so that the scanner zenith was at the horizon 90 degrees from the azimuth of the sun. The automatic hemispherical scan therefore included the terrain measurements for half of the lower hemisphere. Unfortunately, it was difficult to extend the scanner over the side of the truck upon which it was mounted, so most of the near vertical data were not valid terrain measurements. The only valid vertical measurements were made on 24 August 1971 during MET-11. These values are given in the last row of Table 8-2. They fall within the range of data from the flights and within the range of reflectance values from the literature indicated in the next-to-last row of Table 8-2.

The reflectance values for Filter 4 (pseudo-photopic) for the same paths of sight as the airborne data, toward the sun and away from the sun, are graphed in Figure 8-8. No values are given for path of sight zenith angle 95 degrees since it was not practical to take a valid measurement at that angle with the particular experimental configuration used. The graph generally indicates the expected lower reflectances looking toward the sun and viewing the internal shadowing of the textured grass. The higher reflectances of the fully-illuminated grass blades viewed while looking away from the sun are also depicted.

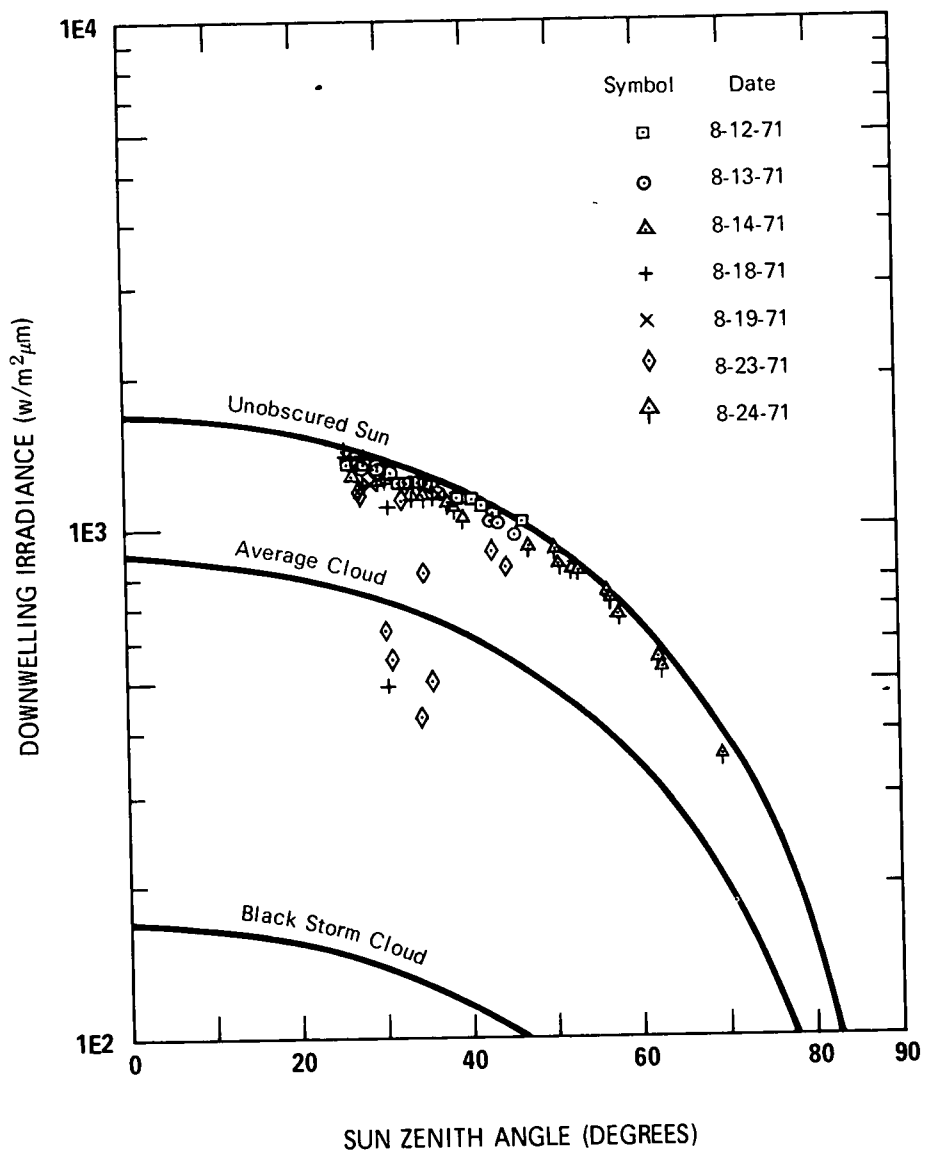


Fig. 8-7. Ground-Based Downwelling Irradiance for Filter 4 (Pseudo-Photopic) Compared to Brown (1952).

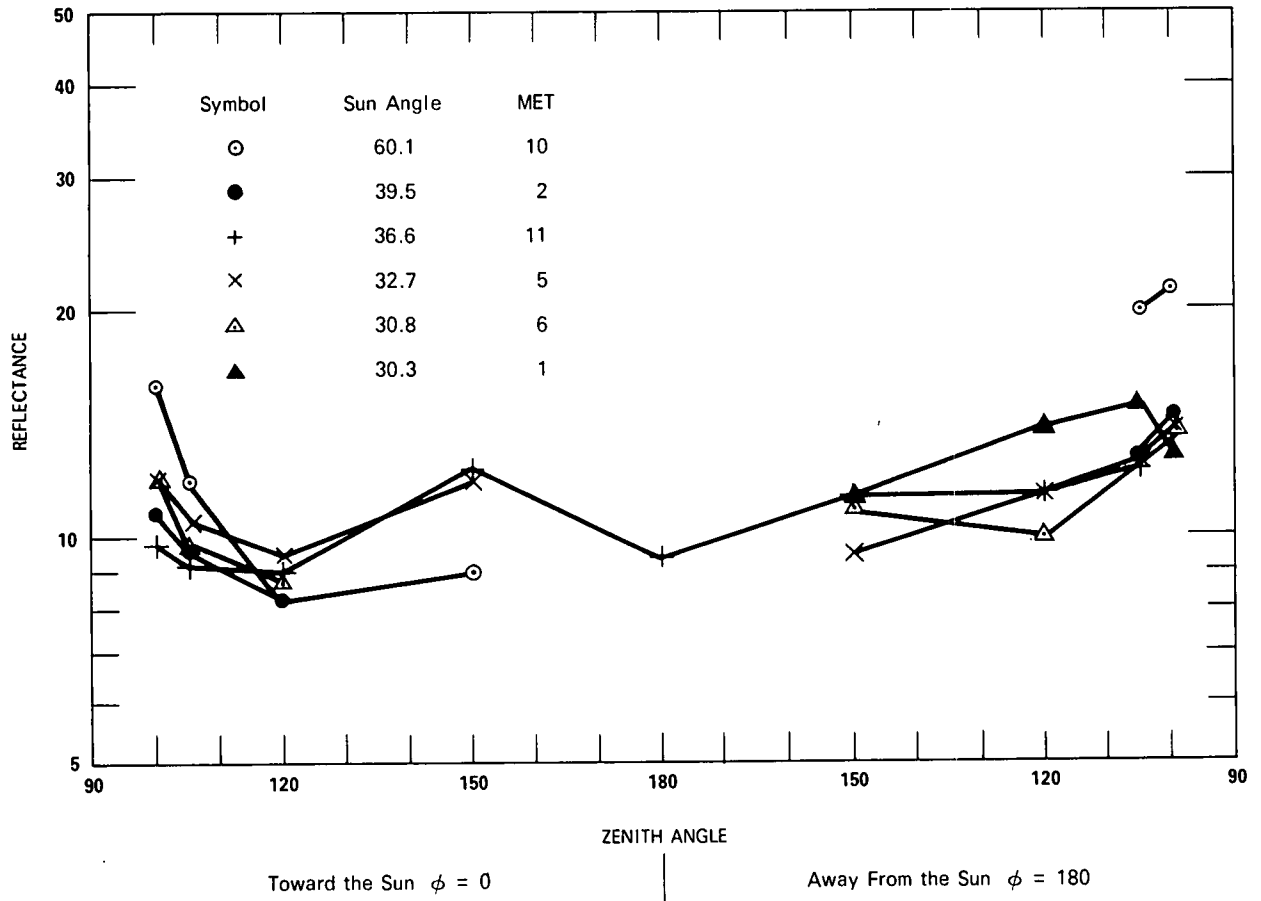


Fig. 8-8. Directional Reflectance of Mowed Grass, Dry and Browning for Filter 4 (Pseudo-Photopic).

8.4 SUMMARY

The derived optical properties for the METRO flights are more consistent as a function of altitude and spectral filter than the equivalent values for ATOM and HAVEN VIEW. This is the direct result of utilizing advanced methods for evaluating and handling the measured values of lighting distribution for the upper hemisphere. First, the apparent sun radiance was separated from the sky radiance array. Then the transmittance from out of the atmosphere to the highest flight altitude was calculated from the ratio of the sky radiances at equivalent angles from the sun. That transmittance, combined with the transmittances derived from the airborne integrating nephelometer data, provided a space-to-altitude beam transmittance for each flight altitude. Next, sky radiances were evaluated as a function of angle from sun, and spurious values resulting from slow phototube decay were corrected. Finally, an average sun zenith angle for the entire flight was established and used for the computation of apparent sun radiance, irradiance, path radiance, and path reflectance. All of these computed optical properties showed consequent improvements in consistency.

These demonstrated improvements in data quality are convincing evidence that the computational techniques used are capable of producing increasingly reliable data. It is necessary that we continue to improve only the precision and accuracy in the measurements of upper and lower hemisphere radiance distributions. Procedural updates to accomplish these ends have been devised and are currently being inserted into the field measurement routines.

9. ACKNOWLEDGEMENTS

To be conducted successfully, Project METRO required the active support of many organizations and individuals. To all of those who so willingly contributed their skills, talents, and inspiration, the authors gratefully acknowledge their debt.

Dr. Robert W. Fenn, Chief, Atmospheric Optics Branch, AFCRL,
Scientific Counsel and Technical Monitor
Major Leo J. Sheehan, USAF, Project Organization and Coordination
Mr. Raymond S. Silva, Operational Services Division, Field Requirements Section
AFCRL, for continuing logistical support and advice

3245th ABGp, L. G. Hanscom Field, for all aircrew assignments:

Lt. Col. Charles E. MacWilliam, pilot
Lt. Col. Robert B. Thorworth, pilot
Lt. Col. D. R. Skinner, pilot
Major Ward A. Myer, pilot
Major S. C. Peterson, pilot
Lt. Col. John D. Morrow, navigator
Major Robert J. Franklin, navigator
M. Sgt. J. H. Bragg, flight engineer
T. Sgt. G. Mello, flight engineer
S. Sgt. W. V. Zito, crew chief
Sgt. J. J. Simas, crew chief
Sgt. C. J. Turner, crew chief

375 AAWg/DMMCC, Scott Air Force Base, for all transient support activities:
Operations Officer Maj. L. L. Bryant
Motor Pool Supervisors: Mr. Church and Sgt. Hammer

Visibility Laboratory, Technical Field Team:
Mr. J. Douglas Bailey, ground station crew
Mr. George F. Simas, ground station crew
Mr. Leonard A. Castro, technical flight crew

Visibility Laboratory, Data Processing and Analysis Team:
Mr. Nils R. Persson, Jr.
Mrs. Janet E. Shields
Mrs. Catharine F. Edgerton
Miss Carolyn M. Williams

Visibility Laboratory, Editorial and Reproduction Team:
Miss Sally L. Poor
Mr. John C. Brown
Mrs. Arlene C. Streed
Mr. James Rodriguez
Miss Alicia G. Enriquez

10. REFERENCES

- Barteneva, O. D. (1960), "Scattering Functions of Light in the Atmospheric Boundary Layer," Bull. Acad. Sci. U.S.S.R., Geophysics Series, 1237 – 1244.
- Boileau, A. R. (1964), "VI. Atmospheric Properties," Appl. Opt. **3**, 570 – 581.
- Boileau, A. R. and J. I. Gordon (1966), "Atmospheric Properties and Reflectances of Ocean Water and Other Surfaces for a Low Sun," Appl. Opt. **5**, 803 – 813.
- Brown, D. R. E. (1952), *Natural Illumination Charts*, Report 374-1, Project Ns-714-100, Department of the Navy, Bureau of Ships, Washington, D. C.
- Changnon, S. A., F. A. Huff and R. G. Semonin (1971), "METROMEX: an investigation of inadvertent weather modification," Bull. Amer. Meteor. Soc. 52 No. 10, October.
- Duntley, S. Q. (1948), "Reduction of Apparent Contrast by the Atmosphere," J. Opt. Soc. Am. **38**, 179 – 191.
- Duntley, S. Q., A. R. Boileau, and R. W. Preisendorfer (1957), "Image Transmission by the Troposphere I," J. Opt. Soc. Am. **47**, 499 – 506.
- Duntley, S. Q. (1964), "Visibility, I. Introduction and II. Summary," Appl. Opt. **3**, 550 – 556.
- Duntley, S. Q. (1969), "Directional Reflectance of Atmospheric Paths of Sight," Duntley Rep. No. 69-1.
- Duntley, S. Q., R. W. Johnson, J. I. Gordon, and A. R. Boileau (1970), "Airborne Measurements of Optical Atmospheric Properties at Night," University of California, San Diego, Scripps Institution of Oceanography, Visibility Laboratory, SIO Ref. 70-7 and AFCRL-70-0137.
- Duntley, S. Q., R. W. Johnson, and J. I. Gordon (1972 a), "Airborne Measurements of Optical Atmospheric Properties in Southern Germany," University of California, San Diego, Scripps Institution of Oceanography, Visibility Laboratory, SIO Ref. 72-64 and AFCRL-72-0255.
- Duntley, S. Q., R. W. Johnson, and J. I. Gordon (1972 b), "Airborne and Ground-Based Measurements of Optical Atmospheric Properties in Central New Mexico," University of California, San Diego, Scripps Institution of Oceanography, Visibility Laboratory, SIO Ref. 72-71 and AFCRL-72-0461.
- Duntley, S. Q., R. W. Johnson, and J. I. Gordon (1972 c), "Airborne Measurements of Optical Atmospheric Properties, Summary and Review," University of California, San Diego, Scripps Institution of Oceanography, Visibility Laboratory, SIO Ref. 72-82 and AFCRL-72-0593.

Duntley, S. O., R. W. Johnson, and J. I. Gordon (1973), "Airborne Measurements of Optical Atmospheric Properties in Southern Illinois," University of California, San Diego, Scripps Institution of Oceanography, Visibility Laboratory, SIO Ref. 73-24 and AFCRL-TR-73-0422.

Edgerton, C. F. (1967), "Relationship Between Meteorological Conditions and Optical Properties of the Atmosphere," University of California, San Diego, Scripps Institution of Oceanography, Visibility Laboratory, SIO Ref. 67-27.

Gordon, J. I., J. L. Harris, and S. O. Duntley (1963), "Earth-to-Space Contrast Transmittance Measurements from Ground Stations," Scripps Institution of Oceanography, University of California, San Diego, SIO Ref. 63-2.

Gordon, J. I. (1964), "III. Optical Properties of Objects and Backgrounds," *Appl. Opt.* **3**, 556 – 562.

Gordon, J. I. (1969), "Model for a Clear Atmosphere," *J. Opt. Soc. Am.* **59**, 14 – 18.

Gordon, J. I. and P. V. Church (1966), "Sky Luminances and Directional Luminous Reflectances of Objects and Backgrounds for a Moderately High Sun," *Appl. Opt.* **5**, 793 – 801.

Gordon, J. I., J. L. Harris, Sr., and S. O. Duntley (1973), "Measuring Earth-to-Space Contrast Transmittance from Ground Stations," *Appl. Opt.* **12**, 1317 – 1323.

Johnson, F. S. (1954), "The Solar Constant," *J. Meteorol.* **11**, 431 – 439.

Kasten, F. (1965), "A New Table and Approximation Formula for the Relative Optical Airmass," *Arch. Met. Geophys. Bioklim.* **B14**, 206 – 233.

Kushpil', V. I. and L. F. Petrova (1971), "Determination of the Atmospheric Transmittance from Sky Brightness Distribution," *Optical Technology* **38**, No. 4, 191 – 193.

Penndorf, R. (1957), "Tables for the Refractive Index for Standard Air and the Rayleigh Scattering Coefficient for the Spectral Region Between 0.2 and 20.0 μ and Their Application to Atmospheric Optics," *J. Opt. Soc. Am.* **47**, 176 – 182.

Preisendorfer, R. W. (1958), "Theory of Attenuation Measurements in Planetary Atmospheres," University of California, San Diego, Scripps Institution of Oceanography, Visibility Laboratory, SIO Ref. 58-81.

Tyler, J. E. and R. W. Preisendorfer (1962), "Light," Chap. 8 in *The Sea*, M. N. Hill, Ed. (Interscience Publishers, Inc., N.Y.), Vol. 1, pp 397 – 451.

USNAF TP-133, U. S. Naval Avionics Facility (1962), "Handbook, Operation and Service Instructions Aerograph Sets AN/AMQ-17 and AN/AMQ-18," Indianapolis 18, Indiana.

U. S. Standard Atmosphere (1962), U. S. Government Printing Office, Washington, D. C. 20402.

U. S. Standard Atmosphere Supplements (1966), U. S. Government Printing Office, Washington, D. C. 20402.

DOCUMENT CONTROL DATA - R&D

(Security classification of title, body of abstract and indexing annotation must be entered when the overall report is classified)

1. ORIGINATING ACTIVITY (Corporate author) University of California, San Diego Visibility Laboratory San Diego, California 92152		2a. REPORT SECURITY CLASSIFICATION UNCLASSIFIED	
		2b. GROUP	
3. REPORT TITLE AIRBORNE AND GROUND-BASED MEASUREMENTS OF OPTICAL ATMOSPHERIC PROPERTIES IN SOUTHERN ILLINOIS			
4. DESCRIPTIVE NOTES (Type of report and inclusive dates) Scientific, Interim			
5. AUTHOR(S) (Last name, first name, initial) Seibert Q. Duntley Richard W. Johnson Jacqueline I. Gordon			
6. REPORT DATE June 1974		7a. TOTAL NO OF PAGES 196	7b. NO OF REFS 29
8a. CONTRACT OR GRANT NO F19628-73-C-0013		9a. ORIGINATOR'S REPORT NUMBER(S) SIO Ref. 74-25 Scientific Report No. 4	
b. Project, Task, Work Unit No. 7621-04-01		9b. OTHER REPORT NO(S) (Any other number that may be assigned this report) AFCRL-TR-74-0298	
c. DoD Element 62101F			
d. DoD Subelement 687621			
10. AVAILABILITY/LIMITATION NOTICES A - Approved for public release; distribution unlimited.			
11. SUPPLEMENTARY NOTES TECH, OTHER		12. SPONSORING MILITARY ACTIVITY Air Force Cambridge Research Laboratories (OP) Hanscom AFB, Massachusetts 01730	
13. ABSTRACT <p>This report presents daytime atmospheric optical data collected chiefly with airborne instruments during a field expedition to southern Illinois in the summer of 1971. Results from four flights and selected ground-based data are presented. The data include the natural irradiance upon horizontal plane surfaces, scalar irradiances, total volume scattering coefficients, atmospheric beam transmittances, path radiances, directional path reflectances, and directional terrain reflectances. Data for sunlight conditions were derived for downward-looking paths of sight inclined at six zenith angles (95, 100, 105, 120, 150, and 180 degrees) from maximum altitudes of 3000 to 5100 meters above ground level and lower in three spectral regions, as follows: two narrow band optical filters with mean wavelengths of 478 and 664 nanometers; and one broad band sensitivity representing the photopic response with a mean wavelength of 557 nanometers.</p>			